

unpublished typescript and the copyright is held by the author. All persons consulting the thesis must read and abide by the Copyright Declaration below.

COPYRIGHT DECLARATION

I recognise that the copyright of the above-described thesis rests with the author and that no quotation from it or information derived from it may be published without the prior written consent of the author.

LOAN

Theses may not be lent to individuals, but the University Library may lend a copy to approved libraries within the United Kingdom, for consultation solely on the premises of those libraries. Application should be made to: The Theses Section, University of London Library, Senate House, Malet Street, London WC1E 7HU.

REPRODUCTION

University of London theses may not be reproduced without explicit written permission from the University of London Library. Enquiries should be addressed to the Theses Section of the Library. Regulations concerning reproduction are given according to the date of acceptance of the thesis and are listed below as guidelines.

- A. Before 1962. Permission granted only upon the prior written consent of the author. (The University Library will provide addresses where possible).
- B. 1962 - 1974. In many cases the author has agreed to permit copying upon completion of a Copyright Declaration.
- C. 1975 - 1988. Most theses may be copied upon completion of a Copyright Declaration.
- D. 1989 onwards. Most theses may be copied.

This thesis comes within category D.

☐

This copy has been deposited in the Library of

UCL

☐

This copy has been deposited in the University of London Library, Senate House, Malet Street, London WC1E 7HU.



Regulation of Endothelial E-selectin Molecule Expression by *Neisseria meningitidis*

Marianne Christina Jacobsen

This thesis is presented to the University of London for the degree of
Doctor of Philosophy

2006

Infectious Diseases and Microbiology Unit
Institute of Child Health
University College London

UMI Number: U592931

All rights reserved

INFORMATION TO ALL USERS

The quality of this reproduction is dependent upon the quality of the copy submitted.

In the unlikely event that the author did not send a complete manuscript and there are missing pages, these will be noted. Also, if material had to be removed, a note will indicate the deletion.



UMI U592931

Published by ProQuest LLC 2013. Copyright in the Dissertation held by the Author.
Microform Edition © ProQuest LLC.

All rights reserved. This work is protected against
unauthorized copying under Title 17, United States Code.



ProQuest LLC
789 East Eisenhower Parkway
P.O. Box 1346
Ann Arbor, MI 48106-1346

Abstract

Group B *Neisseria meningitidis* can induce severe sepsis in children. Whilst intensive care treatment has improved extensively over the last 20 years, morbidity and mortality remains high in patients with meningococcal sepsis. Neutrophil adherence to the endothelium mediated by adhesion molecule expression on both cell types is a prerequisite to the induction of vascular damage and capillary leakage which is characteristic of meningococcal sepsis. *N. meningitidis* and LPS are potent inducer of E-selectin surface expression, an adhesion molecule critical for neutrophil rolling. It has been shown that *N. meningitidis* is more potent than LPS alone at inducing E-selectin expression. This implies a role for LPS-independent mechanisms. This thesis investigates the molecular mechanisms regulating differential E-selectin expression in response to *N. meningitidis* and LPS. E-selectin surface expression was detected by FACS analysis and correlated with mRNA transcription detected by Real-Time RT-PCR. The E-selectin promoter was studied with an optimised transfection method using primary endothelial cells. Live and killed bacteria were able to induce higher levels and prolonged expression of E-selectin when compared to LPS. Bacteria induced E-selectin surface protein expression, which correlated with increased mRNA transcription. This suggested that differential E-selectin expression was largely regulated at the transcriptional level. Studies on the E-selectin promoter suggested that whilst LPS induced E-selectin expression was largely mediated by NF κ B activity, WT bacteria were able to also activate the MAPK pathway. Studies elucidating the molecular mechanisms of disease progression may provide new targets for drug therapy and thereby improve patient outcome in meningococcal sepsis.

Declaration

The work presented in this thesis was solely performed by the researcher. None of the experiments shown in this thesis were executed by anybody else. In chapter 4, the primers for the cyclophilin gene for Real-Time PCR were obtained from Dr. Laila Samady. In Chapter 5 and Chapter 6, the peptides for the transfection experiments were designed and obtained from Dr. Steven Hart and Dr. Michele Writer. The E-selectin promoter plasmids were obtained from Dr. Shosaku Narumi.

Acknowledgements

I would first like to thank my supervisors, Nigel Klein and Steve Hart, for their support. Steve, for your patience and encouragement. Nigel for those hours when you truly became a motivator. Thanks for showing me the bigger picture.

There are two people in particular who deserve a big massive hug and loads of babysitting hours for their support in the final stages of this write up: Meredith Allen and Karolena Kotowicz. I wouldn't have managed this without your encouragement and enthusiasm. Thanks for reading through countless drafts and for discussions which assisted me in broadening my mind and bringing my ideas onto paper. There are no words that can express my gratitude. A big thanks goes to the members of the department, particularly the 'ladies' in the office, Heli Uronen-Hansson, Jessica Strid, Christina Ong, and Hannah Jones who were always there to brighten my days with surreal chats and loads of laughs. I'll miss you all dearly. Katy Newton and Barry Flutter both deserve a thank you for drinks and laughs at the Goose, which made the hard days more bearable. Finally, a special thanks to Garth Dixon and Mona Bajaj-Elliott for all their help in aiding and supporting in getting this work finished.

I would also like to thank my parents, who always supported me in everything that I've done. Thanks for being such wonderful parents and great friends.

Last, but not least, I would like to thank Gav, who put up with me through the best of times and the worst of times. You're probably the only one that knows how much it took to get this far! Thanks for being you.

MJ, December 2005

Table of Contents

ABSTRACT	2
DECLARATION	3
ACKNOWLEDGEMENTS.....	4
TABLE OF CONTENTS	5
TABLE OF FIGURES	10
TABLE OF TABLES.....	12
TABLE OF EQUATIONS.....	13
ABBREVIATIONS	14
CHAPTER 1.....	18
1.1 Introduction	19
1.2 Neisseria meningitidis.....	20
1.2.1 Historical perspectives	20
1.2.2 Epidemiology.....	20
1.2.3 Classification	24
1.2.4 Pathophysiology.....	24
1.2.4.1 Bacterial sepsis and septic shock.....	26
1.2.4.2 Diffuse intravascular coagulation (DIC) during meningococcal disease	27
1.2.4.3 The contribution of shock to the outcome of FMS.....	29
1.3 Bacterial Cell Surface Structure and the role in pathogenesis	30
1.3.1 Capsule	33
1.3.2 Pili.....	34
1.3.3 OMPs	35
1.3.3.1 Porins	35
1.3.3.2 RmpM	37
1.3.3.3 Opa and Opc proteins.....	37
1.3.4 LPS structure and biosynthesis	38
1.3.4.1 LPS induced inflammatory responses	42
1.3.4.2 LPS signalling complex	44
1.3.4.3 LPS signalling via the LPS complex- the NFκB Regulatory Pathways	49
1.3.4.4 LPS signalling via the LPS complex- the MAP Kinase regulatory pathways.....	51
1.4 The use of the LPS-deficient mutant (lpxA-) in elucidating LPS-dependant and independent mechanisms of disease	53
1.5 Endothelium and Inflammation	55
1.5.1 The role of adhesion molecules in leukocyte adhesion and transmigration	56
1.5.1.1 E-selectin.....	59

1.5.1.1.1 E-selectin transcriptional regulation	61
1.5.1.1.2 E-selectin promoter organisation	62
1.5.1.1.3 The role of NFκB in E-selectin transcription	65
1.5.1.1.4 The role of ATF and c-Jun in E-selectin transcription	65
1.5.1.1.5 Final comment on the E-selectin promoter	66
1.5.1.2 ICAM-1	67
1.5.1.3 VCAM-1	69
1.6 Interactions between <i>N. meningitidis</i> and the vascular endothelium.....	71
1.6.1 Mechanisms of bacterial invasion of the endothelium.....	71
1.6.2 Endothelial damage mediated by <i>N. meningitidis</i> LPS	72
1.6.3 Endothelial dysfunction during meningococcal sepsis	72
1.6.3.1 The use of mutants to study interactions between <i>N. meningitidis</i> and the vascular endothelium.....	73
1.7 Aim of PhD project.....	74
CHAPTER 2.....	75
2.1 Reagents.....	76
2.2 Methods	83
2.2.1 Endothelial Cell Culture	83
2.2.1.1 Choice of Endothelial Cell type	83
2.2.1.2 HUVEC Growth and Culture Media	84
2.2.1.3 Choice of FCS	86
2.2.1.4 Endothelial Cell preparation from umbilical cords	87
2.2.1.5 Verification of Endothelial Cell culture	90
2.2.1.6 Endothelial cell passaging.....	92
2.2.2 HMEC-1 Growth and Culture Media.....	92
2.3 Growth and preparation of <i>Neisseria meningitidis</i>	93
2.3.1 <i>N. meningitidis</i> strains used	93
2.3.1.1 <i>N. meningitidis</i> B H44/76.....	93
2.3.1.2 <i>N. meningitidis</i> B H44/76 lpxA- isogenic mutant	93
2.3.2 <i>N. meningitidis</i> culture and preparation	94
2.4 Preparation of LPS from <i>N. meningitidis</i>.....	95
2.5 Surface Immunostaining of HUVEC	96
2.6 Flow Cytometry and FACS analysis	98
2.7 mRNA extraction and cDNA synthesis reaction	98
2.8 PCR reaction conditions and RT-PCR cycling conditions.....	99
2.8.1 Real-Time PCR reaction conditions and cycling conditions.....	100
2.9 Agarose gel electrophoresis.....	101
2.10 Preparation of plasmid DNA	101
2.11 Transfection of Endothelial cells	102
2.11.1 Methodology of LID mediated transfection.....	102
2.11.2 Luciferase Assay	102
2.11.3 Protein Assay	103
2.11.4 Renilla Assay	103
2.12 Statistical analysis.....	104

CHAPTER 3.....	105
3.1 Introduction	106
3.1.1 Aims of Chapter 3.....	108
3.2 Materials and Methods.....	109
3.2.1 HUVEC culture and preparation for experiments.....	109
3.2.2 Preparation of <i>N. meningitidis</i> bacteria.....	109
3.2.3 Immunostaining	110
3.3 Results.....	111
3.3.1 <i>N. meningitidis</i> LPS is a potent activator of endothelial adhesion molecule expression on HUVEC.....	111
3.3.2 <i>N. meningitidis</i> and <i>E. coli</i> LPS are potent activators of endothelial E-selectin expression on HUVEC.....	113
3.3.3 Live <i>N. meningitidis</i> WT and <i>lpxA</i> - bacteria are able to induce high levels of adhesion molecules on HUVEC.....	114
3.3.4 E-selectin surface expression on HUVEC is increased in a dose dependant manner in response to PFA fixed WT <i>N. meningitidis</i> H44/76	117
3.3.5 High concentrations of PFA fixed <i>lpxA</i> - <i>N. meningitidis</i> mutant are able to induce adhesion molecule expression on HUVEC	119
3.3.6 Comparison of adhesion molecule expression in response to PFA fixed WT and <i>lpxA</i> - bacteria and purified LPS demonstrates differential E-selectin expression.....	122
3.3.7 PFA fixed WT <i>N. meningitidis</i> stimulation of HUVEC induces E-selectin, ICAM-1 and VCAM-1 expression in a time-dependant manner.....	124
3.3.8 Adhesion molecule upregulation on HUVEC in response to PFA fixed WT and <i>lpxA</i> - <i>N. meningitidis</i> bacteria and purified meningococcal LPS is time-dependent.....	127
3.4 Discussion	131
CHAPTER 4.....	142
4.1 Introduction	143
4.1.1 Real-time PCR	144
4.1.1.1 Using SYBR® green as a DNA binding dye for Real-Time PCR	147
4.1.2 Cyclophilin: a house-keeping gene for Real-Time RT-PCR.....	149
4.1.3 Quantification of Real-time PCR.....	150
4.1.4 Chapter Aims	151
4.2 Materials and Methods.....	153
4.2.1 Culture of HUVEC and HMEC	153
4.2.2 Detection of adhesion molecule mRNA in HUVEC.....	153
4.2.3 Primers used for RT-PCR and Real-Time RT-PCR.....	153
4.2.4 Primer annealing temperature optimisation	157
4.2.5 Development of standards for Real-Time RT-PCR	157
4.2.6 Data analysis, normalisation of data and statistical analysis.....	159
4.3 Results.....	161
4.3.1 Fixed WT and <i>lpxA</i> - <i>N. meningitidis</i> bacteria and purified meningococcal LPS induce E-selectin mRNA on HUVEC	161
4.3.2 Development and optimisation of Real-Time RT-PCR for endothelial adhesion molecule mRNA	163
4.3.3 Real-Time PCR of standards for Cyclophilin, E-selectin, and VCAM-1	164
4.3.4 Fixed <i>N. meningitidis</i> WT and <i>lpxA</i> - bacteria and purified LPS upregulated E-selectin and VCAM-1 mRNA as detected by Real-Time PCR.....	167
4.3.5 E-selectin mRNA transcription on HUVEC augmented in response to increasing concentrations of fixed WT and <i>lpxA</i> - <i>N. meningitidis</i> and purified LPS	170
4.3.6 E-selectin mRNA levels correlate with E-selectin surface protein expression in HUVEC induced by <i>N. meningitidis</i> WT and <i>lpxA</i> - bacteria.....	172

4.3.7 VCAM-1 mRNA transcription is induced in response to increasing concentrations of fixed WT, <i>lpxA</i> - <i>N. meningitidis</i> and purified LPS	174
4.3.8 VCAM-1 protein expression does not correlate with surface protein levels in WT and LPS induced HUVEC whilst <i>lpxA</i> - induced mRNA and protein expression do	176
4.4 Discussion	178
 CHAPTER 5.....	 186
5.1 Introduction	187
5.1.1 Transfection of Endothelial Cells	188
5.1.2 Improving TE.....	189
5.1.2.1 Use of supplements	189
5.1.2.2 The use of Histone Deacetylation Inhibitors to improve TE.....	190
5.1.2.3 Antibodies and peptides to target transfection	191
5.1.2.4 The use of different promoters and reporter genes to detect TE	192
5.1.2.5 Selection of transfected cells to study a promoter of interest.....	192
5.1.2.6 Differences in TE of cell lines and primary cells	193
5.1.2.7 The use of integrin mediated transfection on endothelial cells	194
5.1.3 Chapter Aims	197
5.2 Materials and Methods.....	198
5.2.1 Culture of HUVEC and HMEC-1	198
5.2.2 Transfection of Endothelial cells	198
5.2.3 Peptide optimisation of LID mediated transfection on HMEC-1 and HUVEC	200
5.2.4 Sodium Butyrate (SB) and Trichostatin A (TSA) Supplement of transfection cocktail	202
5.2.5 Normalisation of data and statistical analysis	202
5.3 Results.....	204
5.3.1 Peptide optimisation of the LID vector system on HMEC-1	204
5.3.2 Transfection of HMEC-1 supplemented with Histone Deacetylation Inhibitors	205
5.3.2.1 SB improves TE of LID mediated transfection of HMEC-1	206
5.3.2.2 TSA was unable to facilitate LID mediated transfection of HMEC-1	207
5.3.3 Peptide optimisation of the LID vector system on HUVEC	208
5.3.4 Transfection kinetics of the LID vector system using Peptide 6 on HUVEC	211
5.3.5 LID vector Transfection of HUVEC supplemented with Histone Deacetylation Inhibitors.....	212
5.3.5.1 SB improves LID mediated transfection of HUVEC	212
5.3.5.2 TSA facilitates LID mediated transfection of HUVEC.....	213
5.3.6 Transfection Kinetics of HUVEC supplemented with SB	214
5.4 Discussion	216
 CHAPTER 6.....	 222
6.1 Introduction	223
6.1.1 Chapter aims	223
6.2 Materials and Methods.....	224
6.2.1 HUVEC culture and preparation for transfection	224
6.2.2 Transfection of HUVEC	224
6.2.3 E-selectin promoter plasmids.....	225
6.2.4 A transfection control plasmid used to normalise E-selectin promoter controlled luciferase activity	227
6.2.5 Verification of E-selectin constructs	228
6.2.6 Luciferase data analysis	228
6.2.7 Preparation of <i>N. meningitidis</i> bacteria and stimulation of E-selectin promoter transfected HUVEC.....	229

6.3 Results.....	230
6.3.1 IL-1 β /PMA induced E-selectin promoter activity in transfected HUVEC	230
6.3.2 Fixed WT and <i>lpxA</i> - <i>N. meningitidis</i> stimulated higher levels of E-selectin promoter activity than purified LPS.....	232
6.3.3 A construct containing only the four regulatory regions of the E-selectin promoter (PDI-IV) (-166) is differentially activated in response to WT and <i>lpxA</i> - <i>N. meningitidis</i> and purified LPS	234
6.3.4 <i>N. meningitidis</i> WT and <i>lpxA</i> - bacteria and LPS do not control E-selectin promoter activity through the promoter region contained between -800 and -166	235
6.3.5 A mutation on the PDII region containing the ATF2/c-Jun site abolishes luciferase activity in response to WT and <i>lpxA</i> - <i>N. meningitidis</i> and purified LPS	238
6.3.6 Maximal E-selectin promoter activity is more reliant on an intact PDII region in response to fixed <i>lpxA</i> - mutant bacteria compared to stimulation with fixed WT bacteria and purified LPS	240
6.3.7 The removal of the PD II region restores the ability of the <i>lpxA</i> - mutant bacteria to induce E-selectin promoter controlled luciferase activity	242
6.3.8 Luciferase activity was not upregulated by WT and <i>lpxA</i> - bacteria and purified LPS when activity was regulated by an irrelevant promoter, such as the CMV promoter,	243
6.4 Discussion	245
CHAPTER 7.....	255
7.1 Endothelial cell adhesion molecule surface expression and mRNA induced by <i>N. meningitidis</i>	256
7.1.1 Does prolonged E-selectin expression affect downstream mechanisms of leukocyte rolling, binding and transmigration?	257
7.1.2 Is prolonged E-selectin expression important for downstream bacterial-cell interactions?	258
7.1.3 Could WT <i>N. meningitidis</i> cross-link with E-selectin and induce clustering, and thereby gene transcription?	259
7.2 Signalling events involved in cellular activation by <i>N. meningitidis</i>	259
7.3 Future work.....	264
7.3.1 The induction of the MAPK signalling pathway and HMG I(Y) by <i>N. meningitidis</i>	264
7.3.2 Neutrophil binding to and transmigration across endothelial layers stimulated with meningococci and purified LPS	265
7.3.3 How is prolonged E-selectin expression maintained and regulated?	266
7.4 Concluding Remarks	266
REFERENCES	268
PUBLICATIONS	325

Table of Figures

Figure 1.1 Reported Meningococcal Disease Distributed By Age (Years) In England And Wales; 1996-2000.....	22
Figure 1.2 Seasonal Variation In <i>N. Meningitidis</i> Serogroups B And C In England And Wales; 1997-2003.....	23
Figure 1.3 Serogroup Variation In Meningococcal Disease Cases In The Uk In 1995.	23
Figure 1.4 Pathophysiology Of Meningococcal Sepsis.	28
Figure 1.5 Electron Micrographs Of <i>N. Meningitidis</i>	30
Figure 1.6 Gram-Negative Bacterial Cell Wall.	32
Figure 1.7 <i>N. Meningitidis</i> Lps Structure, Immunotype 3.	39
Figure 1.8 Meningococcal Lipid A Biosynthesis Pathway.	41
Figure 1.9 The Nuclear Factor-Kappa-B (Nf- κ B) And Activation Transcription Factor-1 (Atf2)/C-Jun Pathway Stimulated By The Lps Signalling Complex.	45
Figure 1.10 The Kinetics Of Surface Expression Of E-Selectin, Icam-1 And Vcam-1 On Huvec In Response To Il-1	57
Figure 1.11 Leukocyte Rolling, Adhesion And Transmigration Through The Endothelium.	58
Figure 1.12 E-Selectin Protein Structure.	60
Figure 1.13 E-Selectin Promoter Organisation.	63
Figure 1.14 Bending Of The E-Selectin Promoter.	64
Figure 1.15 Icam-1 Structure.	67
Figure 1.16 Vcam-1 Protein Structure.	69
Figure 1.17 Characteristic Purpuric Skin Rash (A), And Skin Section From Purpuric (B) Lesion.	73
Figure 2.1 Flow Chart Illustrating Preparation Of Huvec From Umbilical Cords.....	89
Figure 2.2 Microscopic Verification Of Endothelial Cell Culture.....	90
Figure 2.3 Pecam-1 (Cd31) Expression On Huvec As Detected By Facs Analysis.....	91
Figure 2.4 Flow Chart Illustrating The Methodology For Surface Staining Of Adhesion Molecules On Huvec.	97
Figure 3.1 Adhesion Molecule Profiles On Huvec In Response To Increasing Concentrations Of H44/76 <i>N. Meningitidis</i> Lps.	112
Figure 3.2 E-Selectin Expression On Huvec In Response To <i>N. Meningitidis</i> And <i>E. Coli</i> Lps.	114
Figure 3.3 Adhesion Molecule Expression On Huvec In Response To Live Meningococci.	116
Figure 3.4 Adhesion Molecule Profile On Huvec In Response To Increasing Doses Of Fixed Wt H44/76 <i>N. Meningitidis</i>	118
Figure 3.5 Adhesion Molecule Profile On Huvec In Response To Increasing Doses Of Fixed Lpxa-H44/76 <i>N. Meningitidis</i>	120
Figure 3.6 Adhesion Molecule Expression On Huvec In Response To Increasing Concentrations Of Fixed Wt And Lpxa- H44/76 <i>N. Meningitidis</i> Bacteria And Bacterial Lps (10ng/ml)..	123
Figure 3.7 Time Course Of Adhesion Molecule Profile On Huvec In Response To Wt <i>N. Meningitidis</i>	126
Figure 3.8 Time Course Of Adhesion Molecule Expression By Huvec In Response To Wt <i>N. Meningitidis</i>	127
Figure 3.9 Time Dependant Adhesion Molecule Expression On Huvec In Response To Fixed Wt And Lpxa- H44/76 <i>N. Meningitidis</i> And Purified Lps.	129
Figure 3.10 Model For Endothelial Cell Injury Induction By Neutrophil-Endothelial Cell Interactions Leading To Dic.	140
Figure 4.1 Chemistries Used In Real-Time Pcr.	145
Figure 4.2 Dna-Binding Dyes.....	147
Figure 4.3: Diagram Of Genetic Sequence Organisation And Primer Design.....	154
Figure 4.4 Flow Chart Illustrating The Process Undertaken To Produce Plasmids For Standard Curves For Real-Time Pcr.	158
Figure 4.5 Pgem-T Easy Vector (Promega).....	158
Figure 4.6 Induction Of E-Selectin And Vcam-1 By <i>N. Meningitidis</i>	162
Figure 4.7 Real-Time Pcr Primer Optimisation.	164
Figure 4.8 Real-Time Rt-Pcr Optimisation Of Standard Curves For Cyclophilin, E-Selectin And Vcam-1.	166
Figure 4.9 Cyclophilin, E-Selectin And Vcam-1 Mrna Levels In Huvec Stimulated With <i>N. Meningitidis</i> Wt And Lpxa- Bacteria And Purified Lps.	168
Figure 4.10: E-Selectin Mrna Synthesis In Huvec In Response To Fixed <i>N. Meningitidis</i> Bacteria And Meningococcal Lps.	171

Figure 4.11 E-Selectin Mrna And Protein Expression Correlation.....	173
Figure 4.12 Vcam-1 Mrna Synthesis In Huvec In Response To Fixed <i>N. Meningitidis</i> Bacteria And Lps..	175
Figure 4.13 Vcam-1 Mrna And Protein Expression Correlation.	177
Figure 5.1 Lid Mediated Transfection And Trafficking Of Dna.....	195
Figure 5.2 Pci-Luciferase Vector.....	199
Figure 5.3 Time Of Addition Of Supplement To Transfection Reaction.	203
Figure 5.4 Peptide Optimisation Of Lid Vector Transfection On Hmec-1..	205
Figure 5.5 Transfection Of Hmec-1 With Lid Vector Supplemented With Increasing Concentration Of Sb.	206
Figure 5.6 Transfection Of Hmec-1 With Lid Vector Supplemented With Increasing Concentrations Of Tsa.....	208
Figure 5.7 Peptide Optimisation Of Lid Vector Transfection On Huvec..	209
Figure 5.8 Comparison Of Parent And Mutated Peptides Used In Lid Vector Transfections Of Huvec..	210
Figure 5.9: The Kinetics Of Lid Vector Transfection On Huvec.....	211
Figure 5.10 Sb Improves Lid Vector Te On Huvec.	213
Figure 5.11: Tsa Improved Lid Vector Te On Huvec.....	214
Figure 5.12: Sb Only Improves Luciferase Activity On Huvec When Added To The Lid Vector Transfection Cocktail.	215
Figure 6.1: Picagene Basic Vector.....	225
Figure 6.2 E-Selectin Promoter Constructs.....	226
Figure 6.3 Tk Vector. Gene Map Of The Tk Vector.	227
Figure 6.4: E-Selectin Controlled Luciferase Activity Is Detected In Response To Ip..	231
Figure 6.5 Ip Is Able To Induce A 70-Fold Increase In E-Selectin Regulated Luciferase Activity As Compared To Control.....	231
Figure 6.6 Wt And <i>Lpxa</i> - <i>N. Meningitidis</i> Bacteria Are Able To Induce A 9-Fold Increase In Activity Of The -800 E-Selectin Promoter Construct Compared To Control.	233
Figure 6.7 Differential Upregulation Of Luciferase Activity Controlled By The -166 E-Selectin Promoter Deletion Mutant..	235
Figure 6.8 The Region Contained Between The -800 And -166 Promoter Constructs Is Not Involved In The Differential Regulation Of E-Selectin Activation By <i>N. Meningitidis</i> Wt And <i>Lpxa</i> - Bacteria And Purified Lps.	237
Figure 6.9 A Mutation On The Pd Ii Region Of The E-Selectin Promoter Containing The Atf2/C-Jun Site Drastically Reduces Luciferase Activity Induced By Wt And <i>Lpxa</i> - <i>N. Meningitidis</i> And Purified Lps.....	239
Figure 6.10 Induction Of The -166m Demonstrates That The <i>Lpxa</i> - Mutant Relies On The Pdii Site To Induce E-Selectin Promoter Controlled Luciferase Activity.....	241
Figure 6.11 The -129 Mutant, Which Does Not Contain The Pdii Region, Is Differentially Regulated By Wt <i>N. Meningitidis</i> , <i>Lpxa</i> - Mutant, And Purified Lps.....	243
Figure 6.12 The Upregulation Of Luciferase Activity In Response To Wt And <i>Lpxa</i> - <i>N. Meningitidis</i> And Purified Lps Was Specific To The E-Selectin Promoter.....	244
Figure 6.13 E-Selectin Promoter Folding, And The Effect Of A Mutant Or Absent Pdii.	251
Figure 7.1 Model For Differential Signalling By <i>N. Meningitidis</i> And Lps.	263

Table of Tables

Table 2.1 General Reagents	76
Table 2.2 Molecular Biology Reagents, Enzymes And Kits.....	79
Table 2.3 Antibodies.....	81
Table 2.4 General Buffers/Solutions.....	82
Table 2.5 Flow Cytometry Settings For Endothelial Cell Detection.	98
Table 2.6 Cycling Conditions For RT-PCR Reaction.....	99
Table 2.7 Cycling Parameter Conditions For Real-Time RT-PCR Reaction.....	100
Table 4.1 Primers Used For RT PCR.....	155
Table 4.2 Primers Used For Real-Time RT PCR.....	156
Table 4.3 Cycling Conditions For Primer Optimisation PCR Reaction.....	157
Table 5.1 Lipid, Peptide And Dna Concentrations Used For The Transfection Of HUVEC And HMEC-1.	199
Table 5.2 Lid Vector Targeting Peptides	201
Table 6.1 Primers Used For The Sequencing Of E-Selectin Promoter Constructs Inserted Into Picagene Vector.....	228

Table of Equations

Equation 4.1: Mathematical Equation Demonstrating How The Gene Induction Of Gene Of Interest Was
Calculated. *X*=Gene Of Interest (*I.E.* E-Selectin); *Y*=House-Keeping Gene Control (Cyclophilin).
.....160

Abbreviations

ATF-2	Activation Transcription Factor-2
bp	Base pair
BPAEC	Bovine Pulmonary Aortic Endothelial Cells
BSA	Bovine Serum Albumin
cDNA	Complementary DNA
CFU	Colony Forming Units
CHO	Chinese Hamster Ovary
CM	Cytoplasmic Membrane
CMV	Cytomegalovirus
DC	Dendritic cell
DIC	Diffuse Intravascular Coagulation
DMSO	Dimethylsulphoxide
DNA	Deoxyribonucleic acid
dNTPs	Deoxyribonucleotides
ds DNA	Double Stranded DNA
EDTA	Ethylenediaminetetraacetic Acid Disodium Salt
ERK	Extracellular Signal-Regulated Protein Kinases
FACS	Fluorescence Activated Cell Sorter
FCS	Foetal Calf Serum
FMS	Fulminant Meningococcal Sepsis
GAPDH	Glyceraldehydes-3-Phosphate Dehydrogenase
HAEC	Human Aortic Endothelial Cells

HBMEC	Human Brain Microvascular Endothelial Cell (immortalised)
HeLa cells	Henrietta Lack cells
HIMEC	Human Intestinal Microvascular Endothelial Cells
HMEC-1	Human Microvascular Endothelial Cell-1
HMG-I(Y)	High-Mobility-Group protein I(Y)
HMMEC	Human Mucosal Microvascular Endothelial Cells
HUVEC	Human Umbilical Vein Endothelial Cells
ICAM-1	Intracellular Adhesion Molecule-1
IFN- γ	Interferon gamma
Ig	Immunoglobulin
IKK	I κ B kinase
IL	Interleukin
IMS	Industrial Methylated Spirit
IP	IL-1 β /PMA stimulation
IRAK	Interleukin-1 Receptor Associated Kinase
JAM	Junctional Adhesion Molecule
JNK	c-Jun NH ₂ -terminal Kinases
kDA	Kilo Dalton
LAL	Limulus Amebocyte Lysate
LBP	LPS Binding Protein
LID	Lipofectin:Integrin:DNA
LPS	Lipopolysaccharide
LQ	Log of Quantity
MAPK	Mitogen-Activated Protein Kinases
mCD14	Membrane CD14

MFI	Mean Fluorescence Intensity
MKK	MAP Kinase Kinase
MKKK	MAP Kinase Kinase Kinases
mRNA	Messenger Ribonucleic Acid
MyD88	Myeloid Differentiation Factor 88
NF κ B	Nuclear Factor-kappa-B
OM	Outer Membrane
OMP	Outer Membrane Protein
PBMC	Peripheral Blood Mononuclear Cells
PBS	Phosphate-Buffered Saline
PCR	Polymerase Chain Reaction
PD	Positive Domain
PE	Phycoerythrin
PECAM-1	Platelet Endothelial Cell Adhesion Molecule-1
PFA	Paraformaldehyde
PG	Peptidoglycan
PMA	Phorbol 12-myristate 13-acetate
PMN	Polymorphonuclear Leucocytes
PMNL	Polymorphonuclear Neutrophils
PNC	Platelet-Neutrophil Complexes
PRR	Pattern Recognition Receptor
RLU	Relative Luciferase Units
RNA	Ribonucleic acid
RRU	Relative Renilla Units
RT-PCR	Reverse-Transcriptase Polymerase Chain Reaction

SB	Sodium Butyrate
sCD14	Soluble CD14
TAK-1	Transforming Growth Factor- β - Activated Kinase-1
TBE	Tris-Borate-EDTA
TC	Tissue Culture
TGF- β	Transforming Growth Factor beta
TIR	Toll/IL-1 Receptor
TIRAP	TIR Domain-Containing Adapter Protein
TLR	Toll-Like Receptor
TNF- α	Tumour Necrosis Factor-alpha
TRAF-6	TNF Receptor Associated Factor 6
TRAM	TRIF-Related Adaptor Molecule
TSA	Trichostatin A
VCAM-1	Vascular cell adhesion molecule 1
WT	Wild Type

Chapter 1

Introduction

1.1 Introduction

Neisseria meningitidis is a gram negative diplococcus, which is an exclusive human pathogen and is one of the worlds leading causes of meningitis. Despite improvements in treatment and intensive care therapy, overall mortality occurs in 5-10% of disease cases, of which the majority is due to meningococcal sepsis. Meningococcal sepsis is characterised by extensive vascular damage with capillary leakage and intravascular thrombosis leading to shock.

The mechanisms by which the bacterium induces such severe disease are still unclear. High levels of bacteraemia and lipopolysaccharide (LPS) are associated with increased vascular damage. However, exactly how this occurs is still not fully understood. Understanding the molecular mechanisms involved in meningococcal mediated vascular injury will assist in the development of future targeted therapies for shock induced by both meningococci and other agents. These therapies could target specific signalling pathways involved in gene induction, cell surface molecules involved in bacterial entry, or proteins involved in protein trafficking which may be utilised by the bacteria during infection.

1.2 *Neisseria meningitidis*

1.2.1 Historical perspectives

The first account of a meningitis outbreak was made in the 1600 by an English physician named Thomas Willis. However, the first detailed description of an epidemic outbreak was first made in 1805 by a Swiss doctor called Vieusseux. This led to the understanding that the disease occurred in clusters and spread in crowded environments, and could occur as large outbreaks (Cartwright K, 1995). For instance, during the 19th century an epidemic outbreak was associated with the movement of an army regiment through France. Meningococci were first isolated from meningeal exudates from six out of eight cases in 1887 by Anton Weichselbaum (Cartwright K, 1995).

1.2.2 Epidemiology

N. meningitidis is found worldwide. Approximately 10% of the population carry the bacterium as a harmless commensal, a high proportion of which is 15-24 year-olds (Yazdankhah and Caugant, 2004). Carriage increases during epidemic outbreaks or in situations of crowded conditions, such as military barracks, student residences and during the annual pilgrimage to Mecca. Carriage has been reported to be as high as 70% in military recruits (Caugant *et al.*, 1992), and to be as long as 14 months among school children (De Wals and Bouckaert, 1985).

Recent outbreaks of meningococcal disease have affected countries in Europe, Africa and the USA. In 2000, an outbreak in France, the UK and Oman was associated with

pilgrims returning from the Haj. These outbreaks were caused by both *N. meningitidis* serogroup A and W135. In 2003, an epidemic affecting nearly 10,000 people in Burkina Faso and Niger was caused by *N. meningitidis* serogroup A and W135, and widespread vaccination was used in an attempt to prevent further spread of the disease. Smaller outbreaks have occurred in 2004 and 2005 in the meningitis belt, mainly caused by *N. meningitidis* A and W135. Recent outbreaks of *N. meningitidis* serogroup Y have occurred in the USA (www.who.int).

Carriage of *N. meningitidis* elicits the production of protective antibodies. Although infants are initially protected by maternal antibodies they become vulnerable during the development of acquired immunity and consequently are at high risk of *N. meningitidis* infection. Other commensal non-pathogenic bacteria, such as *N. lactamica*, can elicit the production of antibodies which cross-react with *N. meningitidis*, which may give some measure of protection.

Occasionally, the bacterium is able to cause disease, affecting mainly children under 5 years, followed by a secondary peak during teen-age years (Baines and Hart, 2003), (Figure 1.1). Generally, meningococcal disease affects 1-3/100,000 of the European and North American population, and rates as high as 1/100 have been reported in the sub-Saharan African belt (Yazdankhah and Caugant, 2004). What leads to the development of disease is as yet unknown, however, bacterial isolates from disease cases are normally capsulated, whereas 50% of isolates from carriers are unencapsulated bacteria (Yazdankhah and Caugant, 2004). Of those that do develop meningitis or severe sepsis, the overall mortality rate is 10-20%, of which 40% are due to meningococcal sepsis (Tzeng and Stephens, 2000). In 10-20% of survivors there is

significant morbidity, including deafness, permanent renal failure and amputations (Tzeng and Stephens, 2000).

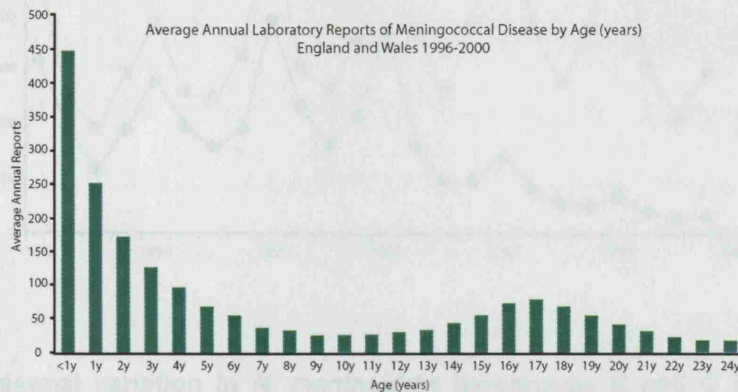


Figure 1.2 Reported meningococcal disease distributed by age (years) in England and Wales; 1996-2000. The figure illustrates the laboratory confirmed cases of meningococcal disease in England and Wales, 1996-2000. The figure was obtained from the Public Health Laboratory Services website.

Figure 1.1 Reported meningococcal disease distributed by age (years) in England and Wales; 1996-2000. Average annual laboratory reports of meningococcal disease by age (years) in England and Wales, 1996-2000. The figure was obtained from the Public Health Laboratory Services website.

There is also seasonal variation in disease incidence (Figure 1.2). Higher levels occur during the winter months (Baines and Hart, 2003). In sub-Saharan Africa, there is a 'meningitis belt' where there are recurrent outbreaks of Group A meningitis every 5-10 years. These outbreaks are mainly associated with the dry season. It has been postulated that dryness of the nasal mucosa may lead to bacterial invasion, thereby allowing the bacteria to enter the bloodstream. Since immunisation with the meningitis C conjugate vaccine, the incidence of meningitis caused by meningococci C bacteria has reduced. *N. meningitidis* B is now the leading cause of meningococcal disease in the UK (Figure 1.3).

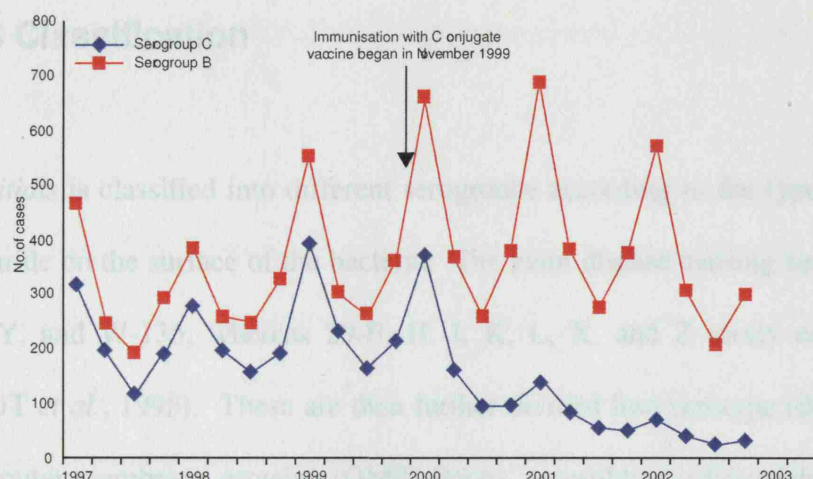


Figure 1.2 Seasonal variation in *N. meningitidis* Serogroups B and C in England and Wales; 1997-2003. The figure illustrates the laboratory confirmed cases of meningococcal disease in England and Wales. Figure obtained from the Public Health Laboratory Services website.

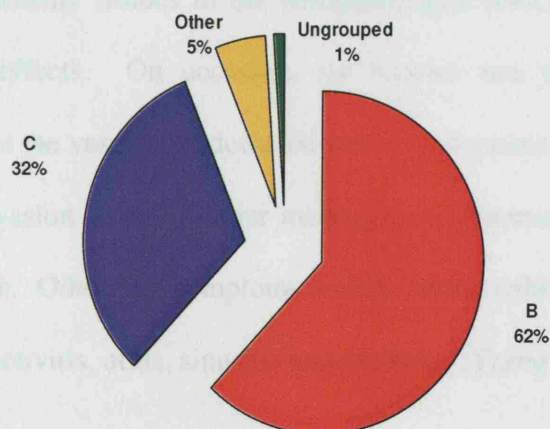


Figure 1.3 Serogroup variation in meningococcal disease cases in the UK in 1995. The figure illustrates the laboratory confirmed cases from 1995 of meningococcal disease by serogroup. Figure was obtained from the Public Health Laboratory Services website.

1.2.3 Classification

N. meningitidis is classified into different serogroups according to the type of capsular polysaccharide on the surface of the bacteria. The main disease causing serogroups are A, B, C, Y, and W-135, whereas 29-E, H, I, K, L, X, and Z rarely cause disease (Poolman JT *et al.*, 1995). These are then further divided into serotype (differences in the major outer membrane proteins (OMP) PorA), serosubtype (differences in PorB), and finally immunotype (differences on LPS structure) (Tzeng and Stephens, 2000). These will be discussed in further detail.

1.2.4 Pathophysiology

N. meningitidis normally resides in the nasopharyngeal tract as part of the host flora with no adverse effects. On occasion, for reasons not yet fully understood, *N. meningitidis* crosses the vascular endothelial barrier and passes into the vascular system. *N. meningitidis* invasion leads to either meningitis (inflammation of the meninges) or sepsis alone or both. Other rare symptoms include septic arthritis, pneumonia, purulent pericarditis, conjunctivitis, otitis, sinusitis and urethritis (Tzeng and Stephens, 2000).

There are three main stages in the development of meningococcal disease: colonisation and penetration, bacteraemia, and localised inflammation (Brandtzaeg P, 1995). The bacterium first colonises the nasopharynx, where-after the bacterium adheres to and induces endocytosis by epithelial cells. Bacteria cross into the circulatory system where bacteraemia occurs, and meningococcal disease develops by 24-48 hours (Brandtzaeg P,

1995), either as meningitis, septicaemia, or both (up to 60% of cases in Europe) (Brandtzaeg P, 1995).

The most important host defence agent for this organism in the blood is the complement system. Deficiency of components of the classical and alternative pathways lead to increased infection rates (50 fold higher). Another component of the innate immune system which may be important against MD is Manos Binding Lectin (MBL). This is a collagenous protein consisting of four exons expressing peptide chains. Three peptide chains join together, and these subunits then make dimmers, trimers, tetramers or hexamers. Different point mutations in the gene cause MBL deficiency affecting the oligomerisation of the protein, whereas mutations of the MBL promoter affect the levels of protein produced (reviewed in Jack, et al., 2001). It has been reported that MBL deficiency may pre-dispose families to meningococcal disease (Bax, et al., 1999). In addition, a family with an MBL deficiency as well as a deficiency in properdin (which is involved in stabilising proteins of the complement pathway) had a high incidence of meningococcal disease (Bathum, et al., 2006).

Although it is unclear what leads to invasion of the epithelial cells in the nasopharynx, phase variation of surface antigens has been suggested as a mechanism (de Vries *et al.*, 1996). For instance, sequences that are prone to phase variation have been identified (Saunders *et al.*, 2000), and these are believed to allow the bacteria to create a variety of different phenotypes expressing different combinations of OMPs. Although LPS immunotypes undergo phase variation by going through high-frequency mutations in LPS synthesis genes (de Vries *et al.*, 1996; Berrington *et al.*, 2002), it has been shown

that variations in LPS isotype do not affect bacterial virulence (Berrington *et al.*, 2002). It remains to be seen if other OMP variations affect bacterial virulence.

1.2.4.1 Bacterial sepsis and septic shock

After colonisation of the nasopharynx, bacteria cross the epithelium by endocytosis (van Deuren *et al.*, 2000). At this stage, the bacteria are capsulated, which protects them from complement-mediated killing (Vogel and Frosch, 1999) and phagocytosis by neutrophils (Klein *et al.*, 1996). This allows the bacteria to multiply, which leads to bacteraemia and fulminant meningococcal sepsis (FMS) may develop. This is characterised by widespread activation of the innate immune response, leading to the production of pro-inflammatory mediators, such as tumour necrosis factor alpha (TNF- α), interleukin-1 β (IL-1 β) and IL-12, and anti-inflammatory mediators such as IL-10, IL-1 receptor antagonist (IL-1RA) and IL-4 (Hackett *et al.*, 2001). The complement cascade is induced by the interaction with blebs produced by the bacteria (Vogel and Frosch, 1999). Whilst the high levels of inflammatory mediators as well as high levels of complement activation are all associated with outcome of meningococcal disease (van Deuren *et al.*, 2000; Westendorp *et al.*, 1995), bacterial levels in the bloodstream are a better predictor of disease severity and outcome, as high levels of bacteraemia are associated with shock (Brandtzaeg *et al.*, 1989; Ovstebo *et al.*, 2004; Hackett *et al.*, 2002) and are responsible for the high levels of inflammatory mediators detected.

1.2.4.2 Diffuse intravascular coagulation (DIC) during meningococcal disease

The clinical presentation of FMS is septic shock and DIC. This is characterised by inadequate organ perfusion which is partly caused by vascular leakage, respiratory distress, vasodilation and inadequate cardiac output. The visual presentation of DIC is skin hemorrhages, where endothelial damage and thrombosis has occurred in small vessels. The pathophysiology leading to DIC is represented on Figure 1.4.

It is necessary to have tight regulation of the coagulation cascade to maintain homeostasis. The coagulation cascade leads to the formation of fibrin, which forms a fibrin clot via the activity of thrombin. There are different activator molecules of thrombin, including the Tissue Factor (TF) VIIa complex on endothelial cells (extrinsic pathway) and via factor XII (intrinsic pathway). At the same time, thrombin can bind thrombomodulin (TM), which, as suggested by its name, modulates the production and action of thrombin by activating Protein C (PC). This in turn 'switches on' the anti-coagulation cascade (Amaral *et al.*, 2004; Faust *et al.*, 2001a; Kurachi *et al.*, 2000).

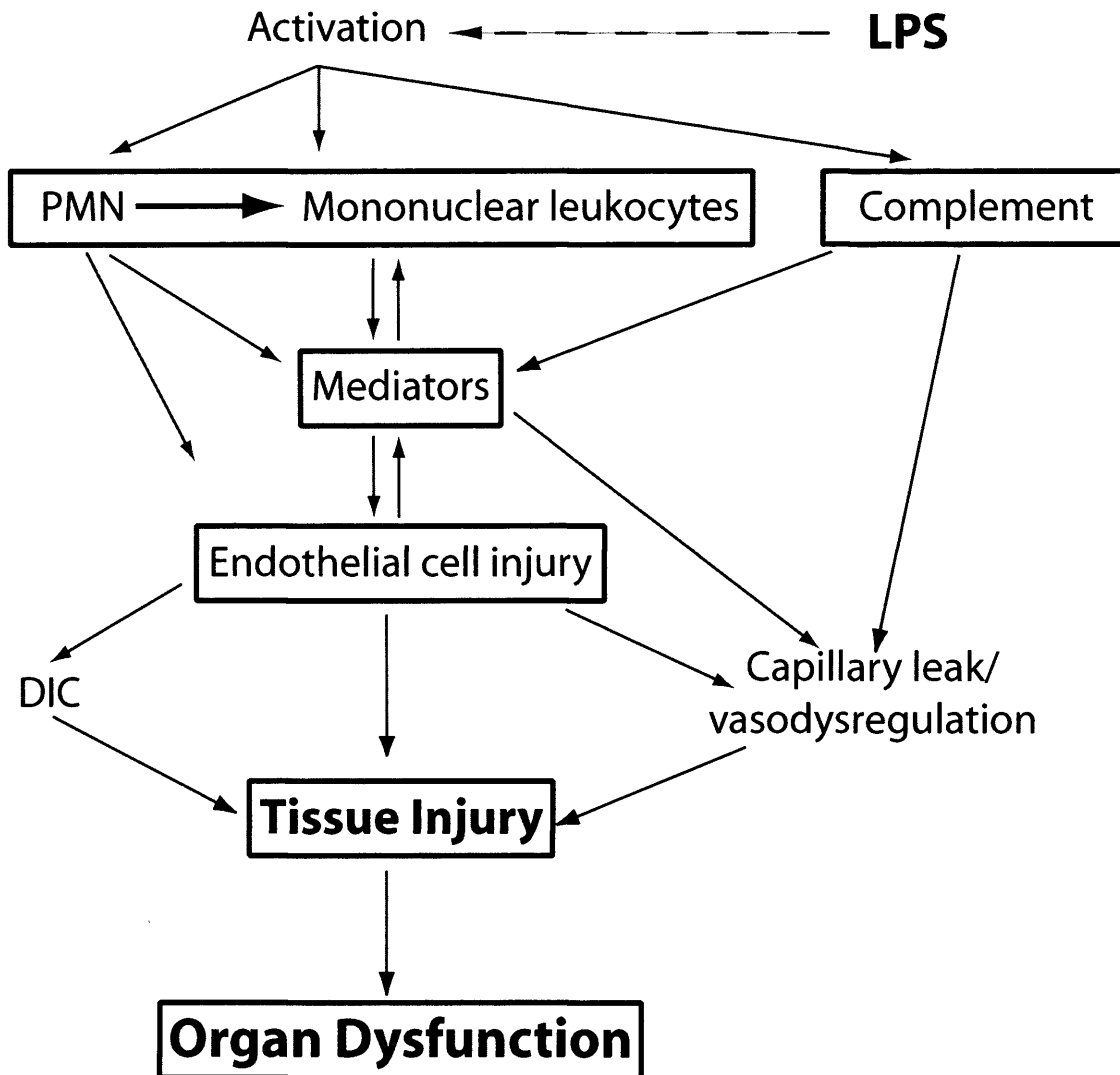


Figure 1.4 Pathophysiology of meningococcal sepsis. The illustration demonstrates the mechanisms which lead to DIC and organ dysfunction. PMN: Polymorphonuclear leucocytes. The figure has been adapted from (de Kleijn et al., 1998).

During meningococcal sepsis, there is reduced TM and Endothelial Protein C Receptor (EPCR) expression on the endothelial cell surface, as well as increased plasma TM levels, and reduced PC, Protein S (a PC co-factor), and anti-TM antigen, as compared to control patients (Faust *et al.*, 2001b). Whilst these factors are depleted, this indicates that: 1) there is either reduced expression and/or production of these factors or 2) they are being consumed during FMS. There is wide support for the later explanation, as

activated endothelial cells express TF in response to *N. meningitidis* (Heyderman *et al.*, 1997), which in turn also activates the coagulation cascade thereby consuming the clotting factors. There are also elevated levels of tissue-type plasminogen activator (t-PA) (which is involved in the degradation of fibrin and fibrin clots), and its inhibitor (Frist *et al.*, 1995) (Amaral *et al.*, 2004), particularly in non-survivors. Hence, although the fibrin degradation pathway is active, there are insufficient factors to counteract the high levels of fibrin being produced. Fibrin clot accumulation and dysfunctional fibrinolysis are instrumental in the multiple organ failure and mortality observed in sepsis (Watanabe *et al.*, 2001).

1.2.4.3 The contribution of shock to the outcome of FMS

Shock is a condition where there is inadequate perfusion of vital organs. When meningococcal disease is associated with shock the mortality rate increases to 10% or more. 50% of reported cases occur in the first 24 hours after the presentation of symptoms. Upto 20% of survivors may require amputation or reconstructive skin surgery.

The mortality rate of patients presenting with meningitis alone is only 1-5%, however, 8-20% of survivors may suffer from brain defects including deafness, mental retardation, epilepsy and seizures, amongst other after-effects.

1.3 Bacterial Cell Surface Structure and the role in pathogenesis

N. meningitidis is a small Gram-negative, encapsulated diplococcus, found exclusively in humans as a commensal organism in the nasopharynx, or as a pathogen causing meningitis and sepsis (Figure 1.5).

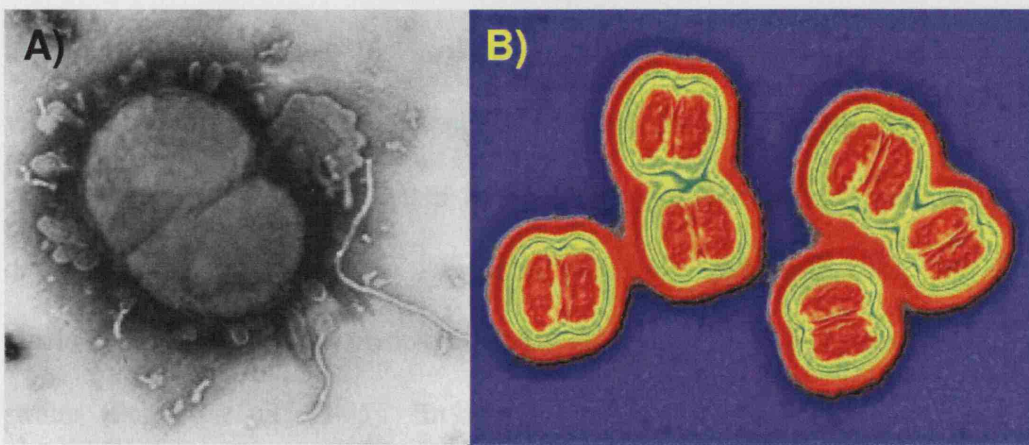


Figure 1.5 Electron micrographs of *N. meningitidis*. A) An electron micrograph of *N. meningitidis*. Image obtained from the King's College London, Randall Division of Cell. B) False colour electron micrograph of *N. meningitidis*. Image obtained from the Molecular Biophysics web site and University of Glasgow, Institute of Biomedical & Life Sciences Website.

The genetic sequences of *N. meningitidis* serogroup A (strain Z2461), serogroup B (MC58) and serogroup C (FAM18) have been elucidated (Parkhill, *et al.*, 2000; Tettelin, *et al.*, 2000; and The Wellcome Trust Sanger Institute, unpublished data). These have resulted in a wide range of information which is beyond the scope of this thesis. The use of this information for the understanding of meningococcal disease is in

its infancy. A few examples of how knowing the genetic sequence of the organism can be helpful are below.

The genome project has assisted in the identification of genome regions of both *N. meningitidis* and *N. gonorrhoeae* that are only found in these two *Neisseria* species and not in the comensal *N. lactamica* (Perrin, et al., 1999), as well as identifying regions that are specific to *N. meningitidis* and not found in *N. gonorrhoeae* (Klee et al., 2000; Perrin, et al., 2002). Some of these regions contain sequences for known factors that are involved in pathogenesis, for instance PilC, and other regions are homologous to virulence regions from other pathogenic bacteria such as *Shigella flexnerii*, *Bacillus cereus* and *Vibrio cholerae* (Perrin, et al., 1999). The use of the genetic sequences to develop microarrays has also supported previously published data, and has also elucidated genetic characteristics that may be specific for uncharacterized *Neisseria* strains (Stabler, et al., 2005). In addition, the genetic sequence of *N. meningitidis* MC58 has been used to identify the transcriptome of this bacteria during in vitro infections of both epithelial and endothelial cells (Dietrich, et al., 2002).

The meningococcal cell surface structure consists of an envelope made up of a cytoplasmic membrane (CM) which is separated from the outer membrane (OM) by peptidoglycan (PG) (Figure 1.6). The CM is mainly made up of phospholipids, whereas the OM is an asymmetrical structure made up of a variety of proteins, which are involved in bacterial colonisation, adherence, and pathogenesis. The OM is surrounded by a polysaccharide capsule. The use of mutant bacteria has been of great use in elucidating the role of the outer membrane molecules in disease progression *in vitro*. These proteins and their roles are discussed further below.

1.3.1 Capsule

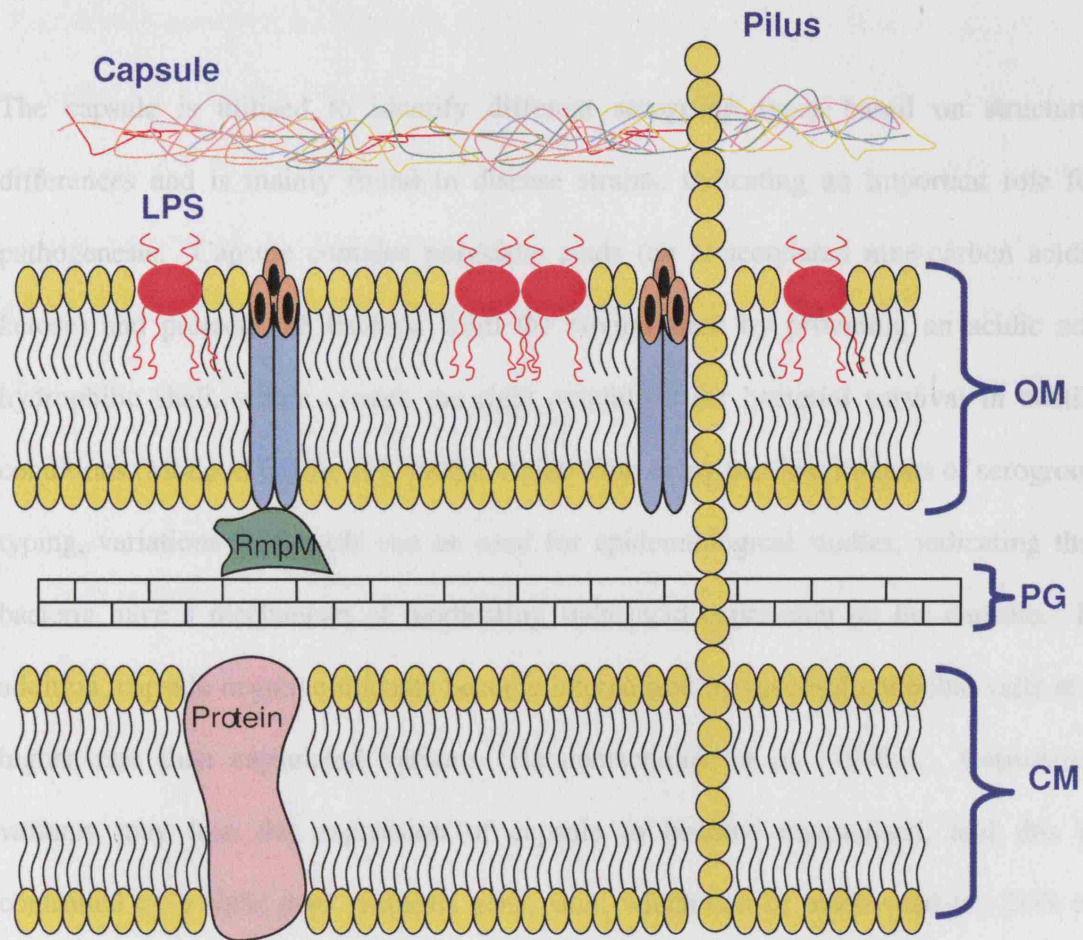


Figure 1.6 Gram-negative bacterial cell wall. The cytoplasm is surrounded by the cytoplasmic membrane (CM), separated from the outer membrane (OM) by a layer of peptidoglycan (PG) in the periplasmic space. The OM is an asymmetrical membrane containing a series of outer membrane proteins (OMPs) including porins, Opa, Opc, and lipopolysaccharide (LPS). Pili are anchored in the CM, crossing through the PG, the OM and the capsule. Adapted from Steeghs *et al.* (2001) and McLeod Griffis (1995).

1.3.1 Capsule

The capsule is utilised to identify different serogroup types based on structural differences and is mainly found in disease strains, indicating an important role for pathogenesis. Capsule contains polysialic acids (an N-acetylated nine-carbon acidic ketose) and protects the bacteria from the environment by providing an acidic and hydrophilic shell, which creates the right conditions for bacterial survival in hostile conditions (McLeod Griffis JM, 1995). Aside from being the determinants of serogroup typing, variations in capsule can be used for epidemiological studies, indicating that bacteria have a mechanism of modulating sialic acid expression on the capsule. In addition, capsule negative mutants become internalised by mucosal epithelial cells at a higher rate than capsulated variants (Hammerschmidt *et al.*, 1996a). Capsulated variants may lose the expression of capsule to become internalised, and this is controlled by a sialic acid synthesis gene, *siaA*, which can be inactivated in ~20% of organisms by the insertion of a movable element referred to as *IS1301* (Hammerschmidt *et al.*, 1996a). This leads to the blocking of capsule synthesis, and hence the generation of unencapsulated bacteria. Another mechanism of regulating capsule switching is by insertion or deletion of a C residue within an oligo-(dC) region within the *siaD* gene (encoding for polysialyltransferase), causing a frame-shift in the gene reading frame, which results in the bacteria losing capsule formation (Hammerschmidt *et al.*, 1996b). Meningococcal strains can also switch capsule serogroup as a result of allelic exchange of the *siaD* gene (Swartley *et al.*, 1997). The mechanism by which this is controlled is probably through transformation and horizontal DNA exchange between bacteria (Swartley *et al.*, 1997).

The capsule protects bacteria from complement mediated killing (Ram *et al.*, 1999; Jack *et al.*, 1998), however, encapsulated bacteria with decreased levels of sialic acid on LPS or mutants lacking sialic acid are not protected from MBL binding (Jack *et al.*, 1998; Jack, *et al.*, 2001). In contrast, the presence or absence of PorA on the meningococcal surface does not affect complement activation by meningococci (Drogari-Apiranthitou *et al.*, 2002). Nevertheless, capsulated organisms are less potent activators of neutrophils and therefore may lead to less endothelial cell injury than unsialylated or unencapsulated organisms (Klein *et al.*, 1996).

1.3.2 Pili

Pili are filamentous extensions found on the outer membrane, and are made up of major pilus subunits called pilins (PilE), minor pilus-associated protein (PilC) and other as yet unknown protein subunits (Meyer *et al.*, 1990). There are two types of pili referred to as class I and class II. *N. meningitidis* Class I pili are structurally and antigenically analogous to *Neisseria gonorrhoeae* pili. Class I and Class II pili from *N. meningitidis* are antigenically and structurally different (Poolman JT *et al.*, 1995); (Perry *et al.*, 1987), which may provide an advantage during host colonisation when invading different tissues (Heckels, 1989).

Pili are involved in initial colonisation of endothelial cells. Pil⁻ mutant strains only adhere to human umbilical vein endothelial cells (HUVEC) at high concentrations and long exposure times compared to pil⁺ isogenic strains (Virji *et al.*, 1991; Virji *et al.*, 1992a; Virji *et al.*, 1993b). Pili mediated adhesion is independent of capsule (Virji *et al.*, 1995). Meningococci expressing class I and class II pili adhere well to HUVEC,

however, alterations in pili structure affect bacterial adhesion to epithelial cells (Virji *et al.*, 1992a; Virji *et al.*, 1993b; Virji, 1996). Differences in adherence capacity to epithelial and endothelial cells within bacterial strains is due to structural variations of pili, modulated by pili primary amino acid sequences, which remove or created *N*-linked glycosylation sites on pilin subunits (Virji *et al.*, 1993b). A single amino acid change of the pilin subunit (Asn-60→Asp) is sufficient to abolish the bacterial adherence capability (Virji *et al.*, 1993b). The structural variation of pili increases bacteria-bacteria interactions, which could in turn reinforce interactions with the eukaryotic cell surface (Marceau *et al.*, 1995; Marceau and Nassif, 1999; Nassif *et al.*, 1999). Pili bind to human CD46 (Kallstrom *et al.*, 1997; Nassif *et al.*, 1994; Nassif *et al.*, 1999; Koomey, 2001) a ubiquitous cell surface molecule, which facilitates pili-mediated intranasal infection of human CD46 expressing mice (Johansson *et al.*, 2003).

1.3.3 OMPs

OMPs have been divided into 5 different classes, based on their molecular weight (Tsai *et al.*, 1981). Class 1 OMPs are PorA proteins, class 2 and 3 are PorB2 and PorB3 respectively, class 4 OMPs is reduction-modifiable protein M (RmpM), and finally class 5 proteins are Opa and Opc proteins. These are described in detail below.

1.3.3.1 Porins

Porins (Tomassen *et al.*, 1990) make up the highest proportion of OMPs on the bacterial cell surface. Porins are made up of three single polypeptides containing high levels of β -pleated sheets interspersed by variable regions creating surface exposed

loops (Derrick *et al.*, 1999;Massari *et al.*, 2003b). The tips of the surface loops are antigenic (Saukkonen *et al.*, 1989), as antibodies raised to these regions are highly bactericidal, particularly antibodies targeting PorA, as PorB is less stable and less exposed on the bacterial cell wall compared to PorA (Minetti *et al.*, 1998). The transmembrane protein conformation of porins is involved in the selective transport of ions, PorA transporting cations and PorB transporting anions (Poolman JT *et al.*, 1995). They also secrete bacterial products. Differences in *N. meningitidis* serotypes are determined by differences in porin structures. There is 60-70% amino acid sequence homology between porin structures from *N. gonorrhoeae* and *N. meningitidis*.

PorB from *N. gonorrhoeae* increase bacterial invasion of epithelial cells. Although this has not been demonstrated for *N. meningitidis* PorB, they do influence actin reorganisation and may insert themselves into the epithelial cell wall in sites of close bacterial-host interactions, thereby influencing pathogenicity. The mechanisms for this have as yet not been elucidated (Massari *et al.*, 2003b).

The role of *Neisseria* porins in apoptosis is contradictory. *N. meningitidis* PorB activate anti-apoptotic genes by interacting with the mitochondrial voltage-dependent anionic channel (Muller *et al.*, 2002a;Massari *et al.*, 2003a). Although PorB from *N. gonorrhoeae* also interact with mitochondria, they induce calcium efflux leading to apoptosis (Muller *et al.*, 2002a).

PorB can stimulate mouse B-cells via Toll-like Receptor 2 (TLR2) and Myeloid Differentiation Factor 88 (MyD88) (Massari *et al.*, 2002), upregulating CD86 (B7-2, a co-stimulatory ligand) on the B-cell surface leading to B-cell proliferation (Wetzler *et*

al., 1996;Snapper *et al.*, 1997). So far, there have been no reports demonstrating that PorB upregulates TLR2 expression.

The use of porins as vaccine adjuvants has also been investigated. The IgG response to a conjugate vaccine incorporating capsular polysaccharide and PorB is significantly reduced upon blockage of CD86 (Mackinnon *et al.*, 1999).

1.3.3.2 RmpM

The class 4 protein RmpM is homologous to *E. coli* RmpA (Klugman *et al.*, 1989), and is associated with porins. It is involved in the anchoring of the outer membrane to the peptidoglycan layer. RmpM has been demonstrated to bind to lactoferrin receptor (LbpA), transferring receptor (TbpA) and siderophore receptor (FrpB), which are all involved in iron-acquisition (Prinz and Tommassen, 2000). Mutations in RmpM cause reduced iron acquisition.

1.3.3.3 Opa and Opc proteins

Opa proteins (referring to opacity proteins) are a family of outer membrane proteins encoded by individual *opa* genes (3-4 in the meningococcal genome), and are expressed on most *N. meningitidis* subgroups (Nassif *et al.*, 1999). The proteins undergo phase variation due to reversible sequence variation found in the 5' coding region of the genes (Stern *et al.*, 1986;Robertson and Meyer, 1992;Nassif *et al.*, 1999;Dehio *et al.*, 1998).

Opc are also a family of proteins found on the outer membrane of the bacteria. Although they are similar in size and physiochemical properties to Opa proteins, they are structurally different (Nassif *et al.*, 1999).

Both Opa and Opc mediate bacterial-host cell (epithelial and endothelial cell) interactions in unencapsulated and non-sialylated bacteria (Virji *et al.*, 1992b; Virji *et al.*, 1993a; Nassif *et al.*, 1999). Attachment and invasion of endothelial cells is facilitated by high expression levels of Opc proteins on the surface of *N. meningitidis*. Opc binds vitronectin, interacting particularly with $\alpha_v\beta_3$ integrins (Virji *et al.*, 1992b; Sarkari *et al.*, 1994; Virji *et al.*, 1994; Virji *et al.*, 1996b; Virji *et al.*, 1995; Nassif *et al.*, 1999).

Opa bind members of the CD66 family, which leads to stronger adhesion and invasion of epithelial cells (Virji *et al.*, 1996a; Virji *et al.*, 1996c) and endothelial cells, where CD66a is upregulated by TNF α (Muenzner *et al.*, 2000). This leads to enhanced endothelial invasion by bacteria directed by Opa-mediated bacterial binding (Muenzner *et al.*, 2000).

1.3.4 LPS structure and biosynthesis

LPS is only found on the OM anchored by the hydrophobic lipid A component (Figure 1.7) which is attached to the surface exposed hydrophilic oligosaccharide core. *Neisseriae* LPS does not contain the O-antigen found in other Gram-negative bacteria, such as *E. coli* and *Salmonellae*, and is therefore often referred to as lipooligosaccharide (LOS) (Erridge *et al.*, 2002).

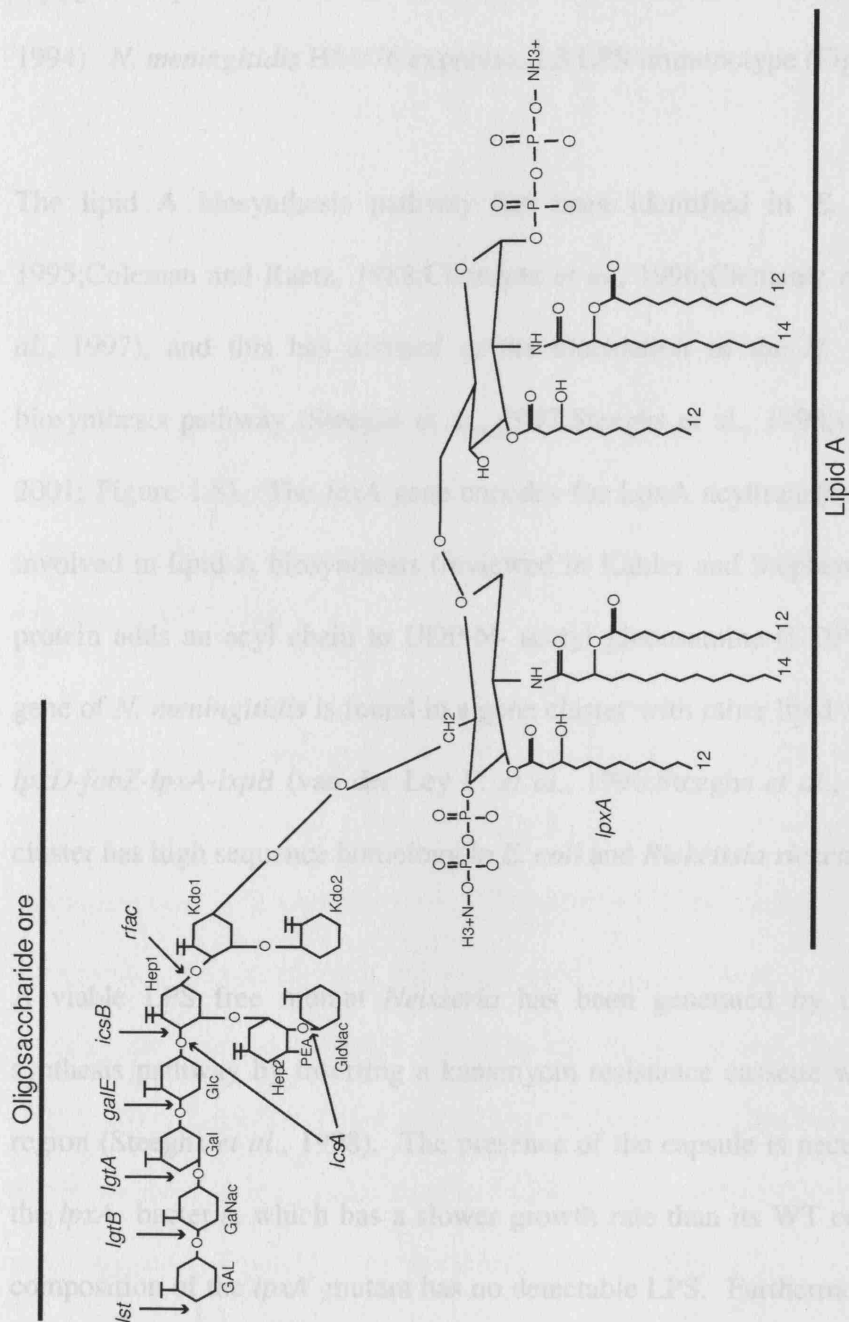


Figure 1.7 *N. meningitidis* LPS structure, immunotype 3. The LPS structure contains a lipid A hydrophobic tail, which anchors the hydrophilic oligosaccharide core to the bacterial outer membrane. Adapted from Hackett *et al.* (2002).

There are 12 LPS *Neisseriae* isotypes initially identified by whole-cell Enzyme-Linked Immunosorbent Assay (ELISA) (Scholten *et al.*, 1994) using monoclonal antibodies (Scholten *et al.*, 1994). Serogroup B meningococci express mainly isotypes L2 and 4, whereas serogroup C meningococci express mainly L1, 3 and 8. However, they are not exclusively expressed. For instance, one serogroup can express higher levels of one isotype compared to another isotype of LPS (Scholten *et al.*, 1994; Scholten *et al.*, 1994). *N. meningitidis* H44/76 expresses L3 LPS immunotype (Figure 1.7).

The lipid A biosynthesis pathway has been identified in *E. coli* (Young *et al.*, 1995; Coleman and Raetz, 1988; Clementz *et al.*, 1996; Clementz *et al.*, 1997; Garrett *et al.*, 1997), and this has assisted in the elucidation of the *N. meningitidis* lipid A biosynthesis pathway (Steeghs *et al.*, 1997; Steeghs *et al.*, 1998; van der Ley P. *et al.*, 2001; Figure 1.8). The *lpxA* gene encodes for LpxA acyltransferase, the first enzyme involved in lipid A biosynthesis (reviewed in Kahler and Stephens, 1998). The LpxA protein adds an acyl chain to UDP-N- acetyl glucosamine (UDP-GlcNac). The *lpxA* gene of *N. meningitidis* is found in a gene cluster with other lipid A biosynthesis genes: *lpxD-fabZ-lpxA-lpxB* (van der Ley P. *et al.*, 1996; Steeghs *et al.*, 1997), and this gene cluster has high sequence homology to *E. coli* and *Rickettsia rickettsii*.

A viable LPS free mutant *Neisseria* has been generated by inactivating the LPS synthesis pathway by inserting a kanamycin resistance cassette within the *lpxA*- gene region (Steeghs *et al.*, 1998). The presence of the capsule is necessary for survival of the *lpxA*- bacteria, which has a slower growth rate than its WT counterpart. The OM composition of the *lpxA*⁻ mutant has no detectable LPS. Furthermore, the proportion of OMPs on the OM is comparable to the WT bacteria, although differences in the

phospholipid composition of the *lpxA*- mutant are present (Steeghs *et al.*, 2001). The *lpxA*- mutant construct has greatly assisted research elucidating LPS independent mechanisms of disease pathogenicity.

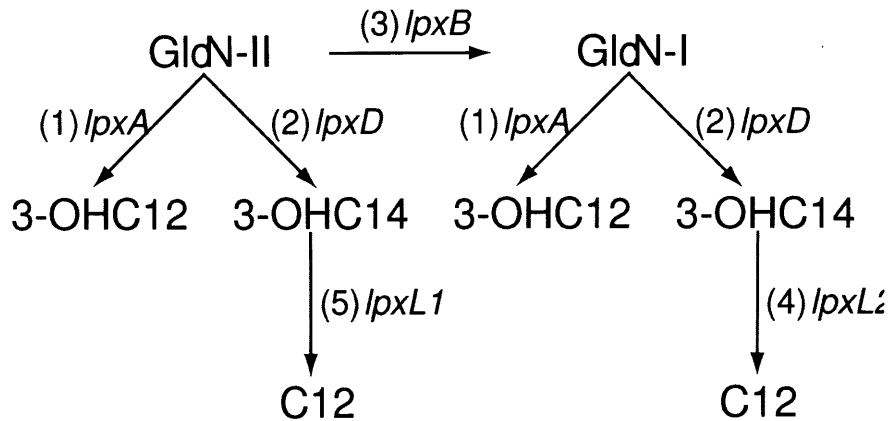


Figure 1.8 Meningococcal Lipid A biosynthesis pathway. UDP-GlcNac is acetylated by *lpxA* and *lpxD*. This is followed by dimerisation of UDP-GlcNac by *lpxB*. *lpxL2* and *lpxL1*, in this order, add the secondary fatty acid chains C12 to N-linked 3-OH C14. Illustration adapted from van der Ley *et al.*, (2001).

The inner core of meningococcal LPS consists of $\text{Glc}\beta 1,4(\text{GlcNAc}_1)\text{Hep}_2\text{Kdo}_2\text{lipidA}$ (Figure 1.7) (van der Ley P. *et al.*, 1997; Stojiljkovic *et al.*, 1997), which is found on all meningococcal LPS immunotypes. The different LPS immunotypes are produced by the addition of sugar residues to the LPS core in a specific order, which is performed by a series of different enzymes found in the LOS glycosyl transferase gene cluster (Banerjee *et al.*, 1998). The action of the individual genes has been determined, and the genes involved in the synthesis of the LPS oligosaccharide core immunotype L3 are demonstrated in Figure 1.7 (Kahler and Stephens, 1998).

Neisseriae serogroups (B, C, Y, and W-135) produce aN LOS sialyltransferase gene, designated *lst* (Lst protein), which sialylates LPS (Kahler and Stephens, 1998). Inactivation of *lst* produces unencapsulated bacteria with unsialylated LPS. Sialylated LPS mimics human carbohydrates, and this allows the bacteria to evade the immune response. For instance, activation of the compliment pathway is reduced by sialylated LPS (Jack *et al.*, 2001). In addition, sialylation of LPS inhibits the uptake of bacteria by neutrophils (McNeil and Virji, 1997).

1.3.4.1 LPS induced inflammatory responses

LPS is a potent inflammatory mediator both *in vivo* and *in vitro*, and can be found in high quantities in plasma during meningococcal disease (Brandtzaeg *et al.*, 1989). LPS plasma levels at the time of hospitalisation can be used as a predictor of outcome of meningococcal disease. LPS plasma levels above 700ng/L are associated with severe septic shock, which may have a fatal outcome due to multiple organ failure, whereas levels below 700ng/L at hospitalisation are associated with reduced morbidity and mortality (Brandtzaeg *et al.*, 1989).

Several LPS isotypes are associated with meningococcal disease. 97% of disease isolates from the UK, Norway and Austria are L3, 7, and 9, and 13% also express L1, 8, and 10 (Jones *et al.*, 1992). Immunotypes L3, 7, 8 and 9 induce significantly higher levels of inflammatory cytokines in a monocyte cell line than do any of the other immunotypes (Braun *et al.*, 2002).

Initial studies exploring LPS immunogenicity and cytotoxicity have used inhibitors of LPS, such as polymyxin B and recombinant bactericidal/permeability-increasing protein (rBPI₂₁)(Heyderman *et al.*, 1999). Cytotoxicity mediated by LPS on HUVEC depends on pili mediated adherence (Dunn *et al.*, 1995). Pili mediated adherence has a synergistic effect on LPS mediated cytotoxicity, as Opc dependent adherence has no effect on LPS mediated cytotoxicity (Dunn *et al.*, 1995).

N. meningitidis activates polymorphonuclear neutrophils (PMNL), which release adhesion molecules and phagocytose bacteria. PMNL activation can be significantly blocked by rBPI₂₁ (Heyderman *et al.*, 1999). rBPI₂₁ has also been used to block *N. meningitidis* WT and LPS induced cytokine production by monocytes (Uronen *et al.*, 2000).

The Lipid A structure of LPS mediates cytotoxicity and is a potent activator of the inflammatory immune response (van der Ley P. *et al.*, 2001; Oliver *et al.*, 2002). Mutant Lipid A (containing five and four fatty acids rather than six fatty acids) lead to reduced cytotoxicity and inflammation as measured by TNF α levels in murine cells (van der Ley P. *et al.*, 2001). Furthermore, mutations leading to abridged LPS oligosaccharide core structures (the *galE* and *lsi* mutant bacteria) have no effect on bacterial cytotoxicity on HUVEC (Jennings *et al.*, 1995).

Mannose-binding lectin (MBL), a member of the complement pathway, binds LPS from *N. gonorrhoeae* (Devyatyarova-Johnson *et al.*, 2000) but not to LPS from WT *N. meningitidis* (Jack *et al.*, 1998). The core structure of *N. gonorrhoeae* LPS is important in mediating MBL binding and complement activation as the addition of sialic acid or

truncation of the core oligosaccharide abolishes MBL binding to LPS (Devyatyarova-Johnson *et al.*, 2000). However, MBL does not bind WT *N. meningitidis* LPS and unsialylated LPS increases binding by MBL (Jack *et al.*, 1998).

1.3.4.2 LPS signalling complex

Several molecules are involved in the binding to and signalling by LPS, and all these combined are referred to as the LPS signalling complex (Figure 1.9). The LPS signalling complex is made up of LPS binding protein (LBP), CD14, TLR4 and MD-1.

LBP has been isolated and purified (Tobias *et al.*, 1986), and binds to LPS (Tobias *et al.*, 1986). It is found at 3-10µg/ml concentrations in plasma, which rises during an acute phase response (Guha and Mackman, 2001). At low concentrations, LBP-LPS complexes are transferred to CD14, whereas high concentrations of LBP can inhibit LPS mediated stimulation on macrophages and monocytes (Hamann *et al.*, 2002;Thompson *et al.*, 2003). LBP also enhances bacterial uptake by macrophages (Klein *et al.*, 2000) and dendritic cells (Baltathakis *et al.*, 2001; Uronen-Hansson *et al.*, 2004).

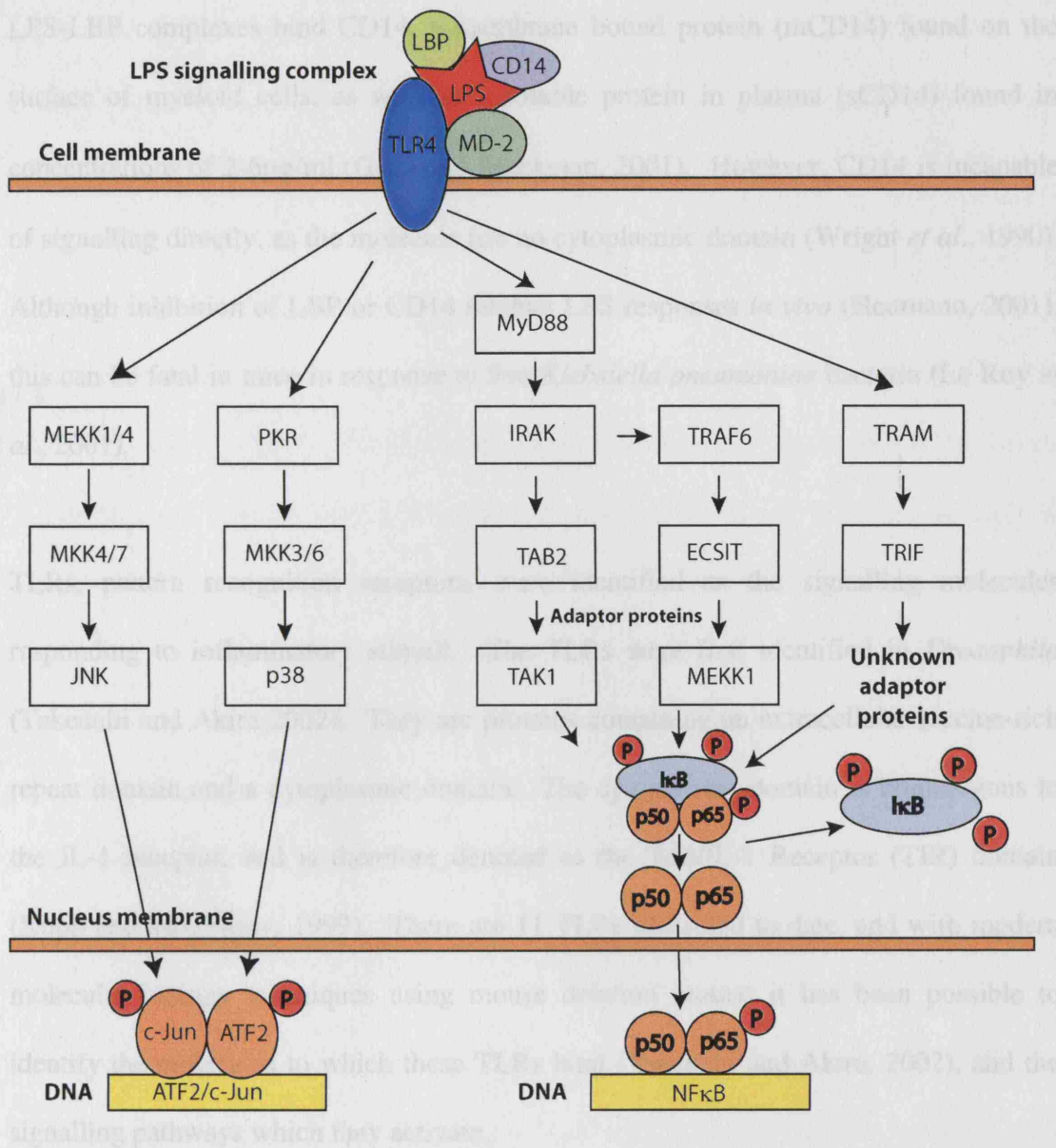


Figure 1.9 The Nuclear Factor-kappa-B (NFκB) and Activation Transcription Factor-1 (ATF2)/c-Jun pathway stimulated by the LPS signalling complex. LPS binds LPS binding protein (LBP) and CD14 (an LPS ligand), and this complex then binds TLR-4. TLR-4 sends downstream signals leading to transcriptional activation by NFκB and ATF2/c-Jun. Illustration adapted from Beutler (2000).

LPS-LBP complexes bind CD14, a membrane bound protein (mCD14) found on the surface of myeloid cells, as well as a soluble protein in plasma (sCD14) found in concentrations of 2-6µg/ml (Guha and Mackman, 2001). However, CD14 is incapable of signalling directly, as the molecule has no cytoplasmic domain (Wright *et al.*, 1990). Although inhibition of LBP or CD14 inhibits LPS responses *in vivo* (Heumann, 2001), this can be fatal in mice in response to live *Klebsiella pneumoniae* bacteria (Le Roy *et al.*, 2001).

TLRs, pattern recognition receptors, were identified as the signalling molecules responding to inflammatory stimuli. The TLRs were first identified in *Drosophila* (Takeuchi and Akira 2002). They are proteins containing an extracellular leucine-rich repeat domain and a cytoplasmic domain. The cytoplasmic domain is homologous to the IL-1 receptor, and is therefore denoted as the Toll/IL-1 Receptor (TIR) domain (Kopp and Medzhitov, 1999). There are 11 TLRs identified to date, and with modern molecular biology techniques using mouse deletion mutant it has been possible to identify the molecules to which these TLRs bind (Takeuchi and Akira, 2002), and the signalling pathways which they activate.

TLR2 knock-out mice, for instance, do not respond to cell wall components of Gram positive bacteria, such as peptidoglycan, as well as lipoproteins from Gram-negative bacteria. TLR2 has been demonstrated to associate with TLR6 to distinguish between the mycoplasma peptide MALP-2 and bacterial lipopeptide, and it has been demonstrated that both the cytoplasmic and extracellular domains of both proteins are required for the recognition and signalling by MALP-2 (Takeuchi and Akira, 2002). Mice susceptible to *Salmonella typhimurium* have been found to have reduced

expression of TLR5, which recognises flagellin. TLR9 knock-out mice have impaired pro-inflammatory cytokine responses, impaired B-cell proliferation, and impaired NF κ B activation in response to unmethylated CpG motifs.

The first TLR to be identified in mammals was TLR4, which was identified through a mutation rendering mice unresponsive to LPS (Politorak *et al.*, 1998). This observation was confirmed in a TLR 4 knock-out mouse model (Hoshino *et al.*, 1999). However, TLR4 does not directly bind LPS alone. It requires the action of MD2, an adaptor protein which is in close proximity to TLR4 on the cell surface (Shimazu *et al.*, 1999; Visintin *et al.*, 2001). MD2 was identified by transfecting TLR4 and MD2 into a non-expressing cell line. The presence of both molecules augmented activation by LPS, compared to single molecule transfected cells (Shimazu *et al.*, 1999). This was confirmed on CHO-CD14 expressing cell lines which are unresponsive to LPS as having a point mutation in the MD2 gene (Schroemm, et al, 2001).

The pathway leading to LPS signalling is therefore governed initially by the binding of LPB and CD14 to LPS, which then binds MD2 and TLR4 on the cell surface, which activates the cell.

Whilst mutations on the TLR4 gene have been known to induce LPS hyporesponsiveness *in vitro* (Arbour *et al.*, 2000), humans with mutations on the TLR4 gene have monocytes (Erridge *et al.*, 2003) and peripheral blood mononuclear cells (PBMCs) (Imahara *et al.*, 2005) that are responsive to LPS from a wide range of bacterial isolates, including *E. coli* and *N. meningitidis* LPS. Furthermore, the severity of meningococcal disease is not associated with mutations on the TLR4 gene (Read *et*

al., 2001). This indicates that although it is clear that TLR4 is the signalling molecule for cell activation by LPS (Poltorak *et al.*, 1998; Tapping *et al.*, 2000; Hoshino *et al.*, 1999), there may be cross-talk between TLRs and other PRRs which may also induce LPS signalling.

Although LPS induced TLR signalling requires the adaptor protein MyD88, MyD88 knockout mice are unable to induce LPS responsive gene expression but still activate NF κ B and mitogen-activated protein kinases (MAPKs) (Kawai *et al.*, 1999). In the MyD88-dependent signalling pathway, MyD88 interacts with the TIR domain (Medzhitov *et al.*, 1998). The death domain region of MyD88 interacts with downstream proteins of the signalling cascade, such as IL-1R associated kinase (IRAK), which become phosphorylated upon stimulation. Phosphorylated IRAK interacts with TNF Receptor associated factor 6 (TRAF-6), which recruits transforming growth factor- β -activated kinase-1 (TAK-1) via the adaptor protein TAB-2, or MEKK1 via the adaptor protein ECSIT (Guha and Mackman, 2001). The signalling pathway eventually leads to the translocation of NF κ B to the nucleus (Kopp and Medzhitov, 1999; Beutler, 2000; Chow *et al.*, 1999; Beutler *et al.*, 2003). NF κ B translocation can also occur in an MyD88 independent manner through the adaptor proteins TRIF-related adaptor molecule (TRAM) (Yamamoto *et al.*, 2003b) and TRIF adaptor protein (Yamamoto *et al.*, 2003a).

The activation of the MAPK pathway also occurs via TLRs (Dong *et al.*, 2002). This occurs via the recruitment by a protein designated TIR domain-containing adapter protein (TIRAP) (Horng *et al.*, 2001; Henneke and Golenbock, 2001), as well as through

IRAK and TRAF6, where the pathway diverges away from the NF κ B pathway (Medzhitov *et al.*, 1998; Muzio *et al.*, 1998; Dong *et al.*, 2002).

Although endothelial cells have traditionally been known to not express CD14, there is one report that demonstrates low expression levels of mCD14 on HUVEC (Jersmann *et al.*, 2001b). Endothelial cell activation by LPS is mediated by LBP and CD14 (Jersmann *et al.*, 2001b; Pugin *et al.*, 1993; Read *et al.*, 1993). Whilst endothelial cells express TLR2 and TLR4 mRNA (Faure *et al.*, 2000; Zeuke *et al.*, 2002) the protein expression of TLR4 is found both intracellularly (Dunzendorfer *et al.*, 2004) and on the cell surface of unstimulated and histamine stimulated endothelial cells (Talreja *et al.*, 2004). TLR2 is also expressed on the endothelial cell surface of unstimulated and stimulated cells (Talreja *et al.*, 2004). TLR4 mediated signalling by LPS leads to NF κ B activation (Faure *et al.*, 2000).

1.3.4.3 LPS signalling via the LPS complex- the NF κ B Regulatory Pathways

NF κ B is an immunoregulatory transcription factor involved both in the innate and adaptive immune response, and is activated in response to cytokines, bacteria and virus.

NF κ B consists of a family of transcription factors designated RelA (p65), NF κ B1 (p50, cleaved off from p105), NF κ B2 (p52, cleaved off from p100), c-Rel, and RelB (Ghosh and Karin, 2002). The structure of these proteins have dimerisation domains, nuclear localisation domains and DNA-binding domains, as well as a transactivation domain, which is involved in the transcriptional activation of NF κ B regulated genes (Murakami

et al., 2000). Although the formation of different homodimers and heterodimers is believed to control the selectivity of NF κ B as a transcription factor (Perkins *et al.*, 1992), homodimers consisting of p50/p50 and p52/p52 repress gene transcription (Zhong *et al.*, 2002).

NF κ B is constitutively found in the cytoplasm, bound to its inhibitor I κ B (Baeuerle, 1998). There are seven different I κ B inhibitors known in mammals, which are designated I κ B α , - β , - ϵ , - γ , Bcl-3, and p100 and p105, of which the last two mentioned bind to Rel proteins (Ghosh and Karin, 2002). Upstream signals, such as TRAF6, activate NF κ B-inducing kinase (NIK), which activates I κ B kinase (IKK). IKK in turn phosphorylates I κ B- α and - β kinases (Ghosh and Karin, 2002; DiDonato *et al.*, 1997). The phosphorylation and degradation of I κ B releases NF κ B into its constituent subunits, and these translocate into the nucleus. Post-translational modification of NF κ B has been reported such as phosphorylation of p65, which is essential for transcriptional activity regulated by NF κ B p65 subunits (Ghosh and Karin, 2002).

I κ B is under the transcriptional control of NF κ B (Chiao *et al.*, 1994), thereby creating a loop to down-regulate NF κ B activity in the nucleus. I κ B binds to NF κ B bound to DNA, and a nuclear-export signal (NES) allows the complex to be transported into the cytoplasm (Ghosh and Karin, 2002). This complex obscures the nuclear localisation signal (NLS) of NF κ B, which becomes active by the phosphorylation and degradation of and release by I κ B.

As mentioned previously, bacterial LPS induces NF κ B through TLR4 signalling. NF κ B can also be activated by different pathogens and pro-inflammatory cytokines like TNF- α and IL-1 (Li and Verma, 2002). LPS induced E-selectin expression is mediated via NF κ B (Dixon *et al.*, 2004; Jersmann *et al.*, 2001a) and is mediated via the MyD88/IRAK/TRAF6 pathway (Zhang *et al.*, 1999). LPS induction of NF κ B also occurs in an MyD88 independent manner via the adaptor proteins TRIF and TRAM (Fitzgerald *et al.*, 2003).

1.3.4.4 LPS signalling via the LPS complex- the MAP Kinase regulatory pathways

MAPKs are signal transducers involved in both innate and adaptive immune responses, as well as development and stress responses (Rincon *et al.*, 2000). Downstream targets of the MAPKs include ATF2 and c-Jun, which are bound to DNA and become active when phosphorylated (Rincon *et al.*, 2000). There are three main groups of MAPKs involved in immune regulation, and these are designated the extracellular signal-regulated protein kinases (ERK), p38, and c-Jun NH₂-terminal kinases (JNK) (Dong *et al.*, 2002). p38 and JNK both phosphorylate ATF2, and c-Jun is only phosphorylated by JNK (Rincon *et al.*, 2000).

Activation of ERK, p38 and JNK occurs on two sites of the proteins, which contain a conserved tripeptide motif Thr-Xaa-Tyr. The phosphorylation of the three different sites is mediated by different MAPKs. p38 is phosphorylated by MAP kinase kinase 3 (MKK3), MKK4, and MKK6, whereas JNK is phosphorylated by MKK4 and MKK7 (Rincon *et al.*, 2000). The upstream kinases of MKKs are known as MAP kinase kinase

kinases (MKKK). The upstream molecules involved in the JNK and p38 pathways activating the MKKKs are from the Rho family GTPases, including Rac and Cdc42 (Barr and Bogoyevitch, 2001; Dong *et al.*, 2002) (Figure 1.9).

There are 10 JNK MAPK isoforms, produced by alternative splicing of the three genes encoding JNK (*JNK1*, *JNK2*, and *JNK3*). The N-terminal domain is involved in binding ATP, whereas the C-terminal region is involved in the recognition of peptide substrates (Barr and Bogoyevitch, 2001). The p38 family has 4 different members, referred to as p38- α , - β , - γ , and - δ , although their individual roles are unclear (Rincon *et al.*, 2000).

Deletions of ATF2 are lethal in mice, however, the use of a mutant producing low levels of ATF-2 demonstrate reduced induction of inflammatory mediators and are more susceptible to death from infections than WT mice (Reimold *et al.*, 2001).

Although a knock-out of c-Jun is lethal in mice, JNK knock-outs survive and are morphologically normal (Barr and Bogoyevitch, 2001). However, *JNK1* and *JNK2* knock-outs have defective T-cell activation and apoptosis. There are no reported defects in the innate immune response in these knock-out mice, indicating that there is some over-lap in the function of the different JNKs in innate immune signalling.

LPS activates both the JNK and p38 pathways (Han *et al.*, 1994; Guha and Mackman, 2001). LPS induction of IL-8 (Hippenstiel *et al.*, 2000) and TF (Wu and Aird, 2005) by endothelial cells is dependent on the activation of the p38 MAPK pathway. In addition, JNK is involved in LPS induced angiogenesis (Pollet *et al.*, 2003). The synergistic upregulation of E-selectin on endothelium by LPS and TNF- α is regulated by p38 and

NF κ B (Jersmann *et al.*, 2001a), whereas in mouse macrophages it is dependent on the stimulation of p38, JNK and ERK (Swantek *et al.*, 1997). JNK and p38 are also involved in the maturation of DCs (Nakahara *et al.*, 2004). These studies demonstrate the wide range of inflammatory mechanisms in which JNK and p38 are involved in.

In endothelial cells, JNK and p38 activity leads to the activation of inflammatory mediators, whereas the involvement of the ERK pathway of MAPKs leads to anti-inflammatory mediator expression (Hoefen and Berk, 2002).

1.4 The use of the LPS-deficient mutant (*lpxA*⁻) in elucidating LPS-dependant and independent mechanisms of disease

The use of the *lpxA*⁻ mutant (Steeghs *et al.*, 1998) has facilitated research elucidating the role of LPS in disease, as well as the role that other OMPs may play in stimulating the inflammatory response. For instance, LPS appears to have an important role in bacterial internalisation into host cells. Adherence and invasion of epithelial cells is affected by the loss of LPS on the bacterial cell surface, as shown with an *lpxA*⁻ (serogroup C) bacterial strain (Albiger *et al.*, 2003). Adhesion by the LPS deficient mutant is 50% lower than the WT bacteria, and there is no epithelial invasion by the mutant bacteria (Albiger *et al.*, 2003). However, invasion of epithelial cells by bacteria was detected at 6 hours. Although WT bacteria are phagocytosed by DCs very rapidly (1 hour), the uptake of the *lpxA*⁻ mutant is slower and less efficient. Uptake of the *lpxA*⁻ mutant is, however, observed at 1 hour, and this continues to increase with time (Uronen-Hansson

et al., 2004). It would be interesting to see if epithelial invasion would increase during prolonged exposure to the *lpxA*⁻ mutant.

Phagocytosis of *N. meningitidis* by mouse macrophages is mediated by a scavenger receptor and is independent of LPS. Whilst phagocytosis of bacteria by mouse macrophages does not correlate with cytokine induction (Peiser *et al.*, 2002), this is in contrast to observations made on human DC. Efficient uptake of bacteria by DC is LPS-dependent and cytokine production is dependent on the internalisation of bacteria. Increasing concentrations of LPS on the bacterial surface enhances phagocytosis of bacteria as well as IL-12 and TNF- α production by DC (Uronen-Hansson *et al.*, 2004).

Whilst high concentrations of *lpxA*⁻ (10^8 organisms/ml) induce TNF- α , IL-1 α and IL-6 levels comparable to WT induction of monocytes (Uronen *et al.*, 2000), PBMCs (Sprong *et al.*, 2001), and DCs (Dixon *et al.*, 2001;Unkmeir *et al.*, 2002a), IL-12 production by DCs is dependant on the presence of LPS on the bacterial cell wall, as there is virtually no IL-12 production in response to the *lpxA*⁻ mutant (Dixon *et al.*, 2001).

Cytokine production has also been demonstrated in human monocyte-derived macrophages in response to WT and *lpxA*⁻. Cytokine induction is ten times greater in response to WT bacteria than the *lpxA*⁻ bacteria (Pridmore *et al.*, 2001;Ingalls *et al.*, 2001). Activation of macrophages by the *lpxA*⁻ mutant is through the TLR2 pathway (Ingalls *et al.*, 2001;Pridmore *et al.*, 2001), whereas WT bacteria activate cells through TLR2 and TLR4 signalling.

The complement pathway is part of the innate immune response, and is activated by pathogenic microorganisms including *N. meningitidis*. Complement activation by *N. meningitidis* can occur independent of LPS (Bjerre *et al.*, 2002), demonstrating that there are other immunogenic OMP components on the bacterial surface.

Although WT bacteria are highly immunogenic, the evidence demonstrates that there are LPS independent mechanisms of activation. Whilst LPS induces strong immunogenic responses in human cells *in vitro*, the LPS structure incorporated onto the bacterial cell wall may be important. The treatment and outcome of meningococcal disease has greatly improved over the last decade, however, there may still be unknown areas in which to target future drug development. In order to elucidate these pathways and mechanisms, the role of bacterial cell components other than LPS must be understood. The use of the *lpxA*- mutant will greatly enhance our understanding of these mechanisms.

1.5 Endothelium and Inflammation

The vascular endothelium is involved in the innate immune response, mediating the tethering, rolling, adhesion and transmigration of leukocytes to sites of infection and inflammation. Adhesion molecules expressed on leukocytes and endothelial cells are important regulators of this process.

1.5.1 The role of adhesion molecules in leukocyte adhesion and transmigration

During an inflammatory immune response, endothelial cells express adhesion molecules which are designed to promote attachment of circulating leukocytes. This mechanism is tightly regulated by the sequential expression of adhesion molecules (Figure 1.10). Tethering is mediated by the expression of selectins (E-, P- and L-selectin), which are initially expressed on the cell surface of endothelial cells (E- and P-selectin) and leukocytes (L-selectin) (Figure 1.11). Firm adhesion is then mediated by the expression of integrins and members of the Ig superfamily, such as intercellular adhesion molecule-1 (ICAM-1/CD54) and vascular cell adhesion molecule-1 (VCAM-1/CD106) (Luscinskas and Gimbrone, Jr., 1996).

The range of cells which adhere to the endothelial surface is governed by the repertoire and kinetics of adhesion molecules expressed on both endothelial cells and leukocyte, and the specific interactions occurring between these molecules (Nourshargh and Marelli-Berg, 2005).

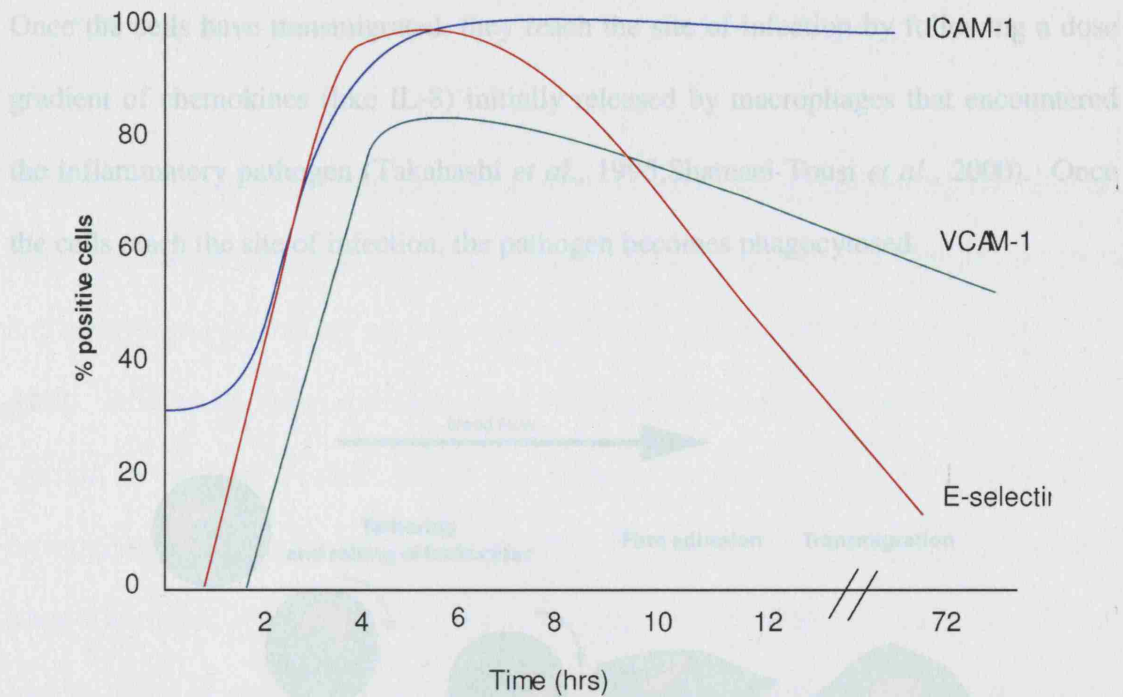


Figure 1.10 The kinetics of surface expression of E-selectin, ICAM-1 and VCAM-1 on HUVEC in response to IL-1 α . Upon stimulation with IL-1 α , E-selectin, ICAM-1 and VCAM-1 are upregulated on endothelial cells. Maximal expression of E-selectin is observed at 4 hours post stimulation, 4-8 hours for VCAM-1, and 6-8 hours for ICAM-1. By 72 hours post infection, there are still high levels of ICAM-1 and lower levels of VCAM-1, whereas E-selectin expression is back to base-line levels. Adapted from Scholz *et al.* (1996).

Figure 1.11 Leukocyte rolling, adhesion and transmigration through the endothelium.

Leukocytes become attracted to sites of infection through IL-8, which is produced by stimulated endothelial cells (Huber, *et al.*, 1991; Smart and Casale, 1994; Zoja, *et al.*, 2002). Leukocyte transmigration is inhibited by IL-8 antibodies (Kuijpers, *et al.*, 1992; Zoja, *et al.*, 2002). Once leukocytes reach activated endothelial cells, they transmigrate at sites of intercellular junctions (Luscinskas and Gimbrone, Jr., 1996), where platelet endothelial cell adhesion molecule-1 (PECAM-1/CD31) and junctional adhesion molecules (JAMs) are expressed (Newman *et al.*, 1990; Simmons *et al.*, 1990; Albelda *et al.*, 1991; Muller, 2003; Martin-Padura *et al.*, 1998; Palmeri *et al.*, 2000). The basement membrane below the endothelial cell layer is then penetrated by proteolytic enzymes.

Once the cells have transmigrated, they reach the site of infection by following a dose gradient of chemokines (like IL-8) initially released by macrophages that encountered the inflammatory pathogen (Takahashi *et al.*, 1995; Shamaei-Tousi *et al.*, 2000). Once the cells reach the site of infection, the pathogen becomes phagocytosed.

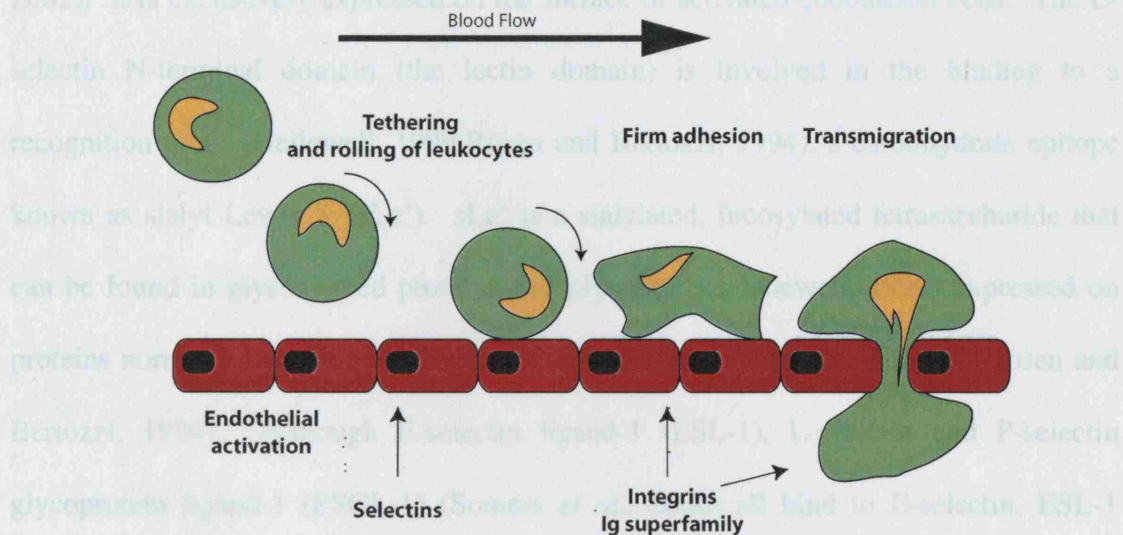


Figure 1.11 Leukocyte rolling, adhesion and transmigration through the endothelium.

Activated endothelium expresses adhesion molecules, which attract leukocytes, mediating their tethering, rolling and firm adhesion, which leads to leukocyte transmigration. Adapted from Kevil and Bullard (1999).

The endothelial adhesion molecules E-selectin, ICAM-1 and VCAM-1 will be discussed in further detail, paying particular attention to the transcriptional regulation of E-selectin.

1.5.1.1 E-selectin

E-selectin is a 115-kDa transmembrane glycoprotein and a member of the selectin family. E-selectin consists of a C-type lectin binding domain, an EGF-like domain, and six complement-regulatory protein regions. (Kevil and Bullard, 1999;Reinhart *et al.*, 2002). It is exclusively expressed on the surface of activated endothelial cells. The E-selectin N-terminal domain (the lectin domain) is involved in the binding to a recognition motif (Hellewell, 1999;Rosen and Bertozzi, 1994), a carbohydrate epitope known as sialyl Lewis X (sLe^x). sLe^x is a sialylated, fucosylated tetrasaccharide that can be found in glycosylated proteins and glycolipids (Hellewell, 1999) expressed on proteins normally found on neutrophils, monocytes and some lymphocytes (Rosen and Bertozzi, 1994). Although E-selectin ligand-1 (ESL-1), L-selectin and P-selectin glycoprotein ligand-1 (PSGL-1) (Somers *et al.*, 2000) all bind to E-selectin, ESL-1 appears to be the only ligand that has a functional role in leukocyte tethering on E-selectin, as antibodies generated against ESL-1 block cell adhesion to soluble E-selectin. L-selectin and PSGL-1 antibodies reduce neutrophil rolling on the endothelium, however, this appears to be due to leukocyte-leukocyte interactions (Patel *et al.*, 2002).

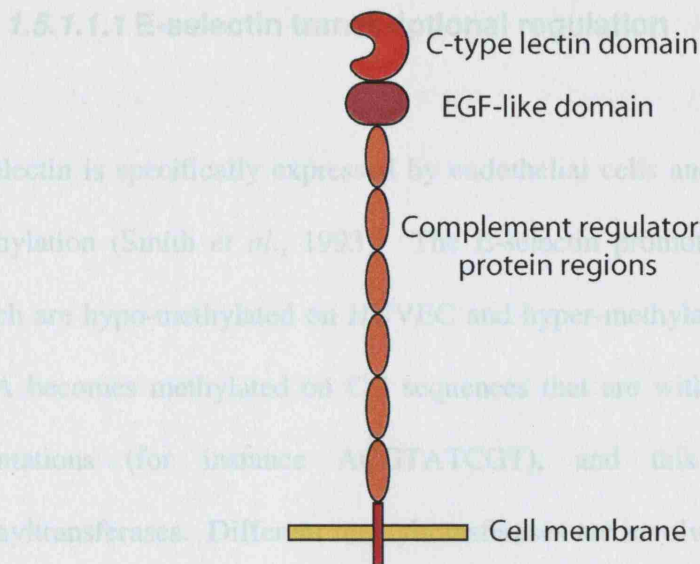


Figure 1.12 E-selectin protein structure. E-selectin consists of a C-type lectin binding domain, an EGF-like domain, and six complement-regulatory protein regions. The cytoplasmic domain contains tyrosine residues which can be phosphorylated.

E-selectin is transiently expressed on the surface of endothelial cells in response to inflammatory stimuli such as TNF- α , IL-1, LPS, and Human Immunodeficiency virus (HIV) Tat protein (Hunt and Jurd, 1997; Montgomery *et al.*, 1991; Wyble *et al.*, 1997; Scholz *et al.*, 1996; Cota-Gomez *et al.*, 2002) (Figure 1.10). Some stimuli can work together to synergistically increase E-selectin expression, as seen with TNF- α and LPS (Jersmann *et al.*, 2001a) and IL-1 and Phorbol 12-myristate 13-acetate (PMA) (Tamaru and Narumi, 1999). Very low levels of E-selectin mRNA have been found in response to IL-2, IL-4, and IL-6 (Montgomery *et al.*, 1991). There are also other inflammation regulatory mediators, such as Transforming Growth Factor β (TGF- β) (Rombouts *et al.*, 2002) IL-4, IL-13, and Interferon- γ (IFN- γ), which inhibit E-selectin expression activated by PMA, IL-1 α and TNF- α on HUVEC (Thornhill and Haskard, 1990; Gamble *et al.*, 1993; Melrose *et al.*, 1998; Etter *et al.*, 1998).

1.5.1.1.1 E-selectin transcriptional regulation

E-selectin is specifically expressed by endothelial cells and this is controlled by gene methylation (Smith *et al.*, 1993). The E-selectin promoter has 3 methylation sites, which are hypo-methylated on HUVEC and hyper-methylated in non-expressing cells. DNA becomes methylated on CG sequences that are within same sequences in both orientations (for instance ACGTATCGT), and this is regulated by DNA methyltransferases. Different methyltransferases are involved during the cell cycle and development, thereby regulating when and where DNA is methylated in different tissues (reviewed in Caiafa and Zampieri, 2005-1062).

E-selectin is transiently and transcriptionally regulated. The primary structure of E-selectin DNA contains a 3' untranslated region with eight ATTTA repeats, encoding AUUUA, and this sequence destabilises the mRNA, which leads to rapid degradation of mRNA transcripts. This sequence is found on several other transiently expressed proteins, including inflammatory cytokines (Bevilacqua *et al.*, 1989), and may be a mechanism of controlling gene expression. This may account for the short half-life of E-selectin mRNA and protein (Drogari-Apiranthitou *et al.*, 2002).

There is no E-selectin transcriptional activity in unstimulated HUVEC, and hence no E-selectin mRNA. Transcriptional activity and E-selectin mRNA is detected in response to TNF- α , IL-1, and LPS (Montgomery *et al.*, 1991; Tamaru and Narumi, 1999; Sugano *et al.*, 2000; Etter *et al.*, 1998; Wyble *et al.*, 1997). Transcriptional activity is detected as early as 30 minutes post stimulation, reaching maximum levels between 2-4 hours, and reaching baseline levels by 24 hours (Montgomery *et al.*, 1991; Whelan *et al.*, 1991). E-

selectin is present on the endothelial cell surface one hour post activation, reaching maximal levels by 4 hours, and declines by 8 hours, reaching baseline levels by 72 hours (Scholz *et al.*, 1996) (Figure 1.10).

There are several downstream pathways that the E-selectin protein may take. It may become soluble through shedding of the cell membrane or via membrane cleavage of the protein leading to its shedding (Wyble *et al.*, 1997). This may explain the presence of soluble E-selectin during inflammation (Kevil and Bullard, 1999; Gearing and Newman, 1993). Another theory is that E-selectin becomes endocytosed and later degraded in lysosomal compartments (von Asmuth *et al.*, 1992; Smeets *et al.*, 1993; Kuijpers *et al.*, 1994).

1.5.1.1.2 E-selectin promoter organisation

Analysis of the E-selectin gene promoter demonstrates that it contains a CAAT and TATA box upstream of the start site, which indicates that the gene is controlled by a minimal promoter (Montgomery *et al.*, 1991).

The E-selectin promoter is divided into 4 positive domains (PD) (Whitley *et al.*, 1994; Collins *et al.*, 1995) (Figure 1.13). These are referred to as PD I, II, III, and IV. These four regions are required for maximal E-selectin promoter activity. These regulatory regions and their positions in relation to each other have been highly conserved in humans, mice and rats (Becker-Andre *et al.*, 1992; Larigan *et al.*, 1992). Interestingly, the positioning between the four regions is equally important to the

function of the promoter as is the cooperation between the four regulatory regions (Meacock *et al.*, 1994).

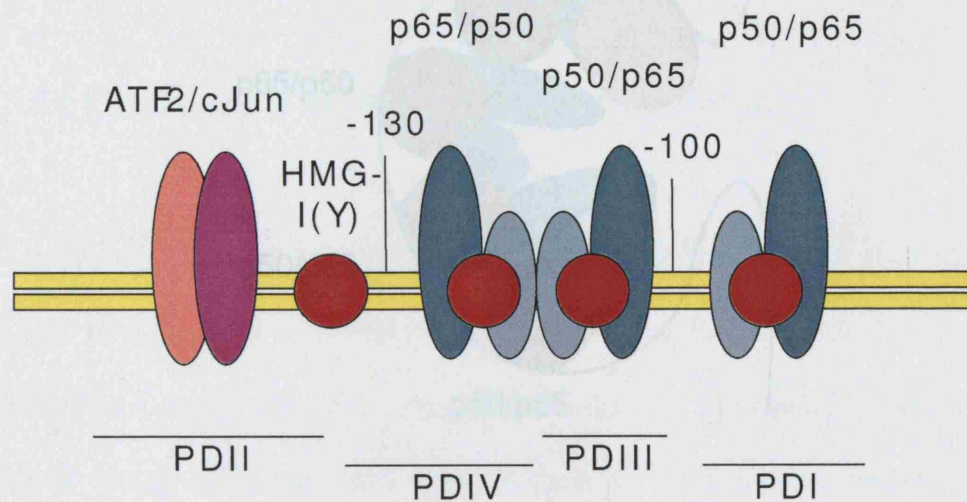


Figure 1.13 Binding of the E-selectin promoter. E-selectin promoter binding is mediated by

Figure 1.13 E-selectin promoter organisation. The regulatory regions (PDI, II, III, and IV) are demonstrated, bound by ATF2/c-Jun, NF κ B and HMG-I(Y). Adapted from Collins *et al.* (1995) and Whitley *et al.* (1994).

NF κ B binds to the PDI, III and IV regions (Whelan *et al.*, 1991; Lewis *et al.*, 1994). Binding of NF κ B to PDIII and IV is enhanced by the binding of High-Mobility-Group protein I(Y) (HMG-I(Y)) (Lewis *et al.*, 1994; Whitley *et al.*, 1994), and this co-operation is essential for maximal E-selectin promoter activity. HMG-I(Y) particularly increases the affinity of p50 homodimers and p50/p65 heterodimers to these three regulatory regions (Whitley *et al.*, 1994) by bending the DNA structure allowing for the initial binding of NF κ B to PDIII (Figure 1.14). PDIII is functionally more important than PDI and IV (Schindler and Baichwal, 1994), as mutations in this region affect promoter activity to a higher degree than mutations on PDI and IV. PDI and III are preferentially bound by p65, p50/p65 and p50 NF κ B (Schindler and Baichwal, 1994).

PDII is also bound by HMG-I(Y) (Whitley *et al.*, 1994), and it has been demonstrated that the activity surrounding the PDII site binds to the other regulatory regions in the E-selectin promoter (Collins *et al.*, 1995).

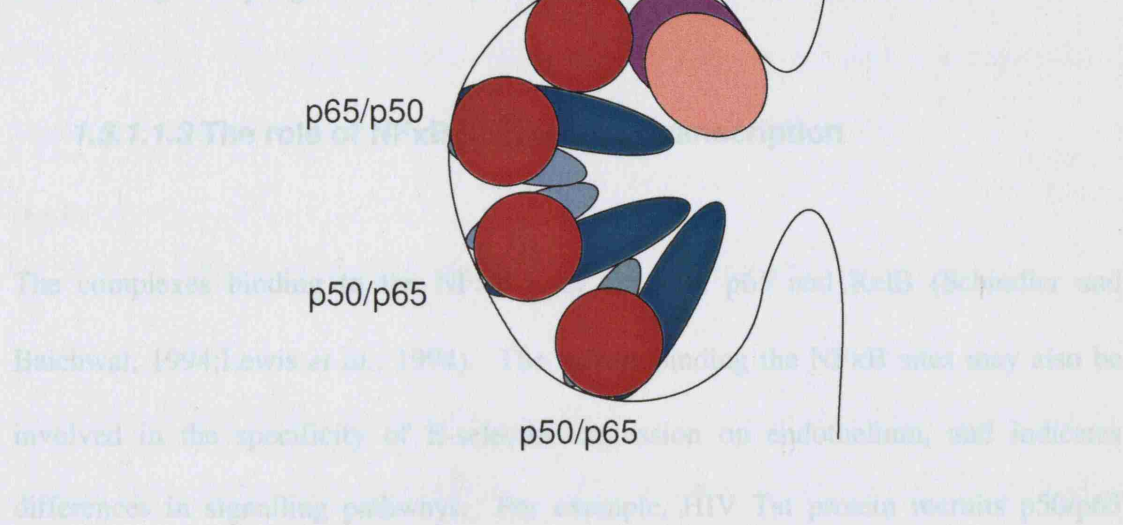


Figure 1.14 Bending of the E-selectin promoter. E-selectin promoter bending is mediated by the binding of HMG-I(Y), which facilitates the binding of the transcription factors to their regulatory regions. Adapted from Collins *et al.* (1995) and Whitley *et al.* (1994).

PD II is an ATF2 consensus site (Hooft *et al.*, 1992;Kaszubska *et al.*, 1993), and this site is constitutively bound by ATF2 and c-Jun (Kaszubska *et al.*, 1993;Read *et al.*,

1997). Deletion of this region reduces maximal E-selectin promoter activity (Schindler and Baichwal, 1994). De Luca and co-workers (1994) found that this site may have both positive and negative regulatory function, as TNF- α activated E-selectin promoter activity is inhibited by cAMP activation. TNF- α increases ATF2 and c-Jun activation, however, cAMP activation only increases ATF2 activation, and this appeared to have a negative effect on E-selectin promoter activity (De Luca *et al.*, 1994).

Another ATF2/c-Jun pathway that has been elucidated is through TRAF2-RAC/CDC42 (Min and Pober, 1997), as over-expression of TRAF2 activates JNK, which in turn phosphorylates c-Jun and ATF2, leading to E-selectin promoter activity. Although c-Jun is transiently phosphorylated, ATF2 appears to remain phosphorylated for a longer period of time (Min and Pober, 1997).

PDII is also bound by HMG-I(Y) (Whitley *et al.*, 1994), and it has been demonstrated that the activity surrounding the PDII site bends the DNA (Figure 1.14), which brings the other regulatory regions in close proximity to each other (Meacock *et al.*, 1994).

1.5.1.1.3 The role of NF κ B in E-selectin transcription

The complexes binding to the NF κ B sites are p50, p65 and RelB (Schindler and Baichwal, 1994; Lewis *et al.*, 1994). The factors binding the NF κ B sites may also be involved in the specificity of E-selectin expression on endothelium, and indicates differences in signalling pathways. For example, HIV Tat protein recruits p50/p65 heterodimers, whereas TNF α recruits a mixture of heterodimers with p50, p65, cRel, and RelB (Cota-Gomez *et al.*, 2002). *N. meningitidis* recruits p65/p50 heterodimers (Dixon *et al.*, 2004).

1.5.1.1.4 The role of ATF and c-Jun in E-selectin transcription

ATF2 and c-Jun are phosphorylated by JNK and p38 through the MAP kinases, MKK3 and 4 in endothelial cells in response to TNF- α (Read *et al.*, 1997). These MAP kinases are all constitutively found in the nucleus of HUVEC, and become phosphorylated by stimulation with TNF- α as early as 15 minutes post activation (Read *et al.*, 1997; Min and Pober, 1997; Jersmann *et al.*, 2001a). Another ATF2/c-Jun pathway that has been elucidated is through TRAF2-RAC/CDC42 (Min and Pober, 1997), as over-expression of TRAF2 activates JNK, which in turn phosphorylates c-JUN and ATF2, leading to E-selectin promoter activity. Although c-Jun is transiently phosphorylated, ATF2 appears to remain phosphorylated for a longer period of time (Min and Pober, 1997).

ATF2 null-mice have defective E-selectin expression (Reimold *et al.*, 1996), indicating that this transcription factor may be essential for E-selectin transcriptional activation. This correlates with the importance of the PDII region, as this region is required for maximal E-selectin promoter activity (Schindler and Baichwal, 1994).

1.5.1.1.5 Final comment on the E-selectin promoter

In summary, the E-selectin promoter is unique, as it requires the full region for E-selectin promoter activity (Hooft *et al.*, 1992; Kaszubska *et al.*, 1993). If one site is abolished, promoter activity is nearly completely abolished. If two PD regions of the E-selectin gene promoter are kept together, they do not synergistically increase their individually PD region activity. It is only with the full region working together that maximal transcriptional activity is observed.

With other promoters that have several transcription factor sites, deletions or mutations of one site reduces the full promoter's activation capacity. For instance, the HIV-1 long terminal repeat enhancer region contains two NFκB sites which co-operate for maximal promoter activity. These two regions are also capable of inducing promoter activity on their own, however, at a reduced capacity (Gaynor *et al.*, 1988).

1.5.1.2 ICAM-1

ICAM-1 is a 80-115-kDa sized molecule and a member of the Ig superfamily (Reinhart *et al.*, 2002). ICAM-1 consists of 5 Ig-like domain repeats, a transmembrane region, and a short cytoplasmic tail (Kevil and Bullard, 1999) (Figure 1.15). ICAM-1 is constitutively expressed in endothelial cells and monocytes, and expression can be increased in response to inflammatory cytokines and other mediators on B- and T-cells, fibroblasts, epithelial cells and endothelial cells, among others (Dustin *et al.*, 1986; Thornhill and Haskard, 1990; Doukas and Pober, 1990; Scholz *et al.*, 1996; Reinhart *et al.*, 2002; Luscinskas and Gimbrone, Jr., 1996).

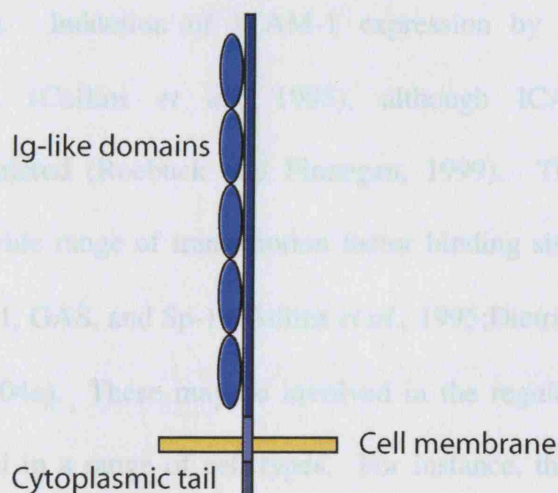


Figure 1.15 ICAM-1 structure. ICAM-1 consists of 5 Ig-like domains, a transmembrane region and a short cytoplasmic tail. ICAM-1 is involved in the firm adhesion of leukocytes to the vascular endothelium.

ICAM-1 serves as a ligand for $\beta 2$ integrins, which are found in CD11a/CD18 (LFA-1), CD11b/CD18 (MAC-1) and CD43 (Dietrich, 2002). These are expressed on the surface of monocytes and lymphocytes (Hertzig *et al.*, 2003). Binding of ICAM-1 to ligand mediates tight adhesion and extravasation of rolling leukocytes preparing for transmigration (Kevil and Bullard, 1999). ICAM-1 null mice have defective neutrophil transmigration through the endothelium, and appear to also be resistant to septic shock (Etzioni *et al.*, 1999), indicating that this molecule has a major role in mediating transmigration of leukocytes through the endothelium.

ICAM-1 surface expression increases as early as 1.5 hours post activation, and reaches maximal levels by 4-6 hours, remaining elevated 72 hours post activation (Scholz *et al.*, 1996) (Figure 1.10). Induction of ICAM-1 expression by $\text{TNF}\alpha$ occurs at the transcriptional level (Collins *et al.*, 1995), although ICAM-1 is also post-transcriptionally regulated (Roebuck and Finnegan, 1999). The ICAM-1 promoter (-1352 - +1) has a wide range of transcription factor binding sites, including sites for $\text{NF}\kappa\text{B}$, C/EBP β , AP-1, GAS, and Sp-1 (Collins *et al.*, 1995; Dietrich, 2002; Chang *et al.*, 2002; Chen *et al.*, 2004a). These may be involved in the regulation of ICAM-1 to a wide range of stimuli in a range of cell types. For instance, the cytokine responsive element of the ICAM-1 promoter requires 250 bp upstream from the transcription start site (Roebuck and Finnegan, 1999). $\text{TNF}\alpha$, IL-1 and LPS induced ICAM-1 promoter activity relies on the presence of an $\text{NF}\kappa\text{B}$ binding site (Ledebur and Parks, 1995) and the upstream C/EBP β binding site (Roebuck *et al.*, 1995). There is also an H_2O_2 responsive region consisting of 960 bp upstream of the transcriptional start site, which contains two AP1/Ets elements (Roebuck *et al.*, 1995; Roebuck, 1999).

1.5.1.3 VCAM-1

VCAM-1, a 110kDa sized protein, is also a member of the immunoglobulin superfamily (reviewed in (Carlos and Harlan, 1994;Hertzig et al., 2003;Kevil and Bullard, 1999;Hellewell, 1999). The structure of VCAM-1 is expressed in two forms, consisting of either six or seven Ig-like domains. It is constitutively expressed at low levels on endothelial cells (Hellewell, 1999), as well as on activated endothelial cells, tissue macrophages, dendritic cells, and bone marrow fibroblasts, myoblasts and myotubes.

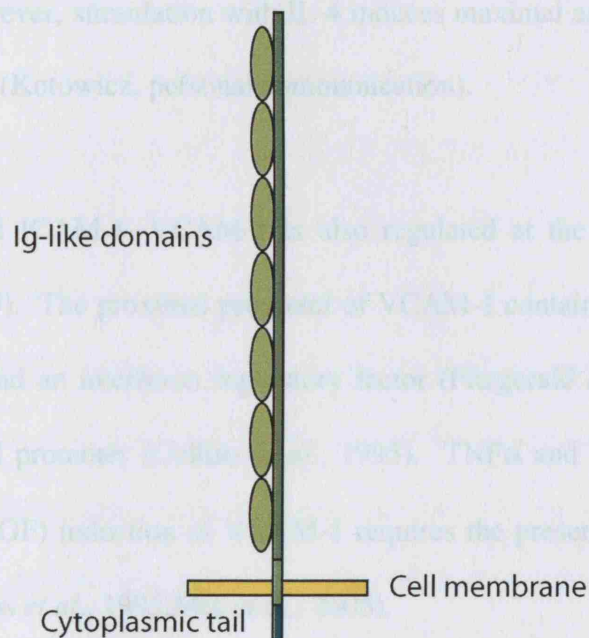


Figure 1.16 VCAM-1 protein structure. VCAM-1 is made up of 6-7 Ig-like domains, a transmembrane region and a short cytoplasmic tail.

The Ig-like extracellular domains of VCAM-1 bind $\alpha 4\beta 1$ (very late antigen-4 (VLA-4)) and $\alpha 4\beta 7$, which are both found on the surface of leukocytes, B-lymphocytes, basophils, and some T-lymphocytes (Luscinskas and Gimbrone, Jr., 1996;Hertzig et al.,

2003). VCAM-1 is involved in the tight adhesion of leukocytes to the endothelium (Osborn *et al.*, 1989) and in leukocyte transmigration.

VCAM-1 expression increases in endothelial cells upon stimulation with inflammatory mediators (Osborn *et al.*, 1989; Swerlick *et al.*, 1992; Kevil and Bullard, 1999; Reinhart *et al.*, 2002). Stimulation of endothelial cells with inflammatory stimuli increases VCAM-1 expression on the cell surface by 1 hour, reaches maximal levels by 4-8 hours, and remains detectable by 72 hours (Scholz *et al.*, 1996), although at lower levels (Figure 1.10). However, stimulation with IL-4 induces maximal and sustained VCAM-1 levels at 24 hours (Kotowicz, personal communication).

Like E-selectin and ICAM-1, VCAM-1 is also regulated at the transcriptional level (Collins *et al.*, 1995). The proximal promoter of VCAM-1 contains two NF κ B binding sites, an Sp1 site and an interferon regulatory factor (Fitzgerald *et al.*, 2003) element within the proximal promoter (Collins *et al.*, 1995). TNF α and Vascular Endothelial Growth Factor (VEGF) induction of VCAM-1 requires the presence of the two NF κ B binding sites (Collins *et al.*, 1995; Min *et al.*, 2005).

1.6 Interactions between *N. meningitidis* and the vascular endothelium

1.6.1 Mechanisms of bacterial invasion of the endothelium

Pili mediate bacterial adherence to endothelial cells (Virji *et al.*, 1991; Virji *et al.*, 1992a) (Section 1.3), and increased adhesion of bacteria is correlated to increased endothelial cell damage (Virji *et al.*, 1991). Expression of Opa and Opc on the bacterial cell surface then leads to firm adhesion and invasion of endothelial cells (Virji *et al.*, 1992b; Virji *et al.*, 1993a; Virji *et al.*, 1994), by interacting with vitronectin, an integrin expressed on the endothelial cell surface (Virji *et al.*, 1992a; Virji *et al.*, 1995), as well as heparin sulphate proteoglycans (Chen, *et al.*, 1995; de Vries *et al.*, 1998). Opa proteins interact with and stimulate expression of carcinoembryonic antigen-related cell adhesion molecule 1 (CEACAM-1/CD66a) on cytokine stimulated endothelial cells (Muenzner *et al.*, 2000; Muenzner *et al.*, 2001), and this binding facilitates invasion of endothelial cells by Opa expressing bacteria. Invasion of endothelial cells requires the activation of the ErbB2 receptor tyrosine kinase pathways, in collaboration with the reorganisation of the actin cytoskeleton (Hoffmann *et al.*, 2001; Eugene *et al.*, 2002). The actin cytoskeleton modifies itself by forming cellular protrusions which appear to engulf and internalise the bacteria (Eugene *et al.*, 2002).

1.6.2 Endothelial damage mediated by *N. meningitidis* LPS

Bacterial LPS is a strong mediator of endothelial cell damage during sepsis (Bannerman and Goldblum, 1999; Bannerman and Goldblum, 2003), inducing apoptosis of stimulated cells. However, whilst *N. meningitidis* LPS induces bacterial-mediated cytotoxicity of endothelial cells, it is independent of the LPS outer core (Jennings *et al.*, 1995) and dependent on pili mediated bacterial adhesion (Dunn *et al.*, 1995).

1.6.3 Endothelial dysfunction during meningococcal sepsis

Although bacterial LPS is believed to be the main cytotoxic component in inducing endothelial damage during sepsis, (Dunn *et al.*, 1995; Jennings *et al.*, 1995), there is evidence to show that there may be other mechanisms involved in endothelial cell dysfunction. These include increased levels of pro-inflammatory cytokines, particularly TNF α and IL-1 β (de Kleijn *et al.*, 1998); and adherence of neutrophils (Bratt and Palmblad, 1997) inducing the release of superoxide anions, hydrogen peroxide and granule enzymes, which target the endothelial cell wall (Varani and Ward, 1994).

Neutrophil binding to endothelium is mediated by adhesion molecules. Skin sections through septic skin show persistent expression of E-selectin, ICAM-1 and VCAM-1 (Klein, personal communication) (Figure 1.17), and *N. meningitidis* activates the expression of these adhesion molecules on the endothelium *in vitro* (Dixon *et al.*, 1999) demonstrating that endothelial activation and increased adhesion molecule expression on the cell surface may play a crucial part in sepsis induced multiple organ failure (Reinhart *et al.*, 2002).

1.7 Aim of PhD project



Figure 1.17 Characteristic purpuric skin rash (A), and skin section from purpuric (B) lesion. E-selectin expression on the vascular endothelium is indicated by the arrow.

1.6.3.1 The use of mutants to study interactions between *N. meningitidis* and the vascular endothelium

Unencapsulated *N. meningitidis* mutants are more potent endothelial adhesion molecule activators than the WT variant (Dixon *et al.*, 1999). Furthermore, the LPS-deficient capsulated mutant, *lpxA*⁻, is capable of activating adhesion molecule expression by endothelial cells (Dixon *et al.*, 2004), in particular E-selectin expression, which is of a similar magnitude as WT induction. It is as yet unclear by which transcription pathway this activation is controlled, as high levels of NF κ B are detected in response to WT bacteria (Dixon *et al.*, 2004; Muenzner *et al.*, 2001), but not in response to the *lpxA*⁻ mutant (Dixon *et al.*, 2004). *N. meningitidis* also activate the MAPK signalling pathway (Sokolova *et al.*, 2004). The activation of JNK is correlated with the invasion of endothelial cells by bacteria, whereas the activation of p38 is involved in the expression of IL-6 and IL-8 by endothelial cells (Sokolova *et al.*, 2004). The NF κ B and JNK pathways are both activated in response to *N. gonorrhoeae* on epithelial cells (Naumann *et al.*, 1997; Naumann *et al.*, 1998).

1.7 Aim of PhD project

The aim of this PhD project is to investigate mechanisms by which *N. meningitidis* controls E-selectin gene expression, by using purified LPS, a WT clinical isolate (Serogroup B H44/76), and an isogenic LPS-free mutant (*lpxA*⁻). Different aspects of E-selectin gene regulation will be examined. In particular:

1. To explore the upregulation of adhesion molecules induced by *N. meningitidis*, and to investigate the endothelial response to live and paraformaldehyde killed bacteria and the kinetics of adhesion molecule expression on endothelium.
2. To develop a Real-Time PCR assay for the detection of adhesion molecule mRNA levels and to explore whether adhesion molecules are controlled by transcriptional or post-transcriptional/translational mechanisms.
3. To optimise a transfection methodology for primary human endothelium.
4. To investigate E-selectin promoter activity mediated by *N. meningitidis*. The E-selectin promoter will be examined in detail for responsive elements to *N. meningitidis*. Deletion mutants will be utilised to explore LPS dependent and independent signalling leading to E-selectin promoter activity.

Chapter 2

Materials and Methods

2.1 Reagents

Table 2.1 General Reagents

Name	Company	Product code
10x Tris-borate-EDTA (TBE)	Sigma	T4415
Accutase	PAA labs	L11-007
Ampicillin	Sigma	A0166
Attachment Factor	TCS Cell Works	ZHS-8949
Bio-Rad Protein Assay Dye Reagent Concentrate	BioRad	500-0006
Bovine Serum Albumin (BSA)	Sigma	A4503
Cell fix	BD	340181
Collagenase Type II	Invitrogen	17101-015
DMEM with L-glutamine, 4500mg/L, D glucose	Invitrogen	41965-039
Dimethylsulphoxide (DMSO)	Sigma	D2650
E. coli LPS, O111B:4, gel purified	Sigma	L3012
Endothelial Cell Attachment Factor (ECAAF)	Sigma	E9765
Endothelial Cell Growth Supplement (ECGS)	PromoCell	C-30180
Epidermal Growth Factor (EGF)	R&D Systems	236-EG-01M

Ethylenediaminetetraacetic acid disodium salt (EDTA)	BDH	100935V
Ethanol	Hayman	UN1170/200-578-6
Foetal Calf Serum (FCS)	Invitrogen	10270-106
Formaldehyde	Sigma	P6148
Fungizone (Amphotericin B)	Invitrogen	15290-026
Gonococcal agar (GC agar)	BD	211275 (4311275)
Interleukin-1 β (2x10 ⁵ IU/ μ g)	R&D Systems	201-LB-005
Isopropanol, molecular biology grade	Sigma	I9516
Kanamycin	Sigma	K0879
L-glutamine	Invitrogen	25030-024
Lipofectin	Invitrogen	18292-011
Low Multiplate 96 well polypropylene microplates- white	GRI	MLL9651
MCDB 131	Invitrogen	10372-019
Nuclease-free H ₂ O	Severn Biotech Ltd	20-9000-01
Optical flat caps, 8 per strip	GRI	TLS-0851
OptiMEM®-1	Invitrogen	31985-047
Paraformaldehyde (PFA)	Sigma	P6148
PBS tablets	Oxoid	BR0014G
Penicillin / Streptomycin	Invitrogen	15140-114
Phorbol 12-myristate 13-acetate (PMA)	Sigma	P1585

Recombinant Human Epidermal Growth Factor (EGF) (2×10^5 IU/mg)	Invitrogen	13247-051
RPMI 1640 (10x) without L-glutamine with NaHCO_3	Invitrogen	22511-026
RPMI 1640 with L-glutamine and 25mM HEPES	Invitrogen	52400-041
RPMI 1640 without L-glutamine and phenol red	Invitrogen	32404-014
Sodium Azide (NaN_3)	BDH Merck	10369
Sodium Butyrate (SB)	Sigma	B5887
24 well tissue culture (TC) plates	Corning	3527
25cm ² TC flasks, Primaria	Becton Dickinson	35-3824
48 well TC plates	Corning	
96 well TC plates	Corning	
Trichostatin A (TSA)	Sigma	T8552
Vitox	Oxoid	SR090A
White polystyrene 96 well luciferase assay plates	Porvair Sciences Ltd	204003

Table 2.2 Molecular Biology Reagents, Enzymes and Kits

Name	Company	Product code
2-mercaptoethanol	BioRad	161-0710
Agarose	Invitrogen	15510-027
AmpliTaq Gold	Applied	N808-0241
Bgl II	Promega	R6081
Coelentrastine	Insight	10010-1
DH5 α -E Electro-competent cells	Invitrogen	11310-019
100 mM dNTP set, PCR Grade	Invitrogen	10297-018
EndoFree Plasmid Maxi-kit	Qiagen	12362
Glycerol (molecular biology grade)		
HindIII	Promega	R6041
iQ SYBR Green super mix	BioRad	170-8880
JM109 High Efficiency competent cells	Promega	L2001
LB agar	Merck	1.10283
LB broth	Merck	1.10285
Luciferase Assay system Freezer 10-Pack	Promega	E4530
Luciferase Assay system Freezer Pack	Promega	E1501
Nuclease Free dH ₂ O	Severn Biotech Ltd	20-9000-01
Oligonucleotide PCR primers	Sigma Genosys	

Peptides	Zinsser Analytic, Alta Biosciences, or Department of Chemistry, University College London	
pGEM-T Easy Vector	Promega	A1360
phRL-TK vector	Promega	E6241
Picagene vector	Toyo Ink, Japan	Obtained from Dr. Narumi (Tamaru and Narumi, 1999)
QIAprep spin miniprep kit	Qiagen	27104
QIAquick Gel Extraction kit	Qiagen	28704
RNeasy Protect Mini-kit	Qiagen	74124
RT-PCR iScript cDNA synthesis kit	BioRad	170-8890
Taq Polymerase	Invitrogen	18038-026
25 base pair (bp) DNA ladder	Promega	G4511
100 bp DNA ladder	Promega	G2101

Table 2.3 Antibodies

Antibody	Supplier	Product code
Goat anti-mouse IgG phycoerythrin (PE) conjugate	Dako	R0490
Mouse anti rat IgG2b (mouse IgG1) negative control	Serotec	MCA195
Mouse anti-human CD31 antibody (mouse IgG1)	Serotec	MCA1738
Mouse anti-human CD62E antibody (mouse IgG1)	Serotec	MCA883
Mouse anti-human ICAM-1 (mouse IgG1)	Serotec	MCA532
Mouse anti-human VCAM-1 (mouse IgG1)	Serotec	MCA907

Table 2.4 General Buffers/solutions

Buffers	Components
Phosphate-buffered Saline (PBS) -Prepared using manufacturers instructions. One tablet of PBS (Oxoid) per 100ml milliQ H ₂ O	137 mM NaCl 2.7 mM KCl 8 mM Na ₂ HPO ₄ 1.5 mM KH ₂ PO ₄
Puck's A Saline with EDTA, FCS and phenol red	0.4 g/L KCl 8 g/L NaCl 0.35 g/L NaHCO ₃ 1 g/L glucose 0.2 % EDTA 10 % FCS 0.005 g/L phenol red
Tris-borate-EDTA (TBE) - prepared 1x TBE by diluting 100 ml 10x TBE (Gaynor et al., 1988) in 900 ml milliQ H ₂ O	45 mM Tris-borate 1 mM EDTA
FACS Wash/Buffer	1x PBS 0.02% Sodium Azide 5% FCS

2.2 Methods

2.2.1 Endothelial Cell Culture

2.2.1.1 Choice of Endothelial Cell type

Endothelial cells line the vasculature and lymphatics, and can be sourced from a variety of tissues, including lung, kidney, bone marrow, skin, saphenous vein, gut and umbilical cords (Bachetti and Morbidelli, 2000;Bicknell, 1996). Although endothelial cells obtained from a range of tissues have been shown to be heterogeneous in their response to different stimuli (Muller *et al.*, 2002b;Bachetti and Morbidelli, 2000;Manconi *et al.*, 2000), HUVEC, large vessel primary endothelial cells, demonstrate properties which are observed in both large vessel and microvascular endothelial cells (Bicknell, 1996). HUVEC are the most readily available source of endothelial cells as umbilical cords are a redundant post-natal tissue. They are therefore the predominant source used to investigate endothelial cell function. It has been reported that HUVEC phenotypic responses to stimuli correspond to *in vivo* observations on the macrovascular and microvasculature endothelium (Muller *et al.*, 2002b;ten Kate *et al.*, 2004).

There may be several disadvantages for using HUVEC as an endothelial cell model. Firstly, HUVEC are large vessel endothelial cells, whereas some of the interactions that are being studied occur mainly in the microvasculature. Second, the main structural difference between HUVEC and brain endothelial cells is the fact that they have GAP junctions, whereas brain endothelial cells have tight junctions. These differences may

be important when mediating leukocyte transmigration, and there may therefore also be differences in the regulation of gene expression and response to different stimuli.

There are several endothelial cell lines available, such as the human microvascular endothelial cell line (HMEC-1). However, immortalised endothelial cells have been shown to lose a number of primary cell characteristics and demonstrate responses that are similar to fibroblasts (Bicknell, 1996). In addition, HMEC-1 do not express E-selectin in response to inflammatory mediators, and have a very weak VCAM-1 responses to TNF α and no response to IL-4 and IL-13 (Kotowicz, personal communication). This may be due to loss of cytokine receptor expression due to continuous cell cycling. Primary endothelial cells are largely quiescent, and divide approximately twice in an adult lifetime (Bicknell, 1996). These observations suggest that responses demonstrated by HMEC-1 do not reflect those of primary cells.

As the gene of interest for this thesis is E-selectin, and endothelial cell lines do not express this molecule, it was important to use a primary endothelial cell source. HUVEC were selected due to the ease of preparation and plentiful source.

2.2.1.2 HUVEC Growth and Culture Media

Growth of endothelial cells requires media rich in amino acids, vitamins, carbohydrates and salts, and high concentrations of FCS, which best reflect the components of serum *in vivo*. MCDB 131 is a media which has been developed specifically for the growth of endothelial cells in culture. Generally, media was kept at 4°C for no longer than 1 month once supplements were added. Frequent warming of the media to 37°C was

avoided by keeping 50ml volume aliquots of working stock solution at 4°C. For experiments where confluent cell monolayers were used, cells were rested in RPMI 1640 media to allow the cells to become quiescent. Resting media was treated in the same manner as endothelial growth media.

1. HUVEC Growth Medium (GM)

For the growth of HUVEC, MCDB 131 was supplemented with 10mM L-glutamine, 100 units/ml penicillin/streptomycin, 0.25µg/ml Amphotericin B and 20% FCS. For the growth of HMEC-1 cells, MCDB 131 was supplemented with 10mM L-glutamine, 100 units/ml penicillin/streptomycin and 10% FCS.

2. Resting Medium-Killed (RMK)

For experiments where PFA killed bacteria were used, HUVEC were rested in RPMI 1640 media supplemented with 10mM L-glutamine, 100 units/ml penicillin/streptomycin and 20% FCS.

3. Resting Medium-Live (RML)

Experiments with live bacteria required the absence of antibiotics in the resting media. In these experiments HUVEC were kept in RPMI 1640 medium supplemented with 10mM L-glutamine and 20% FCS.

4. Cord Preparation Medium (CPM)

Umbilical cords were collected and prepared in RPMI 1640 medium supplemented with 100 units/ml penicillin/streptomycin, 10mM L-glutamine and 2.5µg/ml Amphotericin B.

5. Wash Medium (WM)

To remove blood residue from cords and prepared HUVEC, cells were washed in RPMI 1640 supplemented with 10mM L-glutamine, 100 units/ml penicillin/streptomycin.

6. Super Medium (SM)

For transfection experiments with E-selectin promoter, the use of SM improved Luciferase output. SM media was prepared by supplementing MCDB 131 with 10% FCS, 2ml of ECGS, and 200µl EGF (100µg/µl stock).

2.2.1.3 Choice of FCS

The quality of FCS was of particular importance for optimal growth conditions of HUVEC. Problems were encountered during the study due to poor quality FCS. High quality FCS batches were screened for HUVEC growth, low background levels of endotoxin, as well as E-selectin dose responses to LPS and WT *N. meningitides*. FCS was selected initially based on HUVEC growth, low levels of endotoxin (as determined

by E-selectin background levels) and consistent endothelial cell responses to inflammatory mediators. Low E-selectin background levels was generally a better indicator of low levels of endotoxin contamination than the manufacturers own specs, as E-selectin levels increase with endotoxin levels as low as 0.01ng/ml. Therefore if there were no E-selectin background levels, FCS was said to have endotoxin levels of <0.01ng/ml. FCS was also selected on the basis of reproducible results. A problem arose with a batch that was tested, which allowed for optimum endothelial growth and induced no E-selectin expression in control conditions. However, experiments were not reproducible. High levels of E-selectin expression were at times obtained with low levels of LPS, however, this did not occur consistently. Therefore, FCS was selected on the basis of good endothelial cell growth, no induction of E-selectin expression during control conditions, as well as producing reproducible data. One FCS batch was selected and ordered in bulk for the whole project and kept at -20°C. Prior to use, FCS was heat inactivated at 56°C for 30 minutes and aliquots kept at -20°C until required. Once defrosted, FCS was filtered through at 0.22µm pore filter and kept at 4°C for no longer than 1 month.

2.2.1.4 Endothelial Cell preparation from umbilical cords

Preparation of endothelial cells from umbilical cords was performed as previously described by Kotowicz *et al.* (2000). Ethics approval for the collection of umbilical cords from West Middlesex Hospital, London, was obtained for the Hounslow and Hillingdon Local Research Ethics Committee (Ref. No. 02/712/SV). Umbilical cords were obtained from West Middlesex Hospital, London. Patient consent was obtained at the antenatal clinic for the use of the umbilical cord for scientific research. Cords were

collected in CPM in autoclaved polypropylene bottles, and kept at 4°C for a maximum of 24 hours until processing. Cords were collected on a regular basis, and extraction of HUVEC was generally done no more than 72 hours post-delivery. For cell preparation, cords were removed from the collection bottle, drained of clotted blood and thoroughly washed on the outside with 70% IMS (Figure 2.1). Cords were then washed in fresh CPM to remove excess blood and wash away residual IMS and the ends (5 cm) were cut off to exclude IMS killed endothelial cells and bacteria. The vein was identified and cannulated, and then washed through with CPM. Cells were disassociated from the vessel wall by infusing with warm 0.1% Collagenase Type II in DMEM for 10 minutes at 37°C in 5% CO₂ in air. Cells and collagenase medium were flushed from the cord and collected in a sterile bottle. The vein was then flushed with CPM with 5% FCS and pooled with cell and collagenase collection. The cell extract was centrifuged at 200g for 5 minutes at room temperature, and the supernatant was discarded. Cells were resuspended in GM and seeded on 25cm² flasks coated with attachment factor and grown at 37°C in 5% CO₂ in air.

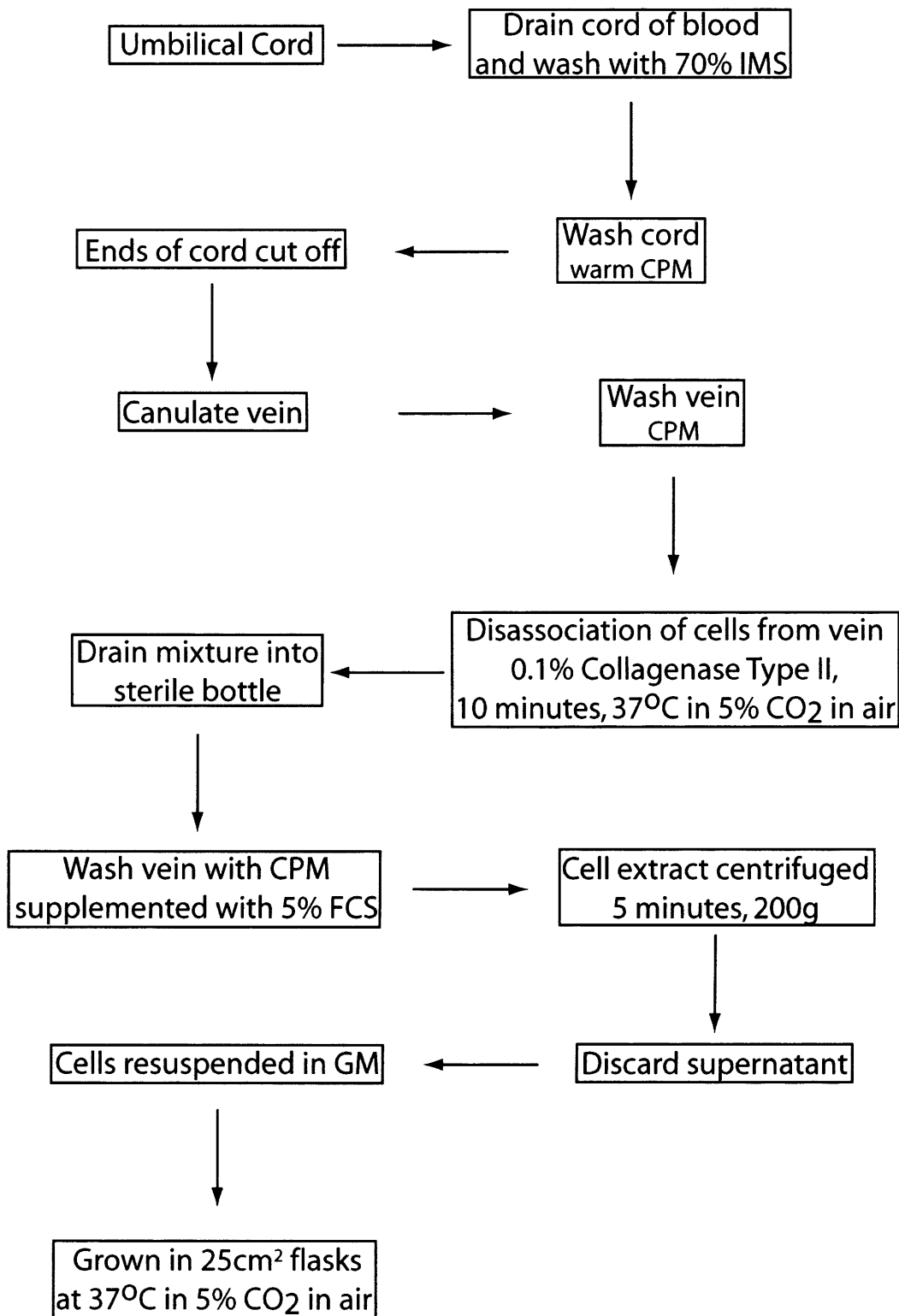


Figure 2.1 Flow chart illustrating preparation of HUVEC from umbilical cords.

2.2.1.5 Verification of Endothelial Cell culture

Verification of endothelial cell culture was determined both morphologically and phenotypically. Endothelial cells were seen to display a typical ‘cobble-stone’ appearance *in vitro* (Figure 2.2). Endothelial cells surface binding of PECAM-1 (CD31) antibody (Figure 2.3) was also performed to verify endothelial cell culture. Although PECAM-1 is expressed on a number of non-adherent lymphoid cells (*e.g.* Neutrophils), it is a specific marker and present in high numbers on primary endothelium. PECAM-1 is therefore a good marker for the verification of endothelial cells in culture.

Figure 2.3 PECAM-1 (CD31) expression in HUVECs as detected by FACS analysis.

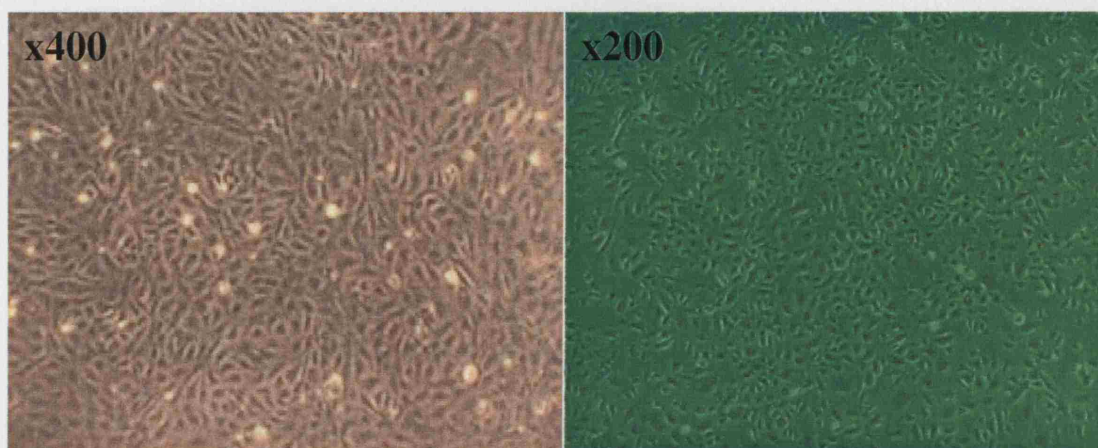


Figure 2.2 Microscopic verification of endothelial cell culture. Images were obtained with an inverted microscope. The image on the left hand side panel was obtained by photographing the endothelial cells through a green filter.

Cells were incubated with the IgG isotype control were negative and found within the first log decade (Figure 2.3C).

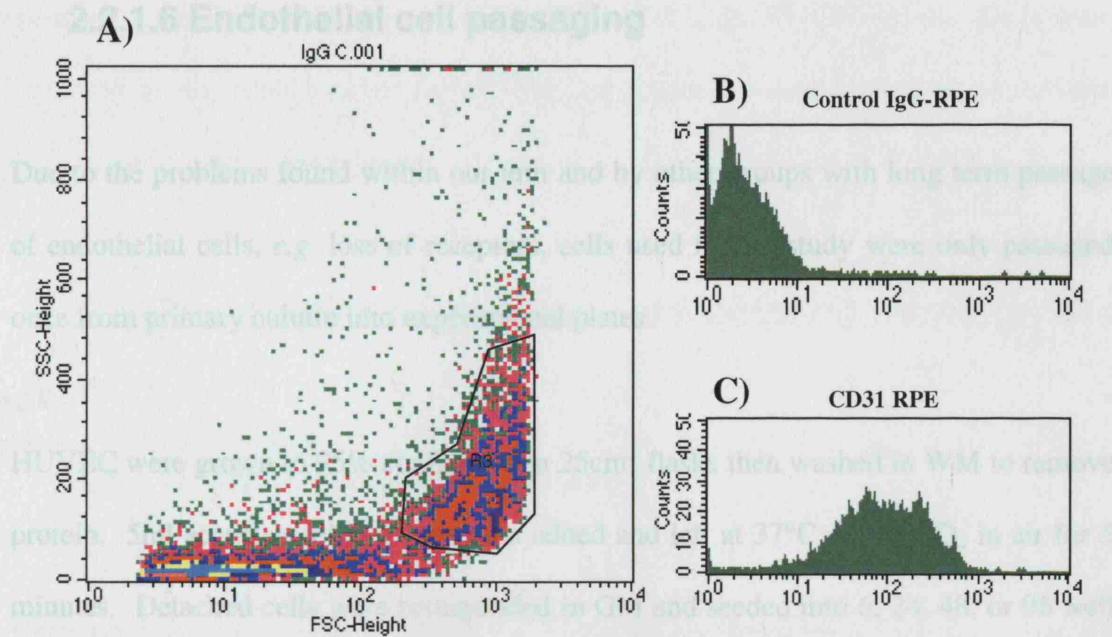


Figure 2.3 PECAM-1 (CD31) expression on HUVEC as detected by FACS analysis.

Endothelial cells were identified by FACS using forward scatter (FSC; size) and side scatter (SSC; complexity and granularity) characteristics (A) endothelial cells identified by gate (R3); (B) control antibody; (C) anti-CD31 (PECAM-1).

Figure 2.3A demonstrates a typical FACS plot of endothelial cells. The endothelial cells, which are large cells, are those found on the right hand side of the plot with a smear leading upwards on the SSC scale. The dots found on the left hand side of the R3 endothelial gate represents debris, dead cells, and smaller cells isolated as part of the endothelial preparation process from the umbilical cord. Cells in this gate (R3) were 98% positive for CD31, indicating a highly purified endothelial cell population (Figure 2.3B). Cells incubated with the IgG isotype control were negative and found within the first log decade (Figure 2.3C).

2.2.1.6 Endothelial cell passaging

Due to the problems found within our unit and by other groups with long term passage of endothelial cells, *e.g.* loss of receptors, cells used in this study were only passaged once from primary culture into experimental plates.

HUVEC were grown to 95% confluence in 25cm² flasks then washed in WM to remove protein. 5ml accutase solution was then added and left at 37°C in 5% CO₂ in air for 5 minutes. Detached cells were resuspended in GM and seeded into 6, 24, 48, or 96 well plates as required. The seeding ratio was usually one 25cm² flask for 1-1½ tissue culture plates, depending on the growth vigour of the cells, which was donor dependent.

For cells used to detect adhesion molecule cell surface and mRNA levels (See Chapters 3 and Chapter 4), secondary culture plates were grown to confluence over 3-7 days and GM was changed every 2-3 days. Once the cells had reached confluence, they were rested in RMK or RML, depending on experimental design. Cells used for transfection experiments (see Chapters 5 and Chapter 6) were grown in GM or SM overnight prior to transfection.

2.2.2 HMEC-1 Growth and Culture Media

HMEC-1 were obtained from the European Collection of Cell Cultures (ECACC). These cells are dermal endothelial cells transformed by simian virus 40 (SV40). HMEC-1 were grown under similar conditions as HUVEC. Cells were grown in MCDB 131 supplemented with 100 units/ml penicillin/streptomycin, 10mM L-

glutamine, and 10% FCS (referred to as GM) at 37°C in 5% CO₂ in air. Cells were passaged in the same manner as HUVEC using accutase and seeded on attachment factor coated tissue culture plates.

2.3 Growth and preparation of *Neisseria meningitidis*

2.3.1 *N. meningitidis* strains used

Bacterial strains used in this study were developed and provided by Dr. Peter van der Ley (RIVM, Bilthoven) and Dr. Liana Steeghs (University Medical Centre Utrecht, the Netherlands).

2.3.1.1 *N. meningitidis* B H44/76

The *N. meningitidis* WT strain used in this study is referred to as H44/76 (Rahman *et al.*, 1998)-type (B:15:P1.7,16), ET-5 complex). This strain was isolated from a fatal human septicaemia case in Norway (Holten, 1979).

2.3.1.2 *N. meningitidis* B H44/76 *lpxA*- isogenic mutant

A viable LPS-free isogenic mutant (*lpxA*-) of the H44/76 WT strain was developed by inactivating the *lpxA*- gene with a kanamycin cassette (Steeghs *et al.*, 1998). The protein product of the *lpxA* gene is involved in the first committed step in the lipid A biosynthesis pathway, and inactivation of the gene prevents the synthesis of bacterial

LPS. The lack of LPS on the bacterial cell wall has been confirmed by Limulus amoebocyte lysate (LAL) assay, gas chromatography/mass spectrometry and whole cell ELISA using LPS specific monoclonal antibodies (Steeghs *et al.*, 1998). WT and *lpxA*- bacteria demonstrate similar binding patterns to monoclonal antibodies for OMPs (Steeghs *et al.*, 1998). Although the assembly of core OMPs is unaffected by the *lpxA*- gene mutation (Steeghs *et al.*, 2001), the LPS-free mutant is only viable in the presence of capsular polysaccharide. The *lpxA*- mutant bacteria shows some evidence of PorA degradation. This is not seen in the WT bacteria (Steeghs, *et al.*, 2002-792). As the *lpxA*- bacteria contains no LPS, this may allow for proteases to have access to and break down OMPs. Furthermore, the *lpxA*- bacteria grows slower than WT bacteria. Purity of the *lpxA*- mutant bacteria was maintained by growth on kanamycin supplemented GC agar plates (100µg/ml).

2.3.2 *N. meningitidis* culture and preparation

Live *N. meningitidis* strains used in this study were cultured and manipulated in a Class I safety cabinet within a category 3 containment facility under negative pressure at the Great Ormond Street Hospital for Children (London, UK). Bacteria were stored at -80°C in Mueller-Hinton broth with 15% glycerol. Bacteria were grown from frozen stock in freshly prepared GC agar plates supplemented with Vitox growth medium, and kept at 35°C in 5% CO₂ in air. As the *lpxA*- mutant bacteria grew more slowly than the WT, it was important that bacteria were used at the stationary phase, and bacteria were therefore used after 16-18 hours of growth (G. Dixon, personal communication).

For experiments requiring live bacteria, bacterial colonies were collected with a sterile cotton swab and suspended in warm RPMI media without phenol red. PFA killed bacteria were prepared by collecting several colonies of bacteria as above and suspended in warm RPMI (without phenol red) supplemented with 0.5% PFA. The bacterial suspension was carefully washed three times with warm RPMI without phenol red.

For both live and PFA killed bacteria, optical density of the bacterial suspension was measured by spectrophotometry at an OD_{540nm}, and the bacterial suspension was adjusted to give a reading of 1. It has been demonstrated that by serial dilutions, plating and viable counts, a suspension of *N. meningitidis* bacteria at stationary phase with an Optical Density (OD) of 540nm (OD_{540nm}) of 1 contains 10⁹ colony forming units per ml (CFU/ml) (Dr. G. Dixon, personal communication).

2.4 Preparation of LPS from *N. meningitidis*

Meningococcal LPS from *N. meningitidis* serogroup B strain H44/76 was prepared by Dr. Liana Steeghs (University Medical Centre, Utrecht, The Netherlands) by hot aqueous phenol extraction, ultra-centrifugation, gel filtration and cold ethanol NaCl gonococcal precipitation. The final product contained <0.3% protein and undetectable nucleic acids (Andersen *et al.*, 1995).

2.5 Surface Immunostaining of HUVEC

Following experimental stimulation of HUVEC, cell media was discarded and cells washed with Puck's A saline with additions (Figure 2.4). Cells were incubated with Puck's A saline for 20 minutes at 37°C in 5% CO₂ in air then removed mechanically and transferred to FACS tubes. HUVEC were then washed with FACS buffer and centrifuged at 200g for 5 minutes at room temperature. The supernatant was discarded and cells were resuspended and incubated with primary antibody for 10 minutes at room temperature before washing with FACS buffer. Cells were centrifuged as above, supernatant discarded, cells were resuspended and incubated with secondary antibody for 10 minutes at room temperature in the dark. Cells were washed with FACS buffer, centrifuged, and resuspended with 1x Cell fix (BD) and kept at 4°C in the dark until FACS acquisition. Generally, FACS acquisition was performed no more than one day after experimental procedure.

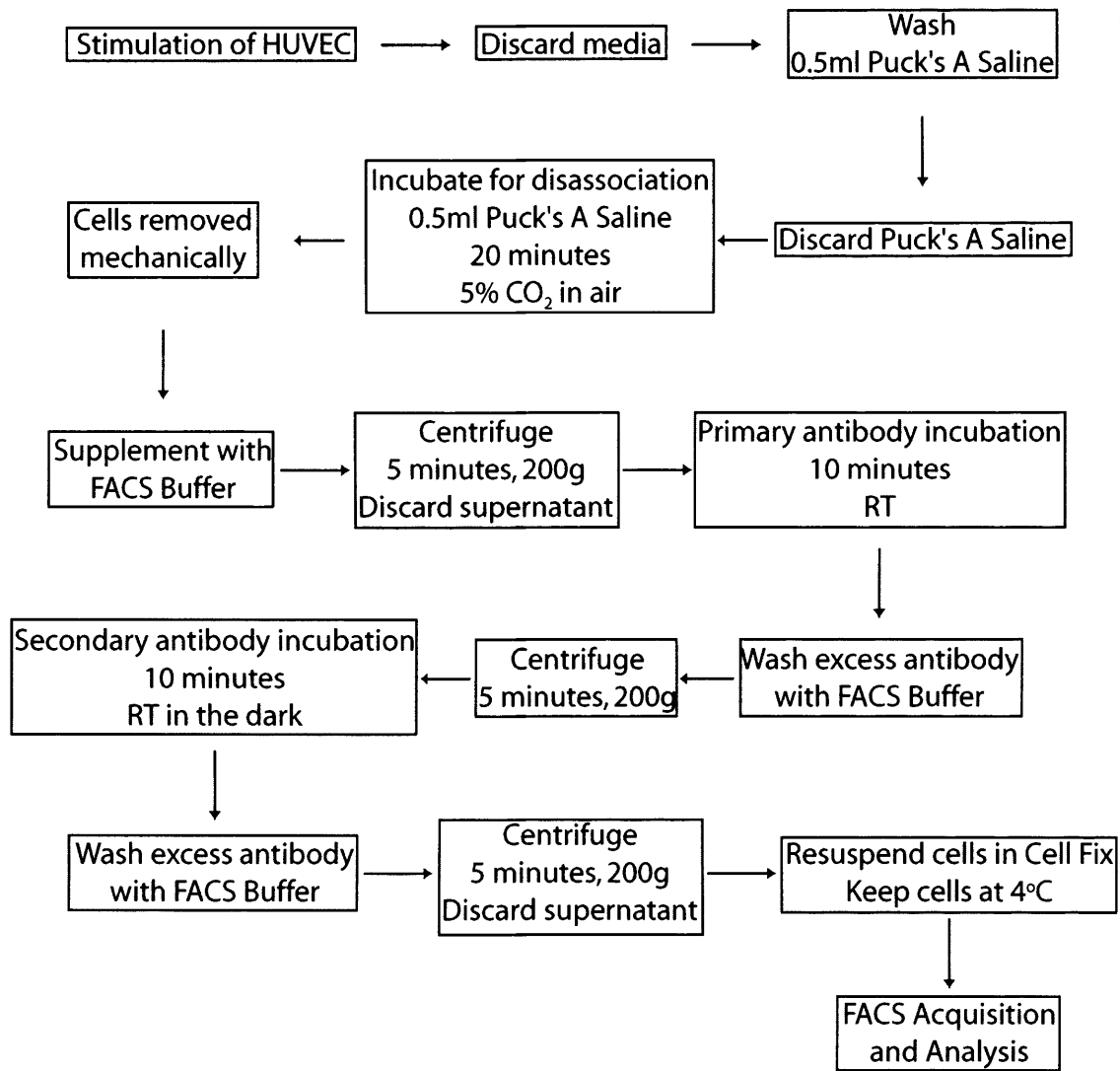


Figure 2.4 Flow chart illustrating the methodology for surface staining of adhesion molecules on HUVEC.

2.6 Flow Cytometry and FACS analysis

Data was acquired from fixed HUVEC and analysed using FACScan (BD) flow cytometer and CellQuest (BD) software. Endothelial cells were gated for as in Section 1.2.1.5 (Figure 2.3), and 5000 events were collected. FACSCalibur acquisition settings are shown in Table 2.5.

Table 2.5 Flow cytometry settings for endothelial cell detection.

Detector	Voltage	Amp gain
Forward Scatter	E-1	1.00
Side Scatter	347	1.00
Fluorescence-2 (PE)	417	1.00

2.7 mRNA extraction and cDNA synthesis reaction

mRNA was extracted using the RNeasy Protect Mini-Kit (Qiagen), and the protocol was followed according to manufacturers instructions. Total RNA was eluted in 30µl of nuclease-free H₂O and stored at -80°C. On average, 15 µg total RNA was extracted from 1x10⁶ cells. Following mRNA extraction, 5 µg of total RNA was used for cDNA synthesis using iScript cDNA synthesis kit (BioRad) in a final volume of 20µl. The iScript cDNA synthesis kit contains the iScript Reverse Transcriptase enzyme and an optimal reaction buffer containing dNTPs, oligo d(T) primer and random hexamer primers (details of concentrations not provided by manufacturers). The reaction carried

out in 20 μ l final volumes. Reactions were incubated for 5 minutes at room temperature for primer annealing, followed by 30 minutes at 42°C for cDNA synthesis, and finally for 5 minutes at 85°C to inactivate the enzyme. After cDNA synthesis, the solution was made up to 40 μ l and stored in 20 μ l aliquots at -20°C.

2.8 PCR reaction conditions and RT-PCR cycling conditions

PCR reactions were carried out in 25 μ l or 50 μ l reaction volumes using AmpliTaq Gold (Dunoyer-Geindre *et al.*, 2002). Manufactures instructions were followed. Briefly, PCR reactions using 1 μ l cDNA were carried out at a 1x concentration of reaction buffer supplemented with 2.5mM MgCl₂, 0.2 mM dNTPs, 1 unit of *Taq* polymerase, and 0.5 μ M of each primer. Reactions were made up to 25 or 50 μ l reactions using nuclease-free H₂O. The PCR reaction was carried out on a Peltier Thermal Cycler PCR machine (MJ Research) using the conditions described on Table 2.6.

Table 2.6 Cycling conditions for RT-PCR reaction

Step	Temperature	Time	Cycles
Initial Denaturation	95°C	10 min	1
Denaturation	95°C	1 min	30
Annealing	60°C	1 min	
Extension	72°C	1 min	
Fluorescence measure	75°C	1 sec	
Melt Curve	55-95.1°C every 0.3°C	1 sec	

2.8.1 Real-Time PCR reaction conditions and cycling conditions

DNA template was amplified using iQ SYBR Green Supermix (BioRad), containing optimum PCR reaction buffer with dNTPs, *Taq* DNA polymerase, and SYBR Green 1, and following manufacturers instructions with some modifications. Briefly, reactions were carried out in 10 μ l volumes using 1 μ l template DNA in 1x iQ SYBR Green Supermix (2x Supermix contains 100mM KCl, 40mM Tris-HCl (pH 8.4), 0.4mM dNTPs (dATP, dCTP, dGTP, and dTTP), i*Taq* DNA polymerase (50 units/ml), 6mM MgCl₂, SYBR Green I, 20 nM fluorescein, and stabilisers). Primers were added at a final concentration of 0.5 μ M. The reaction parameters are shown in Table 2.7. Reactions were performed in duplicate using the MJ Opticon Real-Time PCR instrument (GRI). At the end of the assay, melt-curve analysis was performed. This was used to detect any variation in product size, and hence illustrate if more than one product was amplified.

Table 2.7 Cycling parameter conditions for Real-Time RT-PCR reaction

Step	Temperature	Time	Cycles
Initial Denaturation	95°C	15 min	1
Denaturation	95°C	30 sec	40
Annealing	60°C	30 sec	
Extension	72°C	30 sec	
Melting Temperature	79°C	10 sec	
Fluorescence measure	79°C	1 sec	1
Melt Curve	55-95.1°C every 0.3°C	1 sec	

2.9 Agarose gel electrophoresis

PCR products were viewed by agarose gel electrophoresis. Generally, 1.5% agarose was prepared with 1xTBE. Agarose was melted in a microwave, and a gel cast was prepared. The agarose was allowed to set for at least 1 hour. The set gel was placed into a gel tank containing 1xTBE, and samples were loaded with 6x loading buffer (Promega). Samples and an appropriate size standard were run at 80 volts until bands were resolved. Agarose gels were stained in 1xTBE containing ethidium bromide for 10 minutes, and viewed under UV light.

2.10 Preparation of plasmid DNA

Plasmids were transformed into competent JM109 (Promega) *E. coli* bacterial cells following manufacturers instructions. Positive colonies were grown in LB broth supplemented with 100µg/ml ampicillin and an aliquot of the bacterial culture was frozen at -80°C in 20% sterile glycerol solution. The remaining bacterial solution was used to purify plasmid DAN using Qiagen miniprep kit (Qiagen) or EndoFree Qiagen Maxiprep Kit (Qiagen). Constructs were screened by either restriction enzyme digest or by PCR using primers spanning the sequence of interest. Positive clones were sequenced and compared to the reference gene. DNA quantity was determined by UV spectrophotometry at an OD₂₆₀ and quality was measure as OD₂₆₀/OD₂₈₀≥1.8.

2.11 Transfection of Endothelial cells

2.11.1 Methodology of LID mediated transfection

Chapter 5 describes the development of the LID vector system for use in endothelial cell transfections. Briefly, lipid (Lipofectin, Promega) was combined with peptide, followed by DNA. The final peptide:DNA charge ratio was 7:1. Generally, Peptide 6 was used for LID mediated transfection. The order of the addition of compounds to the mixture is crucial for the LID vector preparation, and has previously been optimised (Hart et al., 1998). The transfection cocktail was made in OptiMEM®-1 reduced serum media. Cells were aspirated, and the transfection mix was added and left on the cells for 4 hours at 37°C 5% CO₂. Cells were then rescued in fresh growth media for HUVEC or HMEC-1 growth media for HMEC-1 overnight.

2.11.2 Luciferase Assay

Transfection reactions were terminated by transferring cells to ice and washing cells twice with ice cold 1x PBS. Cells were harvested in 30µl or 50µl 1x Reporter Lysis Buffer (RLB, Luciferase Assay System-Promega) and kept at -80°C until the luciferase assay was performed. Cells were defrosted on ice, and a 20µl volume was transferred to a white polystyrene 96 well luciferase assay plate (Porvair Sciences Ltd). Lysate and luciferase assay substrate were left at room temperature for 30 minutes to ensure the optimum temperature for the reaction. Luciferase activity was measured using the Luciferase Assay System (Promega) and a Luci-1 Luminometer (Anthos Ltd, Salzburg,

Austria). The machine injected 100 µl of substrate onto the sample well and read the luminescence after 15 seconds.

2.11.3 Protein Assay

For transfection efficiency experiments, transfection reactions were normalised by measuring the amount of protein in each transfected well. This would represent the number of cells present in the transfected well. The protein assay was done using 1xBio-Rad Protein Assay Dye Reagent. Briefly, a standard curve was made by diluting 0, 25, 50, 75, 100 and 125 mg of BSA in PBS. 20 µl of the standard or sample (obtained from the luciferase assay) was added to a flat-bottomed 96 well plate (Greiner Bio-One). 200 µl of 1x protein assay dye was added to the sample and left at room temperature for 10 minutes. The assay was read at OD₅₉₀ using the Luci-1 Luminometer (Anthos Ltd, Salzburg, Austria). Luciferase activity was expressed as Relative Light Units (RLU) per mg of protein (RLU/mg protein).

2.11.4 Renilla Assay

For experiments exploring the activity of the E-selectin promoter, another normalisation technique had to be utilised. Briefly, transfections were performed with both plasmid of interest and a control plasmid expressing Renilla luciferase. This normalises luciferase activity according to the transfection efficiency for each individual well. Renilla substrate was prepared in the following manner: 1mg of Coelenterazine was diluted in 1ml of ethanol and 20µl aliquots were stored in -80°C. Coelenterazine was diluted 1:500 in 1xPBS. A fresh mixture was required for renilla assay. Renilla assay was

performed as the luciferase assay. Briefly, 20µl of lysate was transferred to a white polystyrene 96 well luciferase assay plate (Porvair Sciences Ltd). Lysate and Renilla substrate were left at room temperature for 30 minutes prior to performing assay. Assays were performed on a Luci-1 Luminometer (Anthos Ltd, Salzburg, Austria). The machine injected 40µl of substrate onto the sample well and read the luminescence after 15 seconds. Luciferase activity was expressed as RLU/Relative Renilla Units (RRU).

2.12 Statistical analysis

Statistical analysis of the data was performed using the Graphpad Prism programme. Generally, the ANOVA test was used or paired student t-test, unless otherwise stated.

Chapter 3

***N. meningitidis* LPS dependent and independent activation of endothelial adhesion molecule expression**

3.1 Introduction

The first step in improving patient outcome in meningococcal disease involves a better understanding of FMS. Fulminant vascular damage is characteristic of FMS and meningococcal LPS is directly associated with vascular leakage observed during gram-negative bacterial induced sepsis (Bannerman and Goldblum, 1999). The mechanisms thought to underlie this response involve increased leukocyte rolling and activation on the vascular endothelium and the initial steps in leukocyte adhesion and diapedesis involve increased adhesion molecule expression by the endothelium.

Commercially available *E. coli* LPS has been used to study the sepsis model *in vitro* and *in vivo*. Meningococcal LPS differs from *E. coli* LPS by having only two to five sugar residues attached at the inner core (Kahler and Stephens, 1998), whereas *E. coli* LPS contains a core consisting of ten to twelve sugar residues and an O-specific chain, consisting of repeats of an oligosaccharide chain (Caroff *et al.*, 2002). LPS lacking the O-chain are referred to as 'rough' specified by the morphology of colonies produced by the bacteria. 'Smooth' LPS structures contain the O-chain, and produce 'smooth' looking colonies.

LPS is highly inflammatory, inducing the expression of inflammatory mediators by endothelium, such as cytokines, chemokines and adhesion molecules (Bannerman and Goldblum, 2003). LPS from different bacteria is able to induce differential immune responses, *e.g.* *E. coli* LPS and *Porphyromonas gingivalis* LPS induced different cytokine profiles in mice (Pulendran *et al.*, 2001). Furthermore, varied LPS structures from the same species are able to induce different cytokine responses in human

monocytes, as observed with smooth and rough LPS from *Brucella* species (Rittig *et al.*, 2003).

Whilst *N. meningitidis* LPS is known to be a potent inducer of adhesion molecule expression on endothelial cells, it has been demonstrated that other bacterial components may be involved in bacterial activation of adhesion molecule expression (Dixon *et al.*, 2004). Endothelial cell activation by *N. meningitidis* increases E-selectin, ICAM-1 and VCAM-1 expression (Dixon *et al.*, 1999). Adhesion molecule expression mediates binding of activated neutrophils to the endothelium, and this leads to endothelial damage (Klein *et al.*, 1996).

In order to understand the underlying mechanisms regulating endothelial activation and damage during meningococcal disease, it was necessary to optimise a model which would use and compare LPS induced adhesion molecule expression with induction by live and killed meningococcal bacteria.

3.1.1 Aims of Chapter 3

The aim of this chapter was to investigate the adhesion molecule profile of HUVEC in response to *N. meningitidis*, and in particular to determine:

- the optimal LPS dose needed to stimulate E-selectin, ICAM-1 and VCAM-1 expression.
- endothelial adhesion molecule expression profiles obtained with live *N. meningitidis* WT, purified LPS and the LPS-free mutant, *lpxA*-
- the optimal bacterial concentration required to stimulate adhesion molecule expression in response to PFA killed bacteria
- the optimal bacterial concentration required to stimulate adhesion molecule expression in response to PFA killed *lpxA* bacteria to further investigate the LPS-dependent and independent mechanisms governing endothelial adhesion molecules expression
- the kinetics of adhesion molecule expression by endothelial cells in response to WT and *lpxA*- bacteria and purified LPS

3.2 Materials and Methods

3.2.1 HUVEC culture and preparation for experiments

Details of endothelial cell isolation from umbilical cords, cell culture and maintenance of HUVEC are described in Chapter 2. Once HUVEC reached 95% confluence on primary plates, they were subcultured onto 24 well tissue culture plates coated with attachment factor, and grown until confluent. Cells were then rested in RMK medium for PFA killed bacterial experiments and in RML for live bacterial experiments for 24 hours.

3.2.2 Preparation of *N. meningitidis* bacteria

Bacteria were prepared as described in Chapter 2. For the experiments performed here, bacteria were grown overnight, subcultured once and grown for 16-18 hours. For live bacterial experiments (Section 3.3.3), bacteria were suspended in warm RPMI media without phenol red. For experiments using fixed bacterial, organisms were suspended in 0.5% PFA. Initial experiments described in this chapter utilized frozen (-80°C) stocks of PFA killed bacteria. Freshly grown, killed but not stored meningococci were used in later experiments. The OD₅₄₀ of bacterial solutions was adjusted to a reading of 1, equating to a bacterial concentration of 10⁹ CFU/ml.

3.2.3 Immunostaining

HUVEC immunostaining was described in Chapter 2. Briefly, cells were detached with Puck's A saline supplemented with EDTA and FCS, and collected by centrifugation. Cells were incubated with primary antibodies: CD62E (5µg/ml), CD54 (5µg/ml), CD106 (20µg/ml) and mouse IgG2b (20µg/ml) as negative control. Excess antibody was removed with FACS wash. 20µl fluorescently labelled Goat anti-mouse IgG (F(ab)₂)-PE was used as secondary antibody at a 1:20 dilution. Adhesion molecule expression levels were detected using FACS acquisition, as described in Chapter 2.

3.3 Results

3.3.1 *N. meningitidis* LPS is a potent activator of endothelial adhesion molecule expression on HUVEC

In order to establish the optimal dose of *N. meningitidis* LPS required to activate adhesion molecule expression on the surface of endothelial cells, HUVEC were stimulated with increasing concentrations of purified LPS from *N. meningitidis* H44/76. LPS increased E-selectin, ICAM-1 and VCAM-1 expression in a dose dependent manner. The three adhesion molecules were detected at 0.1ng/ml of LPS, rising to a maximum at 10ng/ml for all three adhesion molecules (Figure 3.1). Concentrations above 10ng/ml LPS did not further increase HUVEC adhesion molecule expression (data not shown). Resting HUVEC and cells stimulated with LPS doses <0.1ng/ml did not express E-selectin. ICAM-1 and VCAM-1 were constitutively expressed in unstimulated HUVEC.

A concentration of 10ng/ml of purified *N. meningitidis* was established as the optimal concentration for stimulating endothelial adhesion molecule expression.

3.3.2 *N. meningitidis* and *E. coli* LPS are potent activators of endothelial E-selectin expression on HUVEC

To compare purified *N. meningitidis* LPS in this system with a commercially available

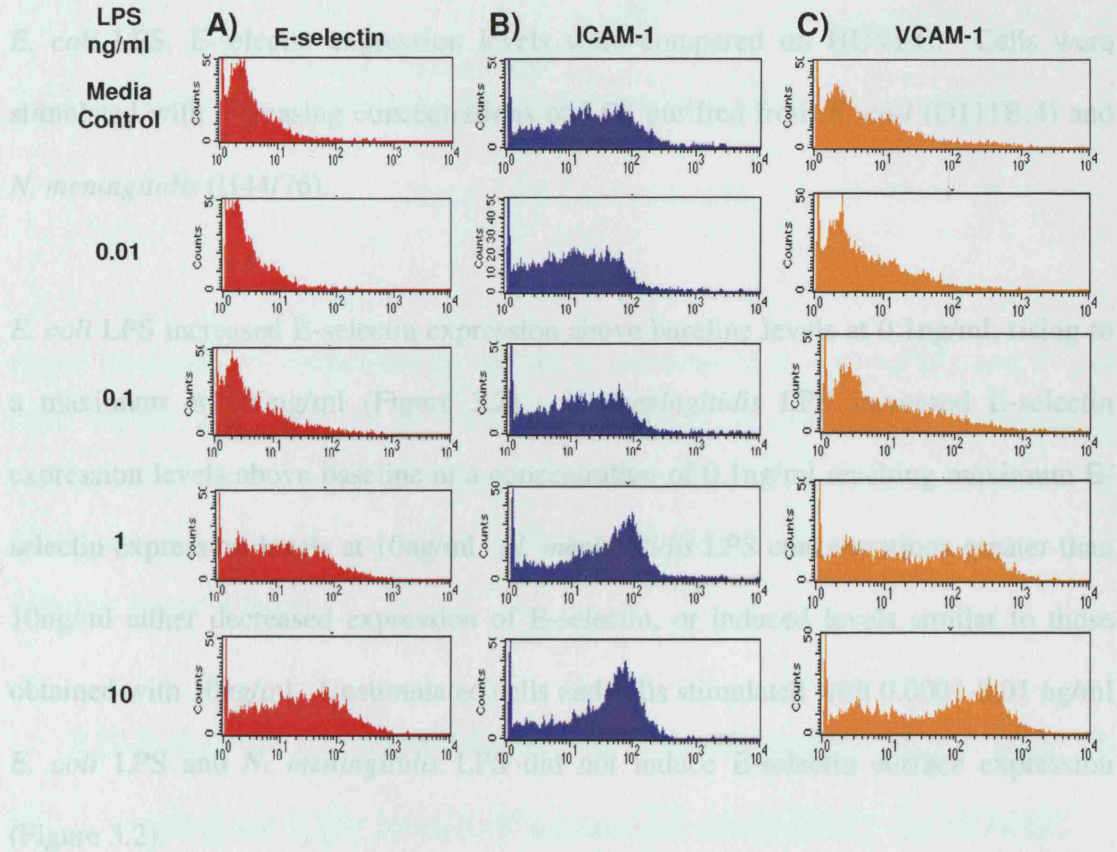


Figure 3.1 Adhesion molecule profiles on HUVEC in response to increasing concentrations of H44/76 *N. meningitidis* LPS. A representative experiment of HUVEC stimulated for 5 hours in response to increasing concentrations of purified LPS or with medium alone. A) E-selectin (■), B) ICAM-1 (■) and C) VCAM-1 (■).

LPS E-selectin induction. Furthermore, *N. meningitidis* LPS induced maximal E-selectin induction at a concentration which was 10-fold lower than *E. coli* LPS. *N. meningitidis* LPS was therefore 5-10 times more stimulatory than *E. coli* LPS in this system.

3.3.2 *N. meningitidis* and *E. coli* LPS are potent activators of endothelial E-selectin expression on HUVEC

To compare purified *N. meningitidis* LPS in this system with a commercially available *E. coli* LPS, E-selectin expression levels were compared on HUVEC. Cells were stimulated with increasing concentrations of LPS purified from *E. coli* (O111B:4) and *N. meningitidis* (H44/76).

E. coli LPS increased E-selectin expression above baseline levels at 0.1ng/ml, rising to a maximum at 100ng/ml (Figure 3.2). *N. meningitidis* LPS increased E-selectin expression levels above baseline at a concentration of 0.1ng/ml reaching maximum E-selectin expression levels at 10ng/ml. *N. meningitidis* LPS concentrations greater than 10ng/ml either decreased expression of E-selectin, or induced levels similar to those obtained with 10ng/ml. Unstimulated cells and cells stimulated with 0.0001-0.01 ng/ml *E. coli* LPS and *N. meningitidis* LPS did not induce E-selectin surface expression (Figure 3.2).

Interestingly, the half-maximum concentration of *N. meningitidis* LPS was approximately 5-fold higher than the half-maximum concentration required for *E. coli* LPS E-selectin induction. Furthermore, *N. meningitidis* LPS induced maximal E-selectin induction at a concentration which was 10-fold lower than *E. coli* LPS. *N. meningitidis* LPS was therefore 5-10 times more stimulatory than *E. coli* LPS in this system.

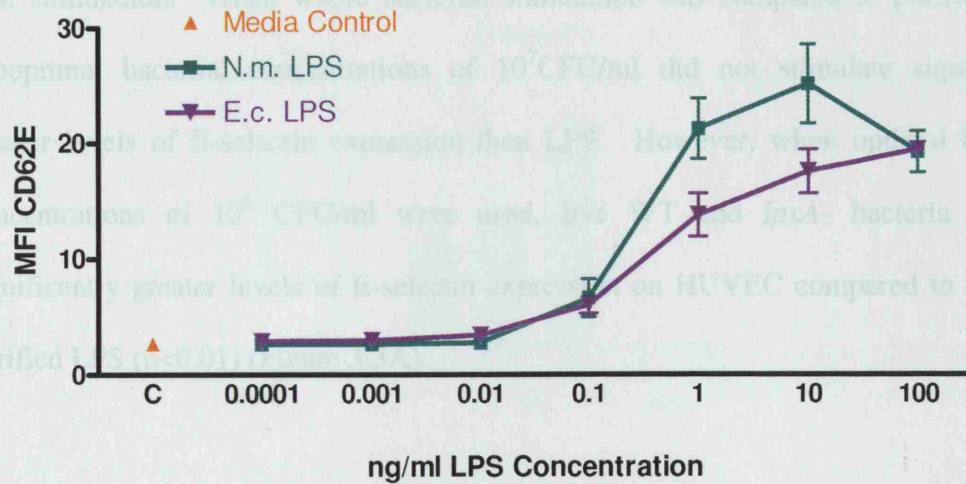


Figure 3.2 E-selectin expression on HUVEC in response to *N. meningitidis* and *E. coli* LPS. HUVEC were stimulated for 5 hours with increasing concentrations of meningococcal LPS (■) and *E. coli* LPS (▼) or with media alone (▲). E-selectin expression was detected by FACS analysis. Results are presented as mean of MFI CD62E \pm SEM, n=4 from endothelial cells from separate donors.

3.3.3 Live *N. meningitidis* WT and *lpxA*- bacteria are able to induce high levels of adhesion molecules on HUVEC

To compare soluble *N. meningitidis* LPS induced adhesion molecule expression with that induced by live meningococci, HUVEC were stimulated with 10^7 and 10^8 CFU/ml live WT and *lpxA*- *N. meningitidis* and 10ng/ml purified LPS for 5 hours. 10ng/ml of purified LPS corresponds to $\sim 10^7$ CFU/ml bacteria, and 100ng/ml of LPS corresponds to $\sim 10^8$ CFU/ml bacteria.

E-selectin expression (Figure 3.3A) increased significantly in response to 10ng/ml purified meningococcal LPS, 10^7 and 10^8 CFU/ml live WT and *lpxA*- bacteria at 5 hours

post stimulation. When whole bacterial stimulation was compared to purified LPS, suboptimal bacterial concentrations of 10^7 CFU/ml did not stimulate significantly greater levels of E-selectin expression than LPS. However, when optimal bacterial concentrations of 10^8 CFU/ml were used, live WT and *lpxA*- bacteria induced significantly greater levels of E-selectin expression on HUVEC compared to 10ng/ml purified LPS ($p < 0.01$) (Figure 3.3A).

For ICAM-1 expression, 10ng/ml LPS, 10^7 and 10^8 CFU/ml WT bacteria, and 10^8 *lpxA*- induced significantly higher ICAM-1 levels compared to unstimulated control, after 5 hours of stimulation (Figure 3.3B). When live WT and *lpxA*- bacterial ICAM-1 stimulation was compared to purified LPS stimulation, levels were not significantly different. 10^7 CFU/ml *lpxA*- bacteria did not induce significantly higher levels of ICAM-1 expression compared to control.

VCAM-1 expression was significantly increased in response to 10ng/ml LPS, and 10^7 and 10^8 CFU/ml WT and *lpxA*- bacteria at 5 hours post stimulation (Figure 3.3C). However, when comparing VCAM-1 expression induced by live WT, *lpxA*- bacteria and LPS induced stimulation, VCAM-1 levels were not significantly different.

Live WT bacteria were better at stimulating E-selectin expression compared to purified LPS. Interestingly, the LPS-free, *lpxA*- mutant bacteria at 10^8 CRU/ml were also able to induce greater levels of E-selectin than purified LPS. However, this differential stimulatory response was not observed for ICAM-1 and VCAM-1 stimulation at 5 hours post stimulation.

3.3.4 E-selectin surface expression on HUVEC is increased

in a dose dependant manner in response to PFA fixed WT *N. meningitidis* H44.

Due to the requirements for quantification of the number of live bacteria was problematic. Therefore a strategy using PFA fixed bacteria was developed and optimised. Bacteria which had been killed with PFA and then stored at -80°C were used for these experiments.

The surface expression of E-selectin on HUVEC in response to fixed WT bacteria in a dose dependent manner (Figure 3.3A). E-selectin expression was enhanced with 10^7 CFU/ml WT bacteria, and 10^8 CFU/ml WT bacteria reached a maximum at 10^8 CFU/ml WT bacteria. There was no E-selectin expression in unstimulated control (Figure 3.3A).

ICAM-1 levels were not induced by 10^7 CFU/ml fixed bacteria, and continued to increase in a dose dependent manner with 10^8 CFU/ml fixed WT bacteria (Figure 3.3B). Control HUVEC stimulated with 10^7 CFU/ml did not further increase ICAM-1 surface expression. Low stimulation with 10^7 CFU/ml did not further increase ICAM-1 surface expression. Low stimulation with 10^7 CFU/ml did not further increase ICAM-1 surface expression.

VCAM-1 levels were not induced by 10^7 CFU/ml fixed bacteria, and continued to increase in a dose dependent manner with 10^8 CFU/ml fixed WT bacteria (Figure 3.3C). Control HUVEC stimulated with 10^7 CFU/ml did not further increase VCAM-1 surface expression. Low stimulation with 10^7 CFU/ml did not further increase VCAM-1 surface expression.

VCAM-1 levels were not induced by 10^7 CFU/ml fixed bacteria, and continued to increase in a dose dependent manner with 10^8 CFU/ml fixed WT bacteria (Figure 3.3C). Control HUVEC stimulated with 10^7 CFU/ml did not further increase VCAM-1 surface expression. Low stimulation with 10^7 CFU/ml did not further increase VCAM-1 surface expression.

VCAM-1 levels were not induced by 10^7 CFU/ml fixed bacteria, and continued to increase in a dose dependent manner with 10^8 CFU/ml fixed WT bacteria (Figure 3.3C). Control HUVEC stimulated with 10^7 CFU/ml did not further increase VCAM-1 surface expression. Low stimulation with 10^7 CFU/ml did not further increase VCAM-1 surface expression.

VCAM-1 levels were not induced by 10^7 CFU/ml fixed bacteria, and continued to increase in a dose dependent manner with 10^8 CFU/ml fixed WT bacteria (Figure 3.3C). Control HUVEC stimulated with 10^7 CFU/ml did not further increase VCAM-1 surface expression. Low stimulation with 10^7 CFU/ml did not further increase VCAM-1 surface expression.

VCAM-1 levels were not induced by 10^7 CFU/ml fixed bacteria, and continued to increase in a dose dependent manner with 10^8 CFU/ml fixed WT bacteria (Figure 3.3C). Control HUVEC stimulated with 10^7 CFU/ml did not further increase VCAM-1 surface expression. Low stimulation with 10^7 CFU/ml did not further increase VCAM-1 surface expression.

VCAM-1 levels were not induced by 10^7 CFU/ml fixed bacteria, and continued to increase in a dose dependent manner with 10^8 CFU/ml fixed WT bacteria (Figure 3.3C). Control HUVEC stimulated with 10^7 CFU/ml did not further increase VCAM-1 surface expression. Low stimulation with 10^7 CFU/ml did not further increase VCAM-1 surface expression.

VCAM-1 levels were not induced by 10^7 CFU/ml fixed bacteria, and continued to increase in a dose dependent manner with 10^8 CFU/ml fixed WT bacteria (Figure 3.3C). Control HUVEC stimulated with 10^7 CFU/ml did not further increase VCAM-1 surface expression. Low stimulation with 10^7 CFU/ml did not further increase VCAM-1 surface expression.

VCAM-1 levels were not induced by 10^7 CFU/ml fixed bacteria, and continued to increase in a dose dependent manner with 10^8 CFU/ml fixed WT bacteria (Figure 3.3C). Control HUVEC stimulated with 10^7 CFU/ml did not further increase VCAM-1 surface expression. Low stimulation with 10^7 CFU/ml did not further increase VCAM-1 surface expression.

VCAM-1 levels were not induced by 10^7 CFU/ml fixed bacteria, and continued to increase in a dose dependent manner with 10^8 CFU/ml fixed WT bacteria (Figure 3.3C). Control HUVEC stimulated with 10^7 CFU/ml did not further increase VCAM-1 surface expression. Low stimulation with 10^7 CFU/ml did not further increase VCAM-1 surface expression.

VCAM-1 levels were not induced by 10^7 CFU/ml fixed bacteria, and continued to increase in a dose dependent manner with 10^8 CFU/ml fixed WT bacteria (Figure 3.3C). Control HUVEC stimulated with 10^7 CFU/ml did not further increase VCAM-1 surface expression. Low stimulation with 10^7 CFU/ml did not further increase VCAM-1 surface expression.

VCAM-1 levels were not induced by 10^7 CFU/ml fixed bacteria, and continued to increase in a dose dependent manner with 10^8 CFU/ml fixed WT bacteria (Figure 3.3C). Control HUVEC stimulated with 10^7 CFU/ml did not further increase VCAM-1 surface expression. Low stimulation with 10^7 CFU/ml did not further increase VCAM-1 surface expression.

VCAM-1 levels were not induced by 10^7 CFU/ml fixed bacteria, and continued to increase in a dose dependent manner with 10^8 CFU/ml fixed WT bacteria (Figure 3.3C). Control HUVEC stimulated with 10^7 CFU/ml did not further increase VCAM-1 surface expression. Low stimulation with 10^7 CFU/ml did not further increase VCAM-1 surface expression.

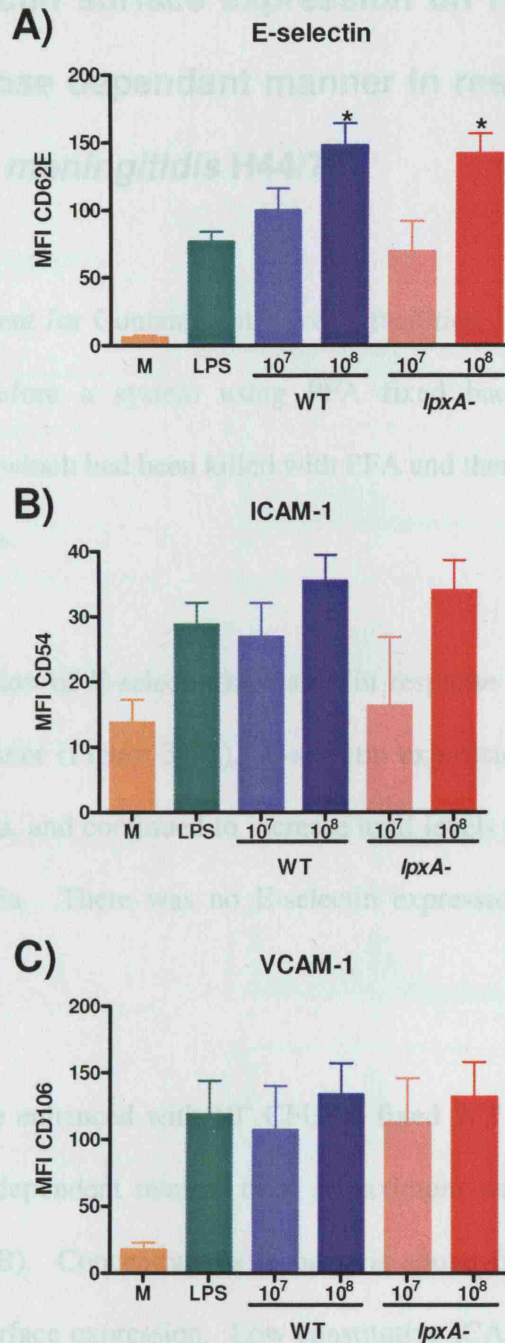


Figure 3.3 Adhesion molecule expression on HUVEC in response to live meningococci.

HUVEC were stimulated for 5 hours with live WT (blue bars), *lpxA*- (red bars) and LPS (green bars). E-selectin (A), ICAM-1 (B) and VCAM-1 (C) were detected using FACS analysis. Results are expressed as mean MFI. $N \geq 2$ from endothelial cells from separate donors. * = $p < 0.01$ when compared to purified LPS (1-way ANOVA).

3.3.4 E-selectin surface expression on HUVEC is increased in a dose dependant manner in response to PFA fixed WT *N. meningitidis* H44/76

Due to the requirement for Containment Level 3 facilities, the use of live bacteria was problematic. Therefore a system using PFA fixed bacteria was developed and optimised. Bacteria which had been killed with PFA and then stored at -80°C were used for these experiments.

The surface expression of E-selectin increased in response to fixed WT bacteria in a dose dependent manner (Figure 3.4A). E-selectin expression was enhanced with 10^4 CFU/ml WT bacteria, and continued to increase until levels reached a maximum at 10^8 CFU/ml WT bacteria. There was no E-selectin expression in unstimulated control (Figure 3.4A).

ICAM-1 levels were enhanced with 10^4 CFU/ml fixed WT bacteria, and continued to increase in a dose dependent manner until a maximum with 10^6 CFU/ml fixed WT bacteria (Figure 3.4B). Concentrations of bacteria above 10^6 CFU/ml did not further increase ICAM-1 surface expression. Low constitutive ICAM-1 levels were expressed in unstimulated HUVEC.

VCAM-1 levels also increased in a dose dependent manner. VCAM-1 expression increased in response to 10^4 CFU/ml fixed WT bacteria reaching a maximum at 10^8 CFU/ml (Figure 3.4C). Low constitutive levels of VCAM-1 were expressed in unstimulated HUVEC.

These results demonstrate that PPA fixed WT bacteria induce adhesion molecule expression in a dose dependent manner (Figure 3.4). Levels of E-selectin and ICAM-1 expression in response to 10^7 and 10^8 CFU/ml PPA fixed WT bacteria were similar to the levels observed for live bacteria (Section 3.3.1).

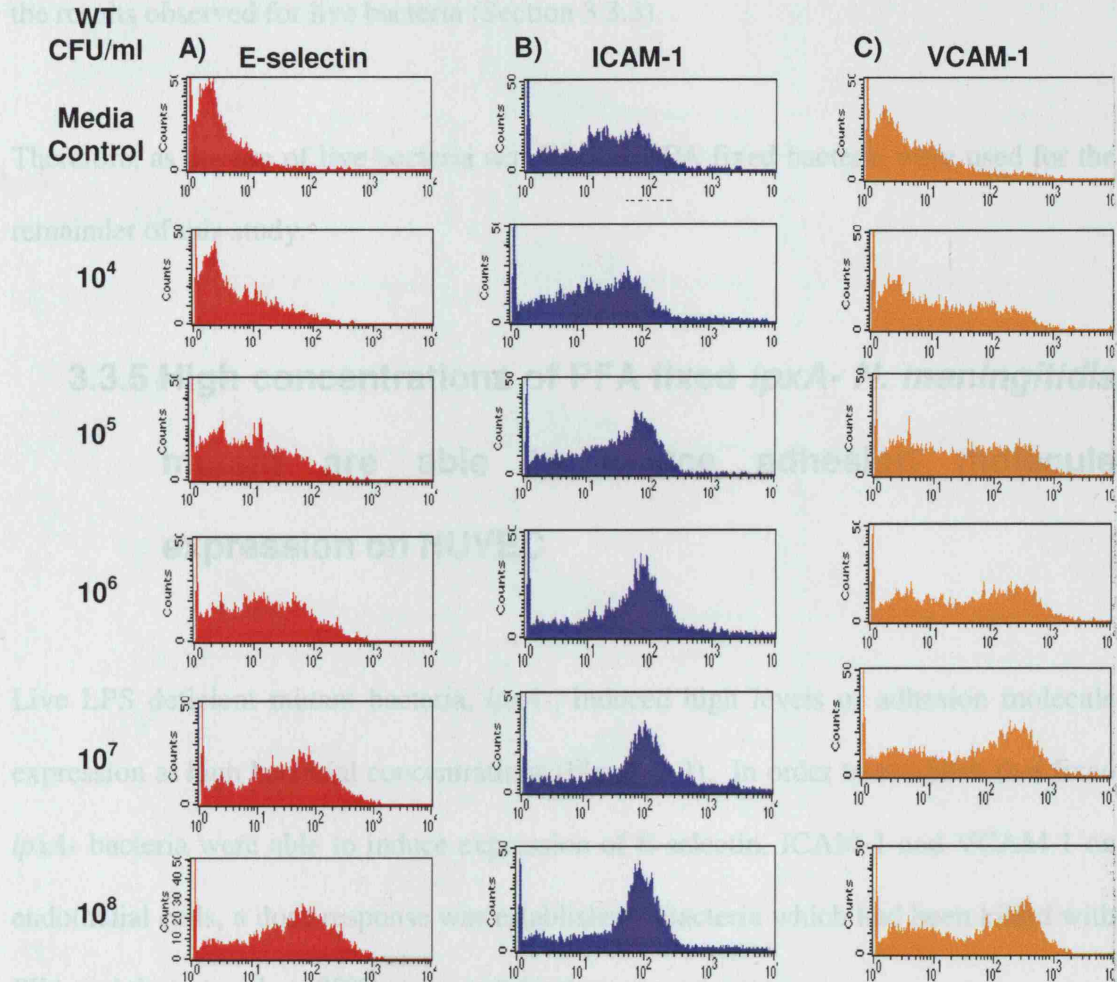


Figure 3.4 Adhesion molecule profile on HUVEC in response to increasing doses of fixed WT H44/76 *N. meningitidis*. HUVEC were stimulated for 5 hours with increasing concentrations of fixed WT bacteria. A) E-selectin (■), B) ICAM-1 (■) and C) VCAM-1 (■). Adhesion molecules were detected by FACS analysis.

These results demonstrate that PFA fixed WT bacteria induce adhesion molecule expression in a dose dependent manner (Figure 3.4). Levels of E-selectin and VCAM-1 expression in response to 10^7 and 10^8 CFU/ml PFA fixed WT bacteria were similar to the results observed for live bacteria (Section 3.3.3).

Therefore, as the use of live bacteria was limited, PFA fixed bacteria were used for the remainder of this study.

3.3.5 High concentrations of PFA fixed *lpxA*- *N. meningitidis* mutant are able to induce adhesion molecule expression on HUVEC

Live LPS deficient mutant bacteria, *lpxA*-, induced high levels of adhesion molecule expression at high bacterial concentrations (Figure 3.3). In order to establish that fixed *lpxA*- bacteria were able to induce expression of E-selectin, ICAM-1 and VCAM-1 on endothelial cells, a dose response was established. Bacteria which had been killed with PFA and then stored at -80°C were used for these experiments.

The *lpxA*- mutant increased levels of E-selectin expression at 10^7 CFU/ml fixed bacteria and was maximal in response to 10^8 CFU/ml (Figure 3.5A). There was no E-selectin expression in response to 10^5 - 10^6 CFU/ml fixed *lpxA*- bacteria. There was undetectable E-selectin expression on unstimulated HUVEC.

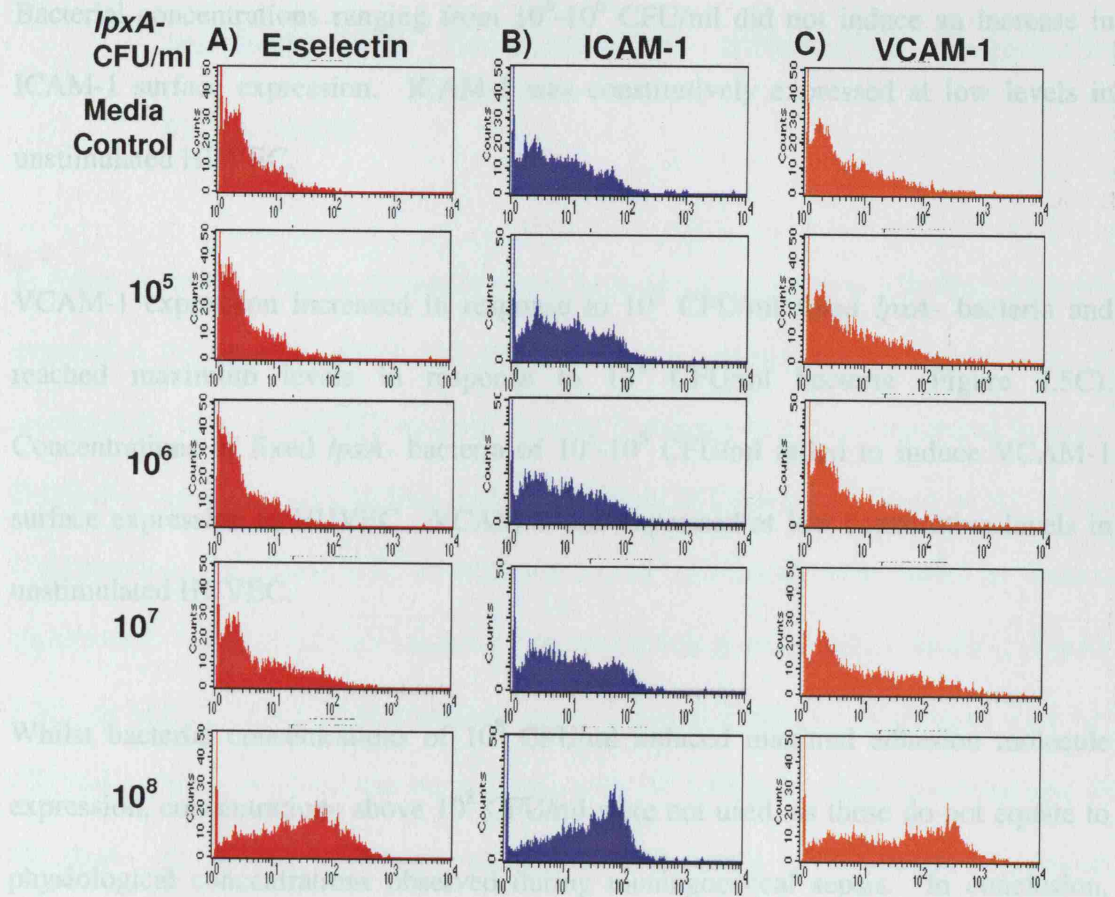


Figure 3.5 Adhesion molecule profile on HUVEC in response to increasing doses of fixed *lpxA*- H44/76 *N. meningitidis*. HUVEC were stimulated for 5 hours with increasing doses of fixed *lpxA*- bacteria. A) E-selectin (■), B) ICAM-1 (■) and C) VCAM-1 (■) adhesion molecules were detected by FACS analysis.

ICAM-1 surface expression increased in response to 10^7 CFU/ml fixed *lpxA*- bacteria and reached maximal levels in response to 10^8 CFU/ml bacteria (Figure 3.5B). Bacterial concentrations ranging from 10^5 - 10^6 CFU/ml did not induce an increase in ICAM-1 surface expression. ICAM-1 was constitutively expressed at low levels in unstimulated HUVEC.

VCAM-1 expression increased in response to 10^7 CFU/ml fixed *lpxA*- bacteria and reached maximum levels in response to 10^8 CFU/ml bacteria (Figure 3.5C). Concentrations of fixed *lpxA*- bacteria of 10^5 - 10^6 CFU/ml failed to induce VCAM-1 surface expression in HUVEC. VCAM-1 was expressed at low constitutive levels in unstimulated HUVEC.

Whilst bacterial concentrations of 10^8 CFU/ml induced maximal adhesion molecule expression, concentrations above 10^8 CFU/ml were not used, as these do not equate to physiological concentrations observed during meningococcal sepsis. In conclusion, high concentrations of fixed *lpxA*- bacteria were able to induce a pattern of adhesion molecule expression, comparable with similar concentrations of live bacteria (Figure 3.3).

3.3.6 Comparison of adhesion molecule expression in response to PFA fixed WT and *lpxA*- bacteria and purified LPS demonstrates differential E-selectin expression

In order to further validate the use of fixed bacteria in this system, adhesion molecule expression responses to fixed WT and *lpxA*- were compared with responses to *N. meningitidis* LPS. Fixed WT bacteria induced E-selectin in a dose-dependent manner. E-selectin expression was highest with 10^8 CFU/ml WT bacteria (Figure 3.6A). High concentrations of fixed WT meningococci (10^8 CFU/ml) were able to induce significantly higher levels of E-selectin expression than purified LPS (10ng/ml) (Figure 3.6A, $p < 0.001$). The LPS-free mutant, *lpxA*-, induced E-selectin expression with 10^7 CFU/ml bacteria, reaching maximum levels with 10^8 CFU/ml. High concentrations of the *lpxA*- mutant (10^8 CFU/ml) induced similar levels of E-selectin expression compared to 10ng/ml LPS.

Fixed WT bacteria induced ICAM-1 in a dose dependent manner (Figure 3.6B). ICAM-1 expression was highest with WT bacterial concentrations of 10^8 CFU/ml. WT bacteria and 10ng/ml purified LPS induced similar levels of ICAM-1 expression in HUVEC. *lpxA*- bacteria induced ICAM-1 expression at a bacterial concentration of 10^7 CFU/ml, reaching maximal levels at 10^8 CFU/ml. *lpxA*- bacteria induced similar levels of ICAM-1 expression as those obtained with 10ng/ml of purified meningococcal LPS (Figure 3.6B).

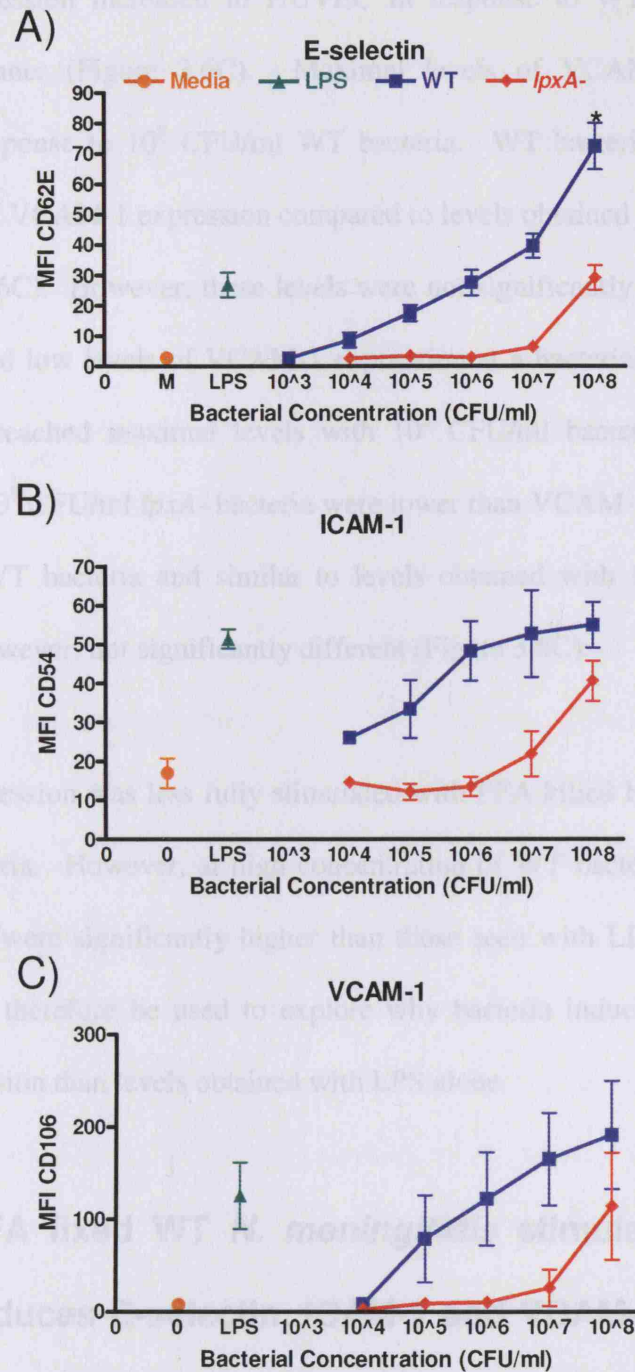


Figure 3.6 Adhesion molecule expression on HUVEC in response to increasing concentrations of fixed WT and *lpxA*- H44/76 *N. meningitidis* bacteria and bacterial LPS (10ng/ml). HUVEC were stimulated for 5 hours with fixed WT (■), *lpxA*- (♦) and 10ng/ml LPS (▲). Results are presented as mean of MFI±SEM, n=3 endothelial cells from separate donors. *is p<0.001 when compared to purified LPS (1-way ANOVA with Bonferroni's correction).

VCAM-1 expression increased in HUVEC in response to WT bacteria in a dose-dependent manner (Figure 3.6C). Maximal levels of VCAM-1 expression were obtained in response to 10^8 CFU/ml WT bacteria. WT bacteria appeared to induce higher levels of VCAM-1 expression compared to levels obtained with 10ng/ml purified LPS (Figure 3.6C). However, these levels were not significantly higher. *lpxA*- mutant bacteria induced low levels of VCAM-1 expression at a bacterial concentration of 10^7 CFU/ml, and reached maximal levels with 10^8 CFU/ml bacteria. VCAM-1 levels induced with 10^8 CFU/ml *lpxA*- bacteria were lower than VCAM-1 levels obtained with 10^8 CFU/ml WT bacteria and similar to levels obtained with 10ng/ml LPS. These levels were, however, not significantly different (Figure 3.6C).

E-selectin expression was less fully stimulated with PFA killed bacteria than that seen with live bacteria. However, at high concentration of WT bacteria (10^8 CFU/ml), E-selectin levels were significantly higher than those seen with LPS alone. PFA killed bacteria could therefore be used to explore why bacteria induce higher levels of E-selectin expression than levels obtained with LPS alone.

3.3.7 PFA fixed WT *N. meningitidis* stimulation of HUVEC induces E-selectin, ICAM-1 and VCAM-1 expression in a time-dependant manner

A time course of adhesion molecule expression was performed in response to fixed WT bacteria. HUVEC were stimulated with fresh grown and PFA fixed *N. meningitides* WT bacteria at a concentration of 10^8 CFU/ml for 28, 10, 8, 6, 4, 2, 1, and 0.5 hours, and E-selectin, ICAM-1 and VCAM-1 expression determined.

Fixed WT bacteria induced low levels of E-selectin expression after 1 hour of stimulation (Figure 3.7A and Figure 3.8). E-selectin levels continued to increase until reaching a maximum at 4 hours, then decreased gradually at 6-28 hours after stimulation. E-selectin levels remained elevated at 28 hours in response to 10^8 CFU/ml.

ICAM-1 levels increased above baseline 2 hours post stimulation with fixed WT bacteria (Figure 3.7B and Figure 3.8). ICAM-1 levels continued to rise until reaching a maximum at 8-10 hours. High levels of ICAM-1 expression were maintained at 28 hours post stimulation. At time points below 2 hours, there was no induction of ICAM-1 expression above baseline.

VCAM-1 expression increased above baseline with fixed WT bacteria at 2 hours post stimulation (Figure 3.7C and Figure 3.8). VCAM-1 levels continued to increase until a maximum was reached at 8-10 hours post stimulation. VCAM-1 levels decreased below maximal levels at 28 hours, although levels were still higher than baseline levels. There was no induction of VCAM-1 expression above baseline in HUVEC stimulated for less than 2 hours.

In conclusion, 4-6 hours was the optimal time point to detect E-selectin expression stimulated by fixed WT bacteria. Furthermore, although 4-6 hours is not optimal for the detection of ICAM-1 and VCAM-1, these were still elevated, allowing further study of these adhesion molecules in response to WT bacteria.

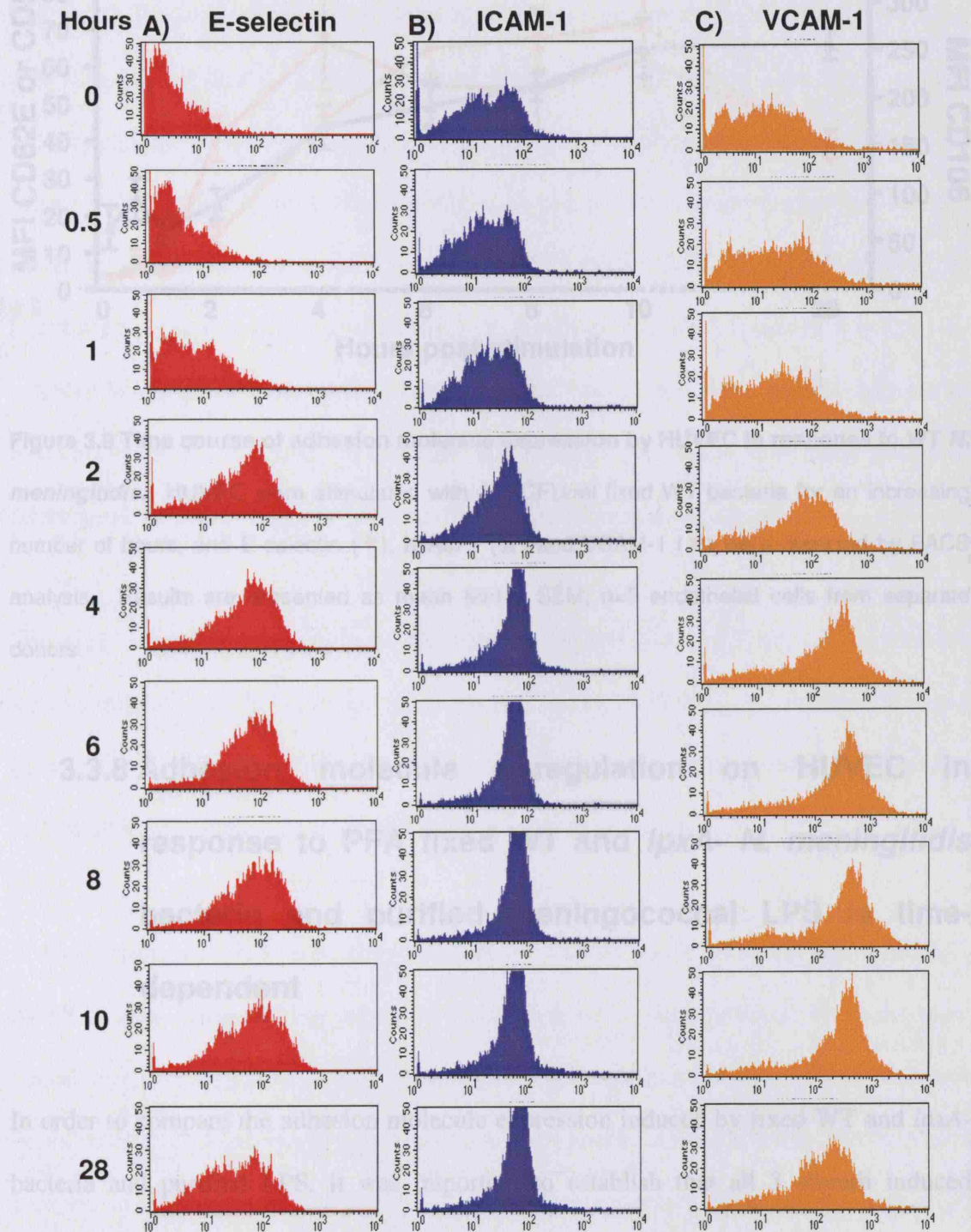


Figure 3.7 Time course of adhesion molecule profile on HUVEC in response to WT *N. meningitidis*. HUVEC were stimulated over a 28 hour time course with 10^8 CFU/ml fixed WT *N. meningitidis*. E-selectin (■), ICAM-1 (■) and VCAM-1 (■) were detected using FACS analysis.

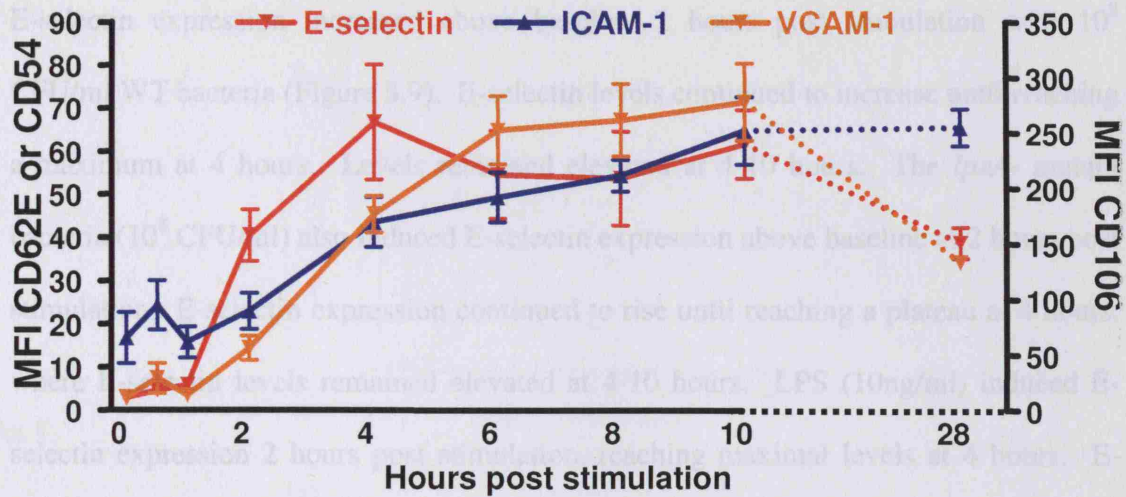


Figure 3.8 Time course of adhesion molecule expression by HUVEC in response to WT *N. meningitidis*. HUVEC were stimulated with 10^8 CFU/ml fixed WT bacteria for an increasing number of hours, and E-selectin (∇), ICAM-1 (\blacktriangle) and VCAM-1 (\blacktriangledown) were detected by FACS analysis. Results are presented as mean MFI \pm SEM, $n=5$ endothelial cells from separate donors.

3.3.8 Adhesion molecule upregulation on HUVEC in response to PFA fixed WT and *lpxA*- *N. meningitidis* bacteria and purified meningococcal LPS is time-dependent

In order to compare the adhesion molecule expression induced by fixed WT and *lpxA*-bacteria and purified LPS, it was important to establish that all 3 stimuli induced optimal or near optimal adhesion molecule expression at 5 hours. A time course was therefore performed in response to freshly grown and PFA fixed *N. meningitidis* WT and *lpxA*- bacteria and purified LPS. HUVEC were stimulated over a 10 hour time period with 10^8 CFU/ml fixed WT and *lpxA*- bacteria and 10ng/ml purified LPS (Figure 3.9).

E-selectin expression increased above baseline 2 hours post stimulation with 10^8 CFU/ml WT bacteria (Figure 3.9). E-selectin levels continued to increase until reaching a maximum at 4 hours. Levels remained elevated at 4-10 hours. The *lpxA*- mutant bacteria (10^8 CFU/ml) also induced E-selectin expression above baseline at 2 hours post stimulation. E-selectin expression continued to rise until reaching a plateau at 4 hours, where E-selectin levels remained elevated at 4-10 hours. LPS (10ng/ml) induced E-selectin expression 2 hours post stimulation, reaching maximal levels at 4 hours. E-selectin levels decreased rapidly between 6-10 hours and were nearly reduced to baseline levels at 10 hours. There was no E-selectin expression at baseline levels (0 hours), and very low levels at 0.5-1 hour in response to all three stimuli.

The *lpxA*- mutant bacteria induced significantly higher levels of E-selectin expression when compared to LPS stimulation levels at 4 hours ($p<0.05$). In addition, WT and *lpxA*- bacteria induced significantly higher levels of E-selectin expression than purified LPS at 10 hours (Figure 3.9A; $p<0.05$ and $p<0.01$, respectively).

ICAM-1 expression increased above baseline at 4 hours post stimulation with fixed WT bacteria, and continued to increase until reaching a maximum at 10 hours post stimulation (Figure 3.9B). Fixed *lpxA*- bacteria also increased ICAM-1 expression at 4 hours post stimulation, reaching a maximum at 10 hours post stimulation. Purified LPS induced an increase in ICAM-1 expression at 4 hours, until reaching a maximum at 10 hours post stimulation. There were no significant differences in ICAM-1 stimulation at any time point in response to fixed WT and *lpxA*- bacteria and purified LPS (Figure 3.9B).

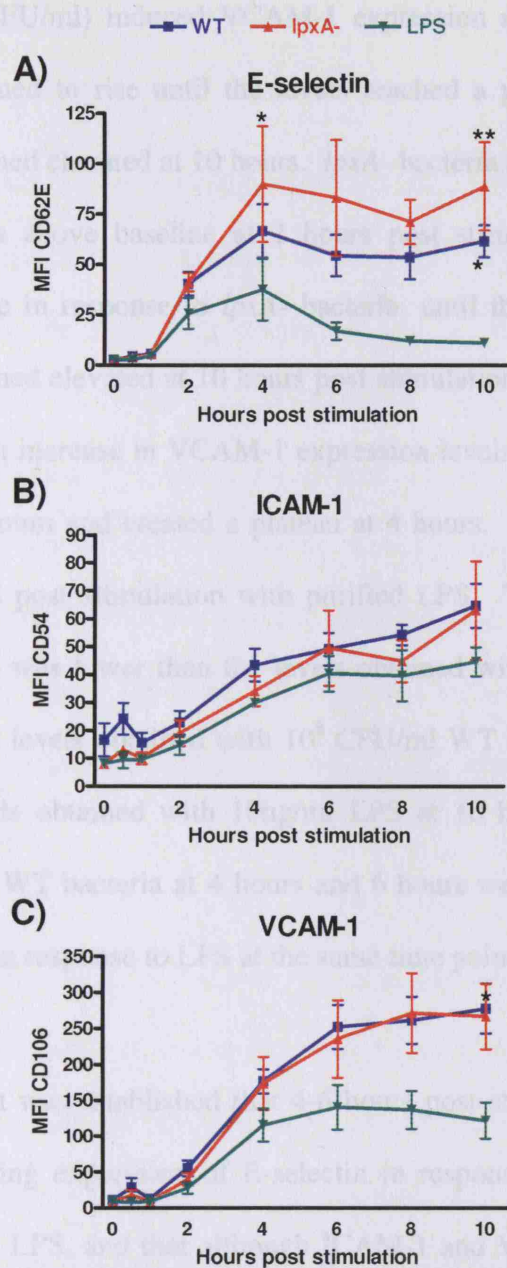


Figure 3.9 Time dependant adhesion molecule expression on HUVEC in response to fixed WT and *lpxA*- H44/76 *N. meningitidis* and purified LPS. HUVEC were stimulated with 10^8 CFU/ml fixed WT bacteria (■), fixed *lpxA*- bacteria (▲) or purified LPS (▼) for 0-10 hours, and E-selectin (A), ICAM-1 (B), and VCAM-1 (C) were detected by FACS analysis. Results are expressed as mean of MFI \pm SEM, $n \geq 3$ endothelial cells from separate donors. *= $p < 0.05$ when compared to purified LPS at the same time point; **= $p < 0.01$ when compared to LPS at the same time point (1-way ANOVA with Bonferroni's correction).

WT bacteria (10^8 CFU/ml) induced VCAM-1 expression above baseline levels at 2 hours, which continued to rise until the levels reached a plateau at 6 hours (Figure 3.9C). Levels remained elevated at 10 hours. *lpxA*- bacteria (10^8 CFU/ml) also induced VCAM-1 expression above baseline at 2 hours post stimulation. VCAM-1 levels continued to increase in response to *lpxA*- bacteria, until they reached a plateau at 6 hours. Levels remained elevated at 10 hours post stimulation with *lpxA*- bacteria. LPS (10ng/ml) induced an increase in VCAM-1 expression levels above baseline at 2 hours and reached a maximum and created a plateau at 4 hours. VCAM-1 levels remained elevated at 10 hours post stimulation with purified LPS. The level of LPS induced VCAM-1 expression was lower than the levels obtained with WT and *lpxA*- bacteria. VCAM-1 expression levels obtained with 10^8 CFU/ml WT bacteria were significantly higher than the levels obtained with 10ng/ml LPS at 10 hours ($p < 0.05$). VCAM-1 levels obtained with WT bacteria at 4 hours and 6 hours were not significantly higher than levels obtained in response to LPS at the same time points (Figure 3.9C).

From these results, it was established that 4-6 hours post stimulation was the optimal time point for studying expression of E-selectin in response to fixed WT and *lpxA*- bacteria and purified LPS, and that although ICAM-1 and VCAM-1 expression levels were sub-optimal at 5 hours, both adhesion molecules were at levels of sufficient magnitude to allow the investigation of adhesion molecule regulation by fixed WT and *lpxA*- bacteria and purified LPS.

3.4 Discussion

The aim of this chapter was to investigate the adhesion molecule profiles induced by meningococci, and particularly to explore the LPS dependent and independent mechanisms that may be regulating meningococcal activation of the endothelium. Purified meningococcal LPS was able to induce E-selectin, ICAM-1 and VCAM-1 expression in HUVEC in a dose dependent manner, as observed in Section 3.3.1-3.3.2. *E. coli* LPS was also able to induce E-selectin expression in a dose dependant manner (Figure 3.2). The LPS dose response obtained in this chapter is consistent with previous studies, which show that E-selectin is upregulated with 0.1ng/ml of *E. coli* LPS (O127:B8), reaching maximal levels at 1-10ng/ml, where a plateau is reached (Jersmann et al., 2001a).

Whilst numerous mechanisms are involved in inducing endothelial damage and sepsis during meningococcal disease, it is widely believed that meningococcal LPS is the main causative agent in this process (Dunn *et al.*, 1995; Jennings *et al.*, 1995), as elevated LPS levels are associated with the severity of meningococcal disease (Brandtzaeg *et al.*, 1989). *E. coli*, a Gram negative bacterium which also contains LPS, is also able to induce sepsis and septic shock in humans. However, *N. meningitidis* induced sepsis is characterised by disseminated vascular damage, which is not generally observed with *E. coli* induced sepsis. It is therefore interesting to note that LPS from *E. coli* caused a milder induction in adhesion molecule expression than *N. meningitidis* LPS (Figure 3.2), which may be reflected in the *in vivo* response.

Interestingly, a study has reported the differences in lethality due to Gram+ bacteria. It was demonstrated that TNF- α is important in inducing *E. coli* LPS induced death in mice, whereas IFN- γ , IL-1 and IL-18 are involved in the lethality caused by *S. typhimurium* (Netea et al., 2001). In addition, a recent study has demonstrated that *N. meningitidis* LPS induces the production of several inflammatory mediators by a range of human cell lines, including TNF- α , IL-1 β , MCP-1, MIP-3 α , IFN- β , nitric oxide, and IFN- γ -inducible protein 10 (IP-10), whereas *E. coli* LPS induced lower levels of IFN- β , nitric oxide, and IP-10 (Zughaier et al., 2005). PBMC's also produce higher levels of TNF- α and IL-1 β in response to *N. meningitidis* LPS than to *E. coli* LPS (Sprong et al., 2004). Van der Meer and colleagues have proposed that these differences may be due to the shape of the lipid A component of LPS (Netea et al., 2002), where a conical shaped LPS is more active than a cylindrical shaped LPS. This shape is believed to interact with different TLRs, where the conical shaped LPS interacts with TLR4, whereas the cylindrical shaped LPS interact with TLR2. Interestingly, *N. meningitidis* LPS interacts with both TLR1 and 2 in combination (Wyllie et al., 2000) and TLR4 alone (Ingalls et al., 2001; Pridmore et al., 2001), and is believed to have a shape that is intermediate between conical and cylindrical (Netea et al., 2002). These findings may explain the differences in E-selectin induction observed with *N. meningitidis* and *E. coli* LPS.

Although meningococcal LPS is able to induce high levels of adhesion molecule expression, it has previously been shown that high concentrations of live WT meningococci induce significantly higher levels of E-selectin expression compared to purified LPS (Dixon *et al.*, 2004). Interestingly, the use of the LPS-free mutant, *lpxA*-, demonstrates that at high concentrations of bacteria, there are LPS-independent

mechanisms inducing high levels of E-selectin expression (Dixon *et al.*, 2004). These findings were confirmed in Section 3.3.3 (Figure 3.3). Although Dixon *et al.* found that 10^7 CFU/ml WT bacteria induced higher levels of E-selectin expression than 10^8 CFU/ml, Figure 3.3 demonstrates that 10^8 CFU/ml WT bacteria induced higher levels of E-selectin expression compared to 10^7 CFU/ml WT bacteria in this study. The reasons for this is unclear, however, one factor that has changed since Dixon *et al.* is the FCS stock. Batches of FCS will differ in their composition of growth factors and hormones, among other things, and these may affect the manner in which cells respond to different stimuli. It may be that the FCS used for this study contained an unknown factor that allowed the cells to survive in the presence of very high bacterial concentrations, which in turn may have allowed the HUVEC to respond to the WT bacteria present. However, the patterns of expression were similar. As can be seen on Figure 3.3, high concentrations of live WT bacteria were able to induce significantly higher levels of E-selectin compared to levels obtained with purified LPS.

Experimental limitations restricted the use of live bacteria, and it was therefore important to establish that PFA killed bacteria were also able to induce adhesion molecule expression in HUVEC. PFA killed WT bacteria were able to induce high levels of E-selectin, ICAM-1 and VCAM-1 expression in stimulated HUVEC (Figure 3.4). The levels of E-selectin were significantly higher than levels obtained with purified LPS (Figure 3.6). The LPS-free mutant, *lpxA*-, was also able to induce adhesion molecule expression when bacterial concentrations were high (10^8 CFU/ml) (Figure 3.5), however, the levels obtained were not significantly higher than levels obtained with purified LPS (Figure 3.6). Dose response experiments were performed with bacteria that had been grown and killed with PFA, and then stored at -80°C for an

indefinite period of time. It may be that freezing the bacteria somehow damages the bacterial membrane. The absence of LPS may affect the *lpxA*- bacterial membrane in a manner that increases its susceptibility to freeze-thawing, which may not be observed in the WT bacterial membrane. It is interesting to note that in time-course experiments (Figure 3.7-Figure 3.9), freshly grown and killed bacteria were utilised. In these experiments, the *lpxA*- mutant was able to induce significantly higher levels of E-selectin expression than levels obtained with purified LPS, and levels were at times higher than those obtained with freshly killed WT bacteria.

Whilst there have been numerous studies performed on LPS and endothelial activation, few have used whole bacteria. *Borrelia crucidurae*, which causes African relapsing fever, induces ICAM-1 and E-selectin expression on HUVEC, and this is dependent on intact live bacteria (Ishii and Takada, 2002). *E. coli* have also been used to activate E-selectin on HUVEC. Interestingly, purified LPS was able to induce higher levels of E-selectin expression than whole inactive bacteria, which required a 10-100 fold higher concentration for the induction of E-selectin expression than purified LPS (Furst-Ladani et al., 1999). However, the authors of the study did not correlate concentration of bacteria to the amount of LPS on the bacterial surface, which makes it difficult to extrapolate the true value of this observation.

The comparison of Gram+ and Gram- bacteria and their induction of E-selectin has also been performed. Interestingly, Gram- bacteria (such as *Bacteroides fragilis*, *Enterobacter cloacae*, *Haemophilus influenzae*, and *Klebsiella pneumoniae*) were able to induce E-selectin expression and mRNA upregulation in a dose dependent manner, and this relied on the presence of sCD14, a protein involved in the LPS signalling

complex described in Section 1.3.4.2. Gram+ bacteria, such as *Staphylococcus aureus*, *Enterococcus faecalis*, and *Streptococcus pneumoniae* were unable to induce E-selectin expression on HUVEC (Noel, et al., 1995). This study also compared the induction of E-selectin in response to live and heat-killed *E. coli*. Whilst both live and killed bacteria were both able to induce E-selectin expression in a dose dependent manner, the killed bacteria induced lower levels of E-selectin expression. This correlates with observation made in this chapter, where live bacteria generally induced higher levels of adhesion molecule expression than killed bacteria (Figure 3.3 and Figure 3.6).

If all these bacteria are able to induce adhesion molecule expression, why do meningococci induce vascular damage, which is not characteristic of sepsis induced by other bacteria? This may be due to other factors, such as cytokine induction, the activation of the coagulation cascade, and the extent of neutrophil binding and transmigration. As mentioned above, there are reported differences in cytokine induction by different bacteria, and this may be due to differences in LPS shape. These factors are likely to contribute to the differential in the extent of sepsis induced by these bacteria. For instance, a recent study has used a whole blood model to study the effects of infected blood on endothelial cell activation. Interestingly, blood infected with *E. coli* induced higher levels of E-selectin expression and endothelial cell permeability than blood infected with *Bacteroides fragilis* or *Enterococcus faecalis* (Nooteboom et al., 2005).

The time-course studies revealed another interesting observation. High concentrations of WT bacteria were able to induce prolonged expression of E-selectin in HUVEC, as

observed by the elevated E-selectin expression levels detected at 28 hours (Figure 3.8 and Figure 3.9). E-selectin expression is known to be upregulated by 5 hours and has been reported to reduce to baseline levels by 24 hours (Scholz *et al.*, 1996). LPS induced E-selectin expression was maximal at 4-6 hours, and then dropped to nearly baseline levels by 10 hours post stimulation (Figure 3.9A). However, the fixed *lpxA*-mutant induced a pattern of E-selectin expression similar to that observed with fixed WT bacteria. Whilst *lpxA*- induced E-selectin expression was maximal at 4-6 hours, levels remained elevated at 10 hours, which was also observed in response to fixed WT bacteria (Figure 3.9A). *lpxA*- induced E-selectin expression was significantly higher than levels obtained with purified LPS at both 4 and 10 hours post stimulation. This may indicate that LPS-independent mechanisms are regulating prolonged E-selectin expression. This could be due to differences in signalling cascades regulating E-selectin transcription or through post-translational mechanisms.

ICAM-1 surface expression levels on HUVEC have been reported to remain elevated at 72 hours (Scholz *et al.*, 1996). Although such a long incubation time was not performed in this study, it was clear that ICAM-1 levels remained elevated in response to WT and *lpxA*- meningococci and purified LPS after 10 hours of stimulation. VCAM-1 levels are maximal at 6-8 hours after cytokine stimulation, with levels declining slowly after this (Scholz *et al.*, 1996). Previous studies have shown that VCAM-1 expression can remain elevated after 72 hours post stimulation (Scholz *et al.*, 1996). Although VCAM-1 expression was elevated in response to WT, *lpxA*- and purified LPS at 10 hours post infection, LPS induced VCAM-1 expression declined after 8 hours. These levels were significantly lower than the VCAM-1 levels detected in response to WT bacteria. There is an indication that prolonged high level expression of VCAM-1

on endothelium is LPS independent, as WT and *lpxA*- bacteria induced higher levels of VCAM-1 expression than LPS at 10 hours.

The data indicates that there are LPS-independent mechanisms governing high expression levels of E-selectin induced by WT meningococci as well as prolonged E-selectin expression. In addition, there may be LPS-independent mechanisms governing prolonged VCAM-1 expression in HUVEC.

The levels of bacteria inducing high levels of E-selectin expression correlate with the bacterial loads detected in patients with meningococcal disease (Ovstebo *et al.*, 2004; Hackett *et al.*, 2002). Levels in septicaemic patients reached as high as 10^7 DNA copies/ml of blood, which equate to the bacterial cell load (Ovstebo *et al.*, 2004; Hackett *et al.*, 2002). LPS levels above 10ng/ml are associated with an 82% fatality rate in meningococcal disease patients (Brandtzaeg *et al.*, 1989). This was the concentration of purified LPS required for maximal E-selectin expression (Figure 3.1 and Figure 3.2).

It is interesting to note that in a whole blood assay of endothelial activation antibiotic treatment of *E. coli* infected blood produced reduced TNF- α levels, however, the antibiotic treated blood induces similar levels of endothelial cell activation as untreated blood (Nooteboom *et al.*, 2005). This may explain why patients presenting with high bacterial loads are likely to still develop sepsis and vascular damage, even after antibiotic therapy.

How does this lead to the vascular damage observed during meningococcal disease? Klein and co-workers have shown that neutrophil binding to the endothelial layer leads to endothelial damage (Klein *et al.*, 1996). Neutrophil binding to the endothelial layer is controlled by the upregulation of adhesion molecules. Dixon *et al.*, (2004) and data presented in this chapter demonstrates that WT bacteria are able to induce high levels of adhesion molecule expression. Interestingly, high concentrations of fixed WT bacteria were able to induce higher levels of E-selectin expression compared to levels obtained in response to purified LPS (Figure 3.6). This differential adhesion molecule induction was not observed for ICAM-1 and VCAM-1 expression, which were stimulated equally well in response to WT bacteria and LPS. E-selectin is an initial surface molecule on endothelial cells involved in the tethering and rolling of neutrophils, and it is therefore interesting to note that WT bacteria are able to induce higher expression levels of E-selectin.

Observations made in this chapter illustrating the induction of high levels and prolonged expression of adhesion molecules, particularly E-selectin, correlate with *in vivo* observations. Sections of purpuric lesions demonstrate high numbers of infiltrating neutrophils (Harrison *et al.*, 2002; Sotto *et al.*, 1976). It has previously been shown that increased numbers of bound neutrophils to the endothelium can cause endothelial damage (Klein *et al.*, 1996).

The question still remains how increased E-selectin expression may induce the vascular damage observed in meningococcal disease. Vascular damage is caused by the inflammatory response and the coagulation cascade (Reinhart *et al.*, 2002; Esmon, 2004). WT *N. meningitidis* induced adhesion molecules expression may promote the

adhesion of large numbers of activated neutrophils. These neutrophils may, in turn, cause vascular damage. This may then trigger the coagulation cascade. In addition, *N. meningitidis* is capable of inducing the coagulation cascade directly by inducing the expression of TF on endothelial cells (Heyderman *et al.*, 1997). These two processes combined (neutrophil-induced endothelial damage and TF expression on the endothelium) may magnify the coagulation cascade to a state where there is no longer any homeostasis and create the characteristic imbalance observed during meningococcal sepsis.

A model illustrating this theory is demonstrated on Figure 3.10. During meningococcal meningitis, there is infiltration by neutrophils into the subarachnoid space (Leib and Tauber, 1999). This is mediated by adhesion molecules on the endothelial and neutrophil cell surfaces. The increase in adhesion molecule expression leads to increased neutrophil adherence to and transmigration across the endothelial cell layer. This in turn may lead to increased endothelial cell damage. During meningococcal disease, there is infiltration of the perivascular space by neutrophils, monocytes/macrophages and platelet-neutrophil complexes (PNC), and these have had to traverse the endothelial cell layer (Harrison *et al.*, 2002; Peters *et al.*, 2003). The resulting endothelial damage may in turn initiate the coagulation cascade, which is dysfunctional during meningococcal sepsis (Section 1.1.3.2) (Figure 3.10).

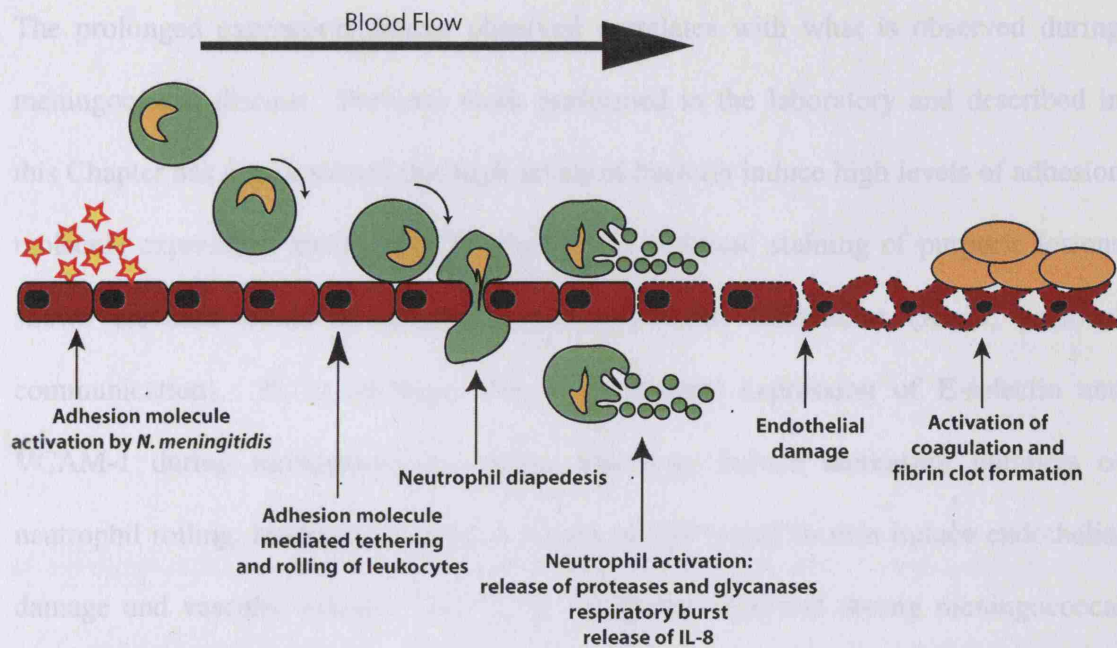


Figure 3.10 Model for endothelial cell injury induction by neutrophil-endothelial cell interactions leading to DIC. Illustration demonstrates a possible mechanism for endothelial cell injury leading to DIC. *N. meningitidis* induces adhesion molecule expression on the endothelium, which leads to neutrophil binding. Neutrophils mediate endothelial cell injury, which induces the coagulation cascade. During meningococcal sepsis there is dysfunctional regulation of the coagulation cascade, which leads to tissue injury and organ dysfunction.

How does prolonged E-selectin and VCAM-1 expression affect this system? The reasons for WT induced prolonged high level expression of E-selectin and VCAM-1 are uncertain. These two surface adhesion molecules are involved at different stages of the pathway leading to leukocyte rolling, firm binding and transmigration on the endothelium. Whereas E-selectin mediates leukocytes rolling, ICAM-1 and VCAM-1 are both involved in the firm adhesion of leukocytes to the endothelium.

The prolonged expression pattern observed correlates with what is observed during meningococcal disease. Previous work performed in the laboratory and described in this Chapter has demonstrated that high levels of bacteria induce high levels of adhesion molecule expression, particularly E-selectin. In addition, staining of purpuric lesions shows elevated levels of E-selectin and neutrophil infiltration (Klein, personal communication). If, in addition, there is prolonged expression of E-selectin and VCAM-1 during meningococcal disease, this may induce increasing numbers of neutrophil rolling, binding and transmigration, which would in turn induce endothelial damage and vascular leakage, the classic symptoms observed during meningococcal disease.

The mechanisms involved in *N. meningitidis* regulation of E-selectin are explored in the following chapters.

Chapter 4

***N. meningitidis* LPS dependent and independent mechanisms mediating upregulation of endothelial cell adhesion molecule mRNA expression**

4.1 Introduction

Since the identification of the DNA sequences of E-selectin (Collins *et al.*, 1991), ICAM-1 (Staunton *et al.*, 1988) and VCAM-1 (Cybulsky *et al.*, 1991), RT-PCR has been the method most extensively utilised to study the mRNA levels of adhesion molecules in tissues and cultured cells. Studies of adhesion molecule mRNA levels have been performed on murine (Everts *et al.*, 2003), bovine (Van Kampen and Mallard, 2001) and human tissues, such as HUVEC (Ishii and Takada, 2002; Kadl *et al.*, 2002; Gupta and Ghosh, 1999; Zhang *et al.*, 2002; Saito *et al.*, 1993; Madan *et al.*, 2001), Human Mucosal Microvascular Endothelial Cells (HMMEC) (Kim *et al.*, 2002) and Human Intestinal Microvascular Endothelial Cells (HIMEC) (Ogawa *et al.*, 2003). RNA protection assay for determining mRNA quantity has also been utilised to investigate E-selectin mRNA expression profiles on HUVEC (Kraiss *et al.*, 2003). However, basic RT-PCR may not be sensitive enough to answer the question required here.

Due to its novelty, Real-Time RT-PCR assays have rarely been used for the detection of adhesion molecule mRNA levels. Although Kadl *et al.* (2002) reported the use of Real-Time RT-PCR in detecting both human and murine inflammatory genes in response to oxidized phospholipids and LPS, at the beginning of this study, a method had not yet been reported for the use of Real-Time PCR in the study of adhesion molecule mRNA expression in HUVEC. Therefore, a model was developed to perform a quantitative assay that would allow for the exploration of the induction of adhesion molecule mRNA in endothelial cells in response to *N. meningitidis*.

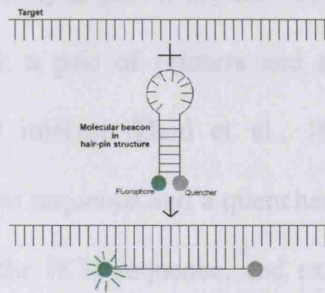
4.1.1 Real-time PCR

RT-PCR is semi-quantitative at best, and this method has therefore been further developed to become quantitative. This method is known as Real-Time PCR, and measures the quantity of PCR product after every cycle. This differs from semi-quantitative RT-PCR, which measures the amount of product at approximately 25 cycles. This gives a very narrow window in which to detect subtle differences in amount of product, and is therefore not very sensitive.

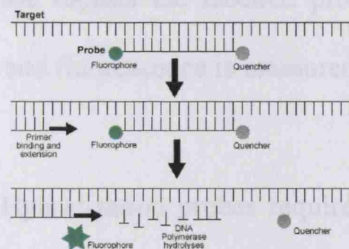
Different chemistries have been developed for use in Real-Time PCR and these can be viewed in Figure 4.1. These are described in further detail below.

1. **Molecular Beacons:** Molecular Beacon reactions consist of specific oligonucleotide primers, which amplify a sequence of interest, and an internal probe, which binds to the sequence of interest (Tyagi and Kramer, 1996). The internal oligoprobes are designed to contain the sequence of interest in the middle and homologous bps at both ends, which then prime together to form a hairpin-like structure. During the annealing step of the Real-Time PCR reaction, the oligoprobe binds to the PCR-amplified complementary sequence, which allows the fluorophore to fluoresce. Fluorescence is measured, thereby allowing for the quantification of the sequence of interest.

A) Molecular Beacons



B) Hydrolysis Probes



C) Hybridisation probes

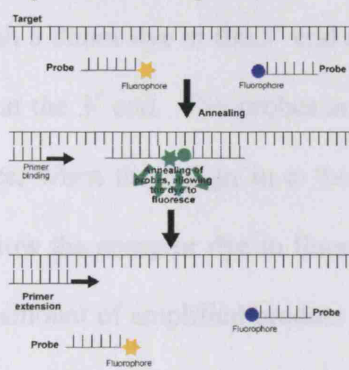


Figure 4.1 Chemistries used in Real-Time PCR. A) Molecular Beacons: The hair-pin structure of the oligoprobe binds to target DNA, allowing the fluorophore to fluoresce and determine the amount of target gene in solution. B) Hydrolysis probe: the probe is degraded by the 5' to 3' nuclease action of the DNA polymerase enzyme, thereby releasing the fluorophore and allowing it to fluoresce. C) Hybridisation probes: the two labelled probes align together in the target sequence, allowing the donor dye and the acceptor dye to come together and fluoresce.

2. Hydrolysis probes: Hydrolysis probes are also known as TaqMan probes. There are two components required: a pair of primers and an internal probe (20-40 bps) specific for the sequence of interest (Heid et al., 1996). The probe contains a fluorophore on the 5' end of the sequence and a quencher at the 3' end of the sequence. Primers and probe anneal to the PCR sequence, and extension of the primers occurs, whereupon the PCR polymerase digests the labelled probe by its 5' to 3' nuclease activity. This releases the dye and fluorescence is measured.

3. Hybridisation probes: Hybridisation probes require three components: a set of primers and two probes that will align adjacent to each other on the sequence of interest. One probe will be labelled with a donor dye at the 5' end and the second probe will be labelled with an acceptor dye at the 3' end. The probes anneal during the denaturation step of the reaction, and hence, when they align in a 'head-to-tail' fashion, the close proximity of the labels will allow the acceptor dye to fluoresce. This fluorescence will be directly proportional to the amount of amplified product in the reaction.

Whilst these three methods are very accurate and produce low background levels, the design of the primers has to be optimal. In addition, the cost of labelled primers is very high, and it can therefore become very expensive to perform Real-Time PCR. A less expensive alternative is SYBR® green, a DNA binding dye.

4.1.1.1 Using SYBR® green as a DNA binding dye for Real-Time PCR

The main DNA-binding dye used in the laboratory for detection of DNA is ethidium bromide. In Real-time PCR assays this has been replaced by SYBR® green 1. This assay only requires a set of sequence specific primers, as SYBR® green binds to any dsDNA. Unbound dye gives out low levels of fluorescence in solution, but as the polymerisation reaction takes place, the dye will bind to dsDNA and emit fluorescence (Figure 4.2).

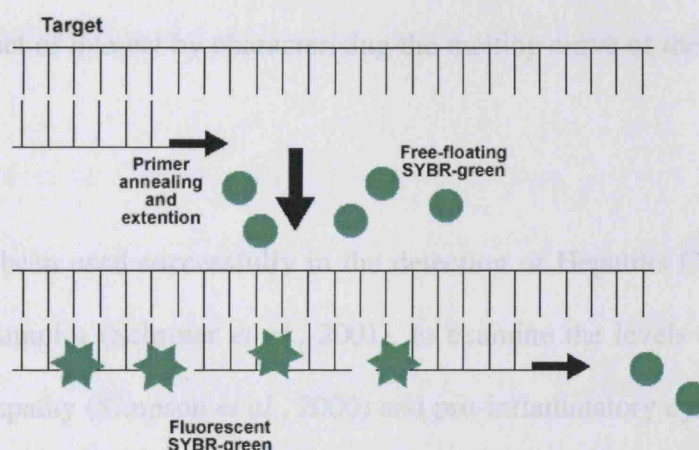


Figure 4.2 DNA-binding dyes. The illustration demonstrates the binding of SYBR-green to dsDNA, allowing the dye to fluoresce.

This property of SYBR® green can, however, cause problems when detecting fluorescence, as the dye does not distinguish between primer-dimers and amplified product. Primer-dimers can be detected by performing a melting curve analysis with the instrumentation programmes. As primer-dimers are smaller than amplified product, they melt at a lower temperature. Therefore, detection of fluorescence can be

performed at a high enough temperature to omit primer-dimer fluorescence but still include amplified product. Primer-dimer formation can also be prevented by performing a 'hot-start' PCR reaction or using a hot-start *Taq* polymerase, which becomes active at high temperature (Kellogg *et al.*, 1994).

The number of SYBR® green molecules binding to PCR product is variable. This may introduce some error in the quantification of product. It is assumed that if two primer pairs have the same amplification efficiency, then the same number of dye molecules will bind, and that the only difference will be if the two sequences amplified differ in product size. Although the level of specificity with this assay relies entirely on the specificity of the primers, it can be ensured that the fluorescence detected is from the amplified product of interest by characterising the melting curve of the product (Ririe *et al.*, 1997).

This assay has been used successfully in the detection of Hepatitis C viral loads from human serum samples (Schroter *et al.*, 2001), to examine the levels of murine VEGF mRNA in retinopathy (Simpson *et al.*, 2000) and pro-inflammatory cytokine production by DC mRNA in response to inflammatory stimuli (Blaschke *et al.*, 2000).

As this product can be used with any primer pair of interest, the cost can be drastically reduced as no labelled probes are required. This method was selected for Real-Time PCR experiments performed in this chapter.

4.1.2 Cyclophilin: a house-keeping gene for Real-Time RT-PCR

Traditionally, house-keeping genes used as mRNA controls have included glyceraldehydes-3-phosphate dehydrogenase (Zhong and Simons, 1999), β -actin and 28S rRNA. Although many studies have used GAPDH and β -actin, there is now increasing evidence that there is variation in gene expression of these genes in a range of cell types and tissues (Spanakis, 1993) and in response to different stimuli such as hypoxia (Zhong and Simons, 1999) and during development (Oikarinen *et al.*, 1991). GAPDH has, in particular, been reported to alter in response to insulin treatment (Nasrin *et al.*, 1990) and in various cancerous cell lines (Bhatia *et al.*, 1994).

In the light of these findings cyclophilin has also been used to normalise gene expression profiles (Zhong and Simons, 1999). 28S rRNA and cyclophilin have been reported to have the least variation in gene expression in response to hypoxia on endothelial cells (Zhong and Simons, 1999; Zhong and Simons, 1999). Therefore cyclophilin is increasingly being utilised as a house-keeping gene (Frist *et al.*, 1995; Ljungberg *et al.*, 2003). In the present study cyclophilin expression was chosen as the control housekeeping gene.

Cyclophilin A is a member of the cyclophilin family, which in humans is made up of at least 8 members (Gothel and Marahiel, 1999-1063) and these are peptidyl-prolyl cis-trans isomerases, which are enzymes involved in protein folding. The cyclophilin A gene is present as one copy in the human genome (Haendler and Hofer, 1990-947).

4.1.3 Quantification of Real-time PCR

There are two ways in which PCR can be quantified: relative or absolute. For most research purposes relative quantification is enough to answer a scientific question, and absolute quantification is therefore mainly used in diagnostic laboratories when viral or bacterial loads have to be determined for treatment purposes (Mackay *et al.*, 2002).

Two methods are commonly used for relative quantification: the standard curve method and the comparative threshold (C_T) method (Livak and Schmittgen, 2001;Giulietti *et al.*, 2001;Overbergh *et al.*, 2003;Bustin, 2000). There are advantages and disadvantages to both methods. For instance, a standard curve is produced by amplifying cDNA of the gene of interest followed by insertion in an appropriate plasmid vector. The plasmid vector is serially diluted to create a standard curve for each Real-Time PCR reaction, thus reducing variability between experiments. Standard curves can also be produced by creating large quantities of mRNA from a cell line expressing both the housekeeping gene and the gene of interests, and serially diluting this to create the standard curve. This relies on the ability to produce large quantities of mRNA. In contrast, a C_T method, such as the $2^{-\Delta\Delta C_T}$ method, does not require the production of a standard curve, as it relies on the relative change in C_T values (for instance, control vs. induction) (Livak and Schmittgen, 2001). However, it assumes that the PCR efficiencies of the housekeeping gene and the gene of interest are equal, which is not always the case. Validation of the C_T and standard curve method has, however, been performed and it has been demonstrated that there is no difference in quantifying mRNA levels when using the relative standard curve method or the $2^{-\Delta\Delta C_T}$ method (Winer *et al.*, 1999;Johnson *et al.*, 2000). Results obtained using these two methods were compared

to the results obtained using Northern Blot analysis. Results obtained by the three methods were comparable (Johnson *et al.*, 2000; Winer *et al.*, 1999).

The relative standard curve method has been used in the literature to measure cytokine gene induction in humans (Overbergh *et al.*, 2003; Giulietti *et al.*, 2001), rat (Peinnequin *et al.*, 2004; Winer *et al.*, 1999) and murine cells (Giulietti *et al.*, 2001; Berti *et al.*, 2002; Overbergh *et al.*, 2003; Chen *et al.*, 2004b). In particular, the use of the relative standard curve method has been favoured when detecting low levels of cytokine mRNA in rat cells (Peinnequin *et al.*, 2004).

4.1.4 Chapter Aims

To better understand the molecular mechanisms governing E-selectin expression observed with WT *N. meningitidis* and purified meningococcal LPS alone, E-selectin mRNA transcription levels were investigated to determine whether the differential expression pattern seen in Chapter 3 could be explained by gene regulation at the transcriptional level or post-transcriptional level (or both). In order to do this, RT-PCR and Real-Time PCR methods were examined.

The aims of this chapter were:

- To examine *N. meningitidis* WT, *lpxA*- and purified meningococcal LPS induced E-selectin and VCAM-1 gene expression on HUVEC by RT-PCR
- To optimise Real-Time PCR primers for the amplification of adhesion molecule mRNA from endothelial cells

- To develop a standard for a house-keeping gene control (cyclophilin), E-selectin and VCAM-1 gene expression
- To utilise the standard curve to determine adhesion molecule mRNA levels in endothelial cells responding to fixed meningococci and LPS

4.2 Materials and Methods

4.2.1 Culture of HUVEC and HMEC

Details of endothelial cell isolation from umbilical cords and cell culture and maintenance of HUVEC and HMEC-1 are described in Chapter 2, Section 2.2.1 and Section 2.2.2. Generally, once HUVEC and HMEC-1 reached 95% confluence, they were subcultured onto tissue culture plates coated with attachment factor and grown to confluence prior to infection with *N. meningitidis* WT and *lpxA*- bacteria and purified LPS.

4.2.2 Detection of adhesion molecule mRNA in HUVEC

Adhesion molecule mRNA expression profiles were investigated using RT-PCR and Real-time RT-PCR, as described in Chapter 2, Section 2.7, 2.8 and 2.9.

4.2.3 Primers used for RT-PCR and Real-Time RT-PCR

Primers for RT-PCR are shown in **Error! Reference source not found.** These primers were obtained from the literature, and produced PCR product sizes ranging from 450-1500 bps. As Real-Time PCR products cannot exceed 350 bps, a different set of primers were designed for Real-Time PCR assays (Table 4.2). These primers were design to produce products of around 200 bps long. Primers were designed to span at

least 2 exons (which is the region of the gene that is translated) and an intron (which a non-translated region), as demonstrated on Figure 4.3.

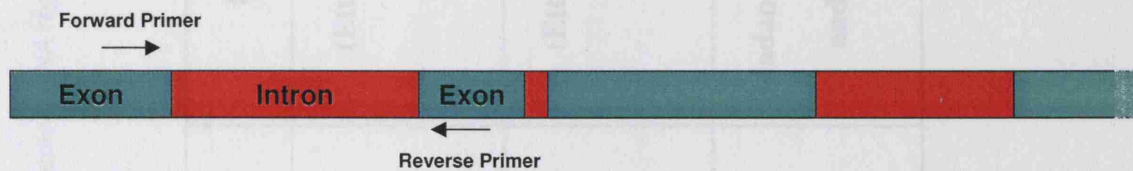


Figure 4.3: Diagram of genetic sequence organisation and primer design. The figure illustrates the organisation of a gene, containing exons (green), which are transcribed into mRNA, and introns (red), which are spliced and are not included in the mRNA sequence. Primers are designed within an exon sequence, and span at least one intron. This allows for the identification of genomic DNA contamination.

Table 4.1 Primers used for RT PCR.

Gene		Primer	Reference
GAPDH	Forward	5'-CACAGTCCATGCCATCACTG-3'	(Etter <i>et al.</i> , 1998)
	Reverse	5'-TACTCCTTGGAGGCCCATGTG-3'	
E-selectin	Forward	5'-TGTGGGCATGTGGAATGATG-3'	(Etter <i>et al.</i> , 1998)
	Reverse	5'-CGAAGCCAGAGGAGAAATG-3'	
VCAM-1	Forward	5'-ACCCCTCCCAAGGCACACACAG-3'	(Madan <i>et al.</i> , 2001; Gupta and Ghosh, 1999)
	Reverse	5'-GTAAGTCTATCTCCAGCCTGTC-3'	

Table 4.2 Primers used for Real-Time RT-PCR.

Gene		Primer	Reference
Cyclophilin	Forward	5'-GTCAGCAATGGTGATCTTCTT-3'	(Samady <i>et al.</i> , 2004)
	Reverse	5'-GCAGAAAATTTTCGTGCTCTG-3'	
E-selectin	Forward	5'-GGGAATTTCGTGTGACCCCTGGCTTC-3'	(Jacobsen <i>et al.</i> , unpublished)
	Reverse	5'-GGAAGCTTGGAAATAGGAGCACTCC-3'	
VCAM-1	Forward	5'-ATGACATGCTTGAGCCAGG-3'	(Zhang <i>et al.</i> , 2002)
	Reverse	5'-GTGTCCTCCTTCTTTGACACT-3'	

4.2.4 Primer annealing temperature optimisation

Primer annealing temperature optimisation was carried out using a Peltier Thermal Cycler PCR machine (MJ Research). A protocol providing a temperature gradient was modified. The programme used can be viewed in Table 4.3. Primers were optimised on HMEC-1 mRNA stimulated for 4 hours with fixed WT bacteria (10^8 CFU/ml).

Table 4.3 Cycling conditions for primer optimisation PCR reaction

Step	Temperature	Time	Cycles
Initial Denaturation	95°C	10 min	1
Denaturation	95°C	1 min	40
Annealing	55-66°C	1 min	
Extension	72°C	1 min	
Final Extension	72°C	10 min	1

4.2.5 Development of standards for Real-Time RT-PCR

To obtain a standard for Real-Time PCR, it was decided to create a product which could be easily prepared in large quantities. Figure 4.4 illustrates the procedure performed to develop a standard curve for Real-Time PCR. The PCR products obtained were inserted into a plasmid which was then grown in large quantities in bacteria and purified for use in PCR. Briefly, PCR product obtained with Real-Time PCR primers were isolated and purified using QIAquick Gel extraction kit (Qiagen). The amount of purified product was determined by gel electrophoresis and compared to a known amount of DNA ladder product.

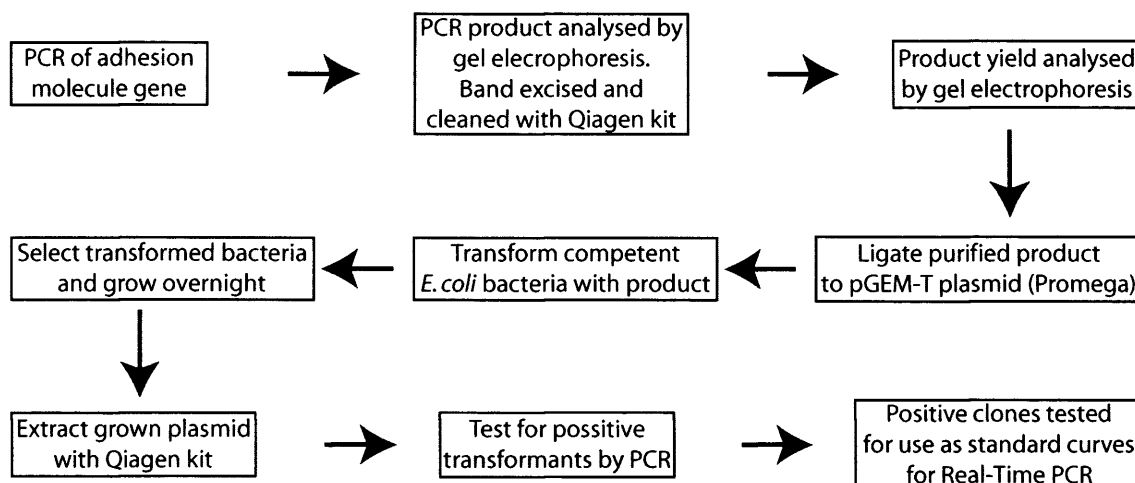


Figure 4.4 Flow chart illustrating the process undertaken to produce plasmids for standard curves for Real-Time PCR.

The purified product was ligated into pGEM-T Easy Vector (Promega, Figure 4.5) following manufacturers instructions. This vector contains a Thymine (T-) overhand, and as the majority of *Taq* polymerase enzymes add an Adenine (A-) overhang to their PCR product, the product can be easily ligated to the pGEM-T vector. Briefly, the PCR product was mixed with the ligation buffer, T4 DNA Ligase, and vector at two optimum molar ratio concentrations (3:1 and 1:1 insert:vector ratios) and left at room temperature for 1 hour.

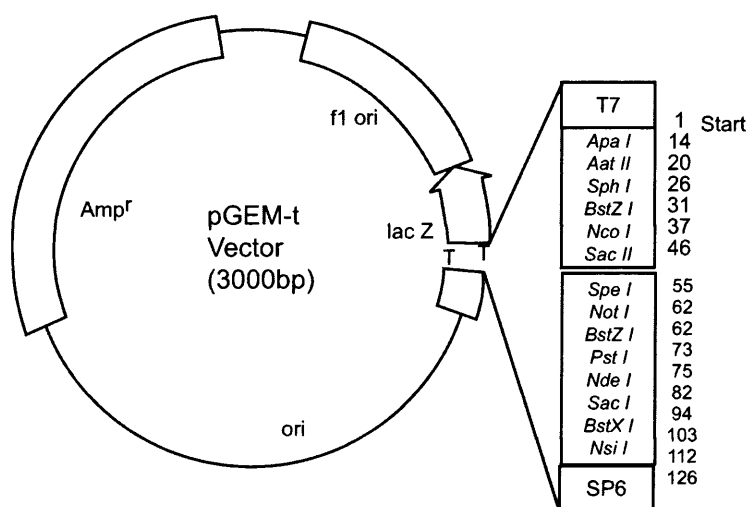


Figure 4.5 pGEM-T Easy Vector (Promega)

The product was used to transform either JM109 (Promega) heat sensitive *E. coli* cells or DH5 α (Invitrogen) electrocompetent *E. coli* cells, following manufacturers instructions. The bacteria were grown overnight on LB agar supplemented with 100 μ g/ml ampicillin. Transformed bacteria would carry the ampicillin resistance gene, allowing them to grow in ampicillin supplemented LB agar.

Colonies were selected and screened for the gene insert by PCR. Selected colonies were grown overnight on LB broth supplemented with 100 μ g/ml ampicillin, and vector was purified using QIAprep spin miniprep kit (Qiagen) following manufacturers instructions. Plasmid was eluted in 30 μ l nuclease free water and serially diluted. Standard curves were generated by 10-fold serial dilutions of plasmids containing each gene of interest. Vector clones that gave consistent and reproducible results were selected and routinely used for Real-Time PCR assays. Diluted plasmids were kept in 5 μ l aliquots at -20°C for long term storage.

4.2.6 Data analysis, normalisation of data and statistical analysis

Data was analysed using an Opticon Monitor (GRI). The threshold curve was set to measure cycle number prior to the exponential expansion of PCR product, as measured by fluorescence intensity of SYBR Green. This was performed by eye. For experimental consistency, standard curves had to have an R^2 value of at least 0.98 or above. If this was not achieved, the Real-Time PCR reaction was repeated. For each primer pair used in a reaction, there would be at least two negative control reactions

containing no template DNA. Real-time PCR reactions that had a positive negative control reaction were repeated.

Data were normalised using a mathematical method, referred to here as *gene induction* (Equation 4.1), took the average of gene of interest (target gene, x) and normalised it to the average of the housekeeping control gene (reference gene, y).

$$gene\ induction = \frac{\bar{x}}{y}$$

Equation 4.1: Mathematical equation demonstrating how the gene induction of gene of interest was calculated. x =gene of interest (*i.e.* E-selectin); y =house-keeping gene control (cyclophilin).

4.3 Results

4.3.1 Fixed WT and *lpxA*- *N. meningitidis* bacteria and purified meningococcal LPS induce E-selectin mRNA on HUVEC

TNF- α induced E-selectin and VCAM-1 expression has previously been detected by RT-PCR 4 hours post induction (Etter *et al.*, 1998; Gupta and Gosh, 1999; Madan *et al.*, 2001). In these studies, GAPDH expression was used to normalise the reactions. In order to compare results obtained in this thesis to previously published work, primers used in the published studies were used to investigate the effect of whole *N. meningitidis* on E-selectin and VCAM-1 gene expression. HUVEC were exposed to PFA killed *N. meningitidis* WT and *lpxA*- and purified LPS for 4 hours prior to RNA extraction followed by RT-PCR.

A modest increase in E-selectin mRNA expression above baseline was observed in response to 10ng/ml meningococcal LPS within 4 hours of culture (Figure 4.6). WT bacteria induced an increase in E-selectin mRNA at 10^6 CFU/ml, with a further increase on exposure to 10^8 CFU/ml WT bacteria. The *lpxA*- mutant induced E-selectin mRNA expression above baseline levels at a concentration of 10^8 CFU/ml bacteria. There was no E-selectin mRNA expression detected by RT-PCR in unstimulated HUVEC and those stimulated with 10^6 CFU/ml *lpxA*- bacteria.

The levels of E-selectin mRNA obtained with 10^8 CFU/ml WT bacteria were higher than the levels obtained with 10ng/ml purified LPS. E-selectin mRNA levels induced

by 10^8 CFU/ml *lpxA*- bacteria reached similar levels to those induced with 10ng/ml purified LPS, however, E-selectin mRNA levels remained low in comparison to WT bacteria.

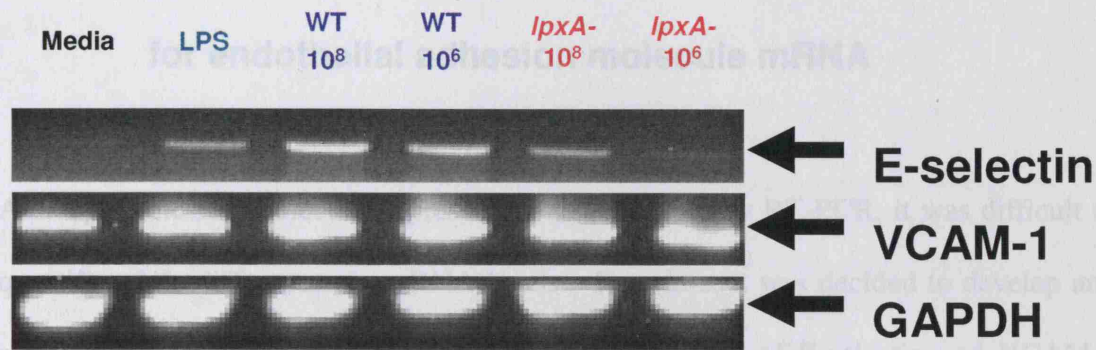


Figure 4.6 Induction of E-selectin and VCAM-1 by *N. meningitidis*. HUVEC were stimulated for 4 hours with *N. meningitidis* WT and *lpxA*- bacteria and 10ng/ml LPS. E-selectin, VCAM-1 and GAPDH were detected by RT-PCR. Primer sequences are demonstrated in **Error! Reference source not found.**, and have previously been used in the literature (Etter *et al.*, 1998;Madan *et al.*, 2001;Gupta and Ghosh, 1999).

VCAM-1 mRNA expression was induced above baseline levels by 10ng/ml purified LPS after 4 hours of stimulation (Figure 4.6). WT bacteria induced VCAM-1 mRNA expression in response to 10^6 and 10^8 CFU/ml. The *lpxA*- mutant bacteria also induced VCAM-1 mRNA expression at a concentration of 10^8 CFU/ml. VCAM-1 mRNA expression in non-stimulated HUVEC was constitutive. Due to the semi-quantitative nature of the detection system, the effect of 10^6 CFU/ml *lpxA*- bacteria on VCAM-1 mRNA expression was inconclusive.

There were no detectable differences in GAPDH mRNA expression in response to WT and *lpxA*- bacteria and purified meningococcal LPS (Figure 4.6), suggesting that there

were no differences in mRNA loading and therefore that the differences in gene induction observed with E-selectin and VCMA-1 are true observations.

4.3.2 Development and optimisation of Real-Time RT-PCR for endothelial adhesion molecule mRNA

Although adhesion molecule expression was detectable by RT-PCR, it was difficult to quantify subtle differences in mRNA levels. Therefore, it was decided to develop and optimise a Real-Time RT-PCR method for the detection of E-selectin and VCAM-1 mRNA to investigate the effects of *N. meningitidis* WT and *lpxA*- bacteria and purified meningococcal LPS.

For Real-Time PCR, product sizes must not exceed 350 bp. Therefore new PCR primers were optimised and tested on HMEC-1 mRNA stimulated with 10^8 CFU/ml WT *N. meningitidis* bacteria, and primer pairs were selected based on their ability to amplify the primed sequence (data not shown). Whilst HMEC-1 do not express E-selectin, these cells did transcribe adhesion molecule mRNA. Figure 4.7 demonstrates the temperature optimisation of the selected primers for cyclophilin, E-selectin and VCAM-1. The cyclophilin and E-selectin primers produced high levels of product at temperatures ranging from 55°-61°C, and levels of product decreased as the temperature was increased to 63°-66°C. However, the VCAM-1 primers produced more product as the temperature increased, reaching optimal levels at 57-61°C. Temperature increases above 61°C inhibited primer annealing to the PCR product. All primers produced good levels of PCR products at 60°C annealing temperature, and this temperature was therefore used as the annealing temperature in Real-Time RT-PCR.

Selctin (Figure 4.8B) and VCAM-1 (Figure 4.8C) produced 1:10 dilutions which exponentially extended at around 3.3 cycles after one another and created standard curves with an R^2 of 0.98. For the majority of the Real-Time PCR data, it was important to create a standard curve with an R^2 of a minimum of 0.98, as assays that produced standards with a lower R^2 value cannot be reliable. Another element to note when creating a good standard is that for every 10 dilution made, the product will appear 3.3 cycles later.

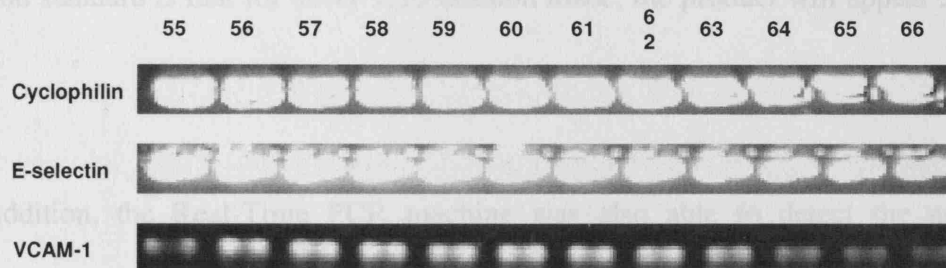


Figure 4.7 Real-time PCR primer optimisation. HMEC-1 cDNA was used to optimisation primer annealing temperature of PCR primers using a temperature gradient programme. Primer sequences can be viewed in Table 4.2.

4.3.3 Real-Time PCR of standards for Cyclophilin, E-selectin, and VCAM-1

Products obtained from the RT-PCR primer temperature optimisation were used to create Real-Time PCR standards, as described in Section 4.2.5. Plasmids were screened for use as standards for Real-Time PCR assays.

Data obtained from Real-Time PCR amplification of the standards for cyclophilin, E-selectin, and VCAM-1 mRNA are shown in Figure 4.8. The highest plasmid concentrations were detected between 10-15 cycles (Figure 4.8i). This allowed the Opticon Instrument to create a base-line of the SYBR-green levels detected. As can be seen on Figure 4.8i and Figure 4.8ii, all three standards (cyclophilin (Figure 4.8A), E-

Selectin (Figure 4.8B), and VCAM-1(Figure 4.8C)) produced 1:10 dilutions which exponentially expanded at around 3.3 cycles after one another and created standard curves with an $R^2 \geq 0.98$. For the analysis of the Real-Time PCR data, it was important to create a standard curve with an R^2 of a minimum of 0.98, as assays that produced standards with a lower R^2 would not be reliable. Another element to note when creating a good standard is that for every 1:10 dilution made, the product will appear 3.3 cycles later.

In addition, the Real-Time PCR machine was also able to detect the number of amplified PCR products. At the end of the Real-Time PCR reaction, the levels of SYBR-green® fluorescence were detected at 0.3°C intervals from 55°C-98°C. As the temperature increased, the SYBR-green® fluorescence remained high, due to the SYBR-green® being bound to dsDNA. Fluorescence levels remained elevated until the temperature reached the melting temperature of the PCR product, where the double-stranded DNA (PCR product) dissociated to become single-stranded. At this point, the SYBR-green® fluorescence rapidly decreased, as can be seen on Figure 4.8iii. The data obtained from the melting curve analysis was used to plot the rate of change of fluorescence with time (Y-axis) as compared to the increase of temperature (X-axis), which created a melting-peak curve for PCR products.

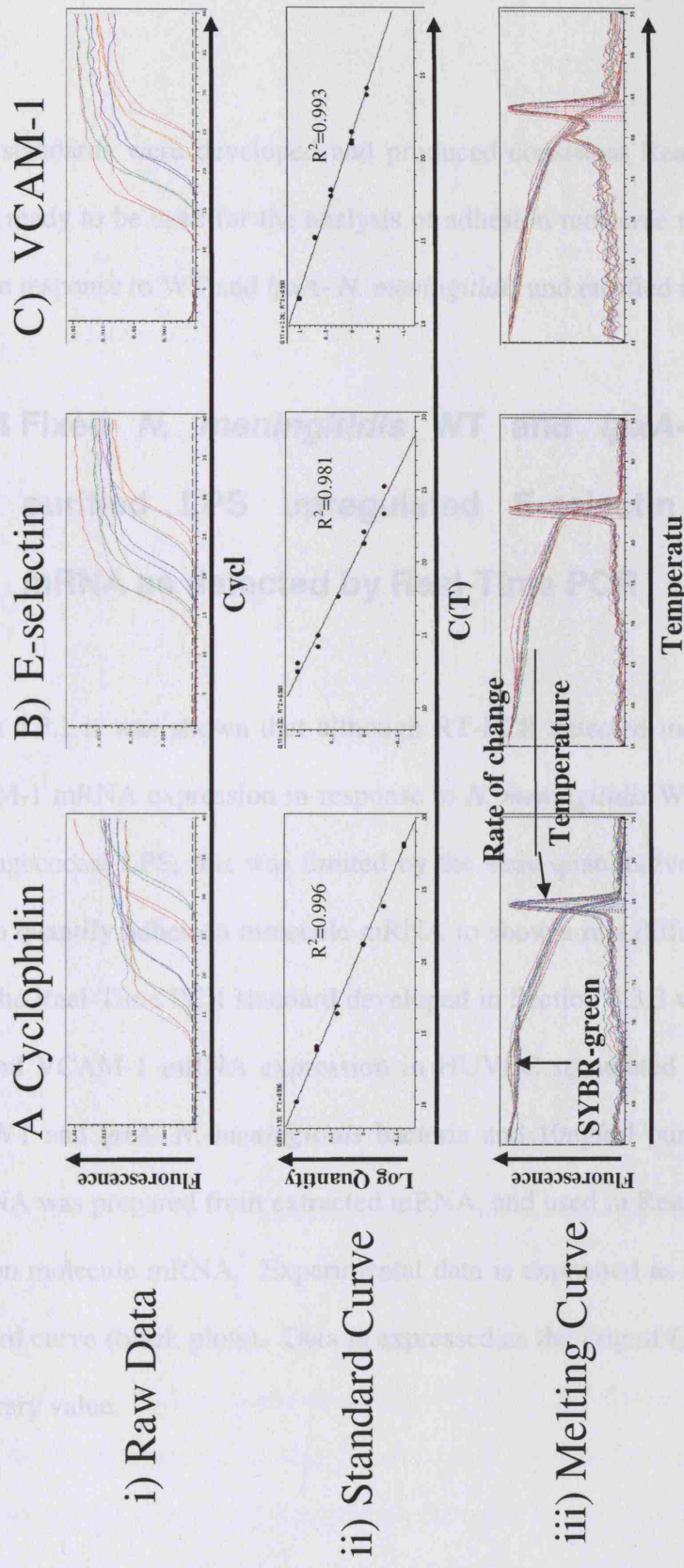


Figure 4.8 Real-time RT-PCR optimisation of standard curves for Cyclophilin, E-selectin and VCAM-1. Standards were created as described in Section 4.2.5. Plasmids were serially diluted and selected for good reproducibility and good standard curve fit ($R^2 \geq 0.98$). A) raw data. B) standard curve. C) melt-curve assay.

Once the standards were developed and produced consistent Real-Time PCR results, they were ready to be used for the analysis of adhesion molecule mRNA expression in HUVEC in response to WT and *lpxA*- *N. meningitidis* and purified meningococcal LPS.

4.3.4 Fixed *N. meningitidis* WT and *lpxA*- bacteria and purified LPS upregulated E-selectin and VCAM-1 mRNA as detected by Real-Time PCR

In Section 4.3.1 it was shown that although RT-PCR detected increases in E-selectin and VCAM-1 mRNA expression in response to *N. meningitidis* WT and *lpxA*- bacteria and meningococcal LPS, this was limited by the semi-quantitative nature of RT-PCR. In order to quantify adhesion molecule mRNA to show a real difference in stimulatory strength, the Real-Time PCR standard developed in Section 4.3.3 was used to detect E-selectin and VCAM-1 mRNA expression in HUVEC stimulated with PFA fixed 10^8 CFU/ml WT and *lpxA*- *N. meningitidis* bacteria and 10ng/ml purified meningococcal LPS. cDNA was prepared from extracted mRNA, and used in Real-Time PCR analysis of adhesion molecule mRNA. Experimental data is expressed as the red plots against the standard curve (black plots). Data is expressed as the Log of Quantity (LQ), which is an arbitrary value.

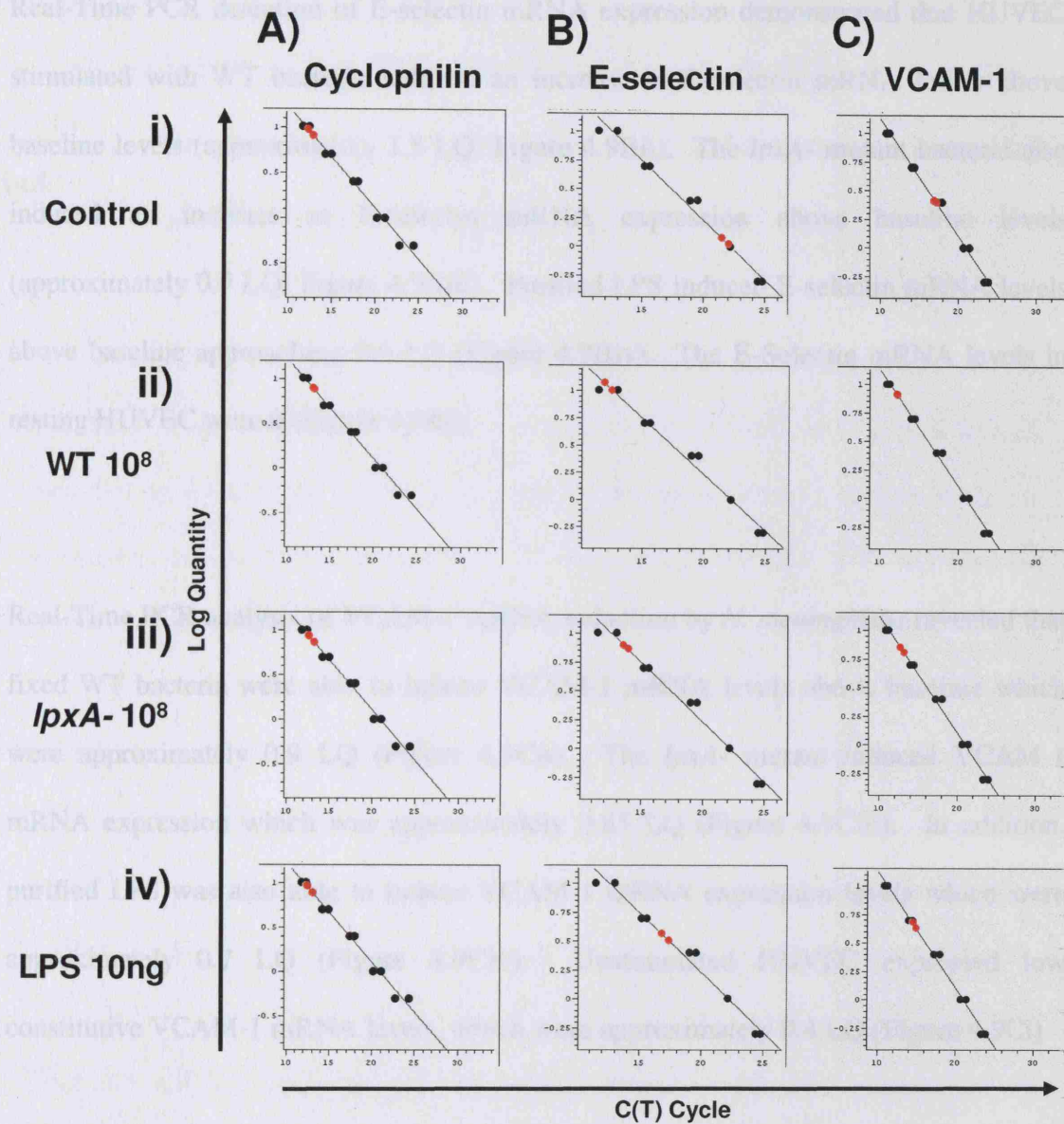


Figure 4.9 Cyclophilin, E-selectin and VCAM-1 mRNA levels in HUVEC stimulated with *N. meningitidis* WT and *lpxA*- bacteria and purified LPS. HUVEC were stimulated for 4 hours, and mRNA levels were detected by Real-Time RT-PCR. The standard curve (black plots) was used to determine the levels of mRNA in the experimental samples (red plots). Cyclophilin (A), E-selectin (B), and VCAM-1 (C) mRNA levels detected in unstimulated control (i), 10^8 CFU/ml WT (ii), 10^8 CFU/ml *lpxA*- (iii), and 10ng/ml LPS. Data is expressed as log of quantity of fluorescence in relation to cycle (C(T)) value.

Real-Time PCR detection of E-selectin mRNA expression demonstrated that HUVEC stimulated with WT bacteria induced an increase in E-selectin mRNA levels above baseline levels (approximately 1.5 LQ; Figure 4.9Bii). The *lpxA*- mutant bacteria also induced an increase in E-selectin mRNA expression above baseline levels (approximately 0.9 LQ; Figure 4.9Biii). Purified LPS induced E-selectin mRNA levels above baseline approaching 0.6 LQ (Figure 4.9Biv). The E-Selectin mRNA levels in resting HUVEC were 0 (Figure 4.9Bi).

Real-Time PCR analysis of VCAM-1 mRNA induction by *N. meningitidis* revealed that fixed WT bacteria were able to induce VCAM-1 mRNA levels above baseline which were approximately 0.9 LQ (Figure 4.9Cii). The *lpxA*- mutant induced VCAM-1 mRNA expression which was approximately 0.85 LQ (Figure 4.9Ciii). In addition, purified LPS was also able to induce VCAM-1 mRNA expression levels which were approximately 0.7 LQ (Figure 4.9Civ). Unstimulated HUVEC expressed low constitutive VCAM-1 mRNA levels, which were approximately 0.4 LQ (Figure 4.9Ci).

The housekeeping gene, cyclophilin, demonstrated no variation in mRNA levels in response to *N. meningitidis* WT and *lpxA*- bacteria and purified LPS and in unstimulated HUVEC (Figure 4.9A). There was very little variation in cyclophilin expression between the different stimuli, and all levels were approximately 0.9 LQ.

4.3.5 E-selectin mRNA transcription on HUVEC augmented in response to increasing concentrations of fixed WT and *lpxA*- *N. meningitidis* and purified LPS

Having established that the increased expression of E-selectin seen on the cell surface in response to whole bacteria and LPS alone was paralleled by increases in cellular mRNA transcription, these findings were investigated further by detecting E-selectin mRNA in response to increasing concentrations of *N. meningitidis* WT and *lpxA*- bacteria and purified meningococcal LPS.

HUVEC were stimulated with 10^5 - 10^8 CFU/ml WT and *lpxA*- bacteria and 0.1-10ng/ml purified LPS. The raw data obtained from the Real-Time RT-PCR reaction was normalised to the housekeeping gene control, cyclophilin, by using the *gene induction* method described in Section 4.2.6, Equation 4.1.

E-selectin mRNA expression increased above baseline with 10^5 CFU/ml WT *N. meningitidis* bacteria (Figure 4.10). E-selectin mRNA expression continued to increase until reaching a maximum in response to 10^8 CFU/ml WT bacteria. Significantly higher levels of E-selectin mRNA expression compared to baseline expression were obtained with 10^8 CFU/ml WT *N. meningitidis* bacteria ($p < 0.001$).

The *lpxA*- bacteria induced low levels of E-selectin mRNA expression above baseline level with 10^6 and 10^7 CFU/ml bacteria (Figure 4.10). E-selectin mRNA levels reached

a maximum in response to 10^8 CFU/ml *lpxA*- bacteria. Significantly high levels of E-selectin mRNA were obtained with 10^8 CFU/ml *lpxA*- bacteria ($p < 0.001$) as compared to control.

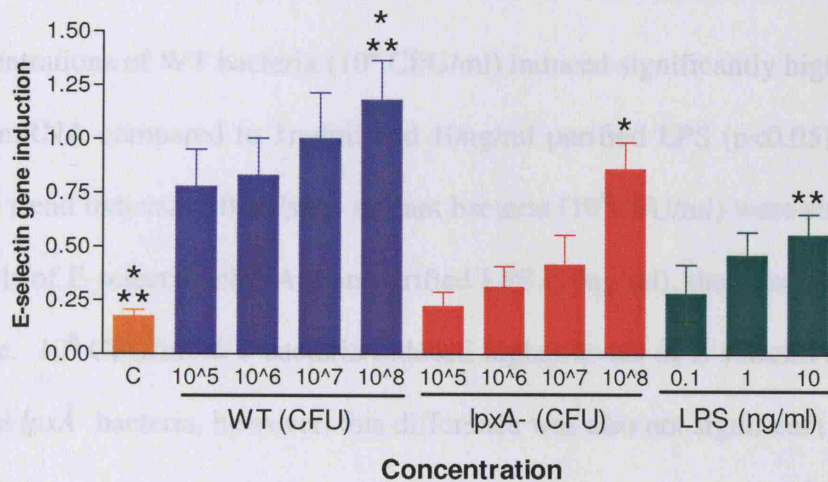


Figure 4.10: E-selectin mRNA synthesis in HUVEC in response to fixed *N. meningitidis* bacteria and meningococcal LPS. HUVEC were stimulated for 4 hours with increasing concentration of WT (blue bars) and *lpxA*- (red bars) bacteria or purified LPS (green bars), and mRNA levels were detected using Real-Time PCR. Data normalised using the *gene induction* method. Results are presented as mean of *gene induction* \pm SEM, $n \geq 4$ from endothelial cells from separate donors *= $p < 0.001$; **= $p < 0.05$ (1-way ANOVA).

E-selectin mRNA expression was also induced in response to increasing concentrations of purified meningococcal LPS (Figure 4.10). Low concentrations of LPS (0.1ng/ml) induced low levels of E-selectin mRNA expression, which continued to increase until

reaching a maximum with 10ng/ml LPS. E-selectin mRNA levels were significantly higher above control when stimulated with 10ng/ml LPS ($p < 0.05$).

Unstimulated HUVEC displayed very low levels of E-selectin mRNA transcription.

High concentrations of WT bacteria (10^8 CFU/ml) induced significantly higher levels of E-selectin mRNA compared to 1ng/ml and 10ng/ml purified LPS ($p < 0.05$). Although there was a trend indicating that *lpxA*- mutant bacteria (10^8 CFU/ml) were able to induce higher levels of E-selectin mRNA than purified LPS (10ng/ml), the data failed to reach significance. 10^8 CFU/ml WT bacteria induced higher levels of E-selectin mRNA than 10^8 CFU/ml *lpxA*- bacteria, however, this difference was also not significant.

4.3.6 E-selectin mRNA levels correlate with E-selectin surface protein expression in HUVEC induced by *N. meningitidis* WT and *lpxA*- bacteria

To verify that increased E-selectin mRNA expression was the cause of the increased E-selectin surface protein expression detected in Chapter 3, it was necessary to correlate the detected mRNA levels with surface protein levels. E-selectin mRNA transcription levels (*gene induction*) stimulated by *N. meningitidis* WT, *lpxA*- mutant and purified LPS were plotted against E-selectin surface protein expression (MFI) levels on stimulated HUVEC (Figure 4.11).

E-selectin mRNA expression levels in HUVEC induced by fixed WT *N. meningitidis* bacteria correlated significantly with E-selectin surface expression levels on HUVEC (Figure 4.11A; $p < 0.05$). In addition, *lpxA*- induced E-selectin mRNA expression in HUVEC also correlated significantly with E-selectin surface expression on HUVEC (Figure 4.11B; $p < 0.01$). Interestingly, there was no correlation between E-selectin mRNA and surface expression levels induced by meningococcal LPS (data not shown).

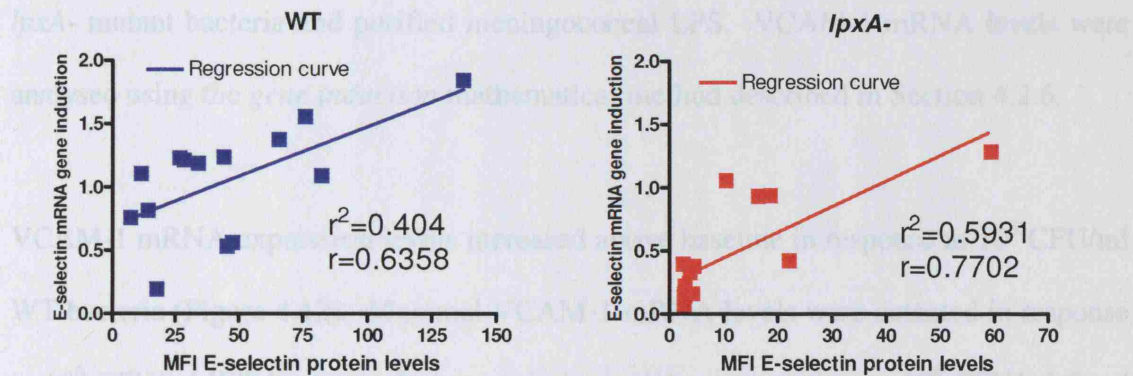


Figure 4.11 E-selectin mRNA and protein expression correlation. HUVEC were stimulated for 4 hours (mRNA) and 5 hours (protein), and E-selectin mRNA and protein expression was detected as described in Chapter 2, Section 2.5 and Section 2.7. mRNA transcription levels were correlated to protein expression using GraphPad Prism, $n=4$ from endothelial cells from separate donors.

4.3.7 VCAM-1 mRNA transcription is induced in response to increasing concentrations of fixed WT, *lpxA*- *N. meningitidis* and purified LPS

In order to investigate if the VCAM-1 surface expression levels were also due to increased transcriptional activity, VCAM-1 mRNA expression patterns were explored in response to increasing concentrations of PFA fixed *N. meningitidis* WT bacteria, *lpxA*- mutant bacteria and purified meningococcal LPS. VCAM-1 mRNA levels were analysed using the *gene induction* mathematical method described in Section 4.2.6.

VCAM-1 mRNA expression levels increased above baseline in response to 10^5 CFU/ml WT bacteria (Figure 4.12). Maximal VCAM-1 mRNA levels were detected in response to 10^6 CFU/ml WT bacteria. Increases in bacterial concentration to 10^8 CFU/ml fixed WT bacteria did not further increase VCAM-1 mRNA expression, however, levels were reduced compared to the levels obtained with 10^6 CFU/ml WT bacteria. VCAM-1 mRNA expression levels were significantly higher above control when stimulate with 10^6 CFU/ml WT bacteria ($p < 0.01$). Whilst increases in WT bacterial concentration did not induce higher levels of VCAM-1 mRNA, levels remained significantly higher in response to 10^8 CFU/ml WT bacteria than levels obtained in unstimulated control HUVEC ($p < 0.001$).

lpxA- bacteria induced VCAM-1 mRNA expression above baseline levels at a concentration of 10^7 CFU/ml bacteria (Figure 4.12). VCAM-1 mRNA expression was

maximal in response to 10^8 CFU/ml *lpxA*- bacteria. *lpxA*- bacterial concentrations of 10^5 and 10^6 CFU/ml did not induce VCAM-1 mRNA transcription as detected by Real-Time PCR. VCAM-1 mRNA expression in HUVEC induced by 10^8 CFU/ml *lpxA*- bacteria were significantly higher than unstimulated control levels ($p < 0.01$).

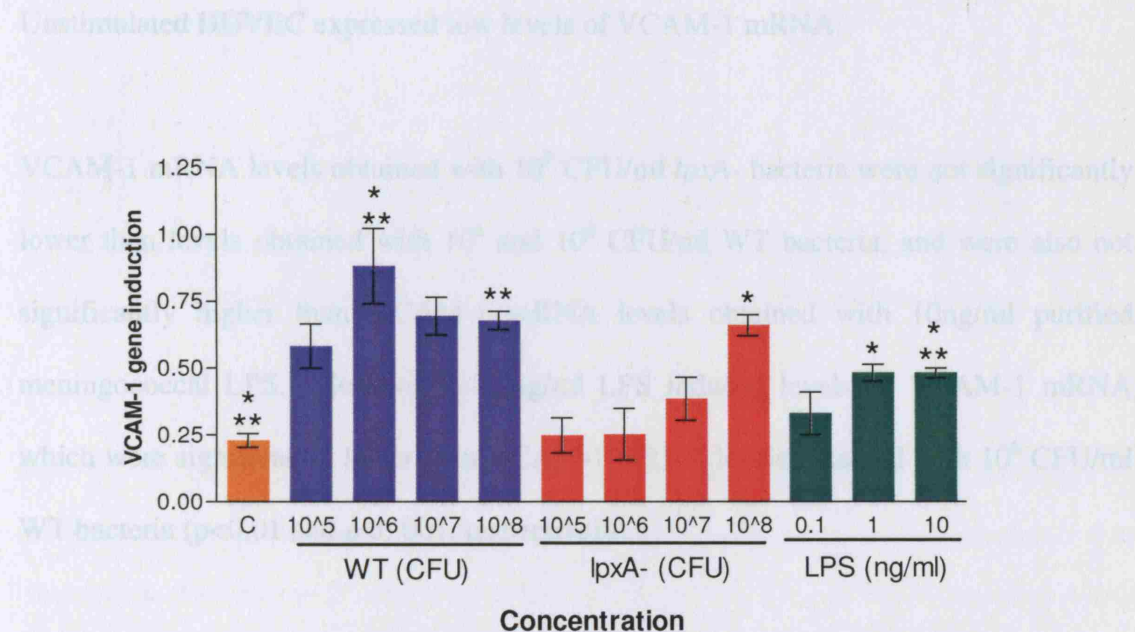


Figure 4.12 VCAM-1 mRNA synthesis in HUVEC in response to fixed *N. meningitidis* bacteria and LPS. HUVEC were stimulated for 4 hours with increasing concentration of WT (blue bars) and *lpxA*- (red bars) bacteria or purified LPS (green bars), and mRNA levels were detected. Data was normalised using the *gene induction* method. Results are presented as mean of *gene induction* \pm SEM, $n=4$ from endothelial cells from separate donors. *= $p < 0.01$; **= $p < 0.001$ (1-way ANOVA).

Low levels of VCAM-1 mRNA expression were induced by 0.1ng/ml purified LPS (Figure 4.12). mRNA levels increased until reaching a plateau in response to 1ng/ml purified LPS, and levels remained elevated in response to 10ng/ml purified LPS.

Unstimulated HUVEC expressed low levels of VCAM-1 mRNA.

VCAM-1 mRNA levels obtained with 10^8 CFU/ml *lpxA*- bacteria were not significantly lower than levels obtained with 10^6 and 10^8 CFU/ml WT bacteria, and were also not significantly higher than VCAM-1 mRNA levels obtained with 10ng/ml purified meningococcal LPS. However, 1-10ng/ml LPS induced levels of VCAM-1 mRNA which were significantly lower than VCAM-1 mRNA levels obtained with 10^6 CFU/ml WT bacteria ($p < 0.01$ and $p < 0.001$, respectively).

4.3.8 VCAM-1 protein expression does not correlate with surface protein levels in WT and LPS induced HUVEC whilst *lpxA*- induced mRNA and protein expression do

VCAM-1 mRNA expression levels were correlated to VCAM-1 surface protein levels (MFI- as detected by FACS) induced by *N. meningitidis* WT and *lpxA*- bacteria and purified LPS (Figure 4.13). WT bacteria induced VCAM-1 mRNA levels that did not correlate with VCAM-1 surface expression, as detected by FACS (Figure 4.13A). LPS induced VCAM-1 mRNA expression also failed to correlate with surface protein expression detected (data not shown). In contrast, correlation of VCAM-1 mRNA and

protein expression induced by the *lpxA*- mutant demonstrated that there was a relationship between the two (Figure 4.13B; $p < 0.05$).

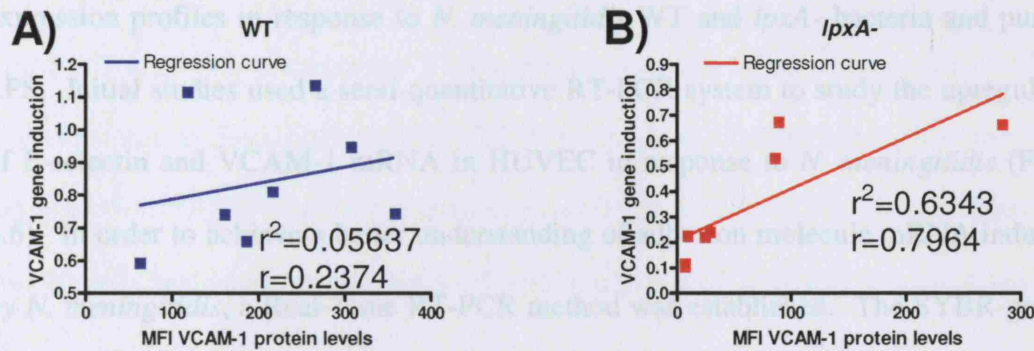


Figure 4.13 VCAM-1 mRNA and protein expression correlation. HUVEC were stimulated for 4 hours (mRNA) and 5 hours (protein), and VCAM-1 mRNA and surface expression was detected as described in Chapter 2, Section 2.5 and Section 2.7. mRNA transcription levels were correlated to protein expression using GraphPad Prism, $n=2$.

4.4 Discussion

The aim of this chapter was to establish endothelial E-selectin and VCAM-1 mRNA expression profiles in response to *N. meningitidis* WT and *lpxA*- bacteria and purified LPS. Initial studies used a semi-quantitative RT-PCR system to study the upregulation of E-selectin and VCAM-1 mRNA in HUVEC in response to *N. meningitidis* (Figure 4.6). In order to achieve a better understanding of adhesion molecule mRNA induction by *N. meningitidis*, a Real-Time RT-PCR method was established. The SYBR-green® method was selected due to practicality and cost of the assay, as it only required a pair of non-labelled primer pairs per gene of interest.

New primer pairs were designed for Real-Time RT-PCR analysis of E-selectin and VCAM-1. During the design of the primers, it was ensured that the product would span at least two exons, as this would allow for the detection of genomic DNA contamination with agarose gel electrophoreses or melting curve analysis. It was ensured that the GC content was between 40-60%, as this is recommended from various primer producing companies. The reason for this percentage is that higher levels of GC bases may lead to incorrect primer annealing of oligos. Primer pair annealing temperature optimisation was performed on all three primer pairs and an annealing temperature of 60° C was selected, as all three primers could prime and produce PCR product at this temperature (Figure 4.7). In addition, higher annealing temperatures are preferable, as they prevent primer-dimers from forming. The development of Real-Time PCR standards was successful for cyclophilin, E-selectin and VCAM-1 (Figure 4.8). The plasmids selected

produced consistently good standards which had an R^2 of above 0.98. The standards were then used to study the stimulation of E-selectin and VCAM-1 mRNA by *N. meningitidis*.

Fixed WT and *lpxA*- bacteria and LPS induced E-selectin mRNA expression at 4 hours post infection, as determined by both RT-PCR and Real-Time RT-PCR (Figure 4.6 and Figure 4.9). 10^8 CFU/ml WT bacteria induced E-selectin mRNA levels which were significantly higher than those obtained with 10ng/ml LPS ($p < 0.05$) (Figure 4.10). WT bacteria induced the highest levels of E-selectin mRNA expression, followed by *lpxA*- and then LPS induction. WT and *lpxA*- bacteria induced E-selectin mRNA levels which correlated with E-selectin surface protein expression (Figure 4.11). Although LPS induced an increase in E-selectin mRNA levels, the E-selectin mRNA dose response curve did not correlate with the dose response curve of E-selectin surface expression. However, E-selectin mRNA did increase in response to purified LPS, and maximal levels were obtained with 1-10ng/ml LPS. Whilst Real-Time PCR is a sensitive method for the detection of mRNA transcription, it may be that the methodology is not as sensitive when mRNA expression levels are very low.

However, the data suggests that WT and *lpxA*- *N. meningitidis* are able to induce higher levels of E-selectin mRNA than purified LPS, indicating that this adhesion molecule is regulated in an LPS-independent manner. The correlation between E-selectin mRNA and surface expression of E-selectin indicates that this may occur at the transcriptional level. If E-selectin were a protein that was stored within cellular organelles, there

would be a rapid increase in E-selectin surface expression. However, this is not observed. A related protein which is stored in cellular granules is P-selectin. P-selectin surface expression increases within minutes of cellular activation with TNF- α (Bischoff and Brasel, 1995). This is followed by increases in P-selectin mRNA expression.

VCAM-1 mRNA was also stimulated in response to *N. meningitidis* WT and *lpxA*-bacteria and purified LPS at 4 hours (Figure 4.6 and Figure 4.12). However, maximal VCAM-1 mRNA expression was induced in response to a lower concentration of bacteria than E-selectin mRNA. VCAM-1 mRNA expression levels were maximal in response to 10^6 CFU/ml WT bacteria. However, VCAM-1 mRNA levels induced by WT bacteria did not correlate with VCAM-1 surface expression (Figure 4.13). In addition, whilst LPS induced maximal VCAM-1 expression levels at a concentration of 10ng/ml, the LPS dose dependent stimulation of VCAM-1 mRNA did not correlate with the dose dependent induction of VCAM-1 surface expression levels obtained (data not shown).

Interestingly, the *lpxA*- bacteria induced maximal VCAM-1 expression at 10^8 CFU/ml (Figure 4.12). Whilst these levels were lower than levels induced by 10^6 CFU/ml WT bacteria, there was a significant correlation between VCAM-1 mRNA expression and surface expression induced by the *lpxA*- bacteria (Figure 4.13B). It may be that there is a limit to how much VCAM-1 mRNA can be produced, and that in response to high concentrations of WT and *lpxA*- bacteria there are secondary mechanisms regulating the transport and stability of VCAM-1 mRNA and protein.

A reason for the weak correlation between VCAM-1 mRNA and surface expression may be due to the low experimental numbers used for this assay.

Although there was no scope to perform a time-course in this study, other groups have performed time-courses detecting adhesion molecule mRNA and surface expression for other organisms and stimuli. For instance, Fuhrmann, *et al.* (2001) performed northern blot analysis to detect adhesion molecule mRNA expression in endothelial cells in response to *Bartonella henselae*, a gram-negative bacteria causing cat scratch disease. E-selectin mRNA levels were detectable at 3 hours, and remained elevated at 4-6 hours. ICAM-1 expression was also detectable at 3 hours, and remained detectable 9 days post stimulation as compared to unstimulated control conditions. Other studies have used 4 hours for the detection of adhesion molecule mRNAs, including E-selectin, ICAM-1 and VCAM-1 mRNA (Gupta and Ghosh, 1999; Madan et al., 2001). This time-point was selected as a suitable time-point to study E-selectin and VCAM-1 mRNA induction by *N. meningitidis*, as this would allow for the detection of both adhesion molecules.

Both E-selectin and VCAM-1 mRNA levels did not always correlate with surface expression levels of these adhesion molecules in response to LPS. Discrepancy between mRNA and protein expression has been previously observed. Everts, *et al.*, (2003) detected E-selectin by both RT-PCR and immunohistochemistry. Although in some inflammatory disease models E-selectin mRNA is detected, there are three disease models that do not demonstrate E-selectin protein expression, even though there are elevated E-selectin mRNA levels. Furthermore, E-selectin expression profiles in response to *B. henselae* have demonstrated that low levels of E-selectin mRNA are

detectable at 24, 36 and 72 hours post infection, however, there is virtually no E-selectin protein detection using ELISA (Fuhrmann *et al.*, 2001). The mechanisms regulating this phenomenon remain unknown. It may be that other unknown mechanisms are regulating the stability of the mRNA transcript at low concentrations, but may not produce detectable protein levels.

There are several elements which regulate the degradation of mRNA transcripts, and these include the 5'-cap structure, the 5'-untranslated region (UTR), the protein coding region, the 3'-UTR and the 3'-polyadenylate tail (Shim and Karin, 2002). The mechanism which regulates the majority of cytokine and chemokine genes is the 3'-UTR mechanism. This consists of AU rich sequence elements which promote mRNA degradation. E-selectin mRNA also contains an AU rich sequence which destabilises E-selectin mRNA and causes rapid degradation of the mRNA transcript (Bevilacqua *et al.*, 1989). However, stability of mRNA transcripts that are normally very unstable has been reported through the stabilisation of the 5'-UTR (Shim and Karin, 2002; Guhaniyogi and Brewer, 2001). For instance, IL-2 mRNA transcripts have been reported to become stable by the activity of JNK on the JNK-responsive element of the 5'-UTR sequence of IL-2 (Chen *et al.*, 1998). Nucleolin and YB-1, two RNA-binding proteins, bind to this sequence and thereby stabilise IL-2 mRNA transcripts (Chen *et al.*, 2000). It may be that *N. meningitidis* may have a similar mechanism for inducing increased E-selectin expression. An mRNA stabilising protein may be induced by *N. meningitidis* and thereby protect mRNA transcripts that would normally be unstable.

The E-selectin gene also contains 3 AATAAA polyadenylation signals (Chu *et al.*, 1994), which produce three different E-selectin transcript sizes referred to as Type I, II and III. These are all expressed in human endothelial cells (Chu *et al.*, 1994). It is interesting to note that the Type I E-selectin molecule omits six out of the eight mRNA destabilisation sites mentioned above, and this transcript is more stable than the longer Type III E-selectin transcript (Chu *et al.*, 1994). Meningococci may somehow induce the production of Type I E-selectin, and thereby induce high E-selectin mRNA and surface protein levels, as the transcripts and protein may be the more stable forms of E-selectin.

It is possible that the WT bacteria can increase E-selectin mRNA stability thereby inducing both high levels and prolonged expression of E-selectin surface protein. For instance, TNF- α stimulated HUVEC have increased and prolonged mRNA and surface expression of E-selectin and VCAM-1 when supplemented with mycophenolic acid (MPA) (Hauser *et al.*, 1997). This is not due to increases in NF κ B activity. MPA appears to increase mRNA stability, however, the mechanisms regulating this remain unclear. The half life of E-selectin mRNA is 2 hours (Ghersa *et al.*, 1992), indicating that E-selectin mRNA is very unstable. Hauser, *et al.*, (1997) has found that E-selectin mRNA stability is 10-fold higher in the presence of MPA. The E-selectin gene has eight ATTTA consensus sequences at the 3' untranslated region (Bevilacqua *et al.*, 1989), and these are believed to render the resulting mRNA sequence unstable. mRNA constructs containing this sequence are rapidly degraded. It may be that MPA somehow interacts with these sites to stabilise mRNA, and that meningococci either express a

protein that interacts with the ATTTA sequence or that they induce the production of a cellular protein that interferes with this site.

Another area in which *N. meningitidis* may be affecting the levels of expressed protein is in the post-translational glycosylation pathway. E-selectin is post-translationally glycosylated in the golgi (Pahlsson *et al.*, 1995). It may be that glycosylation affects E-selectin protein trafficking to the cell membrane, as inhibition of glycosylation reduces E-selectin surface expression. This may be controlled differentially by intact meningococci and purified LPS. For instance, it may be that whole bacteria increase glycosylation of proteins, thereby stabilising E-selectin protein, which is then transported to the surface of the cell. The bacteria may contain a component that may be involved in protein stabilisation at high bacterial concentrations, and hence allow for increased levels of protein to be transported to the surface of the cell membrane.

For instance, LPS has been reported to differentially glycosylate different proteins. LPS induces surface expression of CD83 on monocytes and macrophages. CD83 is stored intracellularly in these cells, and upon LPS stimulation the protein is transported to the cell surface. This involves the glycosylation of the protein (Cao *et al.*, 2005). In contrast, LPS glycosylates IgA inefficiently when compared to the glycosylation of IgA induced by IL-4 and IL-5 stimulation of B-cells, which glycosylate IgA very efficiently (Chintalacharuvu and Emancipator, 1997). These two examples illustrate two contrasting roles which LPS may play in the glycosylation of different inflammatory

proteins, and hence it remains unclear how LPS-dependent and independent regulation may induce mRNA levels that do not always correlate with protein expression.

WT meningococci and purified LPS induced differential E-selectin mRNA expression, which correlated with that observed with the E-selectin surface protein levels (Chapter 3). This suggests that differential E-selectin expression by WT and *lpxA*- bacteria and purified LPS is controlled at the transcriptional level. The data also suggested that the high levels of E-selectin mRNA and surface protein expression are controlled by both LPS-dependant and independent mechanisms. However, it does not rule out mechanisms that may increase the stability of the E-selectin mRNA transcript and protein.

In an attempt to further understand the mechanisms which govern *N. meningitidis* induced adhesion molecule regulation on the endothelium, a study of the E-selectin promoter was undertaken. Prior to this, however, it was necessary to establish a transfection technique on HUVEC, which would allow high levels of transfection efficiency. This method is described in the following chapter.

Chapter 5

Adaptation and optimisation of a Lipid-mediated and Integrin-targeted DNA transfection method for the transfection of primary human endothelial cells

5.1 Introduction

Cell transfection is a technique that has been developed partly for the advancement of gene therapy but is also utilised to study the molecular mechanisms controlling gene expression as well as used to either over-express or inhibit the synthesis of individual proteins.

There are three main techniques that have been described in the literature: 1) electroporation, 2) viral transfection and 3) non-viral transfection. Whilst transfections using electroporation can yield high levels of transfection efficiency (TE), there are many differences in TE reported in the literature (Ear *et al.*, 2001; Iversen *et al.*, 2005; Hernandez *et al.*, 2004). Although viral methods achieve greater levels of TE in a wide range of cell types, their use in an *in vivo* scenario remains limited due to increased risk of cancers, toxicity, and the risk of stimulating the immune response. These problems raise ethical questions for the use of viral vectors to cure genetic disorders. The use of viral vectors to study gene promoters is also limited by the time taken to clone and grow them (about 3 months for a single construct). Hence, there is increased interest in developing non-viral targeted gene-delivery vectors.

5.1.1 Transfection of Endothelial Cells

Historically transfection of endothelial cells has been difficult using the transfection methods listed above. The majority of studies have demonstrated very low levels of transfection in endothelial cells. The use of lipids as a means of non-viral transfection has also shown very different transfection efficiencies. Polyethylenimine-mediated transfection of HUVEC leads to 50% of cells expressing GFP (Zaric *et al.*, 2004). CD-CHOL/DOPE (a cationic liposome at lipid:DNA ratio of 6.4:1) transfects 5.8% of endothelial cells (Fife *et al.*, 1998) and there is increased cytotoxicity at higher lipid:DNA ratios (Fife *et al.*, 1998). In contrast, a recent study has compared the TE of different non-viral, commercially available reagents on HUVEC and a smooth muscle cell line (Kiefer *et al.*, 2004). Transfection efficiencies range from 0.1% to 8% as determined by GFP expression. Superfect (Qiagen) has the highest TE of Human Aorta endothelial cells (HAEC) (8%), but also causes the highest levels of cell toxicity. Lipofectin (Invitrogen) is a poor agent for the transfection of HAEC.

However, recently some groups have achieved reasonable levels of transfection by electroporation of HUVEC. HUVEC transfected at passage two or three have transfection levels of 40% by electroporation when cell isolation and electroporation media are optimum (Ear *et al.*, 2001). High levels of transfection have also been detected on bovine pulmonary aortic endothelial cells (BPAEC) transfected with Eugene 6 (a lipid-based transfection reagent, Roche), where 60-70% of the cells expressed Green Fluorescence Protein (GFP) (Kovalá *et al.*, 2000).

5.1.2 Improving TE

5.1.2.1 Use of supplements

Different drugs and antibodies have been used to supplement the transfection mix in an attempt to improve TE. Apo E (apolipoprotein E, a protein involved in the metabolism of lipoproteins) has been used to improve TE of Lipofectin on HUVEC (Sipehia and Martucci, 1995). When using lipofectin alone, the highest TE is obtained with a DNA:Liposome ratio of 1:8, however, this also causes high levels of cell death, and hence a 1:5 DNA:Liposome ratio combined with Apo E is used. By adding Apo E to the transfection cocktail, efficiency was increased from 16.6% HUVEC to 22.62% of HUVEC expressing β -galactosidase (Sipehia and Martucci, 1995).

Chloroquine, which inhibits the enzymatic degradation of particles within the endosomal vesicles by increasing the pH, has been used to increase TE (Wolfert and Seymour, 1998). However, it inhibits Lipid-Integrin-DNA (LID) complex mediated transfection on endothelial cells, although it improves LID mediated transfection on epithelial cells lines (Hart *et al.*, 1997).

5.1.2.2 The use of Histone Deacetylation Inhibitors to improve TE

Histone deacetylation inhibitors have also been utilised to improve TE. Sodium Butyrate (SB), a short chain fatty acid, is a product produced in the human gut by bacterial fermentation of undigested carbohydrates and fibre. SB acts by inhibiting histone deacetylation, which in turn alters chromatin structure, thereby allowing access of the acetylated DNA to different transcription factors. This reaction appears to occur without directly interacting with the histone deacetylation reaction (Cousens *et al.*, 1979). The mechanism by which SB acts as a histone deacetylation inhibitor is still unclear, although it has been suggested to act by inducing signalling pathways involving serine-threonine-phosphatase activity (Cuisset *et al.*, 1997).

Trichostatin A (TSA) is an antifungal antibiotic obtained from *Streptomyces* and is structurally different from SB. TSA is a specific inhibitor of histone deacetylation which interacting with the deacetylation reaction by inhibiting the removal of acetyl groups from core histones.

SB and TSA reactivate silenced transfected genes in stably transfected HeLa cells (Chen *et al.*, 1997). Up to 80% of transfected HeLa cells have silenced transgenes after 60 days. Transgene activity is dramatically re-established by the addition of SB or TSA to the cell growth media (Chen *et al.*, 1997). SB and TSA induce a 100-fold improvement in transgene expression in viral-transfected cell lines (Dion *et al.*, 1997). In yeast and

Chinese hamster cells, nickel induced gene silencing is reduced by supplementing reactions with TSA (Dion *et al.*, 1997). Gene transcription requires an unfolded nucleosome structure, and this is maintained by histone acetylation (Walia *et al.*, 1998). Histone deacetylation of transgenes is inhibited by SB and TSA, thereby allowing gene transcription.

5.1.2.3 Antibodies and peptides to target transfection

Anti-transferrin receptor antibody in combination with liposome-DNA complexes increases transfection of endothelial cell lines to 75% (Tan *et al.*, 2003). An anti-E-selectin antibody also increases transfection of CHO (Duensing and van Putten, 1997) cells expressing E-selectin, as compared to normal CHO cells (Tan *et al.*, 2003). It has also been demonstrated that by inhibiting lysosomal cysteine proteases, TE of primary fibroblasts is improved (Coonrod *et al.*, 1997).

Peptides that target different cell types have also been demonstrated to improve TE. This method combines lipofectamine with a cell targeting peptide, which induces the cell to ingest the DNA and targets the cell nucleus. Nicklin *et al.* (2000) identified a peptide that targets viral transfection to HUVEC, increasing reporter gene activity up to 15-fold compared to non-targeted viral transfection (Nicklin *et al.*, 2000). This has been further manipulated by re-targeting the coxsackie virus adenovirus receptor (CAR) by inserting the endothelial targeting peptide (Nicklin *et al.*, 2001) into its sequence,

thereby creating a novel viral vector for endothelial cell targeted gene therapy, which transfects 49% of cells (Nicklin *et al.*, 2001).

5.1.2.4 The use of different promoters and reporter genes to detect TE

Tanner *et al.* (1997) compared four different transfection methods: 1) particle-mediated gene transfer; 2) cationic liposomes; 3) calcium phosphate; and 4) DEAE-dextran. The efficiency of transfection of cells at passage 2 depends on three different parameters: vector, promoter sequence and the nature of the reporter gene. The highest TE is achieved with a cationic liposome gene delivery system (20.28%) using an alkaline phosphatase (AP) reporter gene under the control of the CMV promoter. However, the TE with a vector containing the Rous Sarcoma Virus (Oftung *et al.*, 1999) promoter expressing AP is 0.07% compared to 20.28% with a vector containing the CMV promoter (Tanner *et al.*, 1997). This indicates that variations in TE may arise in the literature due to different groups using different promoter and reporter sequences.

5.1.2.5 Selection of transfected cells to study a promoter of interest

In order to enhance a response by a promoter of interest, the system may be further manipulated by separating the transfected cells to then investigate the effect that a promoter of interest has on the transfected cells. For instance, Kovala, *et al.* (2000)

have co-transfected cells using Fugene 6 (Dunoyer-Geindre *et al.*, 2002) with a plasmid expressing GFP under the control of a strong promoter, and a plasmid expressing Red Fluorescence Protein (RFP) under the control of a promoter of interest. Cells expressing GFP are sorted by FACS analysis, and differential levels of RFP are detected on these cells to investigate the promoter of interest. Differential levels of RFP expression are detected on the GFP expressing cells, and these differences are not observed when the whole cell population is analysed (Kovalá *et al.*, 2000). Higher TE is obtained when cells are transfected after trypsinisation, rather than seeding the cells prior to transfection (Kovalá *et al.*, 2000). This methodology has been further manipulated to select transfected cells and observed differences in genes of interest (Garcia *et al.*, 2001; Duval *et al.*, 2003).

5.1.2.6 Differences in TE of cell lines and primary cells

Primary cells have been shown to be resistant to transfection compared to cell lines. Primary cells such as human aortic endothelial cells (HAEC) and Human Aorta Smooth Muscle Cells (HASMC) have much lower transfection efficiencies compared to a cell line (A-10 rat smooth muscle cells) when using different commercially available non-viral vectors (Kiefer *et al.*, 2004). Liposome mediated transfection of immortalised endothelial cell lines yields higher transfection levels compared to primary cell lines (immortalised human brain microvascular endothelial cell (HBMEC) and HMEC-1 compared to HUVEC and HAEC) (Kaiser and Toborek, 2001). Similar differences are

obtained when comparing Lipofectin (Promega) mediated transfection of ECV304 and EA.hy 926 human endothelial cell lines and HUVEC (Teifel *et al.*, 1997).

Although there is 66% of DNA uptake by HUVEC, only 13.8% express the vector (Colombo *et al.*, 2001). Expression of vector DNA is enhanced at increased DNA concentrations and by chloroquine supplement (Colombo *et al.*, 2001). The differential in DNA uptake and DNA expression may be due to rapid degradation of DNA in primary cells.

In human primary fibroblasts, which are difficult to transfect, optimal transfection is obstructed by endosome-lysosome translocation to the nucleus as well as rapid exclusion of transfected DNA from the nucleus (Coonrod *et al.*, 1997). However, in HeLa cells, which are a well recognised cell line, transfected DNA remains in the cell nucleus (Coonrod *et al.*, 1997). The poor levels of TE detected in primary cells may be due to transport of DNA through the obstruction of endosome-lysosome trafficking or through ejection of DNA from the nucleus.

5.1.2.7 The use of integrin mediated transfection on endothelial cells

LID mediated transfection utilises Lipofectin (L; Promega) as the transfection lipid, an integrin targeting peptide (I), and DNA (D). Figure 5.1 illustrates the trafficking through the cell cytoplasm of the LID vector. The integrin targeting peptide binds to its

receptor on the cell membrane, inducing endocytosis of the LID vector. The vector is degraded in the endosome, and DNA is released and travels to the cell nucleus.

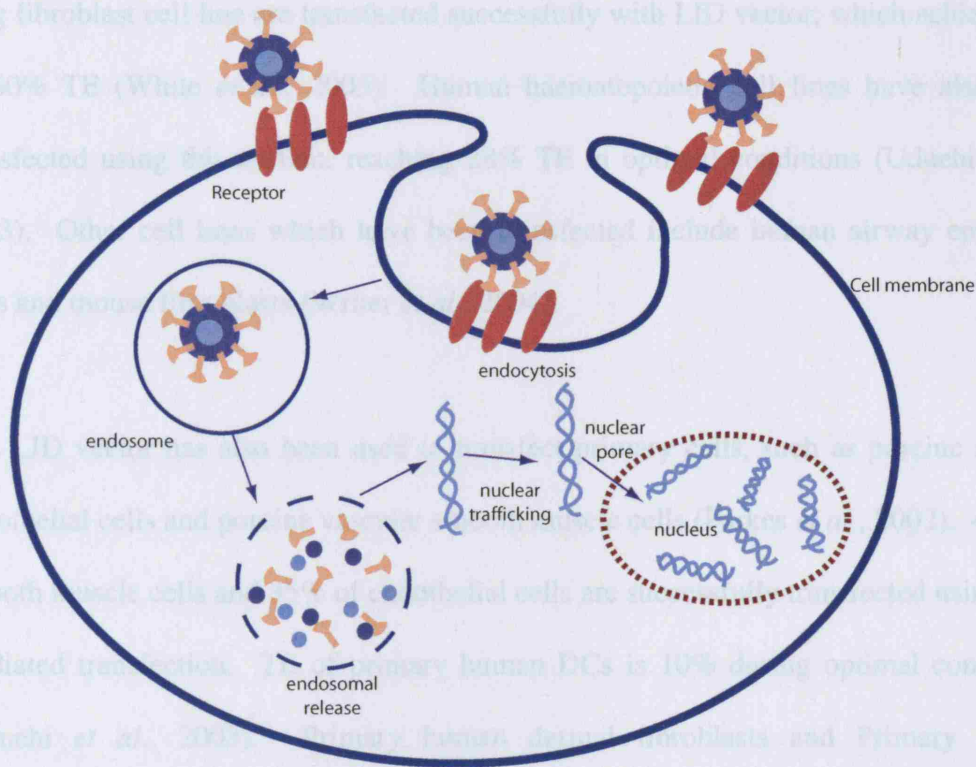


Figure 5.1 LID mediated transfection and trafficking of DNA. LID vector binds to cell receptor via the Integrin-targeting peptide. This promotes endocytosis of the LID vector. The LID vector is degraded in the endosome, and releases the DNA, which travels to the nucleus.

LID vector has been used on a wide range of cell types. In melanoma cell lines and monkey kidney epithelial cells, LID mediated transfection improved TE from 1-10% to above 50% (Hart *et al.*, 1998). A human embryonic kidney cell line and a human foetal lung fibroblast cell line are transfected successfully with LID vector, which achieves up to 60% TE (White *et al.*, 2003). Human haematopoietic cell lines have also been transfected using this system, reaching 28% TE in optimal conditions (Uduehi *et al.*, 2003). Other cell lines which have been transfected include human airway epithelial cells and mouse fibroblasts (Writer *et al.*, 2004).

The LID vector has also been used to transfect primary cells, such as porcine arterial endothelial cells and porcine vascular smooth muscle cells (Parkes *et al.*, 2002). 40% of smooth muscle cells and 35% of endothelial cells are successfully transfected using LID mediated transfection. TE of primary human DCs is 10% during optimal conditions (Uduehi *et al.*, 2003). Primary human dermal fibroblasts and Primary human keratinocytes have also been transfected successfully using different targeting peptides (Writer *et al.*, 2004), demonstrating that the integrin peptide can target different cell types. The LID vector system has been applied successfully to an *in vivo* system in live rats (Jenkins *et al.*, 2000).

LID mediated transfection has been used on endothelial cells. LID transfection improves TE of a human endothelial cell line (ECV304) 100-fold, compared to Integrin-DNA complexes alone (Hart *et al.*, 1998). LID transfection of rabbit corneal endothelium improves TE from 0% to 25% of transfected cells (Hart *et al.*, 1998).

HMEC-1 cells have also been successfully transfected with LID vector with a range of different targeting peptides (Writer *et al.*, 2004). However, the LID system has never been adapted for the transfection of primary human endothelium. This system has been selected for the transfection optimisation of the primary human endothelial cell, HUVEC, and the endothelial cell line HMEC-1 for comparison of endothelial cell specific peptides for targeted gene delivery.

5.1.3 Chapter Aims

Results in Chapter 4 indicated that regulation of E-selectin by *N. meningitidis* occurs at the transcriptional level. To elucidate the mechanisms governing E-selectin regulation, the E-selectin promoter had to be studied in more detail. To accomplish this it was necessary to develop a system which would allow for efficient transfection of primary endothelial cells. LID has not previously been used on HUVEC. The aim of this chapter was to optimise the LID vector transfection system on HMEC-1 and HUVEC.

5.2 Materials and Methods

5.2.1 Culture of HUVEC and HMEC-1

Details of endothelial cell isolation from umbilical cords and cell culture and maintenance of HUVEC and HMEC-1 are described in Chapter 2. Once HUVEC and HMEC-1 reached confluence on primary plates, they were subcultured onto tissue culture plates coated with attachment factor, and grown over-night at 37°C in 5% CO₂ in air prior to transfection experiments.

5.2.2 Transfection of Endothelial cells

Cells were transfected using the LID vector system as described in Chapter 2. Briefly, LID complex was prepared by combining lipofectin lipid and peptide, followed by the addition of DNA plasmid. The transfection cocktail was made in OptiMEM®-1 reduced serum media. Cells were aspirated, and the transfection mix was added and left on the cells for 4 hours at 37°C 5% CO₂ in air. Cells were then rescued in fresh GM overnight.

For the optimisation of peptide:DNA charge ratio on TE, 3:1 and 7:1 charge ratios were attempted. Table 5.1 shows the amounts of lipid, peptide and DNA (pCI-luciferase, Figure 5.2) added to each well, depending on the peptide:DNA charge ratio (3:1 and 7:1) and on well size (24 vs. 96 well plates).

Table 5.1 Lipid, peptide and DNA concentrations used for the transfection of HUVEC and HMEC-1. The table below shows the amounts of reagents used for the transfection of endothelial cells according to the number of cells transfected (which depended on the number of wells per plate). Lipofectin and peptide were combined to form a complex, and DNA was then added to be incorporated into the complex.

Substance	24 well plate	96 well plate
Lipofectin ($\mu\text{g}/\mu\text{l}$)	0.1875	0.09375
Peptide ($\mu\text{g}/\mu\text{l}$) 3:1 ratio	0.45	0.225
Peptide ($\mu\text{g}/\mu\text{l}$) 7:1 ratio	1.05	0.525
Final DNA concentration($\square\text{g}$)	0.5	0.25
Final volume	500 μl	250 μl

For the purpose of optimising the transfection reaction, the pCI-luciferase plasmid (Figure 5.2) was utilised. This plasmid contains the luciferase gene under the control of the CMV promoter.

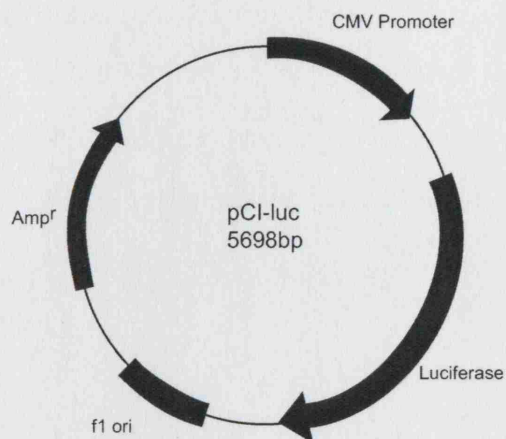


Figure 5.2 pCI-luciferase vector. The illustration above represents the vector used to optimise the LID vector on endothelial cells. The vector contains the luciferase reporter gene (luc^+) controlled by the CMV promoter (Promoter P1). The vector also contains an ampicillin resistance cassette, which allows for antibiotic selection in bacterial cells.

5.2.3 Peptide optimisation of LID mediated transfection on HMEC-1 and HUVEC

A range of peptides were used to optimise the LID vector for endothelial cell transfection. These are shown on Table 5.2. Peptides contained a targeting sequence (previously identified using phage display methods (Koivunen *et al.*, 1995; Writer *et al.*, 2004), two flanking cysteine residues, a 16-lysine (K₁₆) tail, and a –GA spacer. Peptides were synthesised by Zinsser Analytic, Alta Biosciences, or the Department of Chemistry, University College London using standard solid phase synthesis methods using HPLC, and sequences were checked using electrospray mass spectrometry.

Table 5.2 LID vector targeting peptides

Peptide name	Synthesised peptide sequence	Scrambled peptide sequence	Reference
6	[K] ₁₆ GACRRRETEWACG	[K] ₁₆ GACATRWARECG	(Koivunen <i>et al.</i> , 1995; Parkes <i>et al.</i> , 2002)
Y	[K] ₁₆ GACYGLPHKFCG	[K] ₁₆ GACYKHPGFLCG	(Writer <i>et al.</i> , 2004)
E	[K] ₁₆ GACSERSMNFCG	[K] ₁₆ GACNSFMESRCG	(Writer <i>et al.</i> , 2004)
Q	[K] ₁₆ GACLQHKSMPCG		(Writer <i>et al.</i> , 2004)
P	[K] ₁₆ GACLPHKSMPCG		
5	[K] ₁₆ GACDCRGDCFCA		(Koivunen <i>et al.</i> , 1995; Hart <i>et al.</i> , 1997)
G	[K] ₁₆ GACPSGAARACG		(Writer <i>et al.</i> , 2004)

5.2.4 Sodium Butyrate (SB) and Trichostatin A (TSA)

Supplement of transfection cocktail

During the optimisation procedure, TE was improved by supplementing the transfection cocktail with SB or TSA. These compounds were added at the time of transfection to the cocktail and the growth media which was added after the 4 hour incubation period. SB was topped up the following day and left for 6 hours, where after the reaction was terminated. To determine if time of supplement addition affected TE, SB was added after the transfection as demonstrated in Figure 5.3.

5.2.5 Normalisation of data and statistical analysis

Luciferase data was normalised to protein levels in the individual wells to control for cell number in the transfection reaction. Data was plotted using GraphPad Prism, and 1-way ANOVA was performed to assess statistical significance between different groups of data. Probabilities of less than 0.05 were considered significant.

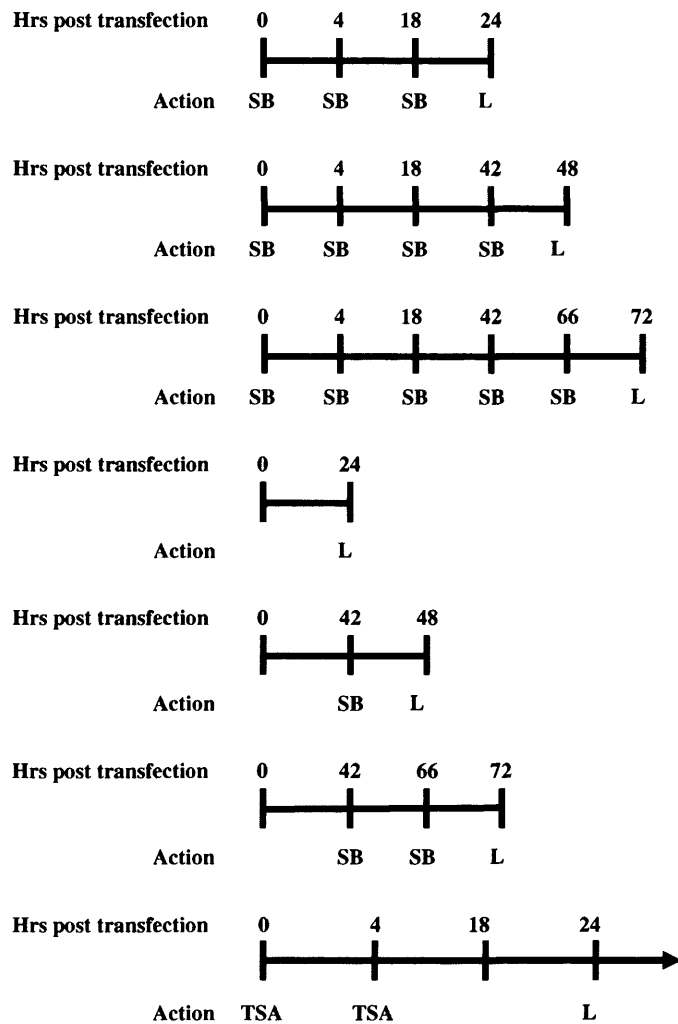


Figure 5.3 Time of addition of supplement to transfection reaction. The above diagram demonstrates the time at which SB or TSA were added to the transfection mix, and at which point the reaction was terminated to detected luciferase activity (LA).

5.3 Results

5.3.1 Peptide optimisation of the LID vector system on HMEC-1

As transfection reactions require a large number of cells, the LID vector system was tested on the transformed endothelial cell line HMEC-1 prior to transfecting HUVEC. HMEC-1 were transfected using the LID vector system with a plasmid expressing luciferase under the control of the CMV promoter (Figure 5.2). A Bio-Rad Protein Assay was performed to control for variation in cell number per reaction. A range of peptides (Table 5.2) were initially tested for their ability to modulate TE.

Figure 5.4 shows a representative experiment of peptide optimisation of LID transfection on HMEC-1. Peptides were tested at a peptide:DNA charge ratio of 3:1 and 7:1, which have been shown to be the optimum ratios to achieve high levels of TE (Hart *et al.*, 1998). There were two peptides which demonstrated high TE of HMEC-1: Peptide 6 and Peptide Y. The optimum peptide:DNA ratio was 7:1 for both peptides. Peptides Q and P were also competent at transfecting HMEC-1, though not as effective as Peptides Y and 6. Peptides E, G and S were poor facilitators of transfection.

These results demonstrated that Peptide 6 and Y were effective mediators of high TE. Peptide 6 was therefore selected for further experiments on HMEC-1 cells at a peptide:DNA charge ratio of 7:1.

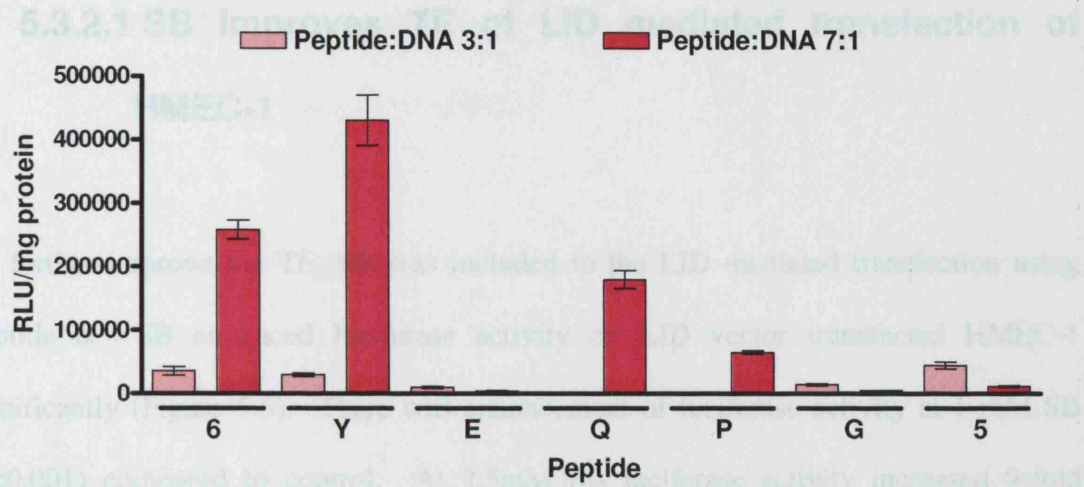


Figure 5.4 Peptide optimisation of LID vector transfection on HMEC-1. HMEC-1 were transfected with LID vector. Lipofectin (Promega) was combined with a wide range of synthesised peptides at a peptide:DNA charge ratio of 3:1 (light pink bars) and 7:1 (dark pink bars). Luciferase activity was detected at Day 1. Results are presented as mean of RLU/mg \pm SEM, n=6. This experiment was performed a minimum of 3 times.

5.3.2 Transfection of HMEC-1 supplemented with Histone Deacetylation Inhibitors

It has been reported that silencing of transfected gene products occurs, and that this can be reversed by using histone deacetylase inhibitors, like TSA and SB (McInerney *et al.*, 2000; Chen *et al.*, 1997; Kitazono *et al.*, 2001).

Figure 5.5 Transfection of HMEC-1 with LID vector supplemented with increasing concentration of SB. HMEC-1 were transfected with LID vector using Peptide 6 and supplemented with SB. Results are presented as mean of RLU/mg \pm SEM, n=6. *p<0.001.

5.3.2.1 SB improves TE of LID mediated transfection of HMEC-1

To further improve the TE, SB was included to the LID mediated transfection using Peptide 6. SB enhanced luciferase activity on LID vector transfected HMEC-1 significantly (Figure 5.5). There was enhancement of luciferase activity at 1 mM SB ($p < 0.001$) compared to control. At 2.5mM SB luciferase activity increased 9-fold ($p < 0.001$) above control. Levels were suboptimal when SB levels were above 5mM. Hence, supplementing transfection reaction with a histone deacetylation inhibitor was able to improve TE of HMEC-1.

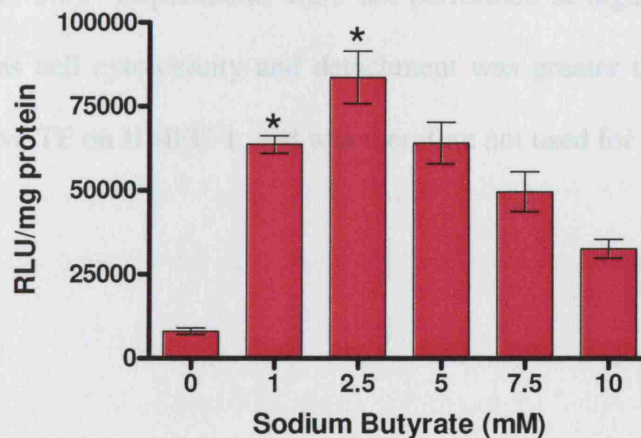


Figure 5.5 Transfection of HMEC-1 with LID vector supplemented with increasing concentration of SB. HMEC-1 were transfected with LID vector using Peptide 6 and supplemented with SB. Results are presented as mean of RLU/mg \pm SEM, $n=6$. *= $p < 0.001$.

5.3.2.2 TSA was unable to facilitate LID mediated transfection of HMEC-1

SB has been demonstrated to inhibit histone deacetylation, and has also been shown to block methylation of DNA. Figure 5.5 demonstrated that SB enhanced luciferase activity in LID vector transfected HMEC-1. To examine the mechanisms by which SB enhanced TE on HMEC-1, another molecule which specifically inhibits histone deacetylation, TSA, was examined to see if there was any enhancement on luciferase activity.

In these experiments TSA did not enhance luciferase activity on LID transfected HMEC-1 (Figure 5.6). Experiments were not performed at higher than 10pmol TSA concentrations as cell cytotoxicity and detachment was greater than 50%. TSA was unable to improve TE on HMEC-1, and was therefore not used for further studies.

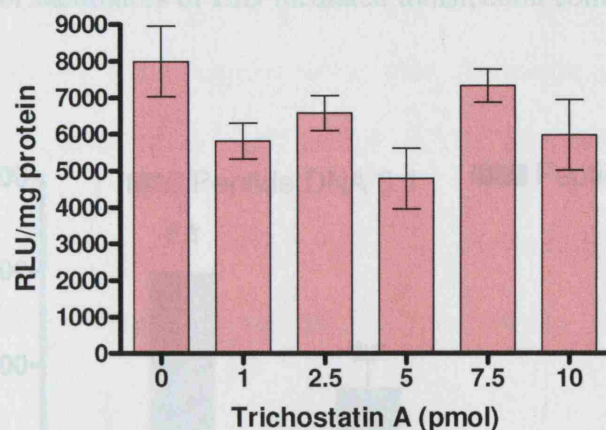


Figure 5.6 Transfection of HMEC-1 with LID vector supplemented with increasing concentrations of TSA. HMEC-1 were transfected with LID vector using Peptide 6 and supplemented with TSA. Results are presented as mean of RLU/mg \pm SEM, n=6.

5.3.3 Peptide optimisation of the LID vector system on HUVEC

Once the LID vector system had been established in the microvascular endothelial cell line, HMEC-1, the system could then be optimised on primary endothelial cells. Figure 5.7 demonstrates the optimisation of peptide and peptide:DNA charge ratio on HUVEC. Peptide 6 was competent at facilitating the transfection HUVEC. The peptide:DNA ratio of 7:1 was up to 7 times more efficient at transfecting HUVEC compared to a 3:1 peptide:DNA charge ratio ($p < 0.001$). Although Peptide Y was also competent at facilitating transfection of HUVEC at the 7:1 peptide:DNA charge ratio, levels were significantly lower than those obtained with Peptide 6 ($p < 0.05$) (Figure 5.8), suggesting a potential role for the parent peptide sequence. The scrambled peptide may have reduced avidity to the targeted integrin.

E and Q were poor facilitators of LID mediated transfection compared to Peptide 6 and Y. HUVEC, and was also significantly lower than its parent counterpart ($p<0.001$).

Peptides E and Q remained poor facilitators of HUVEC transfection (Figure 5.7).

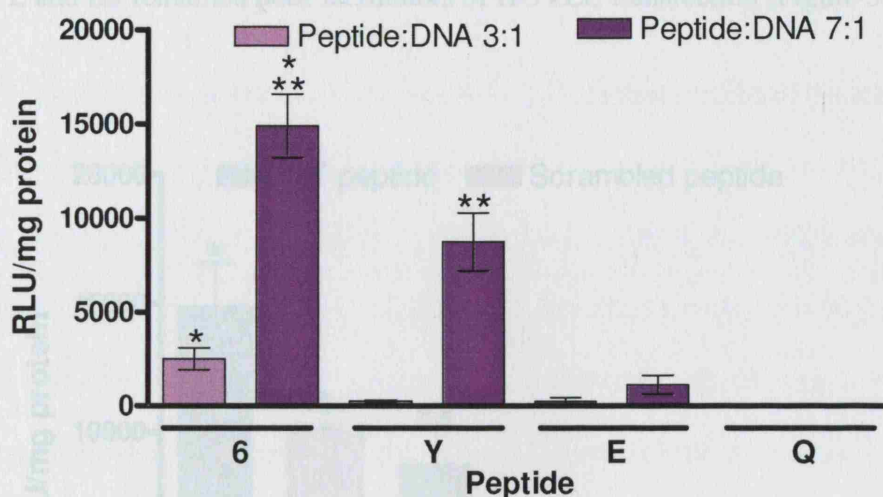


Figure 5.7 Peptide optimisation of LID vector transfection on HUVEC. HUVEC were transfected with LID vector using a range of synthetic peptides at a peptide:DNA charge ratios of 3:1 (light purple bars) and 7:1 (dark purple bars). Results are presented as mean of RLU/mg \pm SEM, n=6. *= $p<0.001$; **= $p<0.01$.

To determine whether the specific peptide sequence or its charge were responsible for the observed increase in TE, scrambled versions of Peptides 6, Y and E were used to transfect HUVEC with LID vector. Scrambled peptides contained the same amino acids but in an altered sequence order. Peptide 6S is the scrambled version of Peptide 6. Although Peptide 6S was able to facilitate LID vector transfection of HUVEC, levels were significantly lower than the levels obtained with Peptide 6 ($p<0.05$) (Figure 5.8), suggesting a potential role for the parent peptide sequence. The scrambled peptide may have reduced avidity to the targeted integrin.

Peptide YS, the scrambled version of Peptide Y, did not facilitate the transfection of HUVEC, and was also significantly lower than its parent counterpart ($p < 0.001$). Peptides E and ES remained poor facilitators of HUVEC transfection (Figure 5.8).

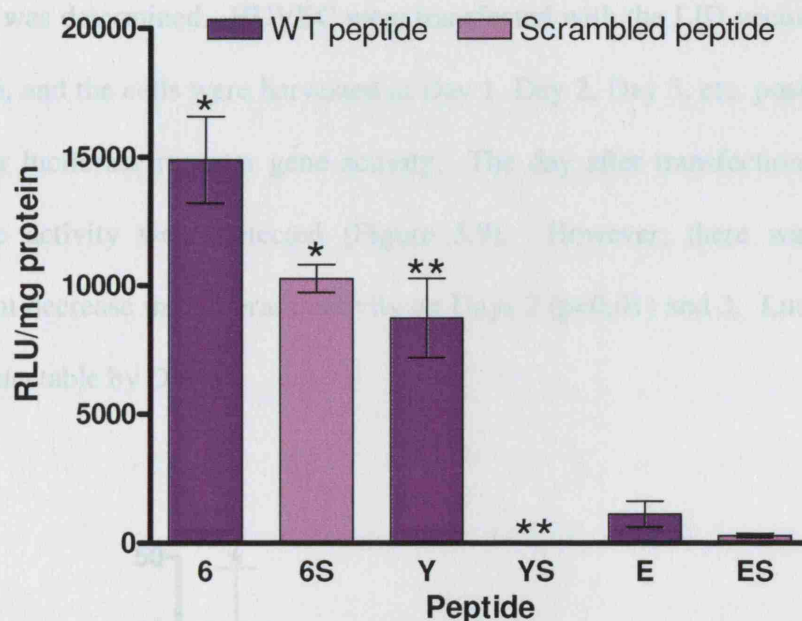


Figure 5.8 Comparison of parent and mutated peptides used in LID vector transfections of HUVEC. HUVEC were transfected with LID vector with a range of synthesised peptides (dark purple bars) and their scrambled counterparts (light purple bars) at a peptide:DNA charge ratio of 7:1. Results are presented as mean of RLU/mg \pm SEM, $n=6$. *= $p < 0.05$; **= $p < 0.001$.

The above series of experiments establish that Peptide 6 significantly enhances LID mediated transfection of HUVEC. Therefore, Peptide 6 was selected at a peptide:DNA charge ratio of 7:1 for further transfection studies.

5.3.4 Transfection kinetics of the LID vector system using Peptide 6 on HUVEC

Once the peptide was selected, the kinetics of LID vector mediated transfection of HUVEC was determined. HUVEC were transfected with the LID vector, facilitated by Peptide 6, and the cells were harvested at Day 1, Day 2, Day 3, etc. post transfection to detect for luciferase reporter gene activity. The day after transfection high levels of luciferase activity were detected (Figure 5.9). However, there was a rapid and significant decrease in luciferase activity on Days 2 ($p<0.01$) and 3. Luciferase activity was undetectable by Day 5.

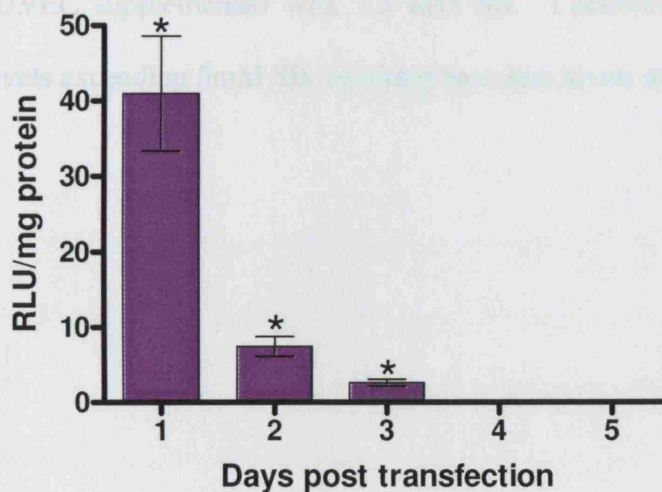


Figure 5.9: The kinetics of LID vector transfection on HUVEC. HUVEC were transfected with LID vector and Peptide 6. Cells were harvested at Days 1, 2 and 3 post transfection. Results are presented as mean of RLU/mg \pm SEM, $n=6$. $*=p<0.01$.

5.3.5 LID vector Transfection of HUVEC supplemented with Histone Deacetylation Inhibitors

5.3.5.1 SB improves LID mediated transfection of HUVEC

As the addition of SB enhanced luciferase activity on transfected HMEC-1 (Figure 5.5), LID mediated transfection of HUVEC was supplemented with increasing concentrations of SB (Figure 5.10). SB augmented LID mediated transfection of HUVEC, mirroring the observation in HMEC-1. Enhancement of luciferase activity on LID vector transfected HUVEC was seen at 1 mM SB ($p < 0.001$), reaching maximal enhancement at 2.5 mM SB ($p < 0.001$). There was a 7-fold increase in luciferase activity on transfected HUVEC supplemented with 2.5 mM SB. Luciferase activity decreased rapidly with levels exceeding 5mM SB, reaching base-line levels at 10 mM SB.

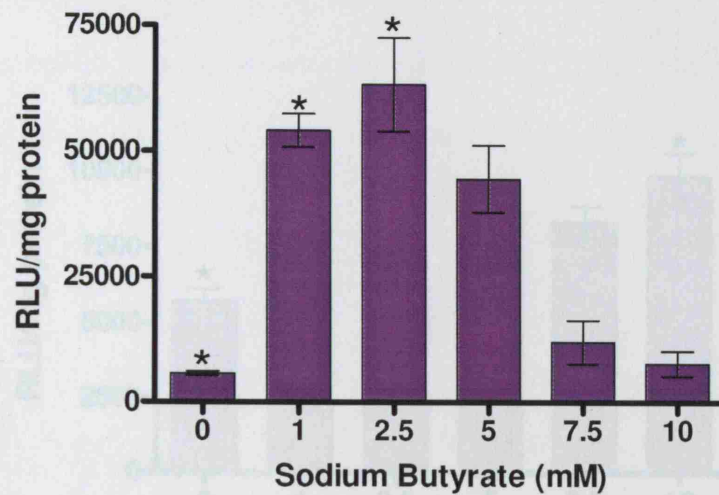


Figure 5.10 SB improves LID vector TE on HUVEC. HUVEC were transfected with LID vector using Peptide 6 and supplemented with SB. Results are presented as mean of RLU/mg \pm SEM, n=6. * p <0.001.

5.3.5.2 TSA facilitates LID mediated transfection of HUVEC

To determine the mechanisms by which SB improves TE in HUVEC, the effects of the specific histone deacetylation inhibitor TSA was explored. TSA enhanced luciferase activity on LID transfected HUVEC (Figure 5.11), although levels were much lower than those obtained with SB. Maximal levels of luciferase activity were obtained with 5-10 pmol TSA. 10pmol TSA significantly improved TE in HUVEC (p <0.01). At these concentrations, TSA enhanced LID vector mediated luciferase activity in HUVEC by nearly 2-fold. HUVEC transfections supplemented with TSA varied considerably, as there were occasions when cytotoxicity occurred the day following transfection. Concentrations above 10pmol TSA were not attempted due to cytotoxicity.

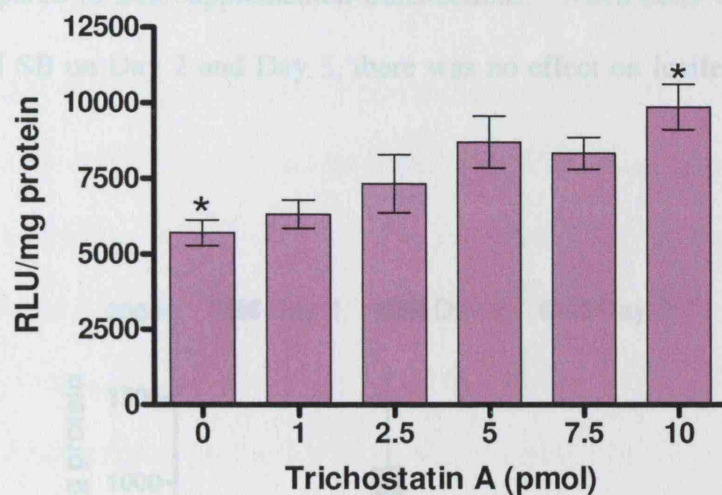


Figure 5.11: TSA improved LID vector TE on HUVEC. HUVEC were transfected with LID vector using Peptide 6 and supplemented with TSA. Results are presented as mean of RLU/mg \pm SEM, n=6. *= $p < 0.01$.

5.3.6 Transfection Kinetics of HUVEC supplemented with SB

HUVEC were transfected using LID supplemented with 2.5 mM SB over 3 days. The transfected cells were either supplemented with SB on the day of transfection (Day 0), or on Day 1, Day 2, and Day 3. As demonstrated on Figure 5.12 luciferase activity on transfected HUVEC without SB was rapidly and significantly reduced by Day 2, and effectively nil by Day 3. Although 2.5 mM SB enhanced luciferase activity on transfected HUVEC when added on Day 0 (*i.e.* supplementing the transfection mix), this did not affect the luciferase activity levels acquired on Day 2 and Day 3, which were as low as those found on transfected HUVEC without SB supplement (Figure

5.12). Supplementing the transfected cells with SB on Day 1 did not augment luciferase activity compared to non-supplemented transfections. When cells were supplemented with 2.5 mM SB on Day 2 and Day 3, there was no effect on luciferase activity (Data not shown).

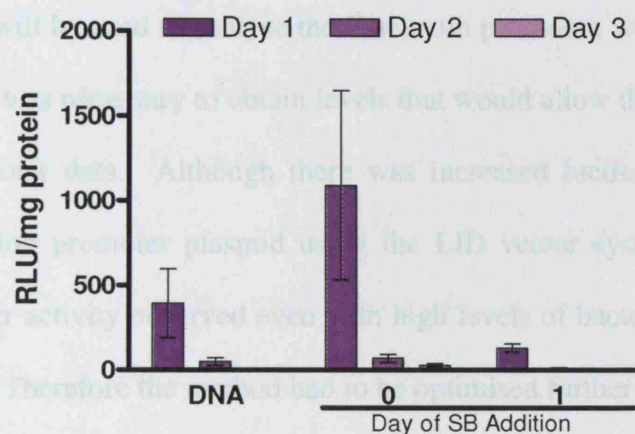


Figure 5.12: SB only improves luciferase activity on HUVEC when added to the LID vector transfection cocktail. HUVEC were transfected with LID vector. The transfection was supplemented with 2.5mM SB at the time of transfection (day 0) or on day 1 post transfection. Results are presented as mean of RLU/mg \pm SEM, n=6.

5.4 Discussion

The aim of this chapter was to adapt and develop the LID vector system to transfect primary human endothelial cells, and specifically HUVEC. The LID vector transfection system has not previously been adapted for use in primary human endothelium, and this unique method will be used to analyse the E-selectin promoter, which will be described in Chapter 6. It was necessary to obtain levels that would allow the interpretation of the E-selectin promoter data. Although there was increased luciferase activity with the CMV optimisation promoter plasmid using the LID vector system, there was no E-selectin promoter activity observed even with high levels of bacteria (see Chapter 6 for further details). Therefore the method had to be optimised further for the promoter to be studied. The results of this chapter are discussed further below.

HMEC-1 demonstrated a wide range of luciferase activity mediated by LID vector transfection using different peptides and peptide:DNA charge ratios. Peptides 6, Y and Q mediated the highest levels of TE at a peptide:DNA charge ratio of 7:1. Peptide 6 and Peptide Y also mediated transfection of HUVEC generating high levels of luciferase activity consistently. Peptide Y had high affinity and avidity for HUVEC and HMEC-1, as the scrambled peptide (Peptide YS) did not mediate high levels of transfection. However, the mutant version of Peptide 6 (Peptide 6S) did not abolish transfection of HUVEC, and the levels were high compared to luciferase activity mediated by other scrambled peptides. This may be due to non-specific binding of Peptide 6S to the cell surface or due to the sequence reducing avidity of the peptide.

The Peptide 6 sequence is homologous to an $\alpha 5 \beta 1$ integrin-targeting motif (Hart *et al.*, 1998). $\alpha 5 \beta 1$ integrins are expressed on the endothelial cell surface and are targeted by different pathogens for cell entry (Kerr, 1999). Peptide Y has sequence homology to an unknown protein expressed by *Legionella pneumophila*, which binds to epithelial cells by an unknown receptor (Writer *et al.*, 2004). The ability of Peptide Y to mediated LID transfection of endothelial cells suggests that the unknown receptor is not unique to epithelial cells. Interestingly, Peptide Q mediated LID transfection of HMEC-1 but did not of HUVEC, compared to Peptide 6 and Peptide Y which transfected both cell types efficiently. Peptide Q has sequence homology to glycoprotein B from human herpes virus, which targets cell surface heparan sulphate (Writer *et al.*, 2004). Heparan sulphate is found on the surface of endothelial cells (Mertens *et al.*, 1992; Netelenbos *et al.*, 2001). It is therefore interesting that this peptide was unable to mediate HUVEC transfection by LID vector.

All peptides mediated higher levels of transfection at a peptide:DNA charge ratio of 7:1. Optimal TE is dependant on complex charge and size, as charge ratios above 4 show the highest levels of TE of both mouse and human neuroblastoma cells (Lee *et al.*, 2003).

Rapid decay of LID mediated transgene expression of HUVEC was observed. Luciferase activity decreased two days post transfection, and levels were almost undetectable at 3 days post infection. Rapid reduction in luciferase activity after 24 hours has been reported previously (Uduehi *et al.*, 2003), and the cellular and molecular mechanisms controlling this phenomenon remain unknown.

One mechanism controlling gene transcription is histone deacetylation. Acetylation of histones allows for gene transcription, and deacetylation is associated with long-term silencing of the chromatin structure (Czermin and Imhof, 2003). It has been demonstrated that different viral sequences are targeted for gene silencing (Chen *et al.*, 1997), and that the silenced viral vectors can be reactivated by using histone deacetylation inhibitors (Chen *et al.*, 1997). Hence it was hypothesised that transgene expression could be enhanced by supplementing the reaction with histone deacetylation inhibitors.

Media was therefore supplemented with SB or TSA. SB improved TE of both HMEC-1 and HUVEC in a dose-dependant manner. In contrast, TSA failed to improve TE on HMEC-1, however, it did improve TE on HUVEC to a minor degree. TSA induces apoptosis (Medina *et al.*, 1997), inhibits cell growth and can be cytotoxic (Kang *et al.*, 2004). Whilst the concentrations of TSA previously reported to improve reporter gene activity range from low concentrations of 0-12.5 pmol (McInerney *et al.*, 2000) to high concentrations of 750 pmol (Chen *et al.*, 1997), the low concentrations used in this study (1-10pmol) were unable to affect TE. It is possible that TSA was inducing apoptosis of HUVEC. Whilst TSA was unable to improve TE, this may be due to the low concentrations utilised in this study. Although histone deacetylation appears to play a role in arresting luciferase reporter gene expression, it is conceivable that other unknown factors may be involved as well.

SB and TSA re-activate silenced transgenes in transfected cell lines (Chen *et al.*, 1997). Stable transfections of HeLa cells with adeno-associated viral vectors are reactivated by supplementing the media with SB or TSA (Chen *et al.*, 1997). Supplementing the transfection reaction with SB at day 1 post-transfection did not improve luciferase reporter gene expression. It is also interesting to note that TSA was not able to induce as high levels of luciferase reporter gene activity as SB, particularly on HMEC-1, where TSA had no effect on luciferase reporter gene activity. The reasons for this are still unclear. However, this indicates that different processes are involved in endothelial cell transgene silencing in the two different cell types.

Another barrier to high levels of TE and sustained transgene expression is methylation of foreign DNA (Hong *et al.*, 2001). Methylation plays a role in the regulation of gene expression, rendering genes inactive (Hermann *et al.*, 2004). Although SB and TSA are both histone deacetylation inhibitors, SB and TSA have also been shown to inhibit methylation of foreign DNA (Collas, 1998). It is interesting to note that activation of silenced genes with SB leads to inhibition of methylation of the foreign DNA as well as increased luciferase reporter gene activity (Collas, 1998). SB extends and improves TE in different systems. Zebrafish eggs have been transfected with a vector expressing luciferase under the control of the CMV promoter. Methylation of the vector occurs within 12 hours, however, supplementing the reaction with SB inhibits the methylation of the vector. Supplementation delays DNA methylation to 3 days post injection (Collas, 1998). However, decreased levels of DNA methylation and increased histone acetylation does not always lead to increased and prolonged luciferase reporter gene

activity, as observed in TSA or 5-azacytidine (Yang and Seto, 2003) supplemented transfection of different cell lines by viral vectors (McInerney *et al.*, 2000). 5-azacytidine and TSA were able to inhibit DNA methylation and deacetylation, respectively, however, this did not lead to increased and prolonged transgene activity (McInerney *et al.*, 2000). The inability of TSA to activate unmethylated vectors (McInerney *et al.*, 2000) may explain why this molecule was less potent at augmenting TE of endothelial cells. There are complex mechanisms involving gene activation, and it may therefore not be enough to inhibit histone deacetylation and methylation to allow for improved gene delivery and expression.

As mentioned in the introduction to this chapter, histone deacetylation inhibitors have previously been used to improve TE on a wide range of cell types. The combination of the LID vector system with this supplement may be useful in other difficult to transfect cell types, such as DCs and other primary cells.

To further understand the mechanisms governing foreign gene regulation on primary cells, it will be interesting to determine whether SB increases DNA uptake or improves reporter gene expression by inhibiting methylation and histone deacetylation of the foreign DNA. This will assist in developing better tools for introducing foreign DNA to primary cells, and may also lead to improved targeting and expression of gene therapy vectors.

The studies performed in this chapter demonstrated that Peptide 6 facilitated LID mediated transfection of HUVEC, and that SB further increased TE on HUVEC. This methodology could now be adapted to study promoters of interest in HUVEC.

Chapter 6

Regulation of the E-selectin promoter by *N. meningitidis*: LPS dependent and independent mechanisms of regulation

6.1 Introduction

Neutrophil rolling and transmigration is one of the critical mechanisms involved in mediating the vascular damage observed during meningococcal disease. Hence, the E-selectin receptor may be important for the aetiology of meningococcal disease, as it mediates neutrophil rolling.

In Chapters 3 and 4 it was shown that WT *N. meningitidis* bacteria could induce high levels of E-selectin mRNA and surface protein expression compared to purified meningococcal LPS alone. To explore the mechanisms governing differential E-selectin expression induced by WT and *lpxA*- *N. meningitidis* bacteria and purified LPS, E-selectin promoter constructs were used in the transfection system optimised in Chapter 5.

6.1.1 Chapter aims

To examine:

- differential stimulation of E-selectin promoter activity by fixed WT and *lpxA*- *N. meningitidis* bacteria and purified meningococcal LPS
- E-selectin promoter deletion mutants to further understand the role of the regulatory regions responding to stimulation by WT bacteria and LPS
- if there are LPS independent mechanisms regulating the E-selectin promoter regulatory regions

6.2 Materials and Methods

6.2.1 HUVEC culture and preparation for transfection

Details of endothelial cell isolation from umbilical cords and cell culture and maintenance of HUVEC are described in Chapter 2, Section 2.2.1. Once HUVEC reached 95% confluence on primary plates, they were subcultured onto tissue culture plates coated with attachment factor, and grown over-night in SM prior to transfection.

6.2.2 Transfection of HUVEC

The transfection methodology optimised in Chapter 5 was utilised to examine E-selectin promoter activity in response to killed WT and *lpxA*- *N. meningitidis* and purified LPS. The transfection mixture was prepared as described in Chapter 2, Section 2.11. Briefly, Peptide 6 was used at a 7:1 peptide:DNA charge ratio. Plasmid DNA was replaced by 210ng of Picagene plasmid (containing the E-selectin promoters; Figure 6.1 and Figure 6.2) and 40ng phRL-TK plasmid (expressing Renilla luciferase) (Figure 6.3). The transfection mixture was supplemented with 2.5 mM SB. Cells were transfected for 4 hours in an incubator at 37°C, 5% CO₂ in air, then rescued in fresh SM supplemented with 2.5 mM SB overnight prior to stimulation. Transfections were performed in 96 well plates.

6.2.3 E-selectin promoter plasmids

Transfections of HUVEC were performed with the Picagene Basic Vector (PGV-B, Toyo Ink, Japan, Figure 6.1). The plasmid was used to insert the E-selectin promoter and deletion mutants of the promoter (Figure 6.2).

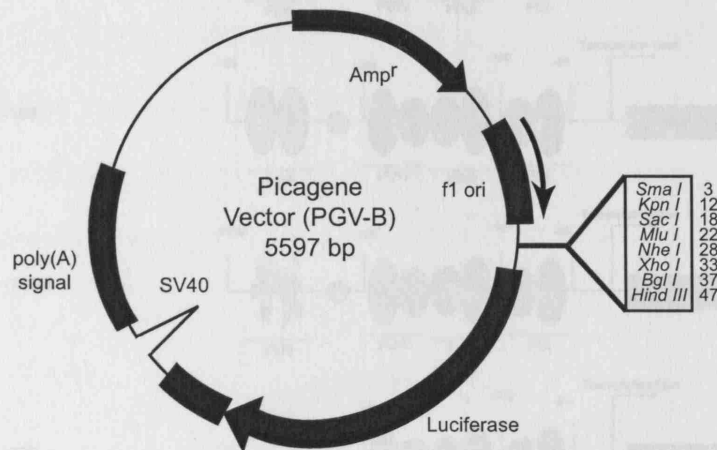


Figure 6.1: Picagene basic vector. The figure shows the gene map of the picagene vector used in this study. The E-selectin promoter sequence was inserted into the plasmid in front of the luciferase reporter gene.

The E-selectin promoter plasmid constructs were a generous gift from Dr. Narumi (Tamaru and Narumi, 1999). The E-selectin promoter constructs were developed by amplifying the E-selectin promoter by PCR, and ligating the fragment with the Picagene vector (Figure 6.1). Primers spanning the E-selectin promoter region were used to create the -166 and -129 promoter construct. The -166M construct was developed by site-directed mutagenesis of the -166 parent construct. By using the -166 construct as

template, the -166M mutant was developed by introducing a mutation on the PCR primer, altering the ATF2/c-Jun site (PD II) from the WT sequence (TGACATCATTG) to a mutant sequence (gtcgAgCcTTG), which has previously been shown to abolish ATF2/c-Jun binding to the E-selectin promoter (Hooft *et al.*, 1992). Figure 6.2 illustrates the deletion constructs used in this study.

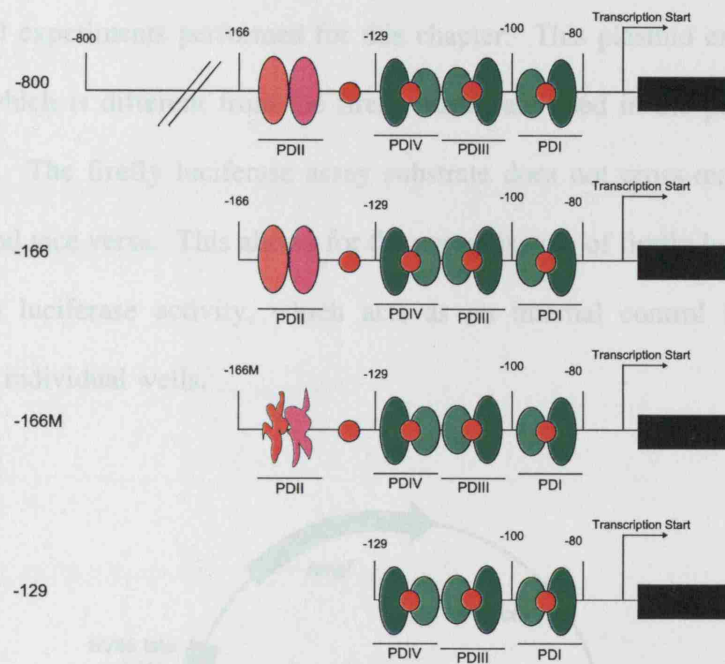


Figure 6.2 E-selectin promoter constructs. The -800 construct contains a long stretch upstream of the transcriptional start site. The -166 construct contains the four known transcription sites, consisting of 3 NF κ B sites (green) and 1 ATF2/C-Jun site (red). The -166M construct contains a mutation on the ATF2/c-Jun site. The -129 has a deletion of the ATF2/c-Jun site. All constructs control the expression of the luciferase reporter gene.

6.2.4 A transfection control plasmid used to normalise E-selectin promoter controlled luciferase activity

The phRL-TK plasmid (Promega, Figure 6.3) was used as an internal transfection control in all experiments performed for this chapter. This plasmid expresses Renilla luciferase, which is different from the firefly luciferase used in the picagene plasmid (Figure 6.1). The firefly luciferase assay substrate does not cross-react with Renilla luciferase, and vice versa. This allows for the normalisation of firefly luciferase activity with Renilla luciferase activity, which acts as an internal control for transfection efficiency in individual wells.

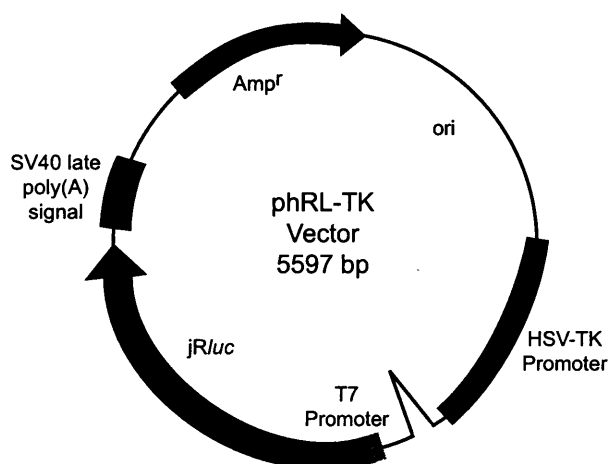


Figure 6.3 TK vector. Gene map of the TK vector.

6.2.5 Verification of E-selectin constructs

Plasmid constructs were screened by either restriction enzyme digest or by PCR using primers spanning the picagene vector (Table 6.1). Positive clones were sequenced and compared to the reference E-selectin promoter sequence (AL021940, (Bevilacqua et al., 1989; Collins et al., 1991).

Table 6.1 Primers used for the sequencing of E-selectin promoter constructs inserted into picagene vector (Toyo Ink, Japan).

Primer	Sequence
PGVB-F	5'-CGGGAGGTACCGAGCTCTTA-3'
PGVB-R	5'-CCTCTAGAGGATAGAATGGC-3'

6.2.6 Luciferase data analysis

Luciferase and Renilla assays are described in Chapter 2. The data obtained was analysed by dividing the RLU by the RRU. This was performed to normalise E-selectin promoter activity to TE obtained in individual wells. This data was then normalised by dividing stimulated activity by unstimulated control activity. Data was expressed as mean of fold increase above control.

6.2.7 Preparation of *N. meningitidis* bacteria and stimulation of E-selectin promoter transfected HUVEC

Bacteria were prepared as described in Chapter 2, Section 2.3. For the experiments performed here, bacteria were seeded from frozen aliquots onto fresh GC plates and grown overnight, then subcultured once and grown for 16-18 hours prior to killing with 0.5% PFA. Freshly grown and killed meningococci were used for all experiments. The OD₅₄₀ of bacterial solutions were adjusted to a reading of 1, to give a working bacterial concentration of 10⁹ CFU/ml.

Stimulation was performed the day after transfection in SM supplemented with 2.5 mM SB and with appropriate concentrations of bacteria, LPS, or 400pg/ml IL-1 β and 100ng/ml PMA simultaneously (IP). Cells were stimulated for 5 hours in an incubator at 37°C, 5% CO₂ in air.

6.3 Results

6.3.1 IL-1 β /PMA induced E-selectin promoter activity in transfected HUVEC

The E-selectin constructs, kindly donated by Dr. Narumi, were sequenced and found to be identical to the published promoter sequence.

In order to establish if the E-selectin promoter constructs were functional with the developed transfection system, E-selectin promoter (-800) transfected HUVEC were stimulated with IL-1 β /PMA (IP).

IP was able to induce luciferase activity in -800 E-selectin promoter transfected HUVEC (Figure 6.4). There was no induction of luciferase activity in transfected unstimulated HUVEC control. The figure demonstrates a representative experiment of luciferase activity.

When luciferase activity was normalised to experimental control activity, IP induced a 70-fold increase in luciferase activity above control (Figure 6.5). Hence, it was possible to induce the -800 E-selectin promoter with IP, which demonstrated that the promoter and transfection system were optimal. IP was used as a positive control for E-selectin promoter activity.

6.3.2 Fixed WT and *lpxA*- *N. meningitidis* stimulated higher

levels of E-selectin promoter activity than purified LPS

Having established that the E-selectin promoter construct is functional in this system, the LPS dependent and independent regulation of E-selectin induction observed in Chapter 3 and Chapter 4 were studied.

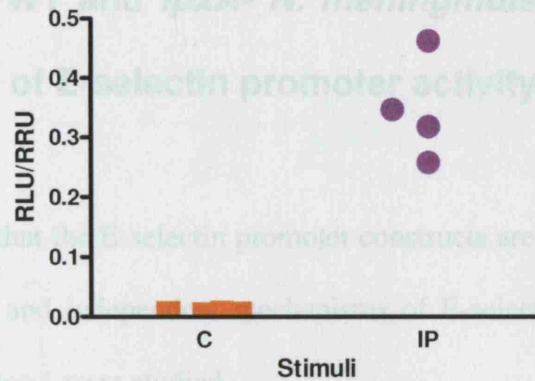


Figure 6.4: E-selectin controlled luciferase activity is detected in response to IP. HUVEC were transfected using LID vector and -800 E-selectin promoter plasmid. HUVEC were then stimulated with IP or media alone (C) for 5 hours. Data is presented as RLU/RRU activity. A representative experiment is illustrated. N=4 from endothelial cells from separate donors.

WT bacteria induced a 2-fold increase in E-selectin promoter activity (Figure 6.5).

Similar to WT, the *lpxA* mutant also induced a 2-fold increase in E-selectin promoter activity. LPS (10µg/ml) induced a 4-fold increase above control of luciferase activity. WT and *lpxA*- bacteria induction of the -800 E-selectin promoter was 2-fold higher than levels obtained with purified LPS. *N. meningitidis* incubated in medium alone exhibited background levels of luciferase activity.

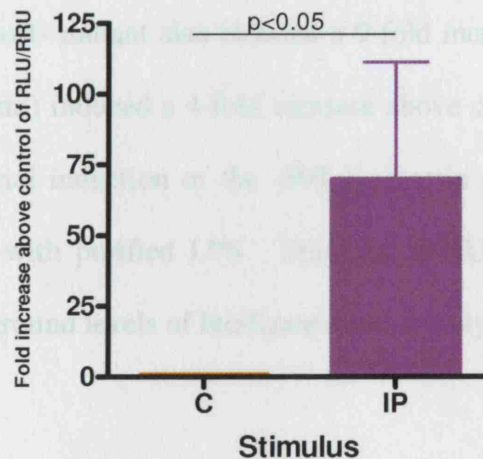


Figure 6.5 IP is able to induce a 70-fold increase in E-selectin regulated luciferase activity as compared to control. Luciferase activity was normalised to Renilla activity and this measure was normalised to the negative control. Results are presented as fold increase above control of RLU/RRU activity, n=5 from endothelial cells from separate donors. P<0.05 (paired student t-test).

6.3.2 Fixed WT and *lpxA*- *N. meningitidis* stimulated higher levels of E-selectin promoter activity than purified LPS

Having established that the E-selectin promoter constructs are functional in this system, the LPS dependent and independent mechanisms of E-selectin induction observed in Chapter 3 and Chapter 4 were studied.

HUVEC transfected with the -800 E-selectin promoter construct were stimulated with 10^8 CFU/ml WT and *lpxA*- bacteria and 10ng/ml LPS to determine if there was transcriptional upregulation of E-selectin by these three stimuli.

WT bacteria induced a 9-fold increase in E-selectin promoter activity (Figure 6.6). Similar to WT, the *lpxA*- mutant also induced a 9-fold increase in E-selectin promoter activity. LPS (10ng/ml) induced a 4-fold increase above control of luciferase activity. WT and *lpxA*- bacterial induction of the -800 E-selectin promoter was 2-fold higher than levels obtained with purified LPS. Transfected HUVEC incubated in medium alone exhibited background levels of luciferase activity only.

6.3.3 A construct containing only the four regulatory regions

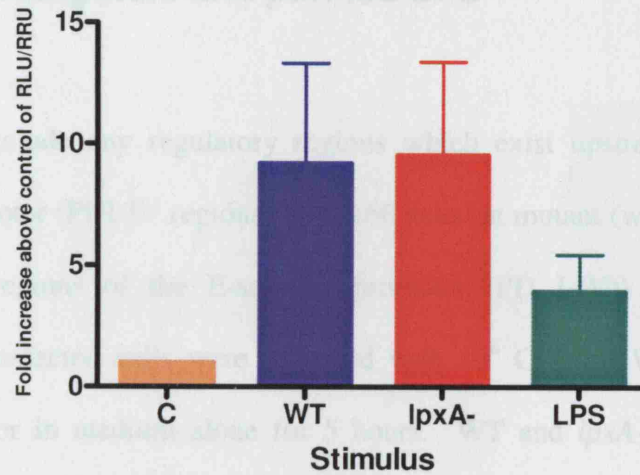
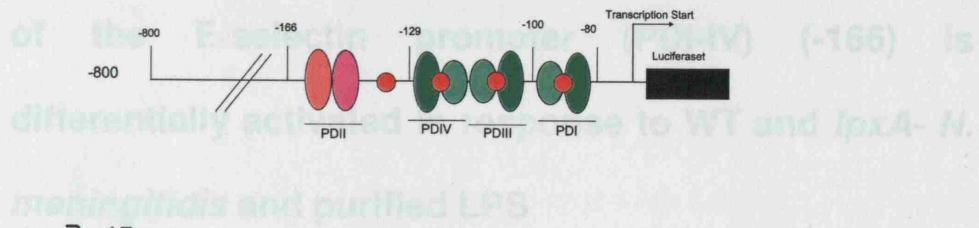


Figure 6.6 WT and *lpxA*- *N. meningitidis* bacteria are able to induce a 9-fold increase in activity of the -800 E-selectin promoter construct compared to control. The -800 E-selectin promoter construct was transfected into HUVEC and stimulated for 5 hours with 10^8 CFU/ml WT or *lpxA*-, 10ng/ml purified LPS or in media alone. Results are presented as mean of fold increase above control of RLU/RRU activity \pm SEM, n=5 from endothelial cells from separate donors

6.3.3 A construct containing only the four regulatory regions of the E-selectin promoter (PDI-IV) (-166) is differentially activated in response to WT and *lpxA*- *N. meningitidis* and purified LPS

In order to exclude any regulatory regions which exist upstream of the E-selectin proximal promoter (PDI-IV regions), the -166 deletion mutant (which contains only the 4 regulatory regions of the E-selectin promoter (PD I-IV)) was transfected into HUVEC. Transfected cells were activated with 10^8 CFU/ml WT or *lpxA*- bacteria, 10ng/ml LPS or in medium alone for 5 hours. WT and *lpxA*- were able to induce luciferase activity, activating increases in activity ranging from 10-12 fold above control (Figure 6.7). LPS alone, however, induced a 4-fold increase in luciferase activity, 60% less than that stimulated by WT and *lpxA*- bacteria. The positive control, IP induced a 15-fold increase in luciferase activity as compared to the negative control.

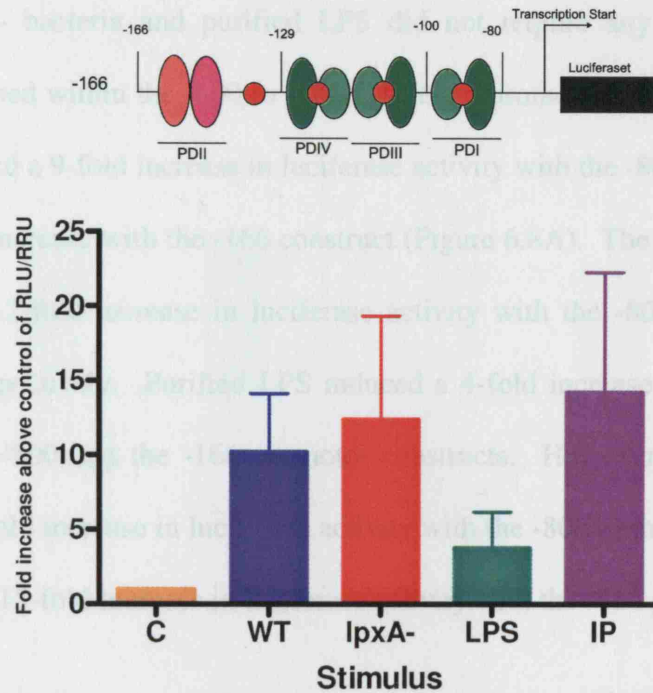


Figure 6.7 Differential upregulation of luciferase activity controlled by the -166 E-selectin promoter deletion mutant. HUVEC were transfected with the -166 E-selectin deletion mutant and stimulated with WT, *lpxA*-, LPS, IP or medium alone for 5 hours. Results are presented as mean of fold increase above control of RLU/RRU activity \pm SEM, n=5 from endothelial cells from separate donors.

6.3.4 *N. meningitidis* WT and *lpxA*- bacteria and LPS do not control E-selectin promoter activity through the promoter region contained between -800 and -166

In order to explore the region contained within the -800 and -166 promoters, the promoter activity of the -800 and -166 promoter constructs were compared to each other in response to WT and *lpxA*- bacteria, purified LPS and IP.

WT and *lpxA*- bacteria and purified LPS did not require any unknown regulatory regions contained within the -800 to -166 E-selectin promoter region (Figure 6.8). WT bacteria induced a 9-fold increase in luciferase activity with the -800 promoter construct and a 10-fold increase with the -166 construct (Figure 6.8A). The *lpxA*- mutant induced a 9 fold and 12-fold increase in luciferase activity with the -800 and -166 promoter constructs, respectively. Purified LPS induced a 4-fold increase in luciferase activity with both the -800 and the -166 promoter constructs. However, stimulation with IP induced a 70-fold increase in luciferase activity with the -800 promoter construct, which decreased to a 15-fold increase in luciferase activity with the -166 promoter construct.

These results indicate that both bacteria and purified LPS induce E-selection promoter activity through the four PD regulatory regions of the E-selectin promoter contained within the consstrcuts, as there was no difference in luciferase activity between the two promoter constructs.

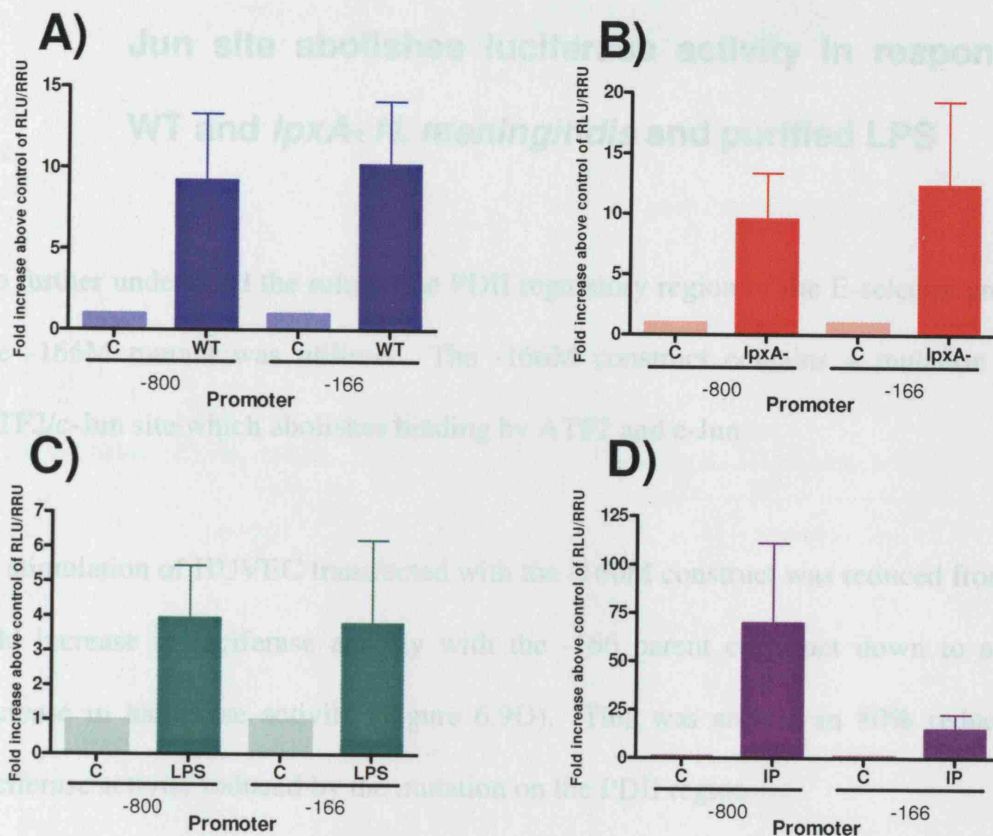


Figure 6.8 The region contained between the -800 and -166 promoter constructs is not involved in the differential regulation of E-selectin activation by *N. meningitidis* WT and *lpxA*⁻ bacteria and purified LPS. HUVEC were transfected with E-selectin deletion mutant constructs and stimulated with 10^8 CFU/ml WT or *lpxA*⁻ bacteria, 10ng/ml purified LPS, IP or media alone for 5 hours. Results are presented as mean of fold increase above control of RLU/RRU activity \pm SEM, n=5 from endothelial cells from separate donors.

6.3.5 A mutation on the PDII region containing the ATF2/c-Jun site abolishes luciferase activity in response to WT and *lpxA*- *N. meningitidis* and purified LPS

To further understand the role of the PDII regulatory region of the E-selectin promoter, the -166M mutant was utilised. The -166M construct contains a mutation on the ATF2/c-Jun site which abolishes binding by ATF2 and c-Jun.

IP stimulation of HUVEC transfected with the -166M construct was reduced from a 15-fold increase in luciferase activity with the -166 parent construct down to a 3-fold increase in luciferase activity (Figure 6.9D). This was around an 80% reduction in luciferase activity induced by the mutation on the PDII region.

E-selectin promoter activity with the -166 construct stimulated with 10^8 CFU/ml WT bacteria induced a 10-fold increase in luciferase activity and this dropped to a 4-fold increase with the mutant -166M construct. This equated to a drop in luciferase activity of about 60% (Figure 6.9A).

The *lpxA*- mutant induced a 12-fold increase in luciferase activity with the -166 construct, and this was reduced to a 2-fold increase with the -166M mutant. This was a reduction of around 90% in luciferase activity caused by the mutation on the PD II site (Figure 6.9B).

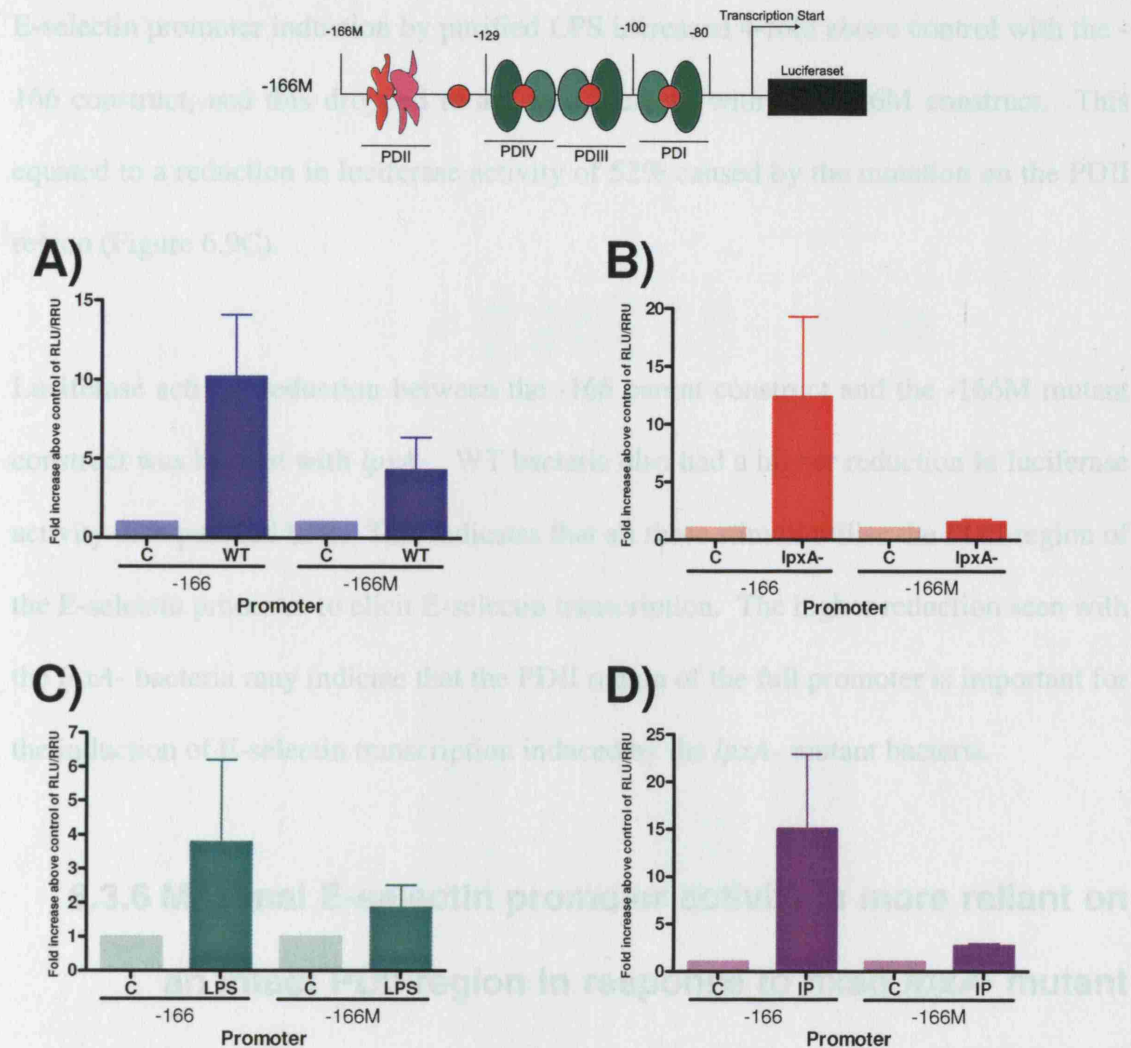


Figure 6.9 A mutation on the PD II region of the E-selectin promoter containing the ATF2/c-Jun site drastically reduces luciferase activity induced by WT and *lpxA*- *N. meningitidis* and purified LPS. HUVEC were transfected with the -166 E-selectin deletion mutant and the -166M mutant and stimulated with 10^8 CFU/ml WT or *lpxA*- bacteria, 10ng/ml purified LPS, IP or media alone for 5 hours. A) 10^8 CFU/ml WT bacterial induction; B) 10^8 CFU/ml *lpxA*- bacterial induction; C) 10ng/ml purified LPS induction; C) IP induction. Results are presented as mean of fold increase above control of RLU/RRU activity \pm SEM, n=3 from endothelial cells from separate donors. The scales of the four graphs differ.

E-selectin promoter induction by purified LPS increased 4-fold above control with the -166 construct, and this dropped to a 2-fold increase with the -166M construct. This equated to a reduction in luciferase activity of 52% caused by the mutation on the PDII region (Figure 6.9C).

Luciferase activity reduction between the -166 parent construct and the -166M mutant construct was highest with *lpxA*⁻. WT bacteria also had a higher reduction in luciferase activity than purified LPS. This indicates that all these stimuli utilise the PDII region of the E-selectin promoter to elicit E-selectin transcription. The higher reduction seen with the *lpxA*⁻ bacteria may indicate that the PDII region of the full promoter is important for the induction of E-selectin transcription induced by the *lpxA*⁻ mutant bacteria.

6.3.6 Maximal E-selectin promoter activity is more reliant on an intact PDII region in response to fixed *lpxA*⁻ mutant bacteria compared to stimulation with fixed WT bacteria and purified LPS

Induction of the -166M mutant by WT, *lpxA*⁻, LPS and IP was compared (Figure 6.10). WT bacteria induced a 4-fold increase in luciferase activity compared to unstimulated control, and LPS was able to induce nearly a 2-fold increase in luciferase activity. However, the *lpxA*⁻ mutant induced less than a 2-fold increase in luciferase activity as compared to the negative control. IP induced a 3-fold increase in luciferase activity of the -166M construct. WT bacteria induced the highest luciferase activity controlled by

the -166M construct, which was followed by LPS and finally *lpxA*-. This indicated that the *lpxA*- mutant bacteria was more reliant on the PDII region for induction of E-selectin controlled luciferase activity than the WT bacteria and purified LPS.

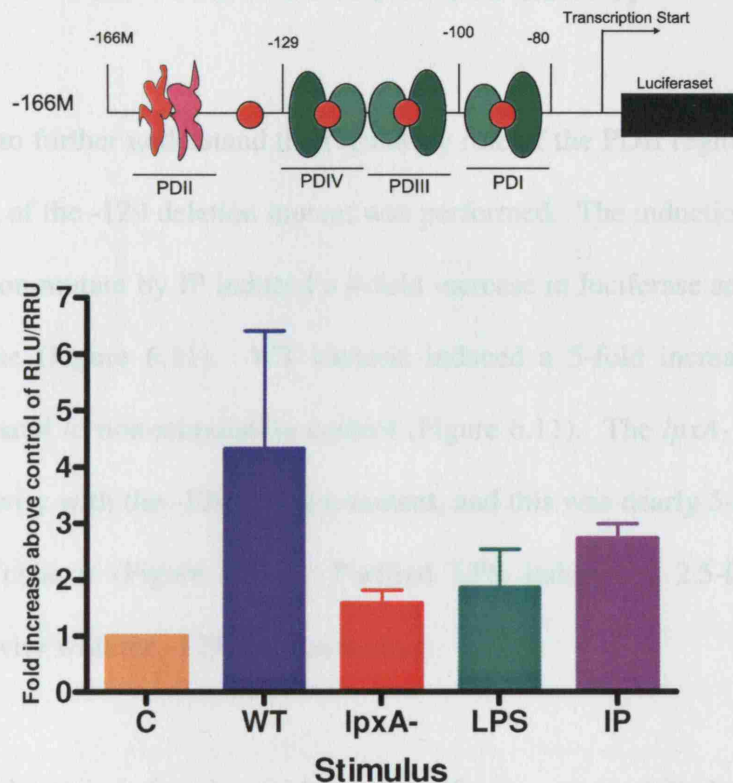


Figure 6.10 Induction of the -166M demonstrates that the *lpxA*- mutant relies on the PDII site to induce E-selectin promoter controlled luciferase activity. HUVEC were transfected with the -166M mutant and stimulated with 10^8 CFU/ml WT or *lpxA*- bacteria, 10ng/ml purified LPS or IP. Results are presented as mean of fold increase above control of RLU/RRU activity \pm SEM, n=5 from endothelial cells from separate donors.

6.3.7 The removal of the PD II region restores the ability of the *lpxA*- mutant bacteria to induce E-selectin promoter controlled luciferase activity

In an attempt to further understand the regulatory role of the PDII region, a comparison of stimulation of the -129 deletion mutant was performed. The induction of the -129 E-selectin deletion mutant by IP induced a 4-fold increase in luciferase activity compared to media alone (Figure 6.11). WT bacteria induced a 5-fold increase in luciferase activity compared to non-stimulation control (Figure 6.11). The *lpxA*- mutant induced luciferase activity with the -129 deletion mutant, and this was nearly 5-fold higher than the negative control (Figure 6.11). Purified LPS induced a 2.5-fold increase in luciferase activity with the -129 deletion mutant.

WT and *lpxA*- bacteria induced equal level of luciferase activity with the -129 E-selectin construct, which were higher than purified LPS. This indicates that although the *lpxA*- mutant relies on the PDII region for optimal E-selectin promoter activity, there may be other regulatory regions involved in LPS-independent induction, which may become active in the absence of the PDII region.

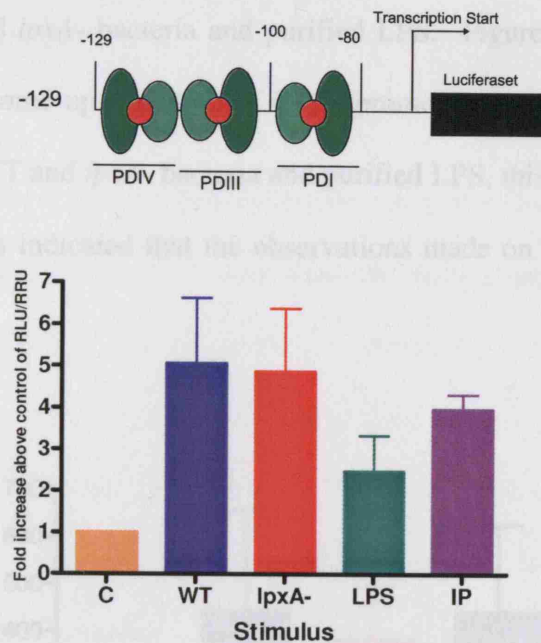


Figure 6.11 The -129 mutant, which does not contain the PDII region, is differentially regulated by WT *N. meningitidis*, *lpxA*- mutant, and purified LPS. HUVEC were transfected with the -129 mutant and stimulated with 10^8 CFU/ml WT or *lpxA*- bacteria, 10ng/ml purified LPS, IP or media alone. Results are presented as mean of fold increase above control of RLU/RRU activity \pm SEM, $n=4$ from endothelial cells from separate donors.

6.3.8 Luciferase activity was not upregulated by WT and *lpxA*- bacteria and purified LPS when activity was regulated by an irrelevant promoter, such as the CMV promoter,

To demonstrate that the activity observed with the E-selectin promoter constructs was specific to the E-selectin promoter and not an artefact, the CMV promoter was utilised to examine the differential upregulation of luciferase activity in response to *N.*

meningitidis WT and *lpxA*- bacteria and purified LPS. Figure 6.12 demonstrates that although there was some upregulation of CMV promoter controlled luciferase activity by *N. meningitidis* WT and *lpxA*- bacteria and purified LPS, this activity did not reach a 2-fold increase. This indicated that the observations made on the E-selectin promoter were specific.

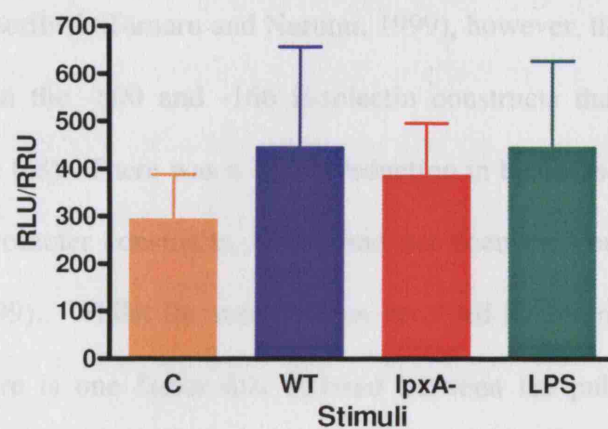


Figure 6.12 The upregulation of luciferase activity in response to WT and *lpxA*- *N. meningitidis* and purified LPS was specific to the E-selectin promoter. HUVEC were transfected with the pCI-luciferase plasmid and stimulated with 10^8 CFU/ml WT or *lpxA*- bacteria, 10ng/ml purified LPS or media alone. Results are presented as mean of fold increase above control of RLU/RRU activity \pm SEM, n=4 from endothelial cells from separate donors.

6.4 Discussion

The aim of this chapter was to explore the regulation of the E-selectin promoter by WT bacteria and purified LPS, and to determine the LPS dependant and independent mechanisms that regulate E-selectin promoter activity by utilising the LPS deficient *lpxA*- mutant bacteria. The constructs utilised in this study responded to IP stimulation, as previously described (Tamaru and Narumi, 1999), however, the pattern observed was different between the -800 and -166 E-selectin constructs than that reported in the literature (Figure 6.8). There was a 78.5% reduction in luciferase activity between the -800 and -166 promoter constructs, which had not been previously observed (Tamaru and Narumi, 1999). Whilst the mechanisms involved in this response have not been investigated, there is one factor that differed between the published results and the experiments performed in this chapter. Tamaru and Narumi (1999) performed transfection experiments on HUVEC that were at passage 6-8. Experiments performed in this chapter were performed on HUVEC which were at passage 1. It is known that passaging HUVEC causes a reduction and eventually a loss of certain inflammatory receptors. It may be that HUVEC at passage 6-8 have lost a receptor responding to IP which would normally signal to an unknown region present in the -800 promoter construct. Therefore, HUVEC transfected and stimulated at passage 1 would be able to signal through an unknown pathway, and thereby induce higher levels of luciferase activity in response to IP.

However, IP stimulation was still useful as a positive control for E-selectin promoter construct transfection and regulation. Although the luciferase activity levels of the -166 construct stimulated with IP were not as high as those observed with the -800 construct, there was still a 15 fold-increase in luciferase activity above control of the -166 construct (Figure 6.5 and Figure 6.7). This showed that the construct was functional.

The levels of luciferase activity obtained in this chapter were much lower than the levels obtained in Chapter 5. This is likely to be an effect of the two different promoters utilised. Whilst the CMV promoter is a strong viral promoter which hijacks the cellular transcription system to produce viral product, the E-selectin promoter is only active on endothelial cells during inflammation and is therefore under tight regulation. The low levels of E-selectin promoter activity produced very low levels of luciferase activity, which made it difficult to analyse the results obtained. Hence, data was normalised to a transfection control plasmid and to unstimulated control. Whilst none of the data is statistically significant, there are trends suggesting that there may be differences in the mechanisms by which WT, *lpxA*- and LPS induce E-selectin transcription.

The stimulation of the full E-selectin promoter (-800 and -166) indicated that there may be differential regulation by WT *N. meningitidis* and purified LPS (Figure 6.6 and Figure 6.7). The *lpxA*- mutant was also able to induce the -800 and -166 E-selectin promoter constructs, demonstrating that the bacteria had LPS independent mechanisms regulating the E-selectin promoter and *de novo* synthesis of E-selectin protein.

The use of the -166M mutant of the -166 promoter construct indicates that the LPS-independent mechanisms of E-selectin regulation may signal through the PDII region, and therefore require this region for maximal promoter activity (Figure 6.9). The highest reduction in luciferase activity between the -166 and -166M was obtained with the *lpxA*- mutant, followed by WT bacteria. The lowest reduction in activity between the -166 and -166M constructs was obtained with purified LPS. Comparison of -166M regulated luciferase activity induced by WT, *lpxA*- and purified LPS demonstrated that the *lpxA*- mutant was more dependent on an intact ATF2/c-Jun site than WT bacteria and purified LPS (Figure 6.10). The differential expression pattern observed with the -800 and -166 promoter constructs stimulated by WT and *lpxA*- bacteria and purified LPS was abolished with the -166M promoter construct (Figure 6.6, Figure 6.7 and Figure 6.10). The WT bacteria was still able to induce higher levels of luciferase activity with the -166M construct compared to the levels observed with purified LPS, however, the *lpxA*- mutant induced lower levels of -166M promoter controlled luciferase activity than WT bacteria and purified LPS. The -166M mutant contains a mutation in the ATF2/c-Jun regulatory site which abolishes the binding of ATF2 (Hooft *et al.*, 1992), and mutations of the ATF2/c-Jun site have been shown to decrease E-selectin promoter activity. This suggests that an intact site is necessary for maximal E-selectin promoter activity in response to cytokines (Hooft *et al.*, 1992; Tamaru and Narumi, 1999), and this was also observed for E-selectin promoter activity induced by WT, *lpxA*- and LPS.

The ATF-2/c-Jun (PDII) region is activated by TNF- α through the phosphorylation of JNK1 and p38 (Read *et al.*, 1997). TNF- α is also able to induce other upstream activators of the MAPK activation pathway (Che *et al.*, 2002). In addition, LPS can also activate p38 and JNK (Jersmann *et al.*, 2001a).

Invasive *N. meningitidis* MC58 (a serogroup B strain) phosphorylates and activates JNK1, JNK2 and p38 (Sokolova *et al.*, 2004). The activation of JNK1 and JNK2 correlates with invasion of endothelial cells by *N. meningitidis*, as a non-invasive strain is unable to induce JNK1 and JNK2 phosphorylation and activation (Sokolova *et al.*, 2004). Blockage of the integrin receptor $\alpha_5\beta_1$, which anchors the bacterium to the endothelial cell surface (Unkmeir *et al.*, 2002b), also inhibits the activation of JNK1 and JNK2 by *N. meningitidis* (Sokolova *et al.*, 2004). This indicates that invasion by meningococci requires the activation of JNK1 and JNK2, whereas p38 is involved in the activation of IL-6 and IL-8 (Sokolova *et al.*, 2004). Hence, the MAPK pathway is activated in response to *N. meningitidis*. Interestingly, the data obtained with the -166M E-selectin promoter construct suggests that LPS-independent activation of the inflammatory response may be more dependant on the MAPK activation pathway.

The mechanisms by which the MAPK pathway may act on the E-selectin promoter when there are low levels of NF κ B activity are still unclear. ATF2 and c-Jun are both capable of protein-protein interactions with NF κ B (Kaszubska *et al.*, 1993). It may be that the LPS independent mechanisms regulating the E-selectin promoter activate greater levels of the MAPK pathway, and that these levels increase ATF2/c-Jun

interactions with NFκB. These interactions may in turn allow low levels of NFκB to bind to the E-selectin promoter and hence induce E-selectin promoter activity. The mutation of the PDII region containing the ATF2/c-Jun site is able to prevent NFκB interacting with its binding sites (Kaszubski *et al.*, 1993), indicating that this regulatory region is important for the binding of NFκB to the E-selectin promoter. Mutations of the PDII region reduce E-selectin promoter activity (Kaszubski *et al.*, 1993; Tamaru and Narumi, 1999; Schindler and Baichwal, 1994), suggesting that an intact PDII region is necessary for maximal E-selectin promoter activity, and this may be due to the interaction between the PDII region and NFκB.

However, when comparing the regulation of luciferase activity by the -129 promoter construct stimulated with WT, *lpxA*- and purified LPS, the luciferase activity pattern appears to revert back to the pattern observed with the -166 and -800 promoter constructs.

This differs to the data obtained with the -166M construct, and does not relate to previously published data, which demonstrates that the *lpxA*- mutant is not able to induce high levels of NFκB activity (Dixon *et al.*, 2004). There are two theories which may explain this phenomenon. First, a crucial stage in the activation of the E-selectin promoter is the folding of the DNA, which allows for the binding of transcription factors. Second, there may be, as yet, unidentified downstream elements which may control E-selectin promoter activity during situations of low NFκB activity.

The relative helix orientation of the PDII region is important for the folding of the E-selectin promoter, which allows for NF κ B binding and brings distant regions together within the promoter (Meacock *et al.*, 1994) (Figure 6.13A). ATF2/c-Jun heterodimers are known to induce DNA bending (Kerppola and Curran, 1993), and activation of the PDII site is essential for the folding of the E-selectin promoter. The mutation of the PDII region abolishes ATF2/c-Jun binding, which prevents the activation of this region. This in turn may prevent the folding of the promoter and abolishes promoter activity (Figure 6.13B). However, the removal of the PDII region may remove its inhibitory potentiality on the promoter (Figure 6.13C). It may be that in the absence of the PDII region, the promoter relies more on the folding exerted by HMG I(Y) binding to the PDIV region.

HMG I(Y) is not a transcription factor, however, it has the ability to enhance promoter activity of a range of genes, including E-selectin, by enhancing the binding of transcription factors to promoter sequences, such as IFN- β (Falvo *et al.*, 1995; Perrella *et al.*, 1999; Lewis *et al.*, 1994; Whitley *et al.*, 1994). The protein bends the promoter to allow for protein-protein interactions between the different transcription factors (Falvo *et al.*, 1995). HMG I(Y) interacts with NF κ B (Brickman *et al.*, 1999) and ATF2 (Du and Maniatis, 1994), and has been shown to increase the binding of NF κ B to the human IFN- β promoter (Falvo *et al.*, 1995), the interleukin-2 receptor α -chain (IL-2R α) (John *et al.*, 1995), and the inducible nitric-oxide synthase promoter/enhancer (iNOS) promoter (Perrella *et al.*, 1999).

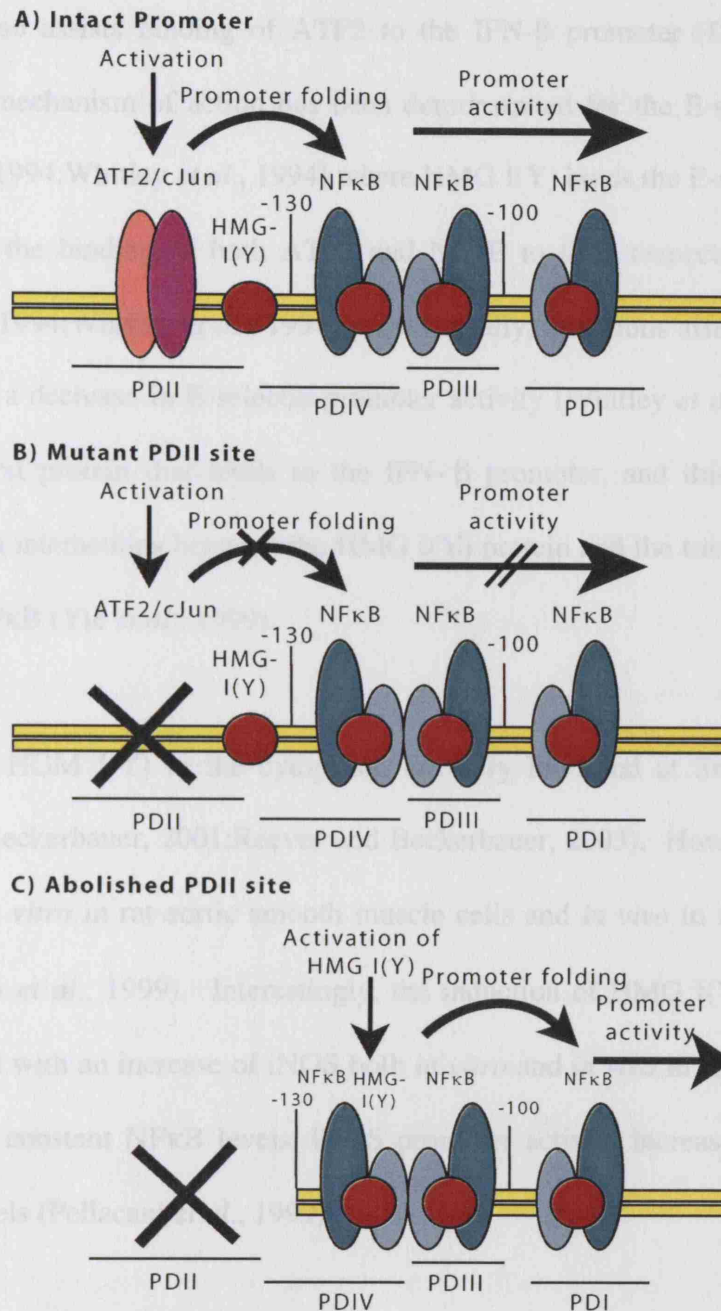


Figure 6.13 E-selectin promoter folding, and the effect of a mutant or absent PDII. A) The intact promoter binds ATF2/c-Jun, which folds the promoter when activated. B) The mutant PDII region prevents ATF2/c-Jun binding, which prevents the folding of the promoter and hence binding by other molecules to the promoter. C) The absent PDII region does not prevent the binding of the other regions to HMG I(Y) and NFκB. HMG I(Y) binding may therefore induce the promoter folding required for promoter activity.

HMG I(Y) also assists binding of ATF2 to the IFN- β promoter (Du and Maniatis, 1994). This mechanism of action has been demonstrated for the E-selectin promoter (Lewis *et al.*, 1994;Whitley *et al.*, 1994) where HMG I(Y) binds the E-selectin promoter and enhances the binding of both ATF2 and NF κ B to their respective binding sites (Lewis *et al.*, 1994;Whitley *et al.*, 1994). Additionally, mutations affecting HMG I(Y) binding cause a decrease in E-selectin promoter activity (Whitley *et al.*, 1994). HMG I(Y) is the first protein that binds to the IFN- β promoter, and this is followed by protein-protein interactions between the HMG I(Y) protein and the transcription factors ATF-2 and NF κ B (Yie *et al.*, 1999).

The levels of HGM I(Y) in the cytoplasm are very low, and at times undetectable (Reeves and Beckerbauer, 2001;Reeves and Beckerbauer, 2003). However, HMG I(Y) is inducible *in vitro* in rat aortic smooth muscle cells and *in vivo* in rat by IL-1 β and LPS (Pellacani *et al.*, 1999). Interestingly, the induction of HMG I(Y) by IL-1 β and LPS correlated with an increase of iNOS both *in vitro* and *in vivo* in rat smooth muscle cells. During constant NF κ B levels, iNOS promoter activity increases by increasing HMG I(Y) levels (Pellacani *et al.*, 1999).

It is possible that the LPS independent mechanisms of E-selectin regulation may be acting on HMG I(Y), and that increasing levels of HMG I(Y) may be important when there are low levels of NF κ B translocation to the nucleus. Increased levels of HMG I(Y) may assist low levels of NF κ B to bind to the promoter and thereby induce promoter activity. This phenomenon in conjunction with the dependence on the

ATF2/c-Jun site may regulate the high levels of E-selectin activity detected in response to the *lpxA*- mutant. Further work will be required to assess this hypothesis.

The p65 subunit of NFκB can also promote bending of DNA (Schreck *et al.*, 1990). This has been demonstrated on the PDIV region of the E-selectin promoter (Meacock *et al.*, 1994). It is possible that removal of the ATF2/c-Jun regulatory site transfer the dependence of promoter folding to the PD IV region binding NFκB. The PDIV and PDIII regions have been shown to be the most important of the 3 NFκB binding sites on the E-selectin promoter (Lewis *et al.*, 1994; Schindler and Baichwal, 1994), as mutations on these sites have the most detrimental effect on E-selectin promoter activity (Schindler and Baichwal, 1994). Although *lpxA*- induces very low levels of NFκB activation, it is possible that the E-selectin promoter is more reliant on the folding of the promoter, and that the quantity of NFκB is secondary to the folding. It may also be that the folding of the PD IV NFκB binding site brings as yet unknown downstream regions together that may play a secondary role in the induction of E-selectin, and that these may be controlled in an LPS independent manner.

There is no evidence to date of downstream regulatory regions on the E-selectin promoter and gene transcript. However, Brostjan *et al.* (1997) used an E-selectin promoter construct which contained 255 bps upstream and 482 bps downstream of the transcriptional start site. The group also used a construct that only contained 30 bps downstream of the transcriptional start site. Deletion of the downstream 450 bp in the translated region causes a reduction in LPS-induced luciferase activity of 40-50%

(Brostjan *et al.*, 1997). Although the group did not comment on this phenomenon, it is an interesting observation which may suggest that regions within the first exon and intron of the E-selectin gene may be required for maximal E-selectin expression. The E-selectin promoter constructs used in this study contained 50 bps downstream of the E-selectin gene transcriptional start site. There could be a regulatory region between -166 and +50 bps of the human E-selectin gene promoter that has yet to be identified. These regions may have LPS-dependent and independent mechanisms of action.

Although it appears that the *lpxA*- mutant induces E-selectin promoter activity via the MAPK pathway, the data suggests an important role for HMG I(Y) controlled E-selectin upregulation induced by LPS-independent mechanisms.

Chapter 7

General Discussion

7.1 Endothelial cell adhesion molecule surface expression and mRNA induced by *N.* *meningitidis*

The aim of this thesis was to investigate the mechanisms by which *N. meningitidis* regulated endothelial E-selectin molecule expression. A range of different approaches were used to investigate the regulation of E-selectin, including the detection of surface protein expression and mRNA expression, as well as a detailed study of the E-selectin promoter.

It was established that E-selectin is differentially regulated in response to both live and killed meningococci and purified LPS. Differential E-selectin expression was LPS-independent, as the *lpxA*- mutant was also able to induce E-selectin surface expression. This difference in protein induction was not as marked with ICAM-1 and VCAM-1 expression stimulated by WT, *lpxA*- and purified LPS. PFA fixed WT bacteria and LPS also induced differential E-selectin mRNA expression. Whilst this does not rule out a possible role for E-selectin post-transcriptional regulation in response to *N. meningitidis*, it suggests that E-selectin protein expression is, at least largely, regulated at the transcriptional level.

Interestingly, there was prolonged E-selectin expression in response to fixed WT and *lpxA*- meningococci, but not purified LPS. Prolonged E-selectin expression is rarely

observed in the literature. E-selectin is upregulated by 4-6 hours and reduced to background levels by 24 hours. Whilst LPS induced E-selectin expression followed such a pattern, WT bacteria induced prolonged high levels of E-selectin expression which remained elevated by 28 hours. The *lpxA*- bacteria induced E-selectin levels which remained elevated at 10 hours post stimulation, and followed the pattern observed with WT bacterial induction of E-selectin. This suggests that prolonged E-selectin expression may also be regulated in an LPS-independent manner.

7.1.1 Does prolonged E-selectin expression affect downstream mechanisms of leukocyte rolling, binding and transmigration?

If there is prolonged E-selectin expression, is there increased and prolonged leukocyte activity on the endothelial layer? Do these interaction increase endothelial damage by leukocytes?

The prolonged E-selectin expression observed, as well as prolonged ICAM-1 and VCAM-1 expression, may be acting as a continuous 'on' switch for leukocyte rolling, activation and transmigration, which in turn may lead to increased endothelial damage due to *N. meningitidis* induced neutrophil-endothelial cell interactions. Endothelial damage and dysfunction of the coagulation cascade are characteristic of FMS, and prolonged high level expression of E-selectin may be a mechanism that sets off a chain reaction inducing continuous neutrophil-mediated damage to the endothelium.

7.1.2 Is prolonged E-selectin expression important for downstream bacterial-cell interactions?

Signalling via E-selectin has been demonstrated. E-selectin clustering occurs upon E-selectin cross-linking mediated by either leukocyte binding (Yoshida *et al.*, 1996) or by an E-selectin cross-linking antibody (Kiely *et al.*, 2003). Clustering of E-selectin is probably regulated by the binding of cytoskeletal proteins. During E-selectin clustering, the endothelium is more resistant to mechanical strain, suggesting that α -actin is involved in this process (Yoshida *et al.*, 1996). This process is controlled by the cytoplasmic domain of E-selectin, which is constitutively phosphorylated (Yoshida *et al.*, 1998). The binding of E-selectin to cytoskeletal proteins is dependant on Rho, a small GTP-binding protein (Wojciak-Stothard *et al.*, 1999). Upon binding of E-selectin by either leukocytes or cross-linking antibodies, the cytoplasmic domain of E-selectin becomes dephosphorylated (Yoshida *et al.*, 1998). Gimbrone and co-workers have proposed a model for E-selectin cross-linking mediated signalling: upon E-selectin cross-linking by leukocytes, E-selectin clustering occurs with caveolin-1. The E-selectin cytoplasmic tail induces binding to signalling molecules which lead to MAPK activation (Hu *et al.*, 2000; Hu *et al.*, 2001) and Ca^{2+} influx (Kiely *et al.*, 2003). MAPK signalling leads to the transcription of down-stream genes, whereas the Ca^{2+} influx leads to cytoskeletal changes in the cell.

7.1.3 Could WT *N. meningitidis* cross-link with E-selectin and induce clustering, and thereby gene transcription?

N. meningitidis does bind recombinant E-selectin (Dixon, personal communication), however, it is unclear if bacteria are able to bind to surface bound E-selectin and if signalling through E-selectin occurs. It is possible that WT *N. meningitidis* cross-links with E-selectin and thereby detains the protein at the cell surface for a prolonged period of time. This, in turn, may induce continued leukocyte rolling and activation, leading to endothelial damage.

However, meningitis and FMS are accidental events. During colonisation, the bacteria will undergo changes to survive, and some of these changes may allow the bacteria to cross into the bloodstream leading to FMS. Whilst bacteria mediate the responses mounted by the host, the extent and severity of the response is likely to be an accident of nature, involving both the bacteria and the host response.

7.2 Signalling events involved in cellular activation by *N. meningitidis*

Studies on the E-selectin promoter suggested that, whilst the full E-selectin promoter responded to WT, *lpxA*- and LPS, the mutation of the PDII region demonstrated the importance of this region for the LPS independent mechanisms of E-selectin

upregulation. Additionally, the data supports a role for HMG I(Y) in meningococcal induced E-selectin expression.

The question arises as to how these stimuli are inducing signal transduction. LPS stimulation occurs via the LPS signalling complex. WT bacteria have also been demonstrated to signal through TLR2 and TLR4 (Pridmore *et al.*, 2001;Pridmore *et al.*, 2003). WT bacterial signalling through TLR2 and TLR4 is not affected by bacterial capsulation or LPS sialylation (Pridmore *et al.*, 2003). In addition, *lpxA*- bacteria signal through TLR2 (Pridmore *et al.*, 2001).

TLR4 binding leads to NF κ B activation and TLR2 binding leads to signalling via the MAPK and NF κ B pathways (Re and Strominger, 2001;Asehnoune *et al.*, 2005). Whilst high concentrations of WT bacteria and purified LPS induce similar levels of NF κ B, they induce differential E-selectin expression. There may be non-LPS components on the bacterial cell surface which mediate cell signalling. For instance, peptidoglycan and *Neisseriae* porins signal through TLR2 (Schwandner *et al.*, 1999;Massari *et al.*, 2002). High numbers of bacteria may be binding to all the available TLR4 molecules on the cell surface, and may therefore start to bind and signalling via the TRL2 receptor through non-LPS components on the bacterial cell surface. This may therefore be augmenting the signal for gene transcription. Meningococcal LPS signals through TLR1 and 2 combined (Wyllie *et al.*, 2000) and through TLR4 (Ingalls *et al.*, 2001;Pridmore *et al.*, 2001). Interestingly, endothelial cells do not express TLR1 protein (Spitzer *et al.*, 2002), and as LPS is not able to signal through TLR2 alone, it

may not augment the signalling cascade to increase gene expression. Further work on meningococcal signalling through TLRs is required to elucidate this question.

Whilst there is conflicting evidence as to whether endothelial cells express TLR receptors on the cell surface or internally, endothelial cells contain TLR mRNA. LPS signalling in endothelial cells has been demonstrated to be mediated by internalisation of LBP-CD14-LPS complexes, which then interacts with internal TLR4, leading to TLR4 mediated signalling (Dunzendorfer *et al.*, 2004). If endothelial TLRs are expressed internally, how do the bacteria interact with the TLRs? Do bacteria have to become internalised to interact with intracellular TLRs, and if so, how do endothelial cells internalise bacteria? Recent work within this department demonstrates that WT *N. meningitidis* bacteria become internalised via the Complement Receptor, CR3. Non-phagocytic cells stably transfected with CR3 are able to phagocytose WT *N. meningitidis* bacteria (Osman, manuscript in preparation). It may be possible that a phagocytic receptor exists on endothelial cells, and that this mediates internalisation of bacteria. Once inside the cell they may be able to then signal through intracellular TLRs.

However, there may be sufficient TLRs expressed on the endothelial surface to induce bacterial signalling without phagocytosis. The data here indicates that there may be differences in signals mediated by WT, *lpxA*- and LPS. It has been shown that differential E-selectin expression by meningococci and LPS is, at least in part, regulated at the transcriptional level, and suggests that the LPS independent mechanisms of E-

selectin upregulation may be activated through the MAPK signalling pathway. WT and LPS induce high levels of NF κ B translocation, whereas *lpxA*- does not (Dixon *et al.*, 2004).

Figure 7.1 illustrates possible mechanisms which may be controlling differential E-selectin upregulation based on the observations made with the E-selectin promoter constructs. It is possible that WT bacteria signal through TLR4 with bacterial bound LPS and TLR2 with porins and other OMP molecules. Binding of TLR4 and TLR2 may induce higher levels of NF κ B translocation and MAPK activation than signalling via TLR4 alone (with purified LPS). Large quantities of *lpxA*- bacteria may signal through TLR2 alone, possibly activating higher levels of the MAPK pathway than purified LPS. The activation of MAPK may in turn lead to increased phosphorylation of the PDII region of the E-selectin promoter, which in turn folds the promoter and recruits NF κ B to the promoter. In addition, WT and *lpxA*- bacteria may also induce increased HMG I(Y) binding to the E-selectin promoter. The mechanisms regulating HMG I(Y) are as yet unknown. There are no reports linking TLRs with HMG I(Y) upregulation or gene induction.

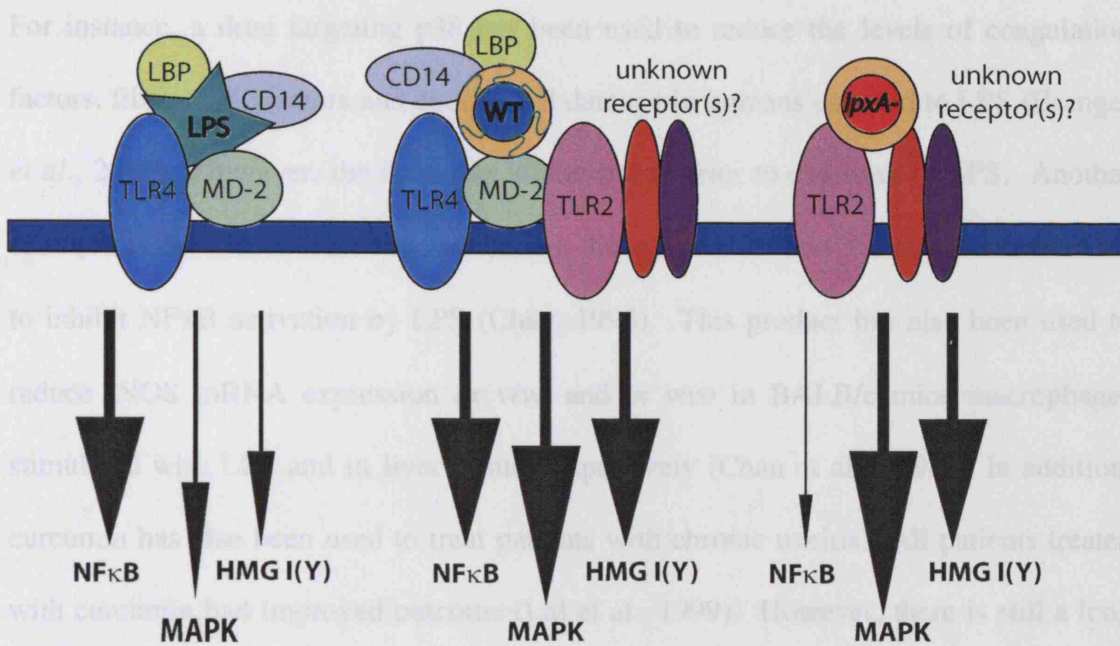


Figure 7.1 Model for differential signalling by *N. meningitidis* and LPS.

7.3 Future work

How can elucidating signalling cascades assist in improving disease outcome? By better understanding the mechanisms governing host responses, targeted drugs may be developed to improve patient outcome. For instance, if increased and prolonged E-selectin expression is contributing to the vast endothelial damage observed during FMS, and this is mediated through the NFκB and MAPK pathways, drugs could be developed to target these signalling cascades to reduce the production of E-selectin. If increased and prolonged E-selectin expression is regulated by increase mRNA stability and glycosylation, drugs could be developed to reverse this process, and thereby return the host to homeostasis.

For instance, a drug targeting p38 has been used to reduce the levels of coagulation factors, fibrinolytic factors and endothelial damage in humans exposed to LPS (Branger *et al.*, 2003). However, the drug was administered prior to exposure to LPS. Another example is the use of curcumin, which is a dietary product and has been demonstrated to inhibit NF κ B activation by LPS (Chan, 1995). This product has also been used to reduce iNOS mRNA expression *ex vivo* and *in vivo* in BALB/c mice macrophages stimulated with LPS and in liver tissue, respectively (Chan *et al.*, 1998). In addition, curcumin has also been used to treat patients with chronic uveitis. All patients treated with curcumin had improved outcome (Lal *et al.*, 1999). However, there is still a long way to go before signalling cascade blockers will become effective drugs to treat disease, partly due to the rapid manner in which the signalling cascades operate.

7.3 Future work

The work in this thesis has raised further questions. There are several areas in which the work has moved to, involving both molecular and cell biology.

7.3.1 The induction of the MAPK signalling pathway and HMG I(Y) by *N. meningitidis*

Firstly, do meningococci signal through the MAPK pathway? And if so, which pathways does it activate? There are two methods which will be used to study this process. Firstly, western blot analysis will be used to investigate the MAPK pathway,

particularly looking at the activation of p38, JNK, and ERK. Secondly, there are inhibitors which block these signalling molecules. These will be used to study their effects on meningococcal induced adhesion molecule expression on HUVEC.

HMG I(Y) upregulation can also be detected by Western blot analysis, and binding to promoter sequence can be determined by Electrophoretic Mobility Shift Assay (Rittig *et al.*, 2003).

7.3.2 Neutrophil binding to and transmigration across endothelial layers stimulated with meningococci and purified LPS

Another question that has arisen from this thesis is whether the differential expression pattern of E-selectin detected in response to meningococci and purified LPS has a downstream effect on leukocyte rolling, adherence and transmigration. This will be studied by using a flow system which allows purified leukocytes to roll over an endothelial monolayer. This can be video-taped and images taken to observe rolling, adherence patterns and transmigration of leukocytes across activated endothelium. Transmigration assays using a transwell system will also give insight into the role that meningococci-activated endothelium play in the transmigration of leukocytes, and may be correlated to what is seen *in vivo*. Endothelial damage induced by neutrophils on meningococci stimulated endothelium could also be investigated.

The use of the signalling pathway inhibitors in the flow and transmigration assays could also be used to study leukocyte-endothelial cell interactions. Some signalling inhibitors are currently going through clinical trials to see if they could be used to improve outcome in different diseases.

7.3.3 How is prolonged E-selectin expression maintained and regulated?

Currently, there is widespread understanding of how genes are regulated through promoters, enhancers, transcription factors, and the signalling pathways leading to gene transcription. However, very little is known about the mechanisms regulating mRNA stability. Work shown in this thesis has demonstrated that WT and *lpxA*-meningococci are able to induce prolonged E-selectin expression, and WT bacteria were shown to maintain elevated E-selectin expression levels for longer than 24 hours after infection. E-selectin expression normally returns to baseline levels by 24 hours. Endothelial infections with meningococci may be used as a model for exploring mechanisms regulating mRNA stability, and may shed light on widespread and specific mechanisms regulating this.

7.4 Concluding Remarks

In conclusion, there appears to be LPS independent mechanisms regulating E-selectin expression induced by meningococci. However, further work is required to fully

understand these processes. In addition, it will be necessary to establish whether differential E-selectin expression may affect the rolling, adhesion and transmigration of neutrophils. By further understanding these processes, future drug therapies may be targeted to reduce the effects induced by meningococci during sepsis. Furthermore, the processes elucidated with this model may give insight to the processes occurring during sepsis in general, thereby allowing for future drugs to be used in the treatment of sepsis induced by a wide range of stimuli and traumas.

References

1. Albelda, S.M., W.A.Muller, C.A.Buck, and P.J.Newman. 1991. Molecular and cellular properties of PECAM-1 (endoCAM/CD31): a novel vascular cell-cell adhesion molecule. *J. Cell Biol.* 114:1059-1068.
2. Albiger, B., L.Johansson, and A.B.Jonsson. 2003. Lipooligosaccharide-deficient *Neisseria meningitidis* shows altered pilus-associated characteristics. *Infect. Immun.* 71:155-162.
3. Amaral, A., S.M.Opal, and J.L.Vincent. 2004. Coagulation in sepsis. *Intensive Care Med.* 30:1032-1040.
4. Andersen, S.R., G.Bjune, J.Lyngby, K.Bryn, and E.Jantzen. 1995. Short-chain lipopolysaccharide mutants of serogroup B *Neisseria meningitidis* of potential value for production of outer membrane vesicle vaccines. *Microb. Pathog.* 19:159-168.
5. Arbour, N.C., E.Lorenz, B.C.Schutte, J.Zabner, J.N.Kline, M.Jones, K.Frees, J.L.Watt, and D.A.Schwartz. 2000. TLR4 mutations are associated with endotoxin hyporesponsiveness in humans. *Nat. Genet.* 25:187-191.
6. Asehnoune, K., D.Strassheim, S.Mitra, K.J.Yeol, and E.Abraham. 2005. Involvement of PKC α / β in TLR4 and TLR2 dependent activation of NF- κ B. *Cell Signal.* 17:385-394.
7. Bachetti, T. and L.Morbidelli. 2000. Endothelial cells in culture: a model for studying vascular functions. *Pharmacol. Res.* 42:9-19.

8. Baeuerle, P.A. 1998. IkappaB-NF-kappaB structures: at the interface of inflammation control. *Cell* 95:729-731.
9. Baines, P.B. and C.A.Hart. 2003. Severe meningococcal disease in childhood. *Br. J. Anaesth.* 90:72-83.
10. Baltathakis, I., O.Alcantara, and D.H.Boldt. 2001. Expression of different NF-kappaB pathway genes in dendritic cells (DCs) or macrophages assessed by gene expression profiling. *J. Cell Biochem.* 83:281-290.
11. Banerjee, A., R.Wang, S.N.Uljon, P.A.Rice, E.C.Gotschlich, and D.C.Stein. 1998. Identification of the gene (lgtG) encoding the lipooligosaccharide beta chain synthesizing glucosyl transferase from *Neisseria gonorrhoeae*. *Proc. Natl. Acad. Sci. U. S. A* 95:10872-10877.
12. Bannerman, D.D. and S.E.Goldblum. 1999. Direct effects of endotoxin on the endothelium: barrier function and injury. *Lab Invest* 79:1181-1199.
13. Bannerman, D.D. and S.E.Goldblum. 2003. Mechanisms of bacterial lipopolysaccharide-induced endothelial apoptosis. *Am. J. Physiol Lung Cell Mol. Physiol* 284:L899-L914.
14. Barr, R.K. and M.A.Bogoyevitch. 2001. The c-Jun N-terminal protein kinase family of mitogen-activated protein kinases (JNK MAPKs). *Int. J. Biochem. Cell Biol.* 33:1047-1063.
15. Becker-Andre, M., v.H.Hooft, C.Losberger, J.Whelan, and J.F.DeLamarter. 1992. Murine endothelial leukocyte-adhesion molecule 1 is a close structural and functional homologue of the human protein. *Eur. J. Biochem.* 206:401-411.

16. Berrington, A.W., Y.C.Tan, Y.Srikhanta, B.Kuipers, L.P.van der, I.R.Peak, and M.P.Jennings. 2002. Phase variation in meningococcal lipooligosaccharide biosynthesis genes. *FEMS Immunol. Med. Microbiol.* 34:267-275.
17. Berti, R., A.J.Williams, J.R.Moffett, S.L.Hale, L.C.Velarde, P.J.Elliott, C.Yao, J.R.Dave, and F.C.Tortella. 2002. Quantitative real-time RT-PCR analysis of inflammatory gene expression associated with ischemia-reperfusion brain injury. *J. Cereb. Blood Flow Metab* 22:1068-1079.
18. Beutler, B. 2000. Tlr4: central component of the sole mammalian LPS sensor. *Curr. Opin. Immunol* 12:20-26.
19. Beutler, B., K.Hoebe, X.Du, and R.J.Ulevitch. 2003. How we detect microbes and respond to them: the Toll-like receptors and their transducers. *J. Leukoc. Biol.* 74:479-485.
20. Bevilacqua, M.P., S.Stengelin, M.A.Gimbrone, Jr., and B.Seed. 1989. Endothelial leukocyte adhesion molecule 1: an inducible receptor for neutrophils related to complement regulatory proteins and lectins. *Science* 243:1160-1165.
21. Bhatia, P., W.R.Taylor, A.H.Greenberg, and J.A.Wright. 1994. Comparison of glyceraldehyde-3-phosphate dehydrogenase and 28S-ribosomal RNA gene expression as RNA loading controls for northern blot analysis of cell lines of varying malignant potential. *Anal. Biochem.* 216:223-226.
22. Bicknell, R. 1996. Endothelial Cell Culture. Cambridge University Press, Cambridge. 1-136 pp.
23. Bischoff, J. and C.Brasel. 1995. Regulation of P-selectin by tumor necrosis factor-alpha. *Biochem. Biophys. Res. Commun.* 210:174-180.

24. Bjerre, A., B.Brusletto, T.E.Mollnes, E.Fritzsønn, E.Rosenqvist, E.Wedeg, E.Namork, P.Kierulf, and P.Brandtzaeg. 2002. Complement activation induced by purified *Neisseria meningitidis* lipopolysaccharide (LPS), outer membrane vesicles, whole bacteria, and an LPS-free mutant. *J. Infect. Dis.* 185:220-228.
25. Blaschke, V., K.Reich, S.Blaschke, S.Zipprich, and C.Neumann. 2000. Rapid quantitation of proinflammatory and chemoattractant cytokine expression in small tissue samples and monocyte-derived dendritic cells: validation of a new real-time RT-PCR technology. *J. Immunol. Methods* 246:79-90.
26. Brandtzaeg P. 1995. Pathogenesis of Meningococcal Infections. In *Meningococcal Disease*. Cartwright K, editor. John Wiley & Sons Ltd, West Sussex. 71-114.
27. Brandtzaeg, P., P.Kierulf, P.Gaustad, A.Skulberg, J.N.Bruun, S.Halvorsen, and E.Sorensen. 1989. Plasma endotoxin as a predictor of multiple organ failure and death in systemic meningococcal disease. *J. Infect. Dis.* 159:195-204.
28. Branger, J., B.B.Van Den, S.Weijer, A.Gupta, S.J.van Deventer, C.E.Hack, M.P.Peppelenbosch, and P.T.van der. 2003. Inhibition of coagulation, fibrinolysis, and endothelial cell activation by a p38 mitogen-activated protein kinase inhibitor during human endotoxemia. *Blood* 101:4446-4448.
29. Bratt, J. and J.Palmblad. 1997. Cytokine-induced neutrophil-mediated injury of human endothelial cells. *J Immunol* 159:912-918.
30. Braun, J.M., C.C.Blackwell, I.R.Poxton, O.E.Ahmer, A.E.Gordon, O.M.Madani, D.M.Weir, S.Giersen, and J.Beuth. 2002. Proinflammatory Responses to Lipooligosaccharide of *Neisseria meningitidis* Immunotype Strains in Relation to Virulence and Disease. *J. Infect. Dis.* 185:1431-1438.

31. Brickman, J.M., M.Adam, and M.Ptashne. 1999. Interactions between an HMG-1 protein and members of the Rel family. *Proc. Natl. Acad. Sci. U. S. A* 96:10679-10683.
32. Brostjan, C., J.Anrather, V.Csizmadia, G.Natarajan, and H.Winkler. 1997. Glucocorticoids inhibit E-selectin expression by targeting NF-kappaB and not ATF/c-Jun. *J. Immunol.* 158:3836-3844.
33. Bustin, S.A. 2000. Absolute quantification of mRNA using real-time reverse transcription polymerase chain reaction assays. *J. Mol. Endocrinol.* 25:169-193.
34. Cao, W., S.H.Lee, and J.Lu. 2005. CD83 is preformed inside monocytes, macrophages and dendritic cells, but it is only stably expressed on activated dendritic cells. *Biochem. J.* 385:85-93.
35. Carlos, T.M. and J.M.Harlan. 1994. Leukocyte-endothelial adhesion molecules. *Blood* 84:2068-2101.
36. Caroff, M., D.Karibian, J.M.Cavaillon, and N.Haeflner-Cavaillon. 2002. Structural and functional analyses of bacterial lipopolysaccharides. *Microbes. Infect.* 4:915-926.
37. Cartwright K. 1995. Introduction and Historical Aspects. *In Meningococcal Disease.* Cartwright K, editor. John Wiley & Sons Ltd, West Sussex. 1-19.
38. Caugant, D.A., E.A.Hoiby, E.Rosenqvist, L.O.Froholm, and R.K.Selander. 1992. Transmission of *Neisseria meningitidis* among asymptomatic military recruits and antibody analysis. *Epidemiol. Infect.* 109:241-253.

39. Chan, M.M. 1995. Inhibition of tumor necrosis factor by curcumin, a phytochemical. *Biochem. Pharmacol.* 49:1551-1556.
40. Chan, M.M., H.I.Huang, M.R.Fenton, and D.Fong. 1998. In vivo inhibition of nitric oxide synthase gene expression by curcumin, a cancer preventive natural product with anti-inflammatory properties. *Biochem. Pharmacol.* 55:1955-1962.
41. Chang, Y.J., M.J.Holtzman, and C.C.Chen. 2002. Interferon-gamma-induced epithelial ICAM-1 expression and monocyte adhesion. Involvement of protein kinase C-dependent c-Src tyrosine kinase activation pathway. *J. Biol. Chem.* 277:7118-7126.
42. Che, W., N.Lerner-Marmarosh, Q.Huang, M.Osawa, S.Ohta, M.Yoshizumi, M.Glassman, J.D.Lee, C.Yan, B.C.Berk, and J.Abe. 2002. Insulin-like growth factor-1 enhances inflammatory responses in endothelial cells: role of Gab1 and MEKK3 in TNF-alpha-induced c-Jun and NF-kappaB activation and adhesion molecule expression. *Circ. Res.* 90:1222-1230.
43. Chen, C.C., M.P.Chow, W.C.Huang, Y.C.Lin, and Y.J.Chang. 2004a. Flavonoids inhibit tumor necrosis factor-alpha-induced up-regulation of intercellular adhesion molecule-1 (ICAM-1) in respiratory epithelial cells through activator protein-1 and nuclear factor-kappaB: structure-activity relationships. *Mol. Pharmacol.* 66:683-693.
44. Chen, C.Y., F.Gatto-Konczak, Z.Wu, and M.Karin. 1998. Stabilization of interleukin-2 mRNA by the c-Jun NH2-terminal kinase pathway. *Science* 280:1945-1949.
45. Chen, C.Y., R.Gherzi, J.S.Andersen, G.Gaietta, K.Jurchott, H.D.Royer, M.Mann, and M.Karin. 2000. Nucleolin and YB-1 are required for JNK-

- mediated interleukin-2 mRNA stabilization during T-cell activation. *Genes Dev.* 14:1236-1248.
46. Chen, L., O.Martinez, L.Overbergh, C.Mathieu, B.S.Prabhakar, and L.S.Chan. 2004b. Early up-regulation of Th2 cytokines and late surge of Th1 cytokines in an atopic dermatitis model. *Clin. Exp. Immunol.* 138:375-387.
 47. Chen, W.Y., E.C.Bailey, S.L.McCune, J.Y.Dong, and T.M.Townes. 1997. Reactivation of silenced, virally transduced genes by inhibitors of histone deacetylase. *Proc. Natl. Acad. Sci. U. S. A* 94:5798-5803.
 48. Chiao, P.J., S.Miyamoto, and I.M.Verma. 1994. Autoregulation of I kappa B alpha activity. *Proc. Natl. Acad. Sci. U. S. A* 91:28-32.
 49. Chintalacharuvu, S.R. and S.N.Emancipator. 1997. The glycosylation of IgA produced by murine B cells is altered by Th2 cytokines. *J. Immunol.* 159:2327-2333.
 50. Chow, J.C., D.W.Young, D.T.Golenbock, W.J.Christ, and F.Gusovsky. 1999. Toll-like receptor-4 mediates lipopolysaccharide-induced signal transduction. *J. Biol. Chem.* 274:10689-10692.
 51. Chu, W., D.H.Presky, R.A.Swerlick, and D.K.Burns. 1994. Alternatively processed human E-selectin transcripts linked to chronic expression of E-selectin in vivo. *J. Immunol.* 153:4179-4189.
 52. Clementz, T., J.J.Bednarski, and C.R.Raetz. 1996. Function of the htrB high temperature requirement gene of *Escherichia coli* in the acylation of lipid A: HtrB catalyzed incorporation of laurate. *J. Biol. Chem.* 271:12095-12102.

53. Clementz, T., Z.Zhou, and C.R.Raetz. 1997. Function of the *Escherichia coli* msbB gene, a multicopy suppressor of htrB knockouts, in the acylation of lipid A. Acylation by MsbB follows laurate incorporation by HtrB. *J. Biol. Chem.* 272:10353-10360.
54. Coleman, J. and C.R.Raetz. 1988. First committed step of lipid A biosynthesis in *Escherichia coli*: sequence of the lpxA gene. *J. Bacteriol.* 170:1268-1274.
55. Collas, P. 1998. Modulation of plasmid DNA methylation and expression in zebrafish embryos. *Nucleic Acids Res.* 26:4454-4461.
56. Collins, T., M.A.Read, A.S.Neish, M.Z.Whitley, D.Thanos, and T.Maniatis. 1995. Transcriptional regulation of endothelial cell adhesion molecules: NF-kappa B and cytokine-inducible enhancers. *FASEB J.* 9:899-909.
57. Collins, T., A.Williams, G.I.Johnston, J.Kim, R.Eddy, T.Shows, M.A.Gimbrone, Jr., and M.P.Bevilacqua. 1991. Structure and chromosomal location of the gene for endothelial- leukocyte adhesion molecule 1. *J. Biol. Chem.* 266:2466-2473.
58. Colombo, M.G., L.Citti, G.Basta, R.De Caterina, A.Biagini, and G.Rainaldi. 2001. Differential ability of human endothelial cells to internalize and express exogenous DNA. *Cardiovasc. Drugs Ther.* 15:25-29.
59. Coonrod, A., F.Q.Li, and M.Horwitz. 1997. On the mechanism of DNA transfection: efficient gene transfer without viruses. *Gene Ther.* 4:1313-1321.
60. Cota-Gomez, A., N.C.Flores, C.Cruz, A.Casullo, T.Y.Aw, H.Ichikawa, J.Schaack, R.Scheinman, and S.C.Flores. 2002. The human immunodeficiency virus-1 Tat protein activates human umbilical vein endothelial cell E-selectin

- expression via an NF-kappa B- dependent mechanism. *J. Biol. Chem.* 277:14390-14399.
61. Cousens, L.S., D.Gallwitz, and B.M.Alberts. 1979. Different accessibilities in chromatin to histone acetylase. *J. Biol. Chem.* 254:1716-1723.
 62. Cuisset, L., L.Tichonicky, P.Jaffray, and M.Delpech. 1997. The effects of sodium butyrate on transcription are mediated through activation of a protein phosphatase. *J. Biol. Chem.* 272:24148-24153.
 63. Cybulsky, M.I., J.W.Fries, A.J.Williams, P.Sultan, R.Eddy, M.Byers, T.Shows, M.A.Gimbrone, Jr., and T.Collins. 1991. Gene structure, chromosomal location, and basis for alternative mRNA splicing of the human VCAM1 gene. *Proc. Natl. Acad. Sci. U. S. A* 88:7859-7863.
 64. Czermin, B. and A.Imhof. 2003. The sounds of silence--histone deacetylation meets histone methylation. *Genetica* 117:159-164.
 65. de Kleijn, E.D., J.A.Hazelzet, R.F.Kornelisse, and R.de Groot. 1998. Pathophysiology of meningococcal sepsis in children. *Eur. J. Pediatr.* 157:869-880.
 66. De Luca, L.G., D.R.Johnson, M.Z.Whitley, T.Collins, and J.S.Pober. 1994. cAMP and tumor necrosis factor competitively regulate transcriptional activation through and nuclear factor binding to the cAMP-responsive element/activating transcription factor element of the endothelial leukocyte adhesion molecule-1 (E-selectin) promoter. *J Biol Chem.* 269:19193-19196.

67. de Vries, F.P., E.A.van Der, J.P.van Putten, and J.Dankert. 1996. Invasion of primary nasopharyngeal epithelial cells by *Neisseria meningitidis* is controlled by phase variation of multiple surface antigens. *Infect. Immun.* 64:2998-3006.
68. De Wals, P. and A.Bouckaert. 1985. Methods for estimating the duration of bacterial carriage. *Int. J. Epidemiol.* 14:628-634.
69. Dehio, C., S.D.Gray-Owen, and T.F.Meyer. 1998. The role of neisserial Opa proteins in interactions with host cells. *Trends Microbiol.* 6:489-495.
70. Derrick, J.P., R.Urwin, J.Suker, I.M.Feavers, and M.C.Maiden. 1999. Structural and evolutionary inference from molecular variation in *Neisseria* porins. *Infect. Immun.* 67:2406-2413.
71. Devyatyarova-Johnson, M., I.H.Rees, B.D.Robertson, M.W.Turner, N.J.Klein, and D.L.Jack. 2000. The lipopolysaccharide structures of *Salmonella enterica* serovar Typhimurium and *Neisseria gonorrhoeae* determine the attachment of human mannose-binding lectin to intact organisms. *Infect. Immun.* 68:3894-3899.
72. DiDonato, J.A., M.Hayakawa, D.M.Rothwarf, E.Zandi, and M.Karin. 1997. A cytokine-responsive I κ B kinase that activates the transcription factor NF- κ B. *Nature* 388:548-554.
73. Dietrich, J.B. 2002. The adhesion molecule ICAM-1 and its regulation in relation with the blood-brain barrier. *J. Neuroimmunol.* 128:58-68.
74. Dion, L.D., K.T.Goldsmith, D.C.Tang, J.A.Engler, M.Yoshida, and R.I.Garver, Jr. 1997. Amplification of recombinant adenoviral transgene products occurs by inhibition of histone deacetylase. *Virology* 231:201-209.

75. Dixon, G.L., R.S.Heyderman, K.Kotovicz, D.L.Jack, S.R.Andersen, U.Vogel, M.Frosch, and N.Klein. 1999. Endothelial adhesion molecule expression and its inhibition by recombinant bactericidal/permeability-increasing protein are influenced by the capsulation and lipooligosaccharide structure of *Neisseria meningitidis*. *Infect. Immun.* 67:5626-5633.
76. Dixon, G.L., R.S.Heyderman, L.P.van der, and N.J.Klein. 2004. High-level endothelial E-selectin (CD62E) cell adhesion molecule expression by a lipopolysaccharide-deficient strain of *Neisseria meningitidis* despite poor activation of NF-kappaB transcription factor. *Clin. Exp. Immunol.* 135:85-93.
77. Dixon, G.L., P.J.Newton, B.M.Chain, D.Katz, S.R.Andersen, S.Wong, L.P.van der, N.Klein, and R.E.Callard. 2001. Dendritic cell activation and cytokine production induced by group B *Neisseria meningitidis*: interleukin-12 production depends on lipopolysaccharide expression in intact bacteria. *Infect. Immun.* 69:4351-4357.
78. Dong, C., R.J.Davis, and R.A.Flavell. 2002. MAP kinases in the immune response. *Annu. Rev. Immunol.* 20:55-72.
79. Doukas, J. and J.S.Pober. 1990. IFN-gamma enhances endothelial activation induced by tumor necrosis factor but not IL-1. *J. Immunol.* 145:1727-1733.
80. Drogari-Apiranthitou, M., E.J.Kuijper, N.Dekker, and J.Dankert. 2002. Complement activation and formation of the membrane attack complex on serogroup B *Neisseria meningitidis* in the presence or absence of serum bactericidal activity. *Infect. Immun.* 70:3752-3758.

81. Du, W. and T.Maniatis. 1994. The high mobility group protein HMG I(Y) can stimulate or inhibit DNA binding of distinct transcription factor ATF-2 isoforms. *Proc. Natl. Acad. Sci. U. S. A* 91:11318-11322.
82. Duensing, T.D. and J.P.van Putten. 1997. Vitronectin mediates internalization of *Neisseria gonorrhoeae* by Chinese hamster ovary cells. *Infect. Immun.* 65:964-970.
83. Dunn, K.L., M.Virji, and E.R.Moxon. 1995. Investigations into the molecular basis of meningococcal toxicity for human endothelial and epithelial cells: the synergistic effect of LPS and pili. *Microb. Pathog.* 18:81-96.
84. Dunoyer-Geindre, S., P.de Moerloose, B.Galve-de Rochemonteix, G.Reber, and E.K.Kruithof. 2002. NFkappaB is an essential intermediate in the activation of endothelial cells by anti-beta(2)-glycoprotein 1 antibodies. *Thromb. Haemost.* 88:851-857.
85. Dunzendorfer, S., H.K.Lee, K.Soldau, and P.S.Tobias. 2004. Toll-like receptor 4 functions intracellularly in human coronary artery endothelial cells: roles of LBP and sCD14 in mediating LPS responses. *FASEB J.* 18:1117-1119.
86. Dustin, M.L., R.Rothlein, A.K.Bhan, C.A.Dinarello, and T.A.Springer. 1986. Induction by IL 1 and interferon-gamma: tissue distribution, biochemistry, and function of a natural adherence molecule (ICAM-1). *J. Immunol.* 137:245-254.
87. Duval, M., S.Bedard-Goulet, C.Delisle, and J.P.Gratton. 2003. Vascular endothelial growth factor-dependent down-regulation of Flk-1/KDR involves Cbl-mediated ubiquitination. Consequences on nitric oxide production from endothelial cells. *J. Biol. Chem.* 278:20091-20097.

88. Ear, T., P.Giguere, A.Fleury, J.Stankova, M.D.Payet, and G.Dupuis. 2001. High efficiency transient transfection of genes in human umbilical vein endothelial cells by electroporation. *J. Immunol. Methods* 257:41-49.
89. Erridge, C., E.Bennett-Guerrero, and I.R.Poxton. 2002. Structure and function of lipopolysaccharides. *Microbes. Infect.* 4:837-851.
90. Erridge, C., J.Stewart, and I.R.Poxton. 2003. Monocytes heterozygous for the Asp299Gly and Thr399Ile mutations in the Toll-like receptor 4 gene show no deficit in lipopolysaccharide signalling. *J. Exp. Med.* 197:1787-1791.
91. Esmon, C.T. 2004. The impact of the inflammatory response on coagulation. *Thromb. Res.* 114:321-327.
92. Etter, H., R.Althaus, H.P.Eugster, L.F.Santamaria-Babi, L.Weber, and R.Moser. 1998. IL-4 and IL-13 downregulate rolling adhesion of leukocytes to IL-1 or TNF-alpha-activated endothelial cells by limiting the interval of E- selectin expression. *Cytokine* 10:395-403.
93. Etzioni, A., C.M.Doerschuk, and J.M.Harlan. 1999. Of man and mouse: leukocyte and endothelial adhesion molecule deficiencies. *Blood* 94:3281-3288.
94. Eugene, E., I.Hoffmann, C.Pujol, P.O.Couraud, S.Bourdoulous, and X.Nassif. 2002. Microvilli-like structures are associated with the internalization of virulent capsulated *Neisseria meningitidis* into vascular endothelial cells. *J. Cell Sci.* 115:1231-1241.
95. Everts, M., S.A.Asgeirsdottir, R.J.Kok, J.Twisk, B.de Vries, E.Lubberts, E.J.Bos, N.Werner, D.K.Meijer, and G.Molema. 2003. Comparison of E-selectin

- expression at mRNA and protein levels in murine models of inflammation. *Inflamm. Res.* 52:512-518.
96. Falvo, J.V., D.Thanos, and T.Maniatis. 1995. Reversal of intrinsic DNA bends in the IFN beta gene enhancer by transcription factors and the architectural protein HMG I(Y). *Cell* 83:1101-1111.
 97. Faure, E., O.Equils, P.A.Sieling, L.Thomas, F.X.Zhang, C.J.Kirschning, N.Polentarutti, M.Muzio, and M.Arditi. 2000. Bacterial lipopolysaccharide activates NF-kappaB through toll-like receptor 4 (TLR-4) in cultured human dermal endothelial cells. Differential expression of TLR-4 and TLR-2 in endothelial cells. *J Biol Chem.* 275:11058-11063.
 98. Faust, S.N., R.S.Heyderman, and M.Levin. 2001a. Coagulation in severe sepsis: a central role for thrombomodulin and activated protein C. *Crit Care Med.* 29:S62-S67.
 99. Faust, S.N., M.Levin, O.B.Harrison, R.D.Goldin, M.S.Lockhart, S.Kondaveeti, Z.Laszik, C.T.Esmon, and R.S.Heyderman. 2001b. Dysfunction of endothelial protein C activation in severe meningococcal sepsis. *N. Engl. J. Med.* 345:408-416.
 100. Fife, K., M.Bower, R.G.Cooper, L.Stewart, C.J.Etheridge, R.C.Coombes, L.Buluwela, and A.D.Miller. 1998. Endothelial cell transfection with cationic liposomes and herpes simplex-thymidine kinase mediated killing. *Gene Ther.* 5:614-620.
 101. Fitzgerald, K.A., D.C.Rowe, B.J.Barnes, D.R.Caffrey, A.Visintin, E.Latz, B.Monks, P.M.Pitha, and D.T.Golenbock. 2003. LPS-TLR4 signaling to IRF-3/7

- and NF-kappaB involves the toll adapters TRAM and TRIF. *J. Exp. Med.* 198:1043-1055.
102. Frist, S.T., H.A.Taylor, Jr., K.A.Kirk, J.R.Grammer, X.N.Li, H.E.Grenett, and F.M.Booyse. 1995. Expression of PAI-1, t-PA and u-PA in cultured human umbilical vein endothelial cells derived from racial groups. *Thromb. Res.* 77:279-290.
 103. Fuhrmann, O., M.Arvand, A.Gohler, M.Schmid, M.Krull, S.Hippenstiel, J.Seybold, C.DeHio, and N.Suttorp. 2001. Bartonella henselae induces NF-kappaB-dependent upregulation of adhesion molecules in cultured human endothelial cells: possible role of outer membrane proteins as pathogenic factors. *Infect. Immun.* 69:5088-5097.
 104. Furst-Ladani, S., H.Redl, A.Haslberger, W.Lubitz, P.Messner, U.B.Sleytr, and G.Schlag. 1999. Bacterial cell envelopes (ghosts) but not S-layers activate human endothelial cells (HUVECs) through sCD14 and LBP mechanism. *Vaccine* 18:440-448.
 105. Gamble, J.R., Y.Khew-Goodall, and M.A.Vadas. 1993. Transforming growth factor-beta inhibits E-selectin expression on human endothelial cells. *J. Immunol.* 150:4494-4503.
 106. Garcia, J.G., F.Liu, A.D.Verin, A.Birukova, M.A.Deichert, W.T.Gerthoffer, J.R.Bamberg, and D.English. 2001. Sphingosine 1-phosphate promotes endothelial cell barrier integrity by Edg-dependent cytoskeletal rearrangement. *J. Clin. Invest* 108:689-701.

107. Garrett, T.A., J.L.Kadmas, and C.R.Raetz. 1997. Identification of the gene encoding the Escherichia coli lipid A 4'- kinase. Facile phosphorylation of endotoxin analogs with recombinant LpxK. *J. Biol. Chem.* 272:21855-21864.
108. Gaynor, R.B., M.D.Kuwabara, F.K.Wu, J.A.Garcia, D.Harrich, M.Briskin, R.Wall, and D.S.Sigman. 1988. Repeated B motifs in the human immunodeficiency virus type I long terminal repeat enhancer region do not exhibit cooperative factor binding. *Proc. Natl. Acad. Sci. U. S. A* 85:9406-9410.
109. Gearing, A.J. and W.Newman. 1993. Circulating adhesion molecules in disease. *Immunol. Today* 14:506-512.
110. Ghera, P., v.H.Hooft, J.Whelan, and J.F.DeLamarter. 1992. Labile proteins play a dual role in the control of endothelial leukocyte adhesion molecule-1 (ELAM-1) gene regulation. *J. Biol. Chem.* 267:19226-19232.
111. Ghosh, S. and M.Karin. 2002. Missing pieces in the NF-kappaB puzzle. *Cell* 109 Suppl:S81-S96.
112. Giulietti, A., L.Overbergh, D.Valckx, B.Decallonne, R.Bouillon, and C.Mathieu. 2001. An overview of real-time quantitative PCR: applications to quantify cytokine gene expression. *Methods* 25:386-401.
113. Guha, M. and N.Mackman. 2001. LPS induction of gene expression in human monocytes. *Cell Signal.* 13:85-94.
114. Guhaniyogi, J. and G.Brewer. 2001. Regulation of mRNA stability in mammalian cells. *Gene* 265:11-23.

115. Gupta, B. and B.Ghosh. 1999. Curcuma longa inhibits TNF-alpha induced expression of adhesion molecules on human umbilical vein endothelial cells. *Int. J. Immunopharmacol.* 21:745-757.
116. Hackett, S.J., M.Guiver, J.Marsh, J.A.Sills, A.P.Thomson, E.B.Kaczmariski, and C.A.Hart. 2002. Meningococcal bacterial DNA load at presentation correlates with disease severity. *Arch. Dis. Child* 86:44-46.
117. Hackett, S.J., A.P.Thomson, and C.A.Hart. 2001. Cytokines, chemokines and other effector molecules involved in meningococcal disease. *J. Med. Microbiol.* 50:847-859.
118. Hamann, L., C.Stamme, A.J.Ulmer, and R.R.Schumann. 2002. Inhibition of LPS-induced activation of alveolar macrophages by high concentrations of LPS-binding protein. *Biochem. Biophys. Res. Commun.* 295:553-560.
119. Hammerschmidt, S., R.Hilse, J.P.van Putten, R.Gerardy-Schahn, A.Unkmeir, and M.Frosch. 1996a. Modulation of cell surface sialic acid expression in *Neisseria meningitidis* via a transposable genetic element. *EMBO J.* 15:192-198.
120. Hammerschmidt, S., A.Muller, H.Sillmann, M.Muhlenhoff, R.Borrow, A.Fox, J.van Putten, W.D.Zollinger, R.Gerardy-Schahn, and M.Frosch. 1996b. Capsule phase variation in *Neisseria meningitidis* serogroup B by slipped-strand mispairing in the polysialyltransferase gene (*siaD*): correlation with bacterial invasion and the outbreak of meningococcal disease. *Mol. Microbiol.* 20:1211-1220.
121. Han, J., J.D.Lee, L.Bibbs, and R.J.Ulevitch. 1994. A MAP kinase targeted by endotoxin and hyperosmolarity in mammalian cells. *Science* 265:808-811.

122. Harrison, O.B., B.D.Robertson, S.N.Faust, M.A.Jepson, R.D.Goldin, M.Levin, and R.S.Heyderman. 2002. Analysis of pathogen-host cell interactions in purpura fulminans: expression of capsule, type IV pili, and PorA by *Neisseria meningitidis* in vivo. *Infect. Immun.* 70:5193-5201.
123. Hart, S.L., C.V.Arancibia-Carcamo, M.A.Wolfert, C.Mailhos, N.J.O'Reilly, R.R.Ali, C.Coutelle, A.J.George, R.P.Harbottle, A.M.Knight, D.F.Larkin, R.J.Levinsky, L.W.Seymour, A.J.Thrasher, and C.Kinnon. 1998. Lipid-mediated enhancement of transfection by a nonviral integrin- targeting vector. *Hum. Gene Ther.* 9:575-585.
124. Hart, S.L., L.Collins, K.Gustafsson, and J.W.Fabre. 1997. Integrin-mediated transfection with peptides containing arginine- glycine-aspartic acid domains. *Gene Ther.* 4:1225-1230.
125. Hauser, I.A., D.R.Johnson, F.Thevenod, and M.Goppelt-Strube. 1997. Effect of mycophenolic acid on TNF alpha-induced expression of cell adhesion molecules in human venous endothelial cells in vitro. *Br. J. Pharmacol.* 122:1315-1322.
126. Heckels, J.E. 1989. Structure and function of pili of pathogenic *Neisseria* species. *Clin. Microbiol. Rev.* 2 Suppl:S66-S73.
127. Heid, C.A., J.Stevens, K.J.Livak, and P.M.Williams. 1996. Real time quantitative PCR. *Genome Res.* 6:986-994.
128. Hellewell, P.G. 1999. Adhesion molecule strategies. *Pulm. Pharmacol. Ther.* 12:137-141.
129. Henneke, P. and D.T.Golenbock. 2001. TIRAP: how Toll receptors fraternize. *Nat. Immunol.* 2:828-830.

130. Hermann, A., H.Gowher, and A.Jeltsch. 2004. Biochemistry and biology of mammalian DNA methyltransferases. *Cell Mol. Life Sci.* 61:2571-2587.
131. Hernandez, J.L., T.Coll, and C.J.Ciudad. 2004. A highly efficient electroporation method for the transfection of endothelial cells. *Angiogenesis.* 7:235-241.
132. Hertzog, T., M.Weber, L.Greifffenberg, B.S.Holthausen, W.Goebel, K.S.Kim, and M.Kuhn. 2003. Antibodies present in normal human serum inhibit invasion of human brain microvascular endothelial cells by *Listeria monocytogenes*. *Infect. Immun.* 71:95-100.
133. Heumann, D. 2001. CD14 and LBP in endotoxemia and infections caused by Gram-negative bacteria. *J. Endotoxin. Res.* 7:439-441.
134. Heyderman, R.S., C.A.Ison, M.Peakman, M.Levin, and N.J.Klein. 1999. Neutrophil response to *Neisseria meningitidis*: inhibition of adhesion molecule expression and phagocytosis by recombinant bactericidal/permeability-increasing protein (rBPI21). *J Infect. Dis.* 179:1288-1292.
135. Heyderman, R.S., N.J.Klein, O.A.Daramola, S.Hammerschmidt, M.Frosch, B.D.Robertson, M.Levin, and C.A.Ison. 1997. Induction of human endothelial tissue factor expression by *Neisseria meningitidis*: the influence of bacterial killing and adherence to the endothelium. *Microb. Pathog.* 22:265-274.
136. Hippenstiel, S., S.Soeth, B.Kellas, O.Fuhrmann, J.Seybold, M.Krull, C.Eichel-Streiber, M.Goebeler, S.Ludwig, and N.Suttorp. 2000. Rho proteins and the p38-MAPK pathway are important mediators for LPS- induced interleukin-8 expression in human endothelial cells. *Blood* 95:3044-3051.

137. Hoefen, R.J. and B.C.Berk. 2002. The role of MAP kinases in endothelial activation. *Vascul. Pharmacol.* 38:271-273.
138. Hoffmann, I., E.Eugene, X.Nassif, P.O.Couraud, and S.Bourdoulous. 2001. Activation of ErbB2 receptor tyrosine kinase supports invasion of endothelial cells by *Neisseria meningitidis*. *J. Cell Biol.* 155:133-143.
139. Holten, E. 1979. Serotypes of *Neisseria meningitidis* isolated from patients in Norway during the first six months of 1978. *J. Clin. Microbiol.* 9:186-188.
140. Hong, K., J.Sherley, and D.A.Lauffenburger. 2001. Methylation of episomal plasmids as a barrier to transient gene expression via a synthetic delivery vector. *Biomol. Eng* 18:185-192.
141. Hooft, v.H., J.Whelan, R.Pescini, M.Becker-Andre, A.M.Schenk, and J.F.DeLamar. 1992. A T-cell enhancer cooperates with NF-kappa B to yield cytokine induction of E-selectin gene transcription in endothelial cells. *J. Biol. Chem.* 267:22385-22391.
142. Horng, T., G.M.Barton, and R.Medzhitov. 2001. TIRAP: an adapter molecule in the Toll signaling pathway. *Nat. Immunol.* 2:835-841.
143. Hoshino, K., O.Takeuchi, T.Kawai, H.Sanjo, T.Ogawa, Y.Takeda, K.Takeda, and S.Akira. 1999. Cutting edge: Toll-like receptor 4 (TLR4)-deficient mice are hyporesponsive to lipopolysaccharide: evidence for TLR4 as the Lps gene product. *J Immunol* 162:3749-3752.
144. Hu, Y., J.M.Kiely, B.E.Szente, A.Rosenzweig, and M.A.Gimbrone, Jr. 2000. E-selectin-dependent signaling via the mitogen-activated protein kinase pathway in vascular endothelial cells. *J. Immunol.* 165:2142-2148.

145. Hu, Y., B.Szente, J.M.Kiely, and M.A.Gimbrone, Jr. 2001. Molecular events in transmembrane signaling via E-selectin. SHP2 association, adaptor protein complex formation and ERK1/2 activation. *J. Biol. Chem.* 276:48549-48553.
146. Hunt, B.J. and K.M.Jurd. 1997. Relation between endothelial-cell activation and infection, inflammation, and infarction. *Lancet* 350:293.
147. Imahara, S.D., S.Jelacic, C.E.Junker, and G.E.O'Keefe. 2005. The TLR4 +896 polymorphism is not associated with lipopolysaccharide hypo-responsiveness in leukocytes. *Genes Immun.* 6:37-43.
148. Ingalls, R.R., E.Lien, and D.T.Golenbock. 2001. Membrane-associated proteins of a lipopolysaccharide-deficient mutant of *Neisseria meningitidis* activate the inflammatory response through toll-like receptor 2. *Infect. Immun.* 69:2230-2236.
149. Ishii, H. and K.Takada. 2002. Bleomycin induces E-selectin expression in cultured umbilical vein endothelial cells by increasing its mRNA levels through activation of NF-kappaB/Rel. *Toxicol. Appl. Pharmacol.* 184:88-97.
150. Iversen, N., B.Birkenes, K.Torsdalen, and S.Djurovic. 2005. Electroporation by nucleofector is the best nonviral transfection technique in human endothelial and smooth muscle cells. *Genet. Vaccines. Ther.* 3:2.
151. Jack, D.L., A.W.Dodds, N.Anwar, C.A.Ison, A.Law, M.Frosch, M.W.Turner, and N.J.Klein. 1998. Activation of complement by mannose-binding lectin on isogenic mutants of *Neisseria meningitidis* serogroup B. *J Immunol* 160:1346-1353.

152. Jack, D.L., G.A.Jarvis, C.L.Booth, M.W.Turner, and N.J.Klein. 2001. Mannose-binding lectin accelerates complement activation and increases serum killing of *Neisseria meningitidis* serogroup C. *J. Infect. Dis.* 184:836-845.
153. Jenkins, R.G., S.E.Herrick, Q.H.Meng, C.Kinnon, G.J.Laurent, R.J.McAnulty, and S.L.Hart. 2000. An integrin-targeted non-viral vector for pulmonary gene therapy. *Gene Ther.* 7:393-400.
154. Jennings, M.P., M.Bisercic, K.L.Dunn, M.Virji, A.Martin, K.E.Wilks, J.C.Richards, and E.R.Moxon. 1995. Cloning and molecular analysis of the *Isi1* (*rfaF*) gene of *Neisseria meningitidis* which encodes a heptosyl-2-transferase involved in LPS biosynthesis: evaluation of surface exposed carbohydrates in LPS mediated toxicity for human endothelial cells. *Microb. Pathog.* 19:391-407.
155. Jersmann, H.P., C.S.Hii, J.V.Ferrante, and A.Ferrante. 2001a. Bacterial lipopolysaccharide and tumor necrosis factor alpha synergistically increase expression of human endothelial adhesion molecules through activation of NF-kappaB and p38 mitogen-activated protein kinase signaling pathways. *Infect. Immun.* 69:1273-1279.
156. Jersmann, H.P., C.S.Hii, G.L.Hodge, and A.Ferrante. 2001b. Synthesis and surface expression of CD14 by human endothelial cells. *Infect. Immun.* 69:479-485.
157. Johansson, L., A.Rytönen, P.Bergman, B.Albiger, H.Kallstrom, T.Hokfelt, B.Agerberth, R.Cattaneo, and A.B.Jonsson. 2003. CD46 in meningococcal disease. *Science* 301:373-375.
158. John, S., R.B.Reeves, J.X.Lin, R.Child, J.M.Leiden, C.B.Thompson, and W.J.Leonard. 1995. Regulation of cell-type-specific interleukin-2 receptor

- alpha-chain gene expression: potential role of physical interactions between Elf-1, HMG-I(Y), and NF-kappa B family proteins. *Mol. Cell Biol.* 15:1786-1796.
159. Johnson, M.R., K.Wang, J.B.Smith, M.J.Heslin, and R.B.Diasio. 2000. Quantitation of dihydropyrimidine dehydrogenase expression by real-time reverse transcription polymerase chain reaction. *Anal. Biochem.* 278:175-184.
 160. Jones D. 1995. Epidemiology of Meningococcal Disease in Europe and the USA. In Meningococcal Disease. Cartwright K, editor. John Wiley & Sons Ltd, West Sussex. 147-157.
 161. Jones, D.M., R.Borrow, A.J.Fox, S.Gray, K.A.Cartwright, and J.T.Poolman. 1992. The lipooligosaccharide immunotype as a virulence determinant in *Neisseria meningitidis*. *Microb. Pathog.* 13:219-224.
 162. Kadl, A., J.Huber, F.Gruber, V.N.Bochkov, B.R.Binder, and N.Leitinger. 2002. Analysis of inflammatory gene induction by oxidized phospholipids in vivo by quantitative real-time RT-PCR in comparison with effects of LPS. *Vascul. Pharmacol.* 38:219-227.
 163. Kahler, C.M. and D.S.Stephens. 1998. Genetic basis for biosynthesis, structure, and function of meningococcal lipooligosaccharide (endotoxin). *Crit Rev. Microbiol.* 24:281-334.
 164. Kaiser, S. and M.Toborek. 2001. Liposome-mediated high-efficiency transfection of human endothelial cells. *J. Vasc. Res.* 38:133-143.
 165. Kallstrom, H., M.K.Liszewski, J.P.Atkinson, and A.B.Jonsson. 1997. Membrane cofactor protein (MCP or CD46) is a cellular pilus receptor for pathogenic *Neisseria*. *Mol. Microbiol.* 25:639-647.

166. Kang, J., J.Chen, D.Zhang, W.Da, and Y.Ou. 2004. Synergistic killing of human leukemia cells by antioxidants and trichostatin A. *Cancer Chemother. Pharmacol.* 54:537-545.
167. Kaszubska, W., v.H.Hooft, P.Ghersa, A.M.DeRaemy-Schenk, B.P.Chen, T.Hai, J.F.DeLamarter, and J.Whelan. 1993. Cyclic AMP-independent ATF family members interact with NF-kappa B and function in the activation of the E-selectin promoter in response to cytokines. *Mol. Cell Biol.* 13:7180-7190.
168. Kawai, T., O.Adachi, T.Ogawa, K.Takeda, and S.Akira. 1999. Unresponsiveness of MyD88-deficient mice to endotoxin. *Immunity.* 11:115-122.
169. Kellogg, D.E., I.Rybalkin, S.Chen, N.Mukhamedova, T.Vlasik, P.D.Siebert, and A.Chenchik. 1994. TaqStart Antibody: "hot start" PCR facilitated by a neutralizing monoclonal antibody directed against Taq DNA polymerase. *Biotechniques* 16:1134-1137.
170. Kerppola, T.K. and T.Curran. 1993. Selective DNA bending by a variety of bZIP proteins. *Mol. Cell Biol.* 13:5479-5489.
171. Kerr, J.R. 1999. Cell adhesion molecules in the pathogenesis of and host defence against microbial infection. *Mol. Pathol.* 52:220-230.
172. Kevil, C.G. and D.C.Bullard. 1999. Roles of leukocyte/endothelial cell adhesion molecules in the pathogenesis of vasculitis. *Am. J. Med.* 106:677-687.
173. Kiefer, K., J.Clement, P.Garidel, and R.Peschka-Suss. 2004. Transfection efficiency and cytotoxicity of nonviral gene transfer reagents in human smooth muscle and endothelial cells. *Pharm. Res.* 21:1009-1017.

174. Kiely, J.M., Y.Hu, G.Garcia-Cardena, and M.A.Gimbrone, Jr. 2003. Lipid raft localization of cell surface E-selectin is required for ligation-induced activation of phospholipase C gamma. *J. Immunol.* 171:3216-3224.
175. Kim, W.J., N.Terada, T.Nomura, R.Takahashi, S.D.Lee, J.H.Park, and A.Konno. 2002. Effect of formaldehyde on the expression of adhesion molecules in nasal microvascular endothelial cells: the role of formaldehyde in the pathogenesis of sick building syndrome. *Clin. Exp. Allergy* 32:287-295.
176. Kitazono, M., Y.Chuman, T.Aikou, and T.Fojo. 2001. Construction of gene therapy vectors targeting thyroid cells: enhancement of activity and specificity with histone deacetylase inhibitors and agents modulating the cyclic adenosine 3',5'- monophosphate pathway and demonstration of activity in follicular and anaplastic thyroid carcinoma cells. *J. Clin. Endocrinol. Metab* 86:834-840.
177. Klein, N.J., C.A.Ison, M.Peakman, M.Levin, S.Hammerschmidt, M.Frosch, and R.S.Heyderman. 1996. The influence of capsulation and lipooligosaccharide structure on neutrophil adhesion molecule expression and endothelial injury by *Neisseria meningitidis*. *J. Infect. Dis.* 173:172-179.
178. Klein, R.D., G.L.Su, C.Schmidt, A.Aminlari, L.Steinstraesser, W.H.Alarcon, H.Y.Zhang, and S.C.Wang. 2000. Lipopolysaccharide-binding protein accelerates and augments *Escherichia coli* phagocytosis by alveolar macrophages. *J. Surg. Res.* 94:159-166.
179. Klugman, K.P., E.C.Gotschlich, and M.S.Blake. 1989. Sequence of the structural gene (rmpM) for the class 4 outer membrane protein of *Neisseria meningitidis*, homology of the protein to gonococcal protein III and *Escherichia coli* OmpA, and construction of meningococcal strains that lack class 4 protein. *Infect. Immun.* 57:2066-2071.

180. Koivunen, E., B.Wang, and E.Ruoslahti. 1995. Phage libraries displaying cyclic peptides with different ring sizes: ligand specificities of the RGD-directed integrins. *Biotechnology (N. Y.)* 13:265-270.
181. Koomey, M. 2001. Implications of molecular contacts and signaling initiated by *Neisseria gonorrhoeae*. *Curr. Opin. Microbiol.* 4:53-57.
182. Kopp, E.B. and R.Medzhitov. 1999. The Toll-receptor family and control of innate immunity. *Curr. Opin. Immunol* 11:13-18.
183. Kotowicz, K., G.L.Dixon, N.J.Klein, M.J.Peters, and R.E.Callard. 2000. Biological function of CD40 on human endothelial cells: costimulation with CD40 ligand and interleukin-4 selectively induces expression of vascular cell adhesion molecule-1 and P-selectin resulting in preferential adhesion of lymphocytes. *Immunology* 100:441-448.
184. Kovala, A.T., K.A.Harvey, P.McGlynn, G.Boguslawski, J.G.Garcia, and D.English. 2000. High-efficiency transient transfection of endothelial cells for functional analysis. *FASEB J.* 14:2486-2494.
185. Kraiss, L.W., N.M.Alto, D.A.Dixon, T.M.McIntyre, A.S.Weyrich, and G.A.Zimmerman. 2003. Fluid flow regulates E-selectin protein levels in human endothelial cells by inhibiting translation. *J. Vasc. Surg.* 37:161-168.
186. Kuijpers, T.W., M.Raleigh, T.Kavanagh, H.Janssen, J.Calafat, D.Roos, and J.M.Harlan. 1994. Cytokine-activated endothelial cells internalize E-selectin into a lysosomal compartment of vesiculotubular shape. A tubulin-driven process. *J. Immunol.* 152:5060-5069.

187. Kurachi, K., K.Zhang, A.Ameri, J.Huo, H.Atoda, and S.Kurachi. 2000. Genetic and molecular mechanisms of age regulation (homeostasis) of blood coagulation. *IUBMB. Life* 49:189-196.
188. Lal, B., A.K.Kapoor, O.P.Asthana, P.K.Agrawal, R.Prasad, P.Kumar, and R.C.Srimal. 1999. Efficacy of curcumin in the management of chronic anterior uveitis. *Phytother. Res.* 13:318-322.
189. Larigan, J.D., T.C.Tsang, J.M.Rumberger, and D.K.Burns. 1992. Characterization of cDNA and genomic sequences encoding rabbit ELAM-1: conservation of structure and functional interactions with leukocytes. *DNA Cell Biol.* 11:149-162.
190. Le Roy, D., F.Di Padova, Y.Adachi, M.P.Glauser, T.Calandra, and D.Heumann. 2001. Critical role of lipopolysaccharide-binding protein and CD14 in immune responses against gram-negative bacteria. *J. Immunol.* 167:2759-2765.
191. Ledebur, H.C. and T.P.Parks. 1995. Transcriptional regulation of the intercellular adhesion molecule-1 gene by inflammatory cytokines in human endothelial cells. Essential roles of a variant NF-kappa B site and p65 homodimers. *J. Biol. Chem.* 270:933-943.
192. Lee, L.K., E.K.Siapati, R.G.Jenkins, R.J.McAnulty, S.L.Hart, and P.A.Shamlou. 2003. Biophysical characterization of an integrin-targeted non-viral vector. *Med. Sci. Monit.* 9:BR54-BR61.
193. Leib, S.L. and M.G.Tauber. 1999. Pathogenesis of bacterial meningitis. *Infect. Dis. Clin. North Am.* 13:527-5vi.

194. Lewis, H., W.Kaszubska, J.F.DeLamarter, and J.Whelan. 1994. Cooperativity between two NF-kappa B complexes, mediated by high- mobility-group protein I(Y), is essential for cytokine-induced expression of the E-selectin promoter. *Mol. Cell Biol.* 14:5701-5709.
195. Livak, K.J. and T.D.Schmittgen. 2001. Analysis of relative gene expression data using real-time quantitative PCR and the 2(-Delta Delta C(T)) Method. *Methods* 25:402-408.
196. Ljungberg, B., J.Jacobsen, S.Haggstrom-Rudolfsson, T.Rasmuson, G.Lindh, and K.Grankvist. 2003. Tumour vascular endothelial growth factor (VEGF) mRNA in relation to serum VEGF protein levels and tumour progression in human renal cell carcinoma. *Urol. Res.* 31:335-340.
197. Luscinskas, F.W. and M.A.Gimbrone, Jr. 1996. Endothelial-dependent mechanisms in chronic inflammatory leukocyte recruitment. *Annu. Rev. Med.* 47:413-421.
198. Mackay, I.M., K.E.Arden, and A.Nitsche. 2002. Real-time PCR in virology. *Nucleic Acids Res.* 30:1292-1305.
199. Mackinnon, F.G., Y.Ho, M.S.Blake, F.Michon, A.Chandraker, M.H.Sayegh, and L.M.Wetzler. 1999. The role of B/T costimulatory signals in the immunopotentiating activity of neisserial porin. *J. Infect. Dis.* 180:755-761.
200. Madan, B., W.N.Gade, and B.Ghosh. 2001. Curcuma longa activates NF-kappaB and promotes adhesion of neutrophils to human umbilical vein endothelial cells. *J. Ethnopharmacol.* 75:25-32.

201. Malhotra, R., R.Priest, and M.I.Bird. 1996. Role for L-selectin in lipopolysaccharide-induced activation of neutrophils. *Biochem. J.* 320 (Pt 2):589-593.
202. Manconi, F., R.Markham, and I.S.Fraser. 2000. Culturing endothelial cells of microvascular origin. *Methods Cell Sci.* 22:89-99.
203. Marceau, M., J.L.Beretti, and X.Nassif. 1995. High adhesiveness of encapsulated *Neisseria meningitidis* to epithelial cells is associated with the formation of bundles of pili. *Mol. Microbiol.* 17:855-863.
204. Marceau, M. and X.Nassif. 1999. Role of glycosylation at Ser63 in production of soluble pilin in pathogenic *Neisseria*. *J. Bacteriol.* 181:656-661.
205. Martin-Padura, I., S.Lostaglio, M.Schneemann, L.Williams, M.Romano, P.Fruscella, C.Panzeri, A.Stoppacciaro, L.Ruco, A.Villa, D.Simmons, and E.Dejana. 1998. Junctional adhesion molecule, a novel member of the immunoglobulin superfamily that distributes at intercellular junctions and modulates monocyte transmigration. *J. Cell Biol.* 142:117-127.
206. Massari, P., P.Henneke, Y.Ho, E.Latz, D.T.Golenbock, and L.M.Wetzler. 2002. Cutting edge: Immune stimulation by neisserial porins is toll-like receptor 2 and MyD88 dependent. *J. Immunol.* 168:1533-1537.
207. Massari, P., C.A.King, A.Y.Ho, and L.M.Wetzler. 2003a. Neisserial PorB is translocated to the mitochondria of HeLa cells infected with *Neisseria meningitidis* and protects cells from apoptosis. *Cell Microbiol.* 5:99-109.
208. Massari, P., S.Ram, H.Macleod, and L.M.Wetzler. 2003b. The role of porins in neisserial pathogenesis and immunity. *Trends Microbiol.* 11:87-93.

209. McInerney, J.M., J.R.Nawrocki, and C.H.Lowrey. 2000. Long-term silencing of retroviral vectors is resistant to reversal by trichostatin A and 5-azacytidine. *Gene Ther.* 7:653-663.
210. McLeod Griffis JM. 1995. Mechanisms of Host Immunity. *In* Meningococcal Disease. Carwright K, editor. Jon Wiley & Sons Ltd, West Sussex. 35-70.
211. McNeil, G. and M.Virji. 1997. Phenotypic variants of meningococci and their potential in phagocytic interactions: the influence of opacity proteins, pili, PilC and surface sialic acids. *Microb. Pathog.* 22:295-304.
212. Meacock, S., R.Pescini-Gobert, J.F.DeLamarter, and v.H.Hooft. 1994. Transcription factor-induced, phased bending of the E-selectin promoter. *J. Biol. Chem.* 269:31756-31762.
213. Medina, V., B.Edmonds, G.P.Young, R.James, S.Appleton, and P.D.Zalewski. 1997. Induction of caspase-3 protease activity and apoptosis by butyrate and trichostatin A (inhibitors of histone deacetylase): dependence on protein synthesis and synergy with a mitochondrial/cytochrome c-dependent pathway. *Cancer Res.* 57:3697-3707.
214. Medzhitov, R., P.Preston-Hurlburt, E.Kopp, A.Stadlen, C.Chen, S.Ghosh, and C.A.Janeway, Jr. 1998. MyD88 is an adaptor protein in the hToll/IL-1 receptor family signaling pathways. *Mol. Cell* 2:253-258.
215. Melrose, J., N.Tsurushita, G.Liu, and E.L.Berg. 1998. IFN-gamma inhibits activation-induced expression of E- and P-selectin on endothelial cells. *J. Immunol.* 161:2457-2464.

216. Mertens, G., J.J.Cassiman, B.H.Van den, J.Vermeylen, and G.David. 1992. Cell surface heparan sulfate proteoglycans from human vascular endothelial cells. Core protein characterization and antithrombin III binding properties. *J. Biol. Chem.* 267:20435-20443.
217. Meyer, T.F., C.P.Gibbs, and R.Haas. 1990. Variation and control of protein expression in *Neisseria*. *Annu. Rev. Microbiol.* 44:451-477.
218. Min, J.K., Y.M.Lee, J.H.Kim, Y.M.Kim, S.W.Kim, S.Y.Lee, Y.S.Gho, G.T.Oh, and Y.G.Kwon. 2005. Hepatocyte growth factor suppresses vascular endothelial growth factor-induced expression of endothelial ICAM-1 and VCAM-1 by inhibiting the nuclear factor-kappaB pathway. *Circ. Res.* 96:300-307.
219. Min, W. and J.S.Pober. 1997. TNF initiates E-selectin transcription in human endothelial cells through parallel TRAF-NF-kappa B and TRAF-RAC/CDC42-JNK-c-Jun/ATF2 pathways. *J. Immunol.* 159:3508-3518.
220. Minetti, C.A., M.S.Blake, and D.P.Remeta. 1998. Characterization of the structure, function, and conformational stability of PorB class 3 protein from *Neisseria meningitidis*. A porin with unusual physicochemical properties. *J. Biol. Chem.* 273:25329-25338.
221. Montgomery, K.F., L.Osborn, C.Hession, R.Tizard, D.Goff, C.Vassallo, P.I.Tarr, K.Bomsztyk, R.Lobb, J.M.Harlan, and . 1991. Activation of endothelial-leukocyte adhesion molecule 1 (ELAM-1) gene transcription. *Proc. Natl. Acad. Sci. U. S. A* 88:6523-6527.
222. Muenzner, P., C.DeHio, T.Fujiwara, M.Achtman, T.F.Meyer, and S.D.Gray-Owen. 2000. Carcinoembryonic antigen family receptor specificity of *Neisseria meningitidis* Opa variants influences adherence to and invasion of

- proinflammatory cytokine-activated endothelial cells. *Infect. Immun.* 68:3601-3607.
223. Muenzner, P., M.Naumann, T.F.Meyer, and S.D.Gray-Owen. 2001. Pathogenic *Neisseria* trigger expression of their carcinoembryonic antigen-related cellular adhesion molecule 1 (CEACAM1; previously CD66a) receptor on primary endothelial cells by activating the immediate early response transcription factor, nuclear factor-kappaB. *J. Biol. Chem.* 276:24331-24340.
 224. Muller, A., J.Rassow, J.Grimm, N.Machuy, T.F.Meyer, and T.Rudel. 2002a. VDAC and the bacterial porin PorB of *Neisseria gonorrhoeae* share mitochondrial import pathways. *EMBO J.* 21:1916-1929.
 225. Muller, A.M., M.I.Hermanns, C.Cronen, and C.J.Kirkpatrick. 2002b. Comparative study of adhesion molecule expression in cultured human macro- and microvascular endothelial cells. *Exp. Mol. Pathol.* 73:171-180.
 226. Muller, W.A. 2003. Leukocyte-endothelial-cell interactions in leukocyte transmigration and the inflammatory response. *Trends Immunol.* 24:327-334.
 227. Murakami, T., C.Mataki, C.Nagao, M.Umetani, Y.Wada, M.Ishii, S.Tsutsumi, T.Kohro, A.Saiura, H.Aburatani, T.Hamakubo, and T.Kodama. 2000. The gene expression profile of human umbilical vein endothelial cells stimulated by tumor necrosis factor alpha using DNA microarray analysis. *J. Atheroscler. Thromb.* 7:39-44.
 228. Muzio, M., G.Natoli, S.Saccani, M.Levrero, and A.Mantovani. 1998. The human toll signaling pathway: divergence of nuclear factor kappaB and JNK/SAPK activation upstream of tumor necrosis factor receptor- associated factor 6 (TRAF6). *J Exp. Med.* 187:2097-2101.

229. Nakahara, T., H.Uchi, K.Urabe, Q.Chen, M.Furue, and Y.Moroi. 2004. Role of c-Jun N-terminal kinase on lipopolysaccharide induced maturation of human monocyte-derived dendritic cells. *Int. Immunol.* 16:1701-1709.
230. Nasrin, N., L.Ercolani, M.Denaro, X.F.Kong, I.Kang, and M.Alexander. 1990. An insulin response element in the glyceraldehyde-3-phosphate dehydrogenase gene binds a nuclear protein induced by insulin in cultured cells and by nutritional manipulations in vivo. *Proc. Natl. Acad. Sci. U. S. A* 87:5273-5277.
231. Nassif, X., J.L.Beretti, J.Lowy, P.Stenberg, P.O'Gaora, J.Pfeifer, S.Normark, and M.So. 1994. Roles of pilin and PilC in adhesion of *Neisseria meningitidis* to human epithelial and endothelial cells. *Proc. Natl. Acad. Sci. U. S. A* 91:3769-3773.
232. Nassif, X., C.Pujol, P.Morand, and E.Eugene. 1999. Interactions of pathogenic *Neisseria* with host cells. Is it possible to assemble the puzzle? *Mol. Microbiol.* 32:1124-1132.
233. Naumann, M., T.Rudel, B.Wieland, C.Bartsch, and T.F.Meyer. 1998. Coordinate activation of activator protein 1 and inflammatory cytokines in response to *Neisseria gonorrhoeae* epithelial cell contact involves stress response kinases. *J Exp. Med.* 188:1277-1286.
234. Naumann, M., S.Wessler, C.Bartsch, B.Wieland, and T.F.Meyer. 1997. *Neisseria gonorrhoeae* epithelial cell interaction leads to the activation of the transcription factors nuclear factor kappaB and activator protein 1 and the induction of inflammatory cytokines. *J. Exp. Med.* 186:247-258.
235. Netea, M.G., B.J.Kullberg, L.A.Joosten, T.Sprong, I.Verschueren, O.C.Boerman, F.Amiot, W.B.van den Berg, and J.W.Van Der Meer. 2001.

- Lethal *Escherichia coli* and *Salmonella typhimurium* endotoxemia is mediated through different pathways. *Eur. J. Immunol.* 31:2529-2538.
236. Netea, M.G., M.van Deuren, B.J.Kullberg, J.M.Cavaillon, and J.W.Van Der Meer. 2002. Does the shape of lipid A determine the interaction of LPS with Toll- like receptors? *Trends Immunol.* 23:135-139.
237. Netelenbos, T., A.M.Drager, H.B.van het, F.L.Kessler, C.Delouis, P.C.Huijgens, B.J.van den, and W.van Dijk. 2001. Differences in sulfation patterns of heparan sulfate derived from human bone marrow and umbilical vein endothelial cells. *Exp. Hematol.* 29:884-893.
238. Newman, P.J., M.C.Berndt, J.Gorski, G.C.White, S.Lyman, C.Paddock, and W.A.Muller. 1990. PECAM-1 (CD31) cloning and relation to adhesion molecules of the immunoglobulin gene superfamily. *Science* 247:1219-1222.
239. Nicklin, S.A., D.J.Von Seggern, L.M.Work, D.C.Pek, A.F.Dominiczak, G.R.Nemerow, and A.H.Baker. 2001. Ablating adenovirus type 5 fiber-CAR binding and HI loop insertion of the SIGYPLP peptide generate an endothelial cell-selective adenovirus. *Mol. Ther.* 4:534-542.
240. Nicklin, S.A., S.J.White, S.J.Watkins, R.E.Hawkins, and A.H.Baker. 2000. Selective targeting of gene transfer to vascular endothelial cells by use of peptides isolated by phage display. *Circulation* 102:231-237.
241. Nooteboom, A., C.J.van der Linden, and T.Hendriks. 2005. Whole blood-mediated endothelial permeability and adhesion molecule expression: a model study into the effects of bacteria and antibiotics. *J. Antimicrob. Chemother.* 55:150-156.

242. Oftung, F., L.M.Naess, L.M.Wetzler, G.E.Korsvold, A.Aase, E.A.Hoiby, R.Dalseg, J.Holst, T.E.Michaelsen, and B.Haneberg. 1999. Antigen-specific T-cell responses in humans after intranasal immunization with a meningococcal serogroup B outer membrane vesicle vaccine. *Infect. Immun.* 67:921-927.
243. Ogawa, H., P.Rafiee, J.Heidemann, P.J.Fisher, N.A.Johnson, M.F.Otterson, B.Kalyanaraman, K.A.Pritchard, Jr., and D.G.Binion. 2003. Mechanisms of endotoxin tolerance in human intestinal microvascular endothelial cells. *J. Immunol.* 170:5956-5964.
244. Oikarinen, A., J.Makela, T.Vuorio, and E.Vuorio. 1991. Comparison on collagen gene expression in the developing chick embryo tendon and heart. Tissue and development time-dependent action of dexamethasone. *Biochim. Biophys. Acta* 1089:40-46.
245. Oliver, K.J., K.M.Reddin, P.Bracegirdle, M.J.Hudson, R.Borrow, I.M.Feavers, A.Robinson, K.Cartwright, and A.R.Gorringe. 2002. *Neisseria lactamica* protects against experimental meningococcal infection. *Infect. Immun.* 70:3621-3626.
246. Osborn, L., C.Hession, R.Tizard, C.Vassallo, S.Luhowskyj, G.Chi-Rosso, and R.Lobb. 1989. Direct expression cloning of vascular cell adhesion molecule 1, a cytokine-induced endothelial protein that binds to lymphocytes. *Cell* 59:1203-1211.
247. Overbergh, L., A.Giulietti, D.Valckx, R.Decallonne, R.Bouillon, and C.Mathieu. 2003. The use of real-time reverse transcriptase PCR for the quantification of cytokine gene expression. *J. Biomol. Tech.* 14:33-43.

248. Ovstebo, R., P.Brandtzaeg, B.Brusletto, K.B.Haug, K.Lande, E.A.Hoiby, and P.Kierulf. 2004. Use of robotized DNA isolation and real-time PCR to quantify and identify close correlation between levels of *Neisseria meningitidis* DNA and lipopolysaccharides in plasma and cerebrospinal fluid from patients with systemic meningococcal disease. *J. Clin. Microbiol.* 42:2980-2987.
249. Pahlsson, P., J.Strindhall, U.Srinivas, and A.Lundblad. 1995. Role of N-linked glycosylation in expression of E-selectin on human endothelial cells. *Eur. J. Immunol.* 25:2452-2459.
250. Palmeri, D., A.van Zante, C.C.Huang, S.Hemmerich, and S.D.Rosen. 2000. Vascular endothelial junction-associated molecule, a novel member of the immunoglobulin superfamily, is localized to intercellular boundaries of endothelial cells. *J. Biol. Chem.* 275:19139-19145.
251. Parkes, R., Q.H.Meng, K.E.Siapati, J.R.Mcewan, and S.L.Hart. 2002. High efficiency transfection of porcine vascular cells in vitro with a synthetic vector system. *Journal of Gene Medicine* 4:292-299.
252. Patel, K.D., S.L.Cuvelier, and S.Wiehler. 2002. Selectins: critical mediators of leukocyte recruitment. *Semin. Immunol.* 14:73-81.
253. Peinnequin, A., C.Mouret, O.Birot, A.Alonso, J.Mathieu, D.Clarencon, D.Agay, Y.Chancerelle, and E.Multon. 2004. Rat pro-inflammatory cytokine and cytokine related mRNA quantification by real-time polymerase chain reaction using SYBR green. *BMC. Immunol.* 5:3.
254. Peiser, L., M.P.De Winther, K.Makepeace, M.Hollinshead, P.Coull, J.Plested, T.Kodama, E.R.Moxon, and S.Gordon. 2002. The class A macrophage scavenger receptor is a major pattern recognition receptor for *Neisseria*

- meningitidis which is independent of lipopolysaccharide and not required for secretory responses. *Infect. Immun.* 70:5346-5354.
255. Pellacani, A., M.T.Chin, P.Wiesel, M.Ibanez, A.Patel, S.F.Yet, C.M.Hsieh, J.D.Paulauskis, R.Reeves, M.E.Lee, and M.A.Perrella. 1999. Induction of high mobility group-I(Y) protein by endotoxin and interleukin-1beta in vascular smooth muscle cells. Role in activation of inducible nitric oxide synthase. *J. Biol. Chem.* 274:1525-1532.
 256. Perkins, N.D., R.M.Schmid, C.S.Duckett, K.Leung, N.R.Rice, and G.J.Nabel. 1992. Distinct combinations of NF-kappa B subunits determine the specificity of transcriptional activation. *Proc. Natl. Acad. Sci. U. S. A* 89:1529-1533.
 257. Perrella, M.A., A.Pellacani, P.Wiesel, M.T.Chin, L.C.Foster, M.Ibanez, C.M.Hsieh, R.Reeves, S.F.Yet, and M.E.Lee. 1999. High mobility group-I(Y) protein facilitates nuclear factor-kappaB binding and transactivation of the inducible nitric-oxide synthase promoter/enhancer. *J. Biol. Chem.* 274:9045-9052.
 258. Perry, A.C., C.A.Hart, I.J.Nicolson, J.E.Heckels, and J.R.Saunders. 1987. Inter-strain homology of pilin gene sequences in *Neisseria meningitidis* isolates that express markedly different antigenic pilus types. *J. Gen. Microbiol.* 133 (Pt 6):1409-1418.
 259. Peters, M.J., R.S.Heyderman, S.Faust, G.L.Dixon, D.P.Inwald, and N.J.Klein. 2003. Severe meningococcal disease is characterized by early neutrophil but not platelet activation and increased formation and consumption of platelet-neutrophil complexes. *J. Leukoc. Biol.* 73:722-730.

260. Pollet, I., C.J.Opina, C.Zimmerman, K.G.Leong, F.Wong, and A.Karsan. 2003. Bacterial lipopolysaccharide directly induces angiogenesis through TRAF6-mediated activation of NF-kappaB and c-Jun N-terminal kinase. *Blood* 102:1740-1742.
261. Poltorak, A., X.He, I.Smirnova, M.Y.Liu, C.V.Huffel, X.Du, D.Birdwell, E.Alejos, M.Silva, C.Galanos, M.Freudenberg, P.Ricciardi-Castagnoli, B.Layton, and B.Beutler. 1998. Defective LPS signaling in C3H/HeJ and C57BL/10ScCr mice: mutations in Tlr4 gene. *Science* 282:2085-2088.
262. Poolman JT, van der Ley PA, and Tommassen J. 1995. Surface structures and secreted products of meningococci. *In* Meningococcal Disease. Cartwright K, editor. John Wiley & Sons Ltd, West Sussex. 21-34.
263. Pridmore, A.C., G.A.Jarvis, C.M.John, D.L.Jack, S.K.Dower, and R.C.Read. 2003. Activation of toll-like receptor 2 (TLR2) and TLR4/MD2 by *Neisseria* is independent of capsule and lipooligosaccharide (LOS) sialylation but varies widely among LOS from different strains. *Infect. Immun.* 71:3901-3908.
264. Pridmore, A.C., D.H.Wyllie, F.Abdillahi, L.Steeghs, L.P.van der, S.K.Dower, and R.C.Read. 2001. A lipopolysaccharide-deficient mutant of *Neisseria meningitidis* elicits attenuated cytokine release by human macrophages and signals via toll- like receptor (TLR) 2 but not via TLR4/MD2. *J. Infect. Dis.* 183:89-96.
265. Prinz, T. and J.Tommassen. 2000. Association of iron-regulated outer membrane proteins of *Neisseria meningitidis* with the RmpM (class 4) protein. *FEMS Microbiol. Lett.* 183:49-53.

266. Pugin, J., C.C.Schurer-Maly, D.Leturcq, A.Moriarty, R.J.Ulevitch, and P.S.Tobias. 1993. Lipopolysaccharide activation of human endothelial and epithelial cells is mediated by lipopolysaccharide-binding protein and soluble CD14. *Proc. Natl. Acad. Sci. U. S. A* 90:2744-2748.
267. Pulendran, B., P.Kumar, C.W.Cutler, M.Mohamadzadeh, T.Van Dyke, and J.Banchereau. 2001. Lipopolysaccharides from distinct pathogens induce different classes of immune responses in vivo. *J. Immunol.* 167:5067-5076.
268. Rahman, M.M., D.S.Stephens, C.M.Kahler, J.Glushka, and R.W.Carlson. 1998. The lipooligosaccharide (LOS) of *Neisseria meningitidis* serogroup B strain NMB contains L2, L3, and novel oligosaccharides, and lacks the lipid-A 4'-phosphate substituent. *Carbohydr. Res.* 307:311-324.
269. Ram, S., F.G.Mackinnon, S.Gulati, D.P.McQuillen, U.Vogel, M.Frosch, C.Elkins, H.K.Guttormsen, L.M.Wetzler, M.Oppermann, M.K.Pangburn, and P.A.Rice. 1999. The contrasting mechanisms of serum resistance of *Neisseria gonorrhoeae* and group B *Neisseria meningitidis*. *Mol. Immunol.* 36:915-928.
270. Re, F. and J.L.Strominger. 2001. Toll-like receptor 2 (TLR2) and TLR4 differentially activate human dendritic cells. *J. Biol. Chem.* 276:37692-37699.
271. Read, M.A., S.R.Cordle, R.A.Veach, C.D.Carlisle, and J.Hawiger. 1993. Cell-free pool of CD14 mediates activation of transcription factor NF-kappa B by lipopolysaccharide in human endothelial cells. *Proc. Natl. Acad. Sci. U. S. A* 90:9887-9891.
272. Read, M.A., M.Z.Whitley, S.Gupta, J.W.Pierce, J.Best, R.J.Davis, and T.Collins. 1997. Tumor necrosis factor alpha-induced E-selectin expression is

- activated by the nuclear factor-kappaB and c-JUN N-terminal kinase/p38 mitogen- activated protein kinase pathways. *J. Biol. Chem.* 272:2753-2761.
273. Read, R.C., J.Pullin, S.Gregory, R.Borrow, E.B.Kaczmariski, F.S.di Giovine, S.K.Dower, C.Cannings, and A.G.Wilson. 2001. A functional polymorphism of toll-like receptor 4 is not associated with likelihood or severity of meningococcal disease. *J. Infect. Dis.* 184:640-642.
 274. Reeves, R. and L.Beckerbauer. 2001. HMGI/Y proteins: flexible regulators of transcription and chromatin structure. *Biochim. Biophys. Acta* 1519:13-29.
 275. Reeves, R. and L.M.Beckerbauer. 2003. HMGA proteins as therapeutic drug targets. *Prog. Cell Cycle Res.* 5:279-286.
 276. Reimold, A.M., M.J.Grusby, B.Kosaras, J.W.Fries, R.Mori, S.Maniwa, I.M.Clauss, T.Collins, R.L.Sidman, M.J.Glimcher, and L.H.Glimcher. 1996. Chondrodysplasia and neurological abnormalities in ATF-2-deficient mice. *Nature* 379:262-265.
 277. Reimold, A.M., J.Kim, R.Finberg, and L.H.Glimcher. 2001. Decreased immediate inflammatory gene induction in activating transcription factor-2 mutant mice. *Int. Immunol.* 13:241-248.
 278. Reinhart, K., O.Bayer, F.Brunckhorst, and M.Meisner. 2002. Markers of endothelial damage in organ dysfunction and sepsis. *Crit Care Med.* 30:S302-S312.
 279. Rincon, M., R.A.Flavell, and R.A.Davis. 2000. The JNK and P38 MAP kinase signaling pathways in T cell-mediated immune responses. *Free Radic. Biol. Med.* 28:1328-1337.

280. Ririe, K.M., R.P.Rasmussen, and C.T.Wittwer. 1997. Product differentiation by analysis of DNA melting curves during the polymerase chain reaction. *Anal. Biochem.* 245:154-160.
281. Rittig, M.G., A.Kaufmann, A.Robins, B.Shaw, H.Sprenger, D.Gemsa, V.Foulongne, B.Rouot, and J.Dornand. 2003. Smooth and rough lipopolysaccharide phenotypes of *Brucella* induce different intracellular trafficking and cytokine/chemokine release in human monocytes. *J. Leukoc. Biol.* 74:1045-1055.
282. Robertson, B.D. and T.F.Meyer. 1992. Genetic variation in pathogenic bacteria. *Trends Genet.* 8:422-427.
283. Roebuck, K.A. 1999. Oxidant stress regulation of IL-8 and ICAM-1 gene expression: differential activation and binding of the transcription factors AP-1 and NF-kappaB (Review). *Int. J. Mol. Med.* 4:223-230.
284. Roebuck, K.A. and A.Finnegan. 1999. Regulation of intercellular adhesion molecule-1 (CD54) gene expression. *J. Leukoc. Biol.* 66:876-888.
285. Roebuck, K.A., A.Rahman, V.Lakshminarayanan, K.Janakidevi, and A.B.Malik. 1995. H₂O₂ and tumor necrosis factor- α activate intercellular adhesion molecule 1 (ICAM-1) gene transcription through distinct cis-regulatory elements within the ICAM-1 promoter. *J. Biol. Chem.* 270:18966-18974.
286. Rombouts, K., T.Niki, P.Greenwel, A.Vandermonde, A.Wielant, K.Hellemans, P.De Bleser, M.Yoshida, D.Schuppan, M.Rojkind, and A.Geerts. 2002. Trichostatin A, a histone deacetylase inhibitor, suppresses collagen synthesis and prevents TGF- β (1)-induced fibrogenesis in skin fibroblasts. *Exp. Cell Res.* 278:184-197.

287. Rosen, S.D. and C.R.Bertozzi. 1994. The selectins and their ligands. *Curr. Opin. Cell Biol* 6:663-673.
288. Saito, I., K.Terauchi, M.Shimuta, S.Nishiimura, K.Yoshino, T.Takeuchi, K.Tsubota, and N.Miyasaka. 1993. Expression of cell adhesion molecules in the salivary and lacrimal glands of Sjogren's syndrome. *J. Clin. Lab Anal.* 7:180-187.
289. Samady, L., J.Dennis, V.Budhram-Mahadeo, and D.S.Latchman. 2004. Activation of CDK4 gene expression in human breast cancer cells by the Brn-3b POU family transcription factor. *Cancer Biol. Ther.* 3:317-323.
290. Sarkari, J., N.Pandit, E.R.Moxon, and M.Achtman. 1994. Variable expression of the Opc outer membrane protein in *Neisseria meningitidis* is caused by size variation of a promoter containing poly- cytidine. *Mol. Microbiol.* 13:207-217.
291. Saukkonen, K., M.Leinonen, H.Abdillahi, and J.T.Poolman. 1989. Comparative evaluation of potential components for group B meningococcal vaccine by passive protection in the infant rat and in vitro bactericidal assay. *Vaccine* 7:325-328.
292. Saunders, N.J., A.C.Jeffries, J.F.Peden, D.W.Hood, H.Tettelin, R.Rappuoli, and E.R.Moxon. 2000. Repeat-associated phase variable genes in the complete genome sequence of *Neisseria meningitidis* strain MC58. *Mol. Microbiol.* 37:207-215.
293. Schindler, U. and V.R.Baichwal. 1994. Three NF-kappa B binding sites in the human E-selectin gene required for maximal tumor necrosis factor alpha-induced expression. *Mol. Cell Biol.* 14:5820-5831.

294. Scholten, R.J., B.Kuipers, H.A.Valkenburg, J.Dankert, W.D.Zollinger, and J.T.Poolman. 1994. Lipo-oligosaccharide immunotyping of *Neisseria meningitidis* by a whole- cell ELISA with monoclonal antibodies. *J. Med. Microbiol.* 41:236-243.
295. Scholz, D., B.Devaux, A.Hirche, B.Potzsch, B.Kropp, W.Schaper, and J.Schaper. 1996. Expression of adhesion molecules is specific and time-dependent in cytokine-stimulated endothelial cells in culture. *Cell Tissue Res.* 284:415-423.
296. Schreck, R., H.Zorbas, E.L.Winnacker, and P.A.Baeuerle. 1990. The NF-kappa B transcription factor induces DNA bending which is modulated by its 65-kD subunit. *Nucleic Acids Res.* 18:6497-6502.
297. Schroter, M., B.Zollner, P.Schafer, R.Laufs, and H.H.Feucht. 2001. Quantitative detection of hepatitis C virus RNA by light cycler PCR and comparison with two different PCR assays. *J. Clin. Microbiol.* 39:765-768.
298. Schwandner, R., R.Dziarski, H.Wesche, M.Rothe, and C.J.Kirschning. 1999. Peptidoglycan- and lipoteichoic acid-induced cell activation is mediated by Toll-like Receptor 2. *J Biol Chem.* 274:17406-17409.
299. Shamaei-Tousi, A., M.J.Burns, J.L.Benach, M.B.Furie, E.I.Gergel, and S.Bergstrom. 2000. The relapsing fever spirochaete, *Borrelia crocidurae*, activates human endothelial cells and promotes the transendothelial migration of neutrophils. *Cell Microbiol.* 2:591-599.
300. Shim, J. and M.Karin. 2002. The control of mRNA stability in response to extracellular stimuli. *Mol. Cells* 14:323-331.

301. Shimazu, R., S.Akashi, H.Ogata, Y.Nagai, K.Fukudome, K.Miyake, and M.Kimoto. 1999. MD-2, a molecule that confers lipopolysaccharide responsiveness on Toll- like receptor 4. *J Exp. Med.* 189:1777-1782.
302. Simmons, D.L., C.Walker, C.Power, and R.Pigott. 1990. Molecular cloning of CD31, a putative intercellular adhesion molecule closely related to carcinoembryonic antigen. *J. Exp. Med.* 171:2147-2152.
303. Simpson, D.A., S.Feeney, C.Boyle, and A.W.Stitt. 2000. Retinal VEGF mRNA measured by SYBR green I fluorescence: A versatile approach to quantitative PCR. *Mol. Vis.* 6:178-183.
304. Sipehia, R. and G.Martucci. 1995. High-efficiency transformation of human endothelial cells by Apo E-mediated transfection with plasmid DNA. *Biochem. Biophys. Res. Commun.* 214:206-211.
305. Smeets, E.F., T.de Vries, J.F.Leeuwenberg, D.H.van den Eijnden, W.A.Buurman, and J.J.Neefjes. 1993. Phosphorylation of surface E-selectin and the effect of soluble ligand (sialyl Lewisx) on the half-life of E-selectin. *Eur. J. Immunol.* 23:147-151.
306. Smith, G.M., J.Whelan, R.Pescini, P.Ghersa, J.F.DeLamarter, and v.H.Hooft. 1993. DNA-methylation of the E-selectin promoter represses NF-kappa B transactivation. *Biochem. Biophys. Res. Commun.* 194:215-221.
307. Snapper, C.M., F.R.Rosas, M.R.Kehry, J.J.Mond, and L.M.Wetzler. 1997. Neisserial porins may provide critical second signals to polysaccharide-activated murine B cells for induction of immunoglobulin secretion. *Infect. Immun.* 65:3203-3208.

308. Sokolova, O., N.Heppel, R.Jagerhuber, K.S.Kim, M.Frosch, M.Eigenthaler, and A.Schubert-Unkmeir. 2004. Interaction of *Neisseria meningitidis* with human brain microvascular endothelial cells: role of MAP- and tyrosine kinases in invasion and inflammatory cytokine release. *Cell Microbiol.* 6:1153-1166.
309. Somers, W.S., J.Tang, G.D.Shaw, and R.T.Camphausen. 2000. Insights into the molecular basis of leukocyte tethering and rolling revealed by structures of P- and E-selectin bound to SLe(X) and PSGL-1. *Cell* 103:467-479.
310. Sotto, M.N., B.Langer, S.Hoshino-Shimizu, and T.de Brito. 1976. Pathogenesis of cutaneous lesions in acute meningococcemia in humans: light, immunofluorescent, and electron microscopic studies of skin biopsy specimens. *J. Infect. Dis.* 133:506-514.
311. Spanakis, E. 1993. Problems related to the interpretation of autoradiographic data on gene expression using common constitutive transcripts as controls. *Nucleic Acids Res.* 21:3809-3819.
312. Spitzer, J.H., A.Visintin, A.Mazzoni, M.N.Kennedy, and D.M.Segal. 2002. Toll-like receptor 1 inhibits Toll-like receptor 4 signaling in endothelial cells. *Eur. J. Immunol.* 32:1182-1187.
313. Sprong, T., M.G.Netea, L.P.van der, T.J.Verver-Jansen, L.E.Jacobs, A.Stalenhoef, J.W.Van Der Meer, and M.van Deuren. 2004. Human lipoproteins have divergent neutralizing effects on *E. coli* LPS, *N. meningitidis* LPS, and complete Gram-negative bacteria. *J. Lipid Res.* 45:742-749.
314. Sprong, T., N.Stikkelbroeck, L.P.van der, L.Steeghs, L.van Alphen, N.Klein, M.G.Netea, J.W.Van Der Meer, and M.van Deuren. 2001. Contributions of

- Neisseria meningitidis LPS and non-LPS to proinflammatory cytokine response. *J. Leukoc. Biol.* 70:283-288.
315. Staunton, D.E., S.D.Marlin, C.Stratowa, M.L.Dustin, and T.A.Springer. 1988. Primary structure of ICAM-1 demonstrates interaction between members of the immunoglobulin and integrin supergene families. *Cell* 52:925-933.
 316. Steeghs, L., H.de Cock, E.Evers, B.Zomer, J.Tommassen, and L.P.van der. 2001. Outer membrane composition of a lipopolysaccharide-deficient Neisseria meningitidis mutant. *EMBO J.* 20:6937-6945.
 317. Steeghs, L., R.den Hartog, A.den Boer, B.Zomer, P.Roholl, and L.P.van der. 1998. Meningitis bacterium is viable without endotoxin. *Nature* 392:449-450.
 318. Steeghs, L., M.P.Jennings, J.T.Poolman, and L.P.van der. 1997. Isolation and characterization of the Neisseria meningitidis lpxD-fabZ- lpxA gene cluster involved in lipid A biosynthesis. *Gene* 190:263-270.
 319. Stern, A., M.Brown, P.Nickel, and T.F.Meyer. 1986. Opacity genes in Neisseria gonorrhoeae: control of phase and antigenic variation. *Cell* 47:61-71.
 320. Stojiljkovic, I., V.Hwa, J.Larson, L.Lin, M.So, and X.Nassif. 1997. Cloning and characterization of the Neisseria meningitidis rfaC gene encoding alpha-1,5 heptosyltransferase I. *FEMS Microbiol. Lett.* 151:41-49.
 321. Sugano, M., K.Tsuchida, and N.Makino. 2000. High-density lipoproteins protect endothelial cells from tumor necrosis factor-alpha-induced apoptosis. *Biochem. Biophys. Res. Commun.* 272:872-876.

322. Swantek, J.L., M.H.Cobb, and T.D.Geppert. 1997. Jun N-terminal kinase/stress-activated protein kinase (JNK/SAPK) is required for lipopolysaccharide stimulation of tumor necrosis factor alpha (TNF-alpha) translation: glucocorticoids inhibit TNF-alpha translation by blocking JNK/SAPK. *Mol. Cell Biol.* 17:6274-6282.
323. Swartley, J.S., A.A.Marfin, S.Edupuganti, L.J.Liu, P.Cieslak, B.Perkins, J.D.Wenger, and D.S.Stephens. 1997. Capsule switching of *Neisseria meningitidis*. *Proc. Natl. Acad. Sci. U. S. A* 94:271-276.
324. Swerlick, R.A., K.H.Lee, L.J.Li, N.T.Sepp, S.W.Caughman, and T.J.Lawley. 1992. Regulation of vascular cell adhesion molecule 1 on human dermal microvascular endothelial cells. *J. Immunol.* 149:698-705.
325. Takahashi, M., J.Masuyama, U.Ikeda, S.Kitagawa, T.Kasahara, M.Saito, S.Kano, and K.Shimada. 1995. Effects of endogenous endothelial interleukin-8 on neutrophil migration across an endothelial monolayer. *Cardiovasc. Res.* 29:670-675.
326. Talreja, J., M.H.Kabir, B.Filla, D.J.Stechschulte, and K.N.Dileepan. 2004. Histamine induces Toll-like receptor 2 and 4 expression in endothelial cells and enhances sensitivity to Gram-positive and Gram-negative bacterial cell wall components. *Immunology* 113:224-233.
327. Tamaru, M. and S.Narumi. 1999. E-selectin gene expression is induced synergistically with the coexistence of activated classic protein kinase C and signals elicited by interleukin-1beta but not tumor necrosis factor-alpha. *J Biol Chem.* 274:3753-3763.

328. Tan, P.H., M.Manunta, N.Ardjomand, S.A.Xue, D.F.Larkin, D.O.Haskard, K.M.Taylor, and A.J.George. 2003. Antibody targeted gene transfer to endothelium. *J. Gene Med.* 5:311-323.
329. Tanner, F.C., D.P.Carr, G.J.Nabel, and E.G.Nabel. 1997. Transfection of human endothelial cells. *Cardiovasc. Res.* 35:522-528.
330. Tapping, R.I., S.Akashi, K.Miyake, P.J.Godowski, and P.S.Tobias. 2000. Toll-like receptor 4, but not toll-like receptor 2, is a signaling receptor for Escherichia and Salmonella lipopolysaccharides. *J Immunol* 165:5780-5787.
331. Teifel, M., L.T.Heine, S.Milbredt, and P.Friedl. 1997. Optimization of transfection of human endothelial cells. *Endothelium* 5:21-35.
332. ten Kate, M., L.J.Hofland, W.M.van Grevenstein, P.V.van Koetsveld, J.Jeel, and C.H.van Eijck. 2004. Influence of proinflammatory cytokines on the adhesion of human colon carcinoma cells to lung microvascular endothelium. *Int. J. Cancer* 112:943-950.
333. Thompson, P.A., P.S.Tobias, S.Viriyakosol, T.N.Kirkland, and R.L.Kitchens. 2003. Lipopolysaccharide (LPS)-binding protein inhibits responses to cell-bound LPS. *J. Biol. Chem.* 278:28367-28371.
334. Thornhill, M.H. and D.O.Haskard. 1990. IL-4 regulates endothelial cell activation by IL-1, tumor necrosis factor, or IFN-gamma. *J. Immunol.* 145:865-872.
335. Tobias, P.S., K.Soldau, and R.J.Ulevitch. 1986. Isolation of a lipopolysaccharide-binding acute phase reactant from rabbit serum. *J. Exp. Med.* 164:777-793.

336. Tommassen, J., P.Vermeij, M.Struyve, R.Benz, and J.T.Poolman. 1990. Isolation of *Neisseria meningitidis* mutants deficient in class 1 (porA) and class 3 (porB) outer membrane proteins. *Infect. Immun.* 58:1355-1359.
337. Tsai, C.M., C.E.Frasch, and L.F.Mocca. 1981. Five structural classes of major outer membrane proteins in *Neisseria meningitidis*. *J. Bacteriol.* 146:69-78.
338. Tyagi, S. and F.R.Kramer. 1996. Molecular beacons: probes that fluoresce upon hybridization. *Nat. Biotechnol.* 14:303-308.
339. Tzeng, Y.L. and D.S.Stephens. 2000. Epidemiology and pathogenesis of *Neisseria meningitidis*. *Microbes. Infect.* 2:687-700.
340. Uduehi, A., C.Mailhos, H.Truman, A.J.Thrasher, C.Kinnon, and S.L.Hart. 2003. Enhancement of integrin-mediated transfection of haematopoietic cells with a synthetic vector system. *Biotechnology and Applied Biochemistry* 38:201-209.
341. Unkmeir, A., U.Kammerer, A.Stade, C.Hubner, S.Haller, A.Kolb-Maurer, M.Frosch, and G.Dietrich. 2002a. Lipooligosaccharide and polysaccharide capsule: virulence factors of *Neisseria meningitidis* that determine meningococcal interaction with human dendritic cells. *Infect. Immun.* 70:2454-2462.
342. Unkmeir, A., K.Latsch, G.Dietrich, E.Wintermeyer, B.Schinke, S.Schwender, K.S.Kim, M.Eigenthaler, and M.Frosch. 2002b. Fibronectin mediates Opc-dependent internalization of *Neisseria meningitidis* in human brain microvascular endothelial cells. *Mol. Microbiol.* 46:933-946.
343. Uronen, H., A.J.Williams, G.Dixon, S.R.Andersen, L.P.van der, M.van Deuren, R.E.Callard, and N.Klein. 2000. Gram-negative bacteria induce

- proinflammatory cytokine production by monocytes in the absence of lipopolysaccharide (LPS). *Clin. Exp. Immunol.* 122:312-315.
344. Uronen-Hansson, H., L.Steeghs, J.Allen, G.L.Dixon, M.Osman, L.P.van der, S.Y.Wong, R.Callard, and N.Klein. 2004. Human dendritic cell activation by *Neisseria meningitidis*: phagocytosis depends on expression of lipooligosaccharide (LOS) by the bacteria and is required for optimal cytokine production. *Cell Microbiol.* 6:625-637.
 345. van der Ley P., M.Kramer, A.Martin, J.C.Richards, and J.T.Poolman. 1997. Analysis of the *icsBA* locus required for biosynthesis of the inner core region from *Neisseria meningitidis* lipopolysaccharide. *FEMS Microbiol. Lett.* 146:247-253.
 346. van der Ley P., M.Kramer, L.Steeghs, B.Kuipers, S.R.Andersen, M.P.Jennings, E.R.Moxon, and J.T.Poolman. 1996. Identification of a locus involved in meningococcal lipopolysaccharide biosynthesis by deletion mutagenesis. *Mol. Microbiol.* 19:1117-1125.
 347. van der Ley P., L.Steeghs, H.J.Hamstra, J.ten Hove, B.Zomer, and L.van Alphen. 2001. Modification of lipid A biosynthesis in *Neisseria meningitidis* *lpxL* mutants: influence on lipopolysaccharide structure, toxicity, and adjuvant activity. *Infect. Immun.* 69:5981-5990.
 348. van Deuren, M., P.Brandtzaeg, and J.W.Van Der Meer. 2000. Update on meningococcal disease with emphasis on pathogenesis and clinical management. *Clin. Microbiol. Rev.* 13:144-66, table.

- 349. Van Kampen, C. and B.A.Mallard. 2001. Regulation of bovine E-selectin expression by recombinant tumor necrosis factor alpha and lipopolysaccharide. *Vet. Immunol Immunopathol.* 79:151-165.
- 350. Varani, J. and P.A.Ward. 1994. Mechanisms of endothelial cell injury in acute inflammation. *Shock* 2:311-319.
- 351. Virji, M. 1996. Studies on the molecular mechanisms of meningococcal interactions with human cells. Towards anti-adhesion measures for the control of meningococcal disease. *Adv. Exp. Med. Biol.* 408:113-122.
- 352. Virji, M., C.Alexandrescu, D.J.Ferguson, J.R.Saunders, and E.R.Moxon. 1992a. Variations in the expression of pili: the effect on adherence of *Neisseria meningitidis* to human epithelial and endothelial cells. *Mol. Microbiol.* 6:1271-1279.
- 353. Virji, M., H.Kayhty, D.J.Ferguson, C.Alexandrescu, J.E.Heckels, and E.R.Moxon. 1991. The role of pili in the interactions of pathogenic *Neisseria* with cultured human endothelial cells. *Mol. Microbiol.* 5:1831-1841.
- 354. Virji, M., K.Makepeace, D.J.Ferguson, M.Achtman, and E.R.Moxon. 1993a. Meningococcal Opa and Opc proteins: their role in colonization and invasion of human epithelial and endothelial cells. *Mol. Microbiol.* 10:499-510.
- 355. Virji, M., K.Makepeace, D.J.Ferguson, M.Achtman, J.Sarkari, and E.R.Moxon. 1992b. Expression of the Opc protein correlates with invasion of epithelial and endothelial cells by *Neisseria meningitidis*. *Mol. Microbiol.* 6:2785-2795.

356. Virji, M., K.Makepeace, D.J.Ferguson, and S.M.Watt. 1996a. Carcinoembryonic antigens (CD66) on epithelial cells and neutrophils are receptors for Opa proteins of pathogenic neisseriae. *Mol. Microbiol.* 22:941-950.
357. Virji, M., K.Makepeace, and E.R.Moxon. 1994. Distinct mechanisms of interactions of Opc-expressing meningococci at apical and basolateral surfaces of human endothelial cells; the role of integrins in apical interactions. *Mol. Microbiol.* 14:173-184.
358. Virji, M., K.Makepeace, I.R.Peak, D.J.Ferguson, M.P.Jennings, and E.R.Moxon. 1995. Opc- and pilus-dependent interactions of meningococci with human endothelial cells: molecular mechanisms and modulation by surface polysaccharides. *Mol. Microbiol.* 18:741-754.
359. Virji, M., K.Makepeace, I.R.Peak, D.J.Ferguson, and E.R.Moxon. 1996b. Pathogenic mechanisms of *Neisseria meningitidis*. *Ann. N. Y. Acad. Sci.* 797:273-276.
360. Virji, M., J.R.Saunders, G.Sims, K.Makepeace, D.Maskell, and D.J.Ferguson. 1993b. Pilus-facilitated adherence of *Neisseria meningitidis* to human epithelial and endothelial cells: modulation of adherence phenotype occurs concurrently with changes in primary amino acid sequence and the glycosylation status of pilin. *Mol. Microbiol.* 10:1013-1028.
361. Virji, M., S.M.Watt, S.Barker, K.Makepeace, and R.Doyonnas. 1996c. The N-domain of the human CD66a adhesion molecule is a target for Opa proteins of *Neisseria meningitidis* and *Neisseria gonorrhoeae*. *Mol. Microbiol.* 22:929-939.

362. Visintin, A., A.Mazzoni, J.A.Spitzer, and D.M.Segal. 2001. Secreted MD-2 is a large polymeric protein that efficiently confers lipopolysaccharide sensitivity to Toll-like receptor 4. *Proc. Natl. Acad. Sci. U. S. A* 98:12156-12161.
363. Vogel, U. and M.Frosch. 1999. Mechanisms of neisserial serum resistance. *Mol. Microbiol.* 32:1133-1139.
364. von Asmuth, E.J., E.F.Smeets, L.A.Ginsel, J.J.Onderwater, J.F.Leeuwenberg, and W.A.Buurman. 1992. Evidence for endocytosis of E-selectin in human endothelial cells. *Eur. J. Immunol.* 22:2519-2526.
365. Walia, H., H.Y.Chen, J.M.Sun, L.T.Holth, and J.R.Davie. 1998. Histone acetylation is required to maintain the unfolded nucleosome structure associated with transcribing DNA. *Journal of Biological Chemistry* 273:14516-14522.
366. Watanabe, R., H.Wada, Y.Watanabe, M.Sakakura, T.Nakasaki, Y.Mori, M.Nishikawa, E.C.Gabazza, T.Nobori, and H.Shiku. 2001. Activity and antigen levels of thrombin-activatable fibrinolysis inhibitor in plasma of patients with disseminated intravascular coagulation. *Thromb. Res.* 104:1-6.
367. Westendorp, R.G., J.A.Langermans, C.E.de Bel, A.E.Meinders, J.P.Vandenbroucke, R.van Furth, and J.T.van Dissel. 1995. Release of tumor necrosis factor: an innate host characteristic that may contribute to the outcome of meningococcal disease. *J. Infect. Dis.* 171:1057-1060.
368. Wetzler, L.M., Y.Ho, H.Reiser, and L.W.Wetzler. 1996. Neisserial porins induce B lymphocytes to express costimulatory B7-2 molecules and to proliferate. *J. Exp. Med.* 183:1151-1159.

369. Whelan, J., P.Ghersa, v.H.Hooft, J.Gray, G.Chandra, F.Talabot, and J.F.DeLamarter. 1991. An NF kappa B-like factor is essential but not sufficient for cytokine induction of endothelial leukocyte adhesion molecule 1 (ELAM-1) gene transcription. *Nucleic Acids Res.* 19:2645-2653.
370. White, R.E., R.Wade-Martins, S.L.Hart, J.Frampton, B.Huey, A.Desai-Mehta, K.M.Cerosaletti, P.Concannon, and M.R.James. 2003. Functional delivery of large genomic DNA to human cells with a peptide-lipid vector. *Journal of Gene Medicine* 5:883-892.
371. Whitley, M.Z., D.Thanos, M.A.Read, T.Maniatis, and T.Collins. 1994. A striking similarity in the organization of the E-selectin and beta interferon gene promoters. *Mol. Cell Biol.* 14:6464-6475.
372. Winer, J., C.K.Jung, I.Shackel, and P.M.Williams. 1999. Development and validation of real-time quantitative reverse transcriptase-polymerase chain reaction for monitoring gene expression in cardiac myocytes in vitro. *Anal. Biochem.* 270:41-49.
373. Wojciak-Stothard, B., L.Williams, and A.J.Ridley. 1999. Monocyte adhesion and spreading on human endothelial cells is dependent on Rho-regulated receptor clustering. *J. Cell Biol.* 145:1293-1307.
374. Wolfert, M.A. and L.W.Seymour. 1998. Chloroquine and amphipathic peptide helices show synergistic transfection in vitro. *Gene Ther.* 5:409-414.
375. Wright, S.D., R.A.Ramos, P.S.Tobias, R.J.Ulevitch, and J.C.Mathison. 1990. CD14, a receptor for complexes of lipopolysaccharide (LPS) and LPS binding protein. *Science* 249:1431-1433.

376. Writer, M.J., B.Marshall, M.A.Pilkington-Miksa, S.E.Barker, M.Jacobsen, A.Kritz, P.C.Bell, D.H.Lester, A.B.Tabor, H.C.Hailes, N.Klein, and S.L.Hart. 2004. Targeted gene delivery to human airway epithelial cells with synthetic vectors incorporating novel targeting peptides selected by phage display. *Journal of Drug Targeting* 12:185-193.
377. Wu, S.Q. and W.C.Aird. 2005. Thrombin, TNF-alpha, and LPS exert overlapping but nonidentical effects on gene expression in endothelial cells and vascular smooth muscle cells. *Am. J. Physiol Heart Circ. Physiol* 289:H873-H885.
378. Wyble, C.W., K.L.Hynes, J.Kuchibhotla, B.C.Marcus, D.Hallahan, and B.L.Gewertz. 1997. TNF-alpha and IL-1 upregulate membrane-bound and soluble E-selectin through a common pathway. *J. Surg. Res.* 73:107-112.
379. Wyllie, D.H., E.Kiss-Toth, A.Visintin, S.C.Smith, S.Boussouf, D.M.Segal, G.W.Duff, and S.K.Dower. 2000. Evidence for an accessory protein function for Toll-like receptor 1 in anti-bacterial responses. *J. Immunol.* 165:7125-7132.
380. Yamamoto, M., S.Sato, H.Hemmi, K.Hoshino, T.Kaisho, H.Sanjo, O.Takeuchi, M.Sugiyama, M.Okabe, K.Takeda, and S.Akira. 2003a. Role of adaptor TRIF in the MyD88-independent toll-like receptor signaling pathway. *Science* 301:640-643.
381. Yamamoto, M., S.Sato, H.Hemmi, S.Uematsu, K.Hoshino, T.Kaisho, O.Takeuchi, K.Takeda, and S.Akira. 2003b. TRAM is specifically involved in the Toll-like receptor 4-mediated MyD88-independent signaling pathway. *Nat. Immunol.* 4:1144-1150.

382. Yang, X.J. and E.Seto. 2003. Collaborative spirit of histone deacetylases in regulating chromatin structure and gene expression. *Current Opinion in Genetics & Development* 13:143-153.
383. Yazdankhah, S.P. and D.A.Caugant. 2004. Neisseria meningitidis: an overview of the carriage state. *J. Med. Microbiol.* 53:821-832.
384. Yie, J., M.Merika, N.Munshi, G.Chen, and D.Thanos. 1999. The role of HMG I(Y) in the assembly and function of the IFN-beta enhanceosome. *EMBO J.* 18:3074-3089.
385. Yoshida, M., B.E.Szente, J.M.Kiely, A.Rosenzweig, and M.A.Gimbrone, Jr. 1998. Phosphorylation of the cytoplasmic domain of E-selectin is regulated during leukocyte-endothelial adhesion. *J. Immunol.* 161:933-941.
386. Yoshida, M., W.F.Westlin, N.Wang, D.E.Ingber, A.Rosenzweig, N.Resnick, and M.A.Gimbrone, Jr. 1996. Leukocyte adhesion to vascular endothelium induces E-selectin linkage to the actin cytoskeleton. *J. Cell Biol.* 133:445-455.
387. Young, K., L.L.Silver, D.Bramhill, P.Cameron, S.S.Eveland, C.R.Raetz, S.A.Hyland, and M.S.Anderson. 1995. The envA permeability/cell division gene of Escherichia coli encodes the second enzyme of lipid A biosynthesis. UDP-3-O-(R-3- hydroxymyristoyl)-N-acetylglucosamine deacetylase. *J. Biol. Chem.* 270:30384-30391.
388. Zaric, V., D.Weltin, P.Erbacher, J.S.Remy, J.P.Behr, and D.Stephan. 2004. Effective polyethylenimine-mediated gene transfer into human endothelial cells. *Journal of Gene Medicine* 6:176-184.

389. Zeuke, S., A.J.Ulmer, S.Kusumoto, H.A.Katus, and H.Heine. 2002. TLR4-mediated inflammatory activation of human coronary artery endothelial cells by LPS. *Cardiovasc. Res.* 56:126-134.
390. Zhang, F.X., C.J.Kirschning, R.Mancinelli, X.P.Xu, Y.Jin, E.Faure, A.Mantovani, M.Rothe, M.Muzio, and M.Arditi. 1999. Bacterial lipopolysaccharide activates nuclear factor-kappaB through interleukin-1 signaling mediators in cultured human dermal endothelial cells and mononuclear phagocytes. *J Biol Chem.* 274:7611-7614.
391. Zhang, X., L.Y.Wang, T.Y.Jiang, H.P.Zhang, Y.Dou, J.H.Zhao, H.Zhao, Z.D.Qiao, and J.T.Qiao. 2002. Effects of testosterone and 17-beta-estradiol on TNF-alpha-induced E-selectin and VCAM-1 expression in endothelial cells. Analysis of the underlying receptor pathways. *Life Sci.* 71:15-29.
392. Zhong, H., M.J.May, E.Jimi, and S.Ghosh. 2002. The phosphorylation status of nuclear NF-kappa B determines its association with CBP/p300 or HDAC-1. *Mol. Cell* 9:625-636.
393. Zhong, H. and J.W.Simons. 1999. Direct comparison of GAPDH, beta-actin, cyclophilin, and 28S rRNA as internal standards for quantifying RNA levels under hypoxia. *Biochem. Biophys. Res. Commun.* 259:523-526.
394. Zughaier, S.M., S.M.Zimmer, A.Datta, R.W.Carlson, and D.S.Stephens. 2005. Differential induction of the toll-like receptor 4-MyD88-dependent and -independent signaling pathways by endotoxins. *Infect. Immun.* 73:2940-2950.

Publications

The following publications have arisen from the work presented in this thesis:

Publications:

Michele J Writer, Barry Marshall, Michael A Pilkington-Miksa, Susie E Barker, **Marianne Jacobsen**, Angelika Kritz, Paul C. Bell, Douglas H Lester, Alethea B Tabor, Helen C Hailes, Nigel Klein, Stephen L Hart. **Targeted Gene Delivery to Human Airway Epithelial Cells with Synthetic Vectors Incorporating Novel Targeting Peptides Selected by Phage Display.** *Journal of Drug Targeting*, 12 (4): 185-193.

Marianne C Jacobsen, Garth LJ Dixon, Liana Steeghs, Stephen L Hart, Nigel J Klein. **The regulation of the E-selectin promoter by *Neisseria meningitidis*.** *Manuscript in preparation.*

Marianne C. Jacobsen, Nigel J Klein, Stephen L Hart. **The transfection of primary human endothelial cells with an integrin targeting synthetic vector.** *Manuscript in preparation.*

Abstract:

Marianne C Jacobsen, Garth LJ Dixon, Rob S Heyderman, Simon R Andersen, Peter vand der Ley, Liana Steeghs, Stephen L Hart, Nigel J Klein. *Neisseria meningitidis* LPS dependent and independent activation of endothelial cells. Poster in the 13th International Pathogenic Neisseria Conference, Oslo, Norway, 2002.

Targeted Gene Delivery to Human Airway Epithelial Cells with Synthetic Vectors Incorporating Novel Targeting Peptides Selected by Phage Display

MICHELE J. WRITER^a, BARRY MARSHALL^b, MICHAEL A. PILKINGTON-MIKSA^c, SUSIE E. BARKER^a,
MARIANNE JACOBSEN^d, ANGELIKA KRITZ^a, PAUL C. BELL^c, DOUGLAS H. LESTER^b, ALETHEA B. TABOR^c,
HELEN C. HAILES^c, NIGEL KLEIN^d and STEPHEN L. HART^{a,*}

^aMolecular Immunology Unit, Institute of Child Health, 30 Guilford Street, London WC1N 1EH, UK; ^bSchool of Contemporary Sciences, University of Abertay, Bell Street, Dundee, UK; ^cDepartment of Chemistry, University College London, Christopher Ingold Laboratories, 20 Gordon Street, London, UK; ^dImmunobiology Unit, Institute of Child Health, 30 Guilford Street, London WC1N 1EH, UK

Human airway epithelial cell targeting peptides were identified by biopanning on 1HAEO-cells, a well characterised epithelial cell line. Bound phage were recovered after three rounds of binding, high stringency washing and elution, leading to the production of an enriched phage peptide population. DNA sequencing of 56 clones revealed 14 unique sequences. Subsequent binding analysis revealed that 13 of these peptides bound 1HAEO-cells with high affinity. Three peptides, SERSMNF, YGLPHKF and PSGAARA were represented at high frequency. Three clearly defined families of peptide were identified on the basis of sequence motifs including ^R/_KSM, ^L/_QHK and ^{PSG}/_TARA. Two peptides, LPHKSMP and LQHKSM contained two motifs. Further detailed sequence analysis by comparison of peptide sequences with the SWISSPROT protein database revealed that some of the peptides closely resembled the cell binding proteins of viral and bacterial pathogens including Herpes Simplex Virus, rotavirus, *Mycoplasma pneumoniae* and rhinovirus, the latter two being respiratory pathogens, as well as peptide YGLPHKF having similarity to a protein of unknown function from the respiratory pathogen *Legionella pneumophila*. Peptides were incorporated into gene delivery formulations with the cationic lipid Lipofectin and plasmid DNA and shown to confer a high degree of transfection efficiency and specificity in 1HAEO-cells. Improved transfection efficiency and specificity was also observed in human endothelial cells, fibroblasts and keratinocytes. Therefore, on the basis of clone frequency after biopanning, cell binding affinity, peptide sequence conservation and pathogenic similarity, we have identified 3 novel peptide families and 5 specific peptides that have the potential for gene transfer to respiratory epithelium *in vivo* as well as providing useful *in vitro* transfection reagents for primary human cell types of scientific and commercial interest.

Keywords: Phage display; Peptide; Airway epithelium; 1HAEO-cells

INTRODUCTION

Clinical trials of cystic fibrosis (CF) gene therapy have established safety parameters and demonstrated proof-of-principle (Caplen *et al.*, 1995; Gill *et al.*, 1997; Porteous *et al.*, 1997; Alton *et al.*, 1999) but gene transfer efficiencies with all vectors in the bronchial epithelium was poor. Murine studies, however, suggested that transfection of as few as 5–10% of epithelial cells may be sufficient for clinical improvement (Dorin *et al.*, 1996). Therefore, even a modest increase in the efficiency of

current vectors may be sufficient. A common problem of vectors based on adenovirus (Pickles *et al.*, 1998; Summerford and Samulski, 1998; Walters *et al.*, 1999), adeno-associated virus (AAV; Bals *et al.*, 1998; Summerford and Samulski, 1998) and cationic liposomes (Matsui *et al.*, 1997), the principal vectors used in clinical trials of CF gene therapy, is the lack of availability of their specific receptors on the apical cell surface of the lung epithelium, limiting cell-binding and entry. Our aim is to develop synthetic vectors for gene therapy of CF and other respiratory diseases. Increased cell binding of synthetic

*Corresponding author. Tel.: +44-020-7905-2228. Fax: +44-020-7831-4366. E-mail: shart@ich.ucl.ac.uk

vectors is an important factor in increasing transfection efficiency and specificity (Schaffer and Lauffenburger, 1998) and is the aim of this study.

Peptides are ideal targeting components for synthetic vectors since even short sequences of 7 amino acids contain sufficient structural complexity for high-affinity and specific receptor targeting. For example, receptor-mediated transfection with short peptides targeted to integrins (Hart *et al.*, 1995; 1997; 1998; Erbacher *et al.*, 1999; Fortunati *et al.*, 2000; Li *et al.*, 2000) and the serpin enzyme complex receptor (Ziady *et al.*, 1997; 2002) have been reported. We have described previously a synthetic vector containing an integrin-targeting peptide motif (RRETAWA) with a 16-lysine tail for DNA complex formation (Hart *et al.*, 1995; 1997; 1998). As well as targeting integrin receptors these lipopolyplex vectors also bind non-specifically to anionic proteoglycan cell-surface moieties due to the polycationic properties of the vector particles. However, in confluent epithelium both proteoglycan and integrin receptors are largely inaccessible, located on the basolateral surfaces. The transfection efficiency of integrin-targeted lipopolyplex in dividing airway epithelial cells was thus, greatly reduced in confluent, non-dividing cells. Vector binding efficiency and thus transfection efficiency in these cells was restored by EGTA treatment, which disrupted the tight junctions, exposing the basolateral surfaces (Meng *et al.*, 2004). However, EGTA treatment would be potentially toxic *in vivo* so a preferable approach would be to retarget the vector to receptors that are accessible and abundant on the apical surface of the airway epithelium by incorporating alternative peptide targeting elements targeted to apical receptors.

In the present study, we aimed to isolate and identify novel peptides that target the apical surface of human airway epithelial cells by panning with a random phage peptide library. Biopanning offers the advantage that prior knowledge of the receptor is unnecessary, receptors do not need to be purified and the receptor is in its native conformation. This approach has been used successfully by others on endothelial cells (Giordano *et al.*, 2001; Nicklin *et al.*, 2001), smooth muscle cells (Michon *et al.*, 2002) and neuroblastoma cells (Zhang *et al.*, 2001) as well as human airway epithelial cells (Romanczuk *et al.*, 1999; Vaysse *et al.*, 2000; Jost *et al.*, 2001).

Phage peptides are usually selected after panning and sequencing by clone frequency and binding affinity to the cell target. However, peptides with a high cell affinity alone may not be optimal for gene transfer. The nature of the receptor targeted by a high affinity peptide, its rate of endocytosis and subsequent route of intracellular trafficking or recycling to the cell surface, may strongly influence the ultimate level of gene transfer and expression.

We report here the isolation of a series of peptides that target the apical surface of human airway epithelial cells. Analysis of the peptide sequences led to the identification of three novel families of peptides containing conserved peptide motifs and their potential homologies to known ligands for airway epithelial cells. We also describe

the utility of these peptides in targeted synthetic vector systems for gene delivery to airway epithelial cells, as well as other cell types. Lipopolyplex vectors with selected peptides displayed a transfection efficiency that was enhanced 10-fold over a previously described integrin-targeted lipopolyplex vector formulation (Hart *et al.*, 1998). Moreover, in comparison to lipopolyplex formulations prepared with control, scrambled peptide sequences, the targeted peptides all displayed a higher degree of receptor specificity. These new peptides may prove useful in the development of synthetic vector systems for clinical gene therapy of respiratory diseases such as CF.

MATERIALS AND METHODS

Cell Lines

The human airway epithelial cell line (1HAEO-) was maintained in Eagle's Minimal Essential Medium (MEM) HEPES modification (Sigma, Poole, UK) containing 10% foetal calf serum (FCS), 100 U/ml penicillin, and 100 µg/ml streptomycin and 2 mM L-glutamine. The mouse fibroblast cell line 3T3, the human fibrosarcoma cell line HT1080, primary human dermal fibroblasts and primary rabbit adventitial fibroblasts RAdF were grown in Dulbecco's MEM with Glutamax-1, with 4500 mg/l glucose, and pyridoxine (Gibco BRL-InVitrogen, Paisley, UK), with 10% FCS, 100 U/ml penicillin and 100 µg/ml streptomycin. The human microvascular endothelium cell line, HMEC-1, was maintained in MCDB31 medium supplemented with L-glutamine, penicillin and streptomycin, and 10% FCS. Primary human keratinocytes (Gibco-BRL-InVitrogen) were cultured in Defined Keratinocyte-SFM containing growth supplement (Gibco-BRL-InVitrogen), with 100 U/ml penicillin and 100 µg/ml streptomycin.

Phage Selection

Panning experiments were performed with a PhD C7C, constrained random peptide library (New England Biolabs, Beverly, MA, USA), a pIII protein display library with 3–5 copies of a heptameric peptide constrained by a cysteine disulfide bridge (CX₇C), displayed at one end of the virion. Three rounds of panning were performed. In the first round, 1HAEO-cells were grown to confluence in 24-well plates then, prior to adding phage, cells were washed twice in Tris-buffered saline (TBS), then blocked by adding 2 ml 2% Marvel, 5% bovine serum albumin (BSA) in TBS (blocking solution) per well for 30 min at 4°C. The blocking solution was then removed and a suspension of 2×10^{11} phage in 1 ml blocking solution was added to wells and incubated for 2 h at 4°C with gentle shaking by rotation. The phage supernatant solution was removed then wells were washed with 2% BSA in TBS (washing solution) with 5 min gentle shaking at 4°C. The washing solution was removed then the washing step was repeated 4 times. This was followed by another five washes for a few seconds only. Cell surface

bound phage were eluted by adding 400 μ l 76 mM citrate buffer, pH 2.5 (elution buffer) to the wells with 10 min rotation shaking at 4°C. The eluate was removed and 1 ml of 30 mM Tris, 1 mM ethylenediaminetetraacetic acid (EDTA), pH 8.0 was added to the cells on ice. Cells were then scraped from the plate, and the cell suspension transferred to a microfuge tube, and vortexed briefly. The phage from this fraction were titrated as plaque forming units (PFU) before amplification of the phage in *Escherichia coli* ER2738 cells using standard methodology (Rider *et al.*, 1996).

Prior to the second round of panning, phage that bind either plastic or components of the blocking solution were cleared by adding 2×10^{11} amplified phage from the first round to a blocked well with no cells for 30 min at 4°C. The supernatant was then passed on to three further wells. This phage sample, cleared of non-specific binders, was then used as the input phage for the second round of panning and the procedure repeated essentially as the first round except that the stringency of washing was increased by the inclusion of a final 10 min wash at 4°C with 1 ml 76 mM citrate buffer, pH 3.5. For the third round of panning, 2×10^{11} amplified phage from the second round was again cleared in five blocked wells containing no cells for 30 min each, followed by incubation in an additional well for 1 h at 4°C. Phage elution of the third round was performed as described for the second round. Following titration of phage from the third round fraction, single, well-isolated plaques were picked, amplified and purified for sequencing and clone binding characterisation by whole cell enzyme-linked immunosorbent assay (ELISA).

The numbers of phage in the collected fractions were calculated by infecting *E. coli* ER2738 cells at log phase of growth ($OD_{600} = 0.5$) with a range of dilutions of phage. These were then added to molten top agar at 45°C and poured onto Luria Bertani (LB) agar plates containing isopropyl- β -D-thiogalactoside (IPTG), 5-bromo-4-chloro-3-indolyl- β -D-galactopyranoside (X-gal) and tetracycline. Plaques on each plate were counted following overnight incubation of the plates at 37°C.

Whole Cell ELISA

Approximately 8×10^4 1HAEO-cells in 100 ml Hank's Balanced Salt Solution (HBSS) were added to each well of a 96-well plate and incubated at 37°C until cells had adhered. The cells were washed gently in HBSS before blocking by the addition of 0.5% BSA in HBSS (ELISA blocking solution) for 30 min. Phage particles, 1×10^{10} , in ELISA blocking solution were added to each well and incubated at room temperature for 40 min. Unbound phage were removed by washing twice with HBSS, and bound phage and cells were fixed by adding 3.7% paraformaldehyde PBS for 10 min. Cells were then washed in phosphate buffered saline (PBS) and incubated in ELISA blocking buffer for 45 min, followed by three more washes in PBS. Bound phage were detected by the addition of horse radish peroxidase (HRP)-conjugated anti-M13

antibody (Amersham Pharmacia Biotech, Amersham, Bucks, UK) diluted 1:5000 in ELISA blocking buffer for 1 h, before washing 3 times in PBS, developing the ELISA with 2,2'-azino-bis(3-ethylbenzthiazoline-6-sulfonic acid) (ABTS), and reading the absorbance at 405 nm.

Phage DNA Sequencing

Phage were precipitated with PEG/NaCl (Rider *et al.*, 1996) from a small overnight culture and single-stranded phage DNA was prepared for sequencing (Bonnycastle *et al.*, 2001). Briefly, the protein coat was removed from the sample by phenol chloroform extraction, and the DNA pelleted by ethanol precipitation, washed with ice cold 70% ethanol then resuspended in 10 mM Tris-HCl, 1 mM EDTA, pH 7.5 (TE).

Between 50 and 100 ng of purified phage, DNA was used in a Big Dye (ABI, Foster City, CA) terminator cycle sequencing reaction using the NEB PhD C7C-96 primer (5'-CCCTCATTAGCGTAACG-3') and purified for loading by ethanol precipitation as described in the kit instructions. The samples were run on an ABI 377 sequencer and the results were analysed using the Vector NTI software (Informax Inc., Oxford, UK).

Peptide Synthesis

Peptides (Table I) consisting of the phage-derived targeting motif, or its scrambled control, cyclised by oxidation of two flanking cysteine residues, and with a 16-lysine (K_{16}) tail and a -GA-spacer, were synthesised by standard solid phase synthesis methods either by Alta Biosciences, Birmingham, or at the Department of Chemistry, University College London. The linear peptides were purified by reverse phase HPLC, then cyclised by oxidation by exposing peptide solutions in water to air for over 48 h. The purity of each peptide was confirmed by analytical HPLC. The identity of the peptides and the success of the cyclisation step were verified by electrospray mass spectrometry (data not shown). All peptides were readily soluble in aqueous media.

Transfections

Lipopolyplex formulations were prepared essentially as described previously (Hart *et al.*, 1998), by mixing the components in the following order: 50 μ l of Lipofectin

TABLE I Peptides synthesised

Name	Sequence	Scrambled (S)
P	[K] ₁₆ -GACLPKSMPCG	[K] ₁₆ -GACHPPMSKLCG
Q	[K] ₁₆ -GACLQHKSMPCG	[K] ₁₆ -GACPLSHQMKCG
Y	[K] ₁₆ -GACYGLPHKFCG	[K] ₁₆ -GACYKHPGFLCG
E	[K] ₁₆ -GACSERSMNFCEG	[K] ₁₆ -GACNSFMESRCG
G	[K] ₁₆ -GACPSGAARACG	[K] ₁₆ -GACAGSARPACG
6	[K] ₁₆ -GACRRETEWACG	[K] ₁₆ -GACEARWARTCG

(Invitrogen Ltd, Paisley, UK; 30 µg/ml in OptiMEM), 70 µl peptide (at between 0.029 and 0.1 mg/ml in OptiMEM, according to peptide charge ratio used), with 50 µl of the luciferase reporter plasmid pCILux at (40 µg/ml in OptiMEM). Plasmid pCILux was prepared by subcloning a luciferase gene from pGL3 Control (Life Technologies, Paisley, UK) into the eukaryotic expression vector pCI (Promega, Southampton, UK). The complex was mixed by pipetting briefly before diluting in OptiMEM to a final volume of 1.57 ml.

The complete growth medium was removed from cells plated at 2×10^4 cells/well overnight in 96-well plates and 200 µl of complex (0.25 µg of plasmid DNA) added to each well, leaving minimal time between preparing the complex and adding to the cells. All transfections were carried out in 6 wells each. The cells were incubated with the complexes for 4 h before replacing with normal media for 24–48 h, after which reporter gene expression was analysed by luciferase assay (Promega).

Luciferase Assays

Cells were washed twice with PBS before the addition of 100 µl of $1 \times$ Reporter Lysis Buffer (Promega) to the cells for 20 min at 4°C before freezing at –20°C for at least 30 min followed by thawing at room temperature ($\pm 20^\circ\text{C}$). Twenty microlitres of the lysate at room temperature was transferred to a white polystyrene 96-well plate (Corning Costar, High Wycombe, UK) and the luciferase activity was measured using the Luciferase Assay System (Promega) and a Lucy-1 Luminometer (Anthos Ltd., Salzburg, Austria). The amount of protein present in each transfection lysate was determined with the Bio-Rad protein assay reagent by the manufacturer's instructions, adding 20 µl from the luciferase test to 200 µl of the reagent diluted 1 in 5 and incubating at room temperature for 10 min before comparing the OD590 to a range of BSA standards. Luciferase activity was expressed as Relative Light Units (RLU) per milligram of protein (RLU/mg). Student's *t* test was performed to assess the statistical significance between different experimental groups with probabilities less than 0.05 ($p < 0.05$) taken to be significant.

Transfection of 1HAEO-cells with pEGFP-N1 Plasmid

Cells were transfected with a plasmid, pEGFP-N1 (Clontech, Palo Alto, CA) encoding an enhanced green fluorescent protein (GFP) reporter gene. The growth medium was removed from subconfluent 1HAEO-cells plated at 5×10^4 cells/well overnight in 6-well plates and transfection complex (3 µg of plasmid DNA, 2.25 µg Lipofectin and the optimum peptide charge ratio (between 3 and 7 to 1 DNA) as determined from luciferase experiments (see legends in Figs. 2 and 3) added to each well in a total volume of 2 ml OptiMEM, adding the complexes to the cells immediately after preparation. All transfections were carried out in triplicate wells.

The cells were incubated with the complexes for 4 h before replacing with normal media for 24 h, after which the cells were examined by fluorescence microscopy and harvested by trypsinisation. The triplicate wells for each transfection were pooled, pelleted by brief centrifugation and resuspended in 300 µl of ice-cold PBS before analysis by flow cytometry using a FACSCalibur (Becton Dickinson, Oxford) using the CellQuest software.

BLAST Search in the SWISSPROT Database

A BLAST (<http://www.ncbi.nlm.nih.gov/blast/>) search of the SWISSPROT database with the phage peptide sequences was carried out to identify homologies with proteins of interest including viral receptor-targeting proteins and cell adhesion molecules.

RESULTS

Analysis of DNA and Peptide Sequences

Sequencing of 56 phage clones from the third round of panning of 1HAEO-cells identified 14 different sequences (Table II). The three most frequent phage clones were present at 32% (SERSMNF), 21% (YGLPHKF) and 16% (PSGAARA), respectively, with the remainder present at 5% and below. Three distinct motifs in the 14 unique sequences were identified, K_R SM (where K and R are both basic residues), L^P/Q HK and PSG^A/T ARA (Table III). Of the 56 clones sequenced, 87% contained one or more of these three motifs. The motifs, L^P/Q HK and K_R SM occurred together in two different peptides, LPHKSMP and LQHKSM.

Analysis of Binding

Whole-cell ELISA was performed to assess and compare the binding affinity of selected phage for the target cell. Results confirmed that 13 of the 14 unique peptide sequences bound 1HAEO-cells with significantly higher affinity than insertless phage except for the clone

TABLE II The 56 sequenced phage clones from the third round of panning of 1HAEO-cells were represented by 14 different sequences

Sequence	Number	Percentage
SERSMNF	18	32
YGLPHKF	12	21
PSGAARA	9	16
LQHKSM	3	5
VKSMVTH	3	5
SQSRMNF	2	4
QPLRHHQ	2	4
LPHKSMP	1	2
PSGTARA	1	2
KQRPWL	1	2
IPMNAPW	1	2
SLPFARN	1	2
GPARI SF	1	2
MGLPLRF	1	2

TABLE III Frequency of peptide sequence motifs

Motif	No. of different peptides	Percentage of clones
KSM/RSM	5	48
LXHK	3	29
PSGXARA	2	18

MGLPLRF, which was present in a single copy, which bound equally well in cell-free wells indicating a peptide with high affinity for plastic or components of the blocking solution. Relative binding affinities of the six peptides selected for further investigation compared to a negative control of phage bearing no insert are shown (Fig. 1)

Peptide Sequence Analysis by BLAST

The 13 cell-binding peptides were analysed to identify similar sequences in the SWISSPROT protein databases by BLAST (Table IV). Close similarities were found to several molecules of interest, which may bind receptors present on the surface of epithelial cells in the lung. In particular, four sequences were similar to receptor-binding proteins of viral and bacterial pathogens (Table IV). Peptide SERSMNF shares a close similarity with parts of the receptor targeting proteins of the respiratory pathogens rhinovirus (Mengaud *et al.*, 1996) and *Listeria monocytogenes* (Glaser *et al.*, 2001). Peptide VKSMVTH resembles the epithelial cell receptor-binding proteins of both rotavirus, VP4 (Jolly *et al.*, 2001) and the adhesion protein of *Mycoplasma pneumoniae* (Gabridge, 1982). Peptide YGLPHKF resembles a protein of unknown function of the respiratory pathogen *Legionella pneumophila* (Sequence i.d.CAB65216 in the SWISSPROT database). Peptide LPHKSMP, as well as containing two recurring motifs identified by panning, LPHK and KSM, shares close similarity to glycoprotein B

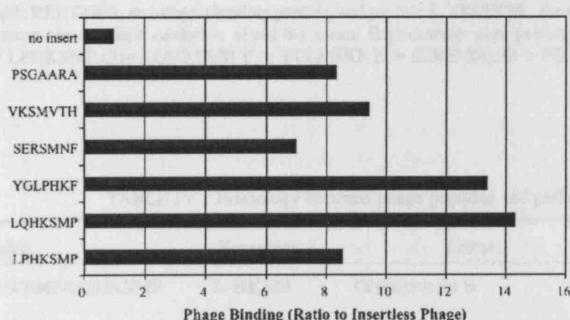


FIGURE 1 Binding of phage to 1HAEO-cells in 96-well plates detected by anti-M13 HRP antibody was quantified in a whole cell ELISA. Values of the phage binding to 1HAEO-cells were determined after subtracting the value phage binding to plate only then expressed as a ratio of binding relative to insertless phage. Values are the means of six wells and the experiment was performed 3 times. Data from a representative experiment is shown.

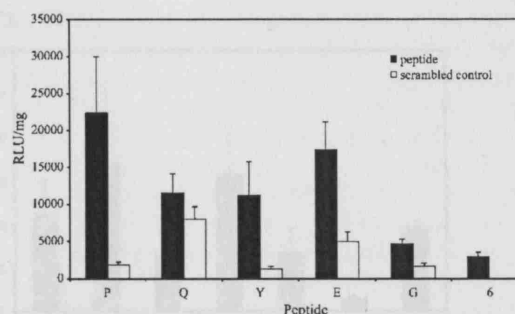


FIGURE 2 Transfection of 1HAEO-cells with phage derived peptides and their scrambled controls was carried out with a range of peptide: DNA charge ratios including 1.5:1, 3:1 and 7:1. For peptides P, Q, E, G, and 6 and their scrambled controls the optimal ratio was 7, whereas for Y and its scrambled control it was ratio 3. Controls include cells with no transfection complexes added (OptiMEM only) and peptide RRETAWA, an integrin binding peptide. Each result is the mean of 6 values and error bars represent the standard deviation about the mean. Peptide P = LPHKSMP, Q = LQHKSMF, Y = YGLPHKF, E = SERSMNF, G = PSGAARA, 6 = RRETAWA. See Table I for scrambled controls.

of Herpes Simplex Virus (HSV), the viral ligand for the cell surface receptor moiety, heparan sulphate (Herold *et al.*, 1994). While HSV is not regarded as a respiratory pathogen, heparan sulphate receptors are abundant on epithelial cell surfaces. The sequences PSGAARA closely resemble part of the coagulation factor XII which binds to cytokeratin (Mahdi *et al.*, 2002).

Transfections

Of the 14 phage sequences, the 4 most frequent were selected, while LPHKSMP was also selected as it contains two of the conserved motifs (Table III) and also resembles glycoprotein B of Herpes Simplex Virus. The 5 peptides were synthesised, with a DNA-binding K_{16} domain linked by a GA sequence to the phage sequence, the latter flanked by two C residues to form a cyclic, conformationally constrained targeting moiety (Table I). These peptides were tested for their ability to transfect 1HAEO-cells in a lipopolyplex formulation (Fig. 2). Transfection efficiency, as measured by luciferase activity, was significantly increased by the addition of the phage-derived peptides compared to their scrambled controls and also compared to the positive control, the integrin binding peptide RRETAWA ($p < 0.05$). One of the peptides, LPHKSMP, consistently produced transfection efficiencies of around 5 times the value of that obtained with peptide RRETAWA and around 10 times the transfection efficiencies obtained with the scrambled version of the peptide. The significantly lower transfection efficiencies obtained when using scrambled versions of the peptides ($p < 0.05$) suggest that the increase in efficiency seen with the phage peptides is sequence dependant and not due to charge or other overall properties of the peptide. Fluorescence activated cell sorting (FACS) analysis of the percentage of cells transfected (Table V) showed

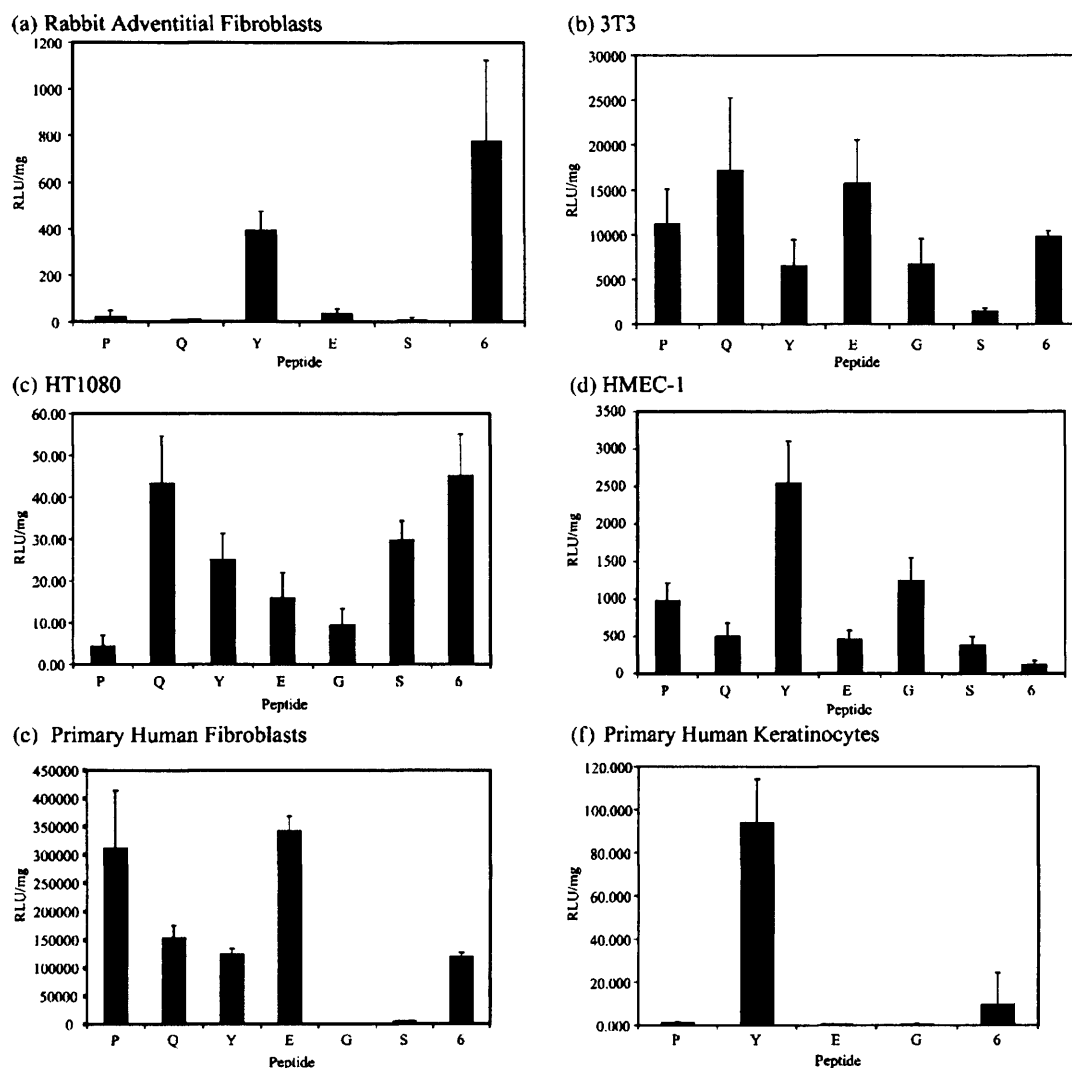


FIGURE 3 Transfections with lipid:peptide: DNA complexes containing phage-derived peptides were performed in (a) primary rabbit adventitial fibroblasts, (b) murine 3T3 fibroblasts, (c) human fibrosarcoma, HT1080 cells, (d) human microvascular endothelial cells, HMEC-1, (e) human primary skin fibroblasts and (f) human primary keratinocytes. Complexes were prepared with a range of peptide: DNA charge ratios including 1.5:1, 3:1 and 7:1. For rabbit adventitial fibroblasts and HMEC-1 cells, all peptides were optimal at ratio 7. For 3T3 cells, all peptides were optimal at ratio 7, except peptide Y which was optimal at ratio 3. For HT1080 cells, peptide P, Q and Y were optimal at ratio 3, while peptides E, G and 6 were optimal at ratio 7, and peptide S at ratio 1.5. For primary human fibroblasts, all peptides were optimal at ratio 3, except peptide G which was used at ratio 7. For primary human keratinocytes, peptides P, E and G were optimal at ratio 3, whereas peptides Y and 6 were optimal at ratio 7. Luciferase expression levels were compared relative to transfection complexes containing peptide RRETAWA, an integrin binding peptide, and peptide S, YKHPGFL, the scrambled version of peptide Y. Each result is the mean of 6 values and error bars represent the standard deviation about the mean. Experiments were performed 3 times and results of a representative experiment are shown. Peptide P = LPHKSMP, Q = LQHKSMF, Y = YGLPHKF, E = SERSMNF, G = PSGAARA, S = YKHPGFL, 6 = RRETAWA. See Table I for scrambled controls.

TABLE IV Homology between phage peptides and pathogens from BLAST (Identical regions are shown in bold)

Peptide	Homology	Protein	Pathogen	Receptor
LPHKSMP/LQHKSMF	L-HKSM	Glycoprotein B	Human herpesvirus	Cell surface heparan sulphate (Herold <i>et al.</i> , 1994)
SERSMNF	SDRSMN	Capsid binding protein VP2	Human rhinovirus	ICAM-1 or LDL receptor family
YGLPHKF	ERSMNF YGLPHK	Internalin (Glaser <i>et al.</i> , 2001)	<i>Listeria monocytogenes</i>	E-cadherin (Mengaud <i>et al.</i> , 1996)
		Unknown function (SWISSPROT: CAB65216).	<i>L. pneumophila</i>	Unknown epithelial cell receptors
VKSMVTH	VKSMITQ	Adhesin P1	<i>M. pneumoniae</i>	Cell surface sialo-glycoproteins (Gabridge, 1982)
	KSMATH	VP4-cell receptor binding	Rotavirus	VLA-2 (Coulson <i>et al.</i> , 1997)

TABLE V Percentage of cells transfected by Lipid: peptide vector by FACS

Peptide used in lipopolyplex	Percentage of cells transfected
LPHKSMP	36.4
LPHKSMP scrambled	19.3
RRETAWA	21.2
RRETAWA scrambled	19.6

that peptide LPHKSMP transfected 36% of cells, compared to 21% when peptide RRETAWA was used, and 19% when scrambled peptide controls were used, suggesting that the increase in transfection efficiency is due at least in part to a greater number of cells being transfected, hence more vectors binding and internalising in a sequence-specific manner.

Transfections were also performed with rabbit adventitial fibroblast and murine fibroblasts 3T3 cells, HMEC-1 and HT1080 human cell lines, and primary keratinocytes and primary fibroblasts (Fig. 3). Transfections with the phage peptides in HT1080 and rabbit adventitial fibroblast cells were of similar efficiency or lower than with peptide RRETAWA. Phage-derived peptides in HMEC-1 cells, however, were all significantly better than peptide RRETAWA ($p < 0.05$). Most notably, peptide YGLPHKF generated luciferase expression levels 20 times higher than peptide RRETAWA, while peptide PSGAARA was 10 times better, and peptide LPHKSMP 8 times better. In murine fibroblasts 3T3 cells, only transfection efficiencies of phage peptides Q and E were higher than levels achieved with peptide RRETAWA ($p < 0.05$). Of the two human primary cell types transfected, peptide YGLPHKF transfection efficiencies were 10 times higher than that of peptide 6 in human keratinocytes whereas in human skin fibroblasts peptides SERSMNF and LPHKSMP both produced efficiencies almost 3 times higher than peptide RRETAWA. In GFP transfections of both primary human fibroblasts and keratinocytes, transfection efficiencies of around 20% were achieved with peptide-optimised lipopolyplex formulations (data not shown).

DISCUSSION

We have developed synthetic vectors systems for efficient, receptor-mediated transfection in lung epithelial cells with the aim of developing enhanced vectors for gene therapy of respiratory diseases such as CF. Novel targeting peptides were identified and assessed after biopanning on 1HAEO-airway epithelial cell line (Cozens *et al.*, 1992) in monolayer with a constrained 7-amino acid phage-display library. Lipopolyplex vectors incorporating these new targeting peptides displayed transfection efficiencies up to 7-fold higher than an equivalent integrin-targeted vector systems and up to 10-fold higher transfection efficiency than scrambled control peptides, indicating receptor-mediated transfection specificity.

Systematic analysis of sequence data in this study, led to the identification of three new families of epithelial-cell binding peptides containing conserved peptide sequence motifs. From 56 sequenced clones, 13 unique peptide sequences with cell binding properties were isolated with the majority containing at least 1 of 3 recurring amino acid motifs, R/KSM , L^P/QHK and $PSG^A/TARA$. Two of these motifs, R/KSM and L^P/QHK , occurred together in two similar phage peptides, LPHKSMP and LQHSMP. The binding affinity of the phage peptides to 1HAEO-cells was at levels of 7–14 times that of control phage, with peptide LQHSMP giving the strongest signal and peptide SERSMNF the weakest. These levels of enhanced binding are comparable to that of the peptide THALWHT isolated by Jost and colleagues (2001), where binding was approximately 8 times that of the control phage.

The BLAST analysis of peptide similarities to the protein sequence database provides an insight into which receptors might be bound by the peptides. Four peptides displayed close similarity to the receptor-targeting proteins of pathogens, three of them lung pathogens. The use of peptides in gene delivery systems that exploit pathogenic infectious pathways is attractive and may present a new approach for achieving efficient transfection despite the many barriers to gene therapy of the lung (Ferrari *et al.*, 2003). At this stage, however, the sequence similarity to pathogenic receptor binding ligands, however intriguing, is only suggestive of homology and further biochemical analysis will be necessary to evaluate this apparent homology further. One frequent peptide/motif, $PSG^A/TARA$ had no similarity to pathogenic sequences but was similar to Factor XII which, interestingly, binds to cytokeratin-1, an epithelial receptor.

Previous studies of biopanning on human airway epithelial cells have yielded alternative sequences which bear no resemblance to the peptides or motifs discovered here or with each other (Romanczuk *et al.*, 1999; Vaysse *et al.*, 2000; Jost *et al.*, 2001). This could be due to differences in the peptide libraries, differences in panning procedure and cells. Two peptides, RFDSLKV and GRGDGDV, were identified by Vaysse and colleagues (2000), by biopanning on CFT-2, a human foetal tracheal cell line derived from a CF patient. The latter peptide contains an integrin-targeting RGD motif. In contrast, none of the peptides we describe in this study contain known integrin receptor binding motifs. Jost and colleagues (2001) identified a single peptide sequence, THALWHT, that occurred in multiple phage clones after biopanning on 16HBE14o-, a human bronchial epithelial cell line. This peptide's receptor is unknown although in transfection experiments it conferred receptor-mediated transfection in epithelial cells. In the report of Romanczuk and colleagues (1999), a phage peptide library of random 12-mers was used for biopanning on primary normal human bronchial epithelial (NHBE) cells. In 20 sequences obtained, 4 families were identified containing the motifs RXLA, HXTF, TFXOT and SDXLAXXS, where X refers to non-identical amino

acids (Romanczuk *et al.*, 1999). No sequence similarities or homologies were suggested in that publication and none of the individual peptides nor the conserved motifs resemble the peptides we have described.

The five peptides synthesised in the form $[K]_{16}GAC[X]_7C$, where X is any amino acid, for inclusion in lipopolyplex vectors were selected not only on the basis of clone frequency but also after consideration of sequence motifs and similarities to pathogenic ligands. All five peptides synthesised were capable of increasing the transfection efficiency when incorporated into lipopolyplex vectors to a level above that seen with the integrin binding peptide RRETAWA and also above that of their scrambled controls. All were found to increase the efficiency of transfection of 1HAEo-cells above that of integrin binding peptide, with the highest, peptide LPHKSMP, giving over 7 times the efficiency of peptide RRETAWA. Peptide LPHKSMP produced RLU/mg values approximately 12 times that of its scrambled control indicating a high degree of receptor specific transfection: this equals or exceeds values seen with other phage derived peptides in non-viral (Vaysse *et al.*, 2000; Jost *et al.*, 2001) and viral vectors (Romanczuk *et al.*, 1999). In other cell types tested, preliminary observations suggest that the peptides display species specificity as well as receptor specificity. For example, none of the peptides is better at transfection of rabbit and murine fibroblasts than complexes with the integrin-targeted peptide RRETAWA although primary human fibroblasts are transfected 2–3 times better with peptides LPHKSMP and SERSMNF and primary keratinocytes 10 times better with peptide YGLPHKF. These different transfection efficiencies are a likely consequence of differential receptor expression and distribution.

In previous biopanning studies, the most frequent clone sequence or the peptide with the highest binding affinity was usually selected for subsequent study (Romanczuk *et al.*, 1999; Nicklin *et al.*, 2000; Vaysse *et al.*, 2000; Jost *et al.*, 2001; Morpurgo *et al.*, 2002). Interestingly, peptide SERSMNF, the most frequent clone, was neither the best binder nor the best transfection peptide in 1HAEo-cells. Peptide LPHKSMP, generated the highest transfection efficiency in 1HAEo-cells, over 7 times that seen with the integrin binding peptide RRETAWA, although it only occurred once in the 56 phage peptide clones. Peptide LPHKSMP was selected for further study on the basis that it contained two conserved motifs, and had close sequence similarity to a cell binding protein of Human Herpes Virus. Peptide LQHKSMF, which only varies by one amino acid from peptide LPHKSMP and contains the same two conserved motifs, R/KSM and L^P/QHK , gave considerably lower transfection efficiency than peptide LPHKSMP, although in phage binding assays it displayed considerably higher binding values. These observations suggest that high receptor binding affinity of a ligand in gene vectors does not necessarily correlate with gene transfer efficiency. The differences between binding data and transfection efficiencies of peptide ligands may reflect

the need for a balance between initial high affinity receptor binding to promote internalisation, and release of the complex once internalised from the receptors suggested similarly for synthetic mannosylated transfection complexes (Fajac *et al.*, 2002).

The main aim of this study was to increase efficiency of transfection of human airway epithelial cells by isolating peptides capable of increasing binding and internalisation of complexes. As such these peptides may also be of use in targeting other forms of drug to the lung epithelium in many diseases. These peptides could also be used in targeting viral vectors to the lung since peptides of this size can be incorporated into the viral coat to retarget vector types including adenovirus (Xia *et al.*, 2000; Nicklin *et al.*, 2001; Koizumi *et al.*, 2003), AAV (Grifman *et al.*, 2001; Shi and Bartlett, 2003) and retroviruses, e.g. Maloney Murine Leukaemia Virus (MMLV; Gollan and Green, 2002).

Acknowledgements

1HAEo-cells were a generous gift of Professor Dieter Gruenert (San Francisco). We thank Jo Buddle and Samantha Hardy for expert technical assistance. This work was funded by the Biotechnology and Biological Sciences Research Council (grants 1/E11945 and 39/GTH12550), Cystic Fibrosis Trust (grant PJ513) and the Engineering and Physical Sciences Research Council.

References

- Alton, E.W., Stern, M., Farley, R., Jaffe, A., Chadwick, S.L., Phillips, J., Davies, J., Smith, S.N., Browning, J., Davies, M.G., Hodson, M.E., Durham, S.R., Li, D., Jeffery, P.K., Scallan, M., Balfour, R., Eastman, S.J., Cheng, S.H., Smith, A.E., Meeker, D. and Geddes, D.M. (1999) "Cationic lipid-mediated CFTR gene transfer to the lungs and nose of patients with cystic fibrosis: a double-blind placebo-controlled trial", *Lancet* **353**, 947–954.
- Bals, R., Wang, X., Zasloff, M. and Wilson, J.M. (1998) "The peptide antibiotic LL37/hCAP-18 is expressed in epithelia of the human lung where it has broad antimicrobial activity at the airway surface", *Proc. Natl Acad. Sci. USA* **95**, 9541–9546.
- Bonnycastle, L.L.C., Menendez, A. and Scott, J.K. (2001) "General phage methods", In: Barbas, III, C.F., Burton, D.R., Scott, J.K. and Silverman, G.J., eds, *Phage Display: A Laboratory Manual* (Cold Spring Harbor Laboratory Press, New York) **30**, pp 15.1–15.30.
- Caplen, N.J., Alton, E.W.F.W., Middleton, P.G., Dorin, J.R., Stevenson, B.J., Gao, X., Durham, S.R., Jeffery, P.K., Hodson, M.E., Coutelle, C., Huang, L., Porteous, D.J., Williamson, R. and Geddes, D.M. (1995) "Liposome-mediated CFTR gene transfer to the nasal epithelium of patients with cystic fibrosis", *Nat. Med.* **1**, 39–46.
- Coulson, B.S., Londrigan, S.L. and Lee, D.J. (1997) "Rotavirus contains integrin ligand sequences and a disintegrin-like domain that are implicated in virus entry into cells", *Proc. Natl Acad. Sci. USA* **94**, 5389–5394.
- Cozens, A.L., Yezzi, M.J., Yamaya, M., Steiger, D., Wagner, J.A., Garber, S.S., Chin, L., Simon, E.M., Cutting, G.R., Gardner, P., *et al.* (1992) "A transformed human epithelial cell line that retains tight junctions post crisis", *In Vitro Cell Dev. Biol.* **28A**, 735–744.
- Dorin, J.R., Farley, R., Webb, S., Smith, S.N., Farini, E., Delaney, S.J., Wainwright, B.J., Alton, E.W. and Porteous, D.J. (1996) "A demonstration using mouse models that successful gene therapy for cystic fibrosis requires only partial gene correction", *Gene Ther.* **3**, 797–801.
- Erbacher, P., Remy, J.-S. and Behr, J.-P. (1999) "Gene transfer with synthetic virus-like particles via the integrin-mediated endocytosis pathway", *Gene Ther.* **6**, 138–145.

- Fajac, I., Grosse, S., Briand, P. and Monsigny, M. (2002) "Targeting of cell receptors and gene transfer efficiency: a balancing act", *Gene Ther.* **9**, 740–742.
- Ferrari, S., Griesenbach, U., Geddes, D.M. and Alton, E. (2003) "Immunological hurdles to lung gene therapy", *Clin. Exp. Immunol.* **132**, 1–8.
- Fortunati, E., Ehlert, E., van Loo, N.D., Wyman, C., Eble, J.A., Grosveld, F. and Scholte, B.J. (2000) "A multi-domain protein for beta1 integrin-targeted DNA delivery", *Gene Ther.* **7**, 1505–1515.
- Gabridge, M.G. (1982) "A review of the morphological and biochemical features of the attachment process in infections with *Mycoplasma pneumoniae*", *Rev. Infect. Dis.* **4**, S179–S184.
- Gill, D.R., Southern, K.W., Mofford, K.A., Seddon, T., Huang, L., Sorgi, F., Thomson, A., MacVinish, L.J., Ratcliff, R., Bilton, D., Lane, D.J., Littlewood, J.M., Webb, A.K., Middleton, P.G., Colledge, W.H., Cuthbert, A.W., Evans, M.J., Higgins, C.F. and Hyde, S.C. (1997) "A placebo-controlled study of liposome-mediated gene transfer to the nasal epithelium of patients with cystic fibrosis", *Gene Ther.* **4**, 199–209.
- Giordano, R.J., Cardo-Vila, M., Lahdenranta, J., Pasqualini, R. and Arap, W. (2001) "Biopanning and rapid analysis of selective interactive ligands", *Nat. Med.* **7**, 1249–1253.
- Glaser, P., Frangeul, L., Buchrieser, C., Rusniok, C., Amend, A., Baquero, F., Berche, P., Bloeker, H., Brandt, P., Chakraborty, T., Charbit, A., Chetouani, F., Couve, E., de Daruvar, A., Dehoux, P., Domann, E., Dominguez-Bernal, G., Duchaud, E., Durant, L., Dussurget, O., Entian, K.D., Fsihi, H., Portillo, F.G., Garrido, P., Gautier, L., Goebel, W., Gomez-Lopez, N., Hain, T., Hauf, J., Jackson, D., Jones, L.M., Kaerst, U., Kreft, J., Kuhn, M., Kunst, F., Kurapkat, G., Madueno, E., Maitournam, A., Vicente, J.M., Ng, E., Nedjari, H., Nordsiek, G., Novella, S., de Pablos, B., Perez-Diaz, J.C., Purcell, R., Rimmel, B., Rose, M., Schluter, T., Simoes, N., Tierrez, A., Vazquez-Boland, J.A., Voss, H., Wehland, J. and Cossart, P. (2001) "Comparative genomics of *Listeria species*", *Science* **294**, 849–852.
- Gollan, T.J. and Green, M.R. (2002) "Redirecting retroviral tropism by insertion of short, non-disruptive peptide ligands into envelope", *J. Virol.* **76**, 3558–3563.
- Grifman, M., Trepel, M., Speece, P., Gilbert, L.B., Arap, W., Pasqualini, R. and Weitzman, M.D. (2001) "Incorporation of tumor-targeting peptides into recombinant adeno-associated virus capsids", *Mol. Ther.* **3**, 964–975.
- Hart, S.L., Harbottle, R.P., Cooper, R., Miller, A., Williamson, R. and Coutelle, C. (1996) "Gene delivery and expression mediated by an integrin-binding peptide", [published erratum *Gene Ther.* 1996 Nov;3(11):1032–3] *Gene Ther.* **2**, 552–554.
- Hart, S.L., Collins, L., Gustafsson, K. and Fabre, J.W. (1997) "Integrin-mediated transfection with peptides containing arginine-glycine-aspartic acid domains", *Gene Ther.* **4**, 1225–1230.
- Hart, S.L., Arancibia-Carcamo, C.V., Wolfert, M.A., Mailhos, C., O'Reilly, N.J., Ali, R.R., Coutelle, C., George, A.J., Harbottle, R.P., Knight, A.M., Larkin, D.F., Levinsky, R.J., Seymour, L.W., Thrasher, A.J. and Kinnon, C. (1998) "Lipid-mediated enhancement of transfection by a nonviral integrin-targeting vector", *Hum. Gene Ther.* **9**, 575–585.
- Herold, B.C., Visalli, R.J., Susmarski, N., Brandt, C.R. and Spear, P.G. (1994) "Glycoprotein C-independent binding of herpes simplex virus to cells requires cell surface heparan sulphate and glycoprotein B", *J. Gen. Virol.* **75**, 1211–1222.
- Jolly, C.L., Huang, J.A. and Holmes, I.H. (2001) "Selection of rotavirus VP4 cell receptor binding domains for MA104 cells using a phage display library", *J. Virol. Methods* **98**, 41–51.
- Jost, P.J., Harbottle, R.P., Knight, A., Miller, A.D., Coutelle, C. and Schneider, H. (2001) "A novel peptide, THALWHT, for the targeting of human airway epithelia", *FEBS Lett.* **489**, 263–269.
- Koizumi, N., Mizuguchi, H., Utoguchi, N., Watanabe, Y. and Hayakawa, T. (2003) "Generation of fiber-modified adenovirus vectors containing heterologous peptides in both the HI loop and C-terminus of the fiber knob", *J. Gene Med.* **5**, 267–276.
- Li, J.M., Collins, L., Zhang, X., Gustafsson, K. and Fabre, J.W. (2000) "Efficient gene delivery to vascular smooth muscle cells using a nontoxic, synthetic peptide vector system targeted to membrane integrins: a first step toward the gene therapy of chronic rejection", *Transplantation* **70**, 1616–1624.
- Mahdi, F., Madar, Z.S., Figueroa, C.D. and Schmaier, A.H. (2002) "Factor XII interacts with the multiprotein assembly of urokinase plasminogen activator receptor, gC1qR, and cytokeratin 1 on endothelial cell membranes", *Blood* **99**, 3585–3596.
- Matsui, H., Johnson, L.G., Randell, S.H. and Boucher, R.C. (1997) "Loss of binding and entry of liposome-DNA complexes decreases transfection efficiency in differentiated airway epithelial cells", *J. Biol. Chem.* **272**, 1117–1126.
- Meng, Q.-H., Robinson, D., Jenkins, R., McAnulty, R. and Hart, S. (2004) "Efficient transfection of non-proliferating human airway epithelial cells with a synthetic vector system", *J. Gene Med.* **6**, 210–221.
- Mengaud, J., Ohayon, H., Gounon, P., Mège, R.-M. and Cossart, P. (1996) "E-cadherin is the receptor for internalin, a surface protein required for entry of *L. monocytogenes* into epithelial cells", *Cell* **84**, 923–932.
- Michon, I., Hauer, A., von der Thüsen, J., Molenaar, T., van Berkel, T., Biessen, E. and Kuiper, J. (2002) "Targeting of peptides to restenotic vascular smooth muscle cells using phage display *in vitro* and *in vivo*", *Biochim. Biophys. Acta* **1591**, 87.
- Morpurgo, M., Kirschner, M. and Radu, A. (2002) "An approach to increased polyplex gene delivery by peptides selected from a phage display library", *J. Biochem. Biophys. Methods*, 1574.
- Nicklin, S.A., White, S.J., Watkins, S.J., Hawkins, R.E. and Baker, A.H. (2000) "Selective targeting of gene transfer to vascular endothelial cells by use of peptides isolated by phage display", *Circulation* **102**, 231–237.
- Nicklin, S.A., Von Seggern, D.J., Work, L.M., Pek, D.C., Dominiczak, A.F., Nemerow, G.R. and Baker, A.H. (2001) "Ablating adenovirus type 5 fiber-CAR binding and HI loop insertion of the SIGYPLP peptide generate an endothelial cell-selective adenovirus", *Mol. Ther.* **4**, 534–542.
- Pickles, R.J., McCarty, D., Matsui, H., Hart, P.J., Randell, S.H. and Boucher, R.C. (1998) "Limited entry of adenovirus vectors into well-differentiated airway epithelium is responsible for inefficient gene transfer", *J. Virol.* **72**, 6014–6023.
- Porteous, D.J., Dorin, J.R., McLachlan, G., Davidson-Smith, H., Davidson, H., Stevenson, B.J., Carothers, A.D., Wallace, W.A., Moralee, S., Hoenes, C., Kallmeyer, G., Michaelis, U., Naujoks, K., Ho, L.P., Samways, J.M., Imrie, M., Greening, A.P. and Innes, J.A. (1997) "Evidence for safety and efficacy of DOTAP cationic liposome mediated CFTR gene transfer to the nasal epithelium of patients with cystic fibrosis", *Gene Ther.* **4**, 210–218.
- Rider, J.E., Sparks, A.B., Adey, N.B. and Kay, B.K. (1996) "Microbiological methods", In: Kay, B.K., Winter, J. and McCafferty, J., eds, *Phage Display of Peptides and Proteins* (Academic Press, San Diego), pp 55–65.
- Romanczuk, H., Galer, C.E., Zabner, J., Barsomian, G., Wadsworth, S.C. and O'Riordan, C.R. (1999) "Modification of an adenoviral vector with biologically selected peptides: a novel strategy for gene delivery to cells of choice", *Hum. Gene Ther.* **10**, 2615–2626.
- Schaffer, D.V. and Lauffenburger, D.A. (1998) "Optimization of cell surface binding enhances efficiency and specificity of molecular conjugate gene delivery", *J. Biol. Chem.* **273**, 28004–28009.
- Shi, W. and Bartlett, J.S. (2003) "RGD inclusion in VP3 provides adeno-associated virus type 2 (AAV 2)-based vectors with a heparan sulfate-independent cell entry mechanism", *Mol. Ther.* **7**, 515–525.
- Summerford, C. and Samulski, R.J. (1998) "Membrane-associated heparan sulfate proteoglycan is a receptor for adeno-associated virus type 2 virions", *J. Virol.* **72**, 1438–1445.
- Vaysse, L., Burgelin, I., Merlio, J.P. and Arveiler, B. (2000) "Improved transfection using epithelial cell line-selected ligands and fusogenic peptides", *Biochim. Biophys. Acta* **1475**, 369–376.
- Walters, R.W., Grunst, T., Bergelson, J.M., Finberg, R.W., Welsh, M.J. and Zabner, J. (1999) "Basolateral localization of fiber receptors limits adenovirus infection from the apical surface of airway epithelia", *J. Biol. Chem.* **274**, 10219–10226.
- Xia, H., Anderson, B., Mao, Q. and Davidson, B.L. (2000) "Recombinant human adenovirus: targeting to the human transferrin receptor improves gene transfer to brain microcapillary endothelium", *J. Virol.* **74**, 11359–11366.
- Zhang, J., Spring, H. and Schwab, M. (2001) "Neuroblastoma tumor cell-binding peptides identified through random peptide phage display", *Cancer Lett.* **171**, 153–164.
- Ziady, A.G., Perales, J.C., Ferkol, T., Gerken, T., Beegen, H., Perlmutter, D.H. and Davis, P.B. (1997) "Gene transfer into hepatoma cell lines via the serpin enzyme complex receptor", *Am. J. Physiol.* **273**, G545–G552.
- Ziady, A.-G., Kelley, T.J., Milliken, E., Ferkol, T. and Davis, P.B. (2002) "Functional evidence of CFTR gene transfer in nasal epithelium of cystic fibrosis mice *in vivo* following luminal application of DNA complexes targeted to the serpin-enzyme complex receptor", *Mol. Ther.* **5**, 413–419.